An Analysis of the Role of Glutathione and p53 in the Response to Oxidative Injury

Jonathan P Coe

Submitted for the degree of Doctor of Philosophy

University of Edinburgh

2002

Declaration

The work presented in this thesis has been carried out by myself except where specifically indicated in the text.

Jonathan Coe

August 2002

Contents

Acknowledgements

I owe much to various disparate groups for assisting my progress throughout this project. In particular, I am in debt to Professors David and Alan for their boundless enthusiasm, insight, and time. Thanks to Irfan for guidance, editing and advice throughout the redox sections, and the ELEGI laboratory for use of hardware.

Special respect to Dom, Chris and Scotty: a collective of more robust philosophers and debauched visionaries would be difficult to conceive. I am sure none of us will ever forget the process. Additionally, I acknowledge Jason for providing a supply of fresh *arabica* and *adobe* tuition.

Cheers also to Eleanor, Stefan, Liz, Jan and others who provided daily support and advice, whilst Dave, Dunc, Tegan, Sumen, Su, Roo *et al* supplied a continual stream of diverse and creative diversions outwith the radioactive confines of Teviot Place. In the latter stages, I would also have had difficulty maintaining carbohydrate levels without the express services of Colin.

I dedicate this thesis to my parents for providing unswerving moral and financial support - without which this thesis would have been even more difficult to complete, and withholding comment regarding the unusual behavioural characteristics of a wayward PhD student.

Abbreviations

AIF	Apoptosis inhibitory factor
Amp	Ampicilin
AP-1	Activator protein-1
APS	Ammonium persulphate
ARE	Antioxidant response element
ATP	Adenosine triphosphate
BER	Base excision repair
bp	Base pairs
BSA	Bovine serum albumin
BSO	Buthionine sulfoximine
cAMP	Cyclic adonosine monophosphate
CDK	Cyclin-dependent kinase
cDNA	Complimentary DNA
ddH2O	Distilled, de-ionized water
DEM	Diethylmaleate
DMSO	Dimethylsulfoxide
DNA	Deoxyribonucleic acid
dNTP(s)	Deoxyribonucleotide phosphates
DTNB	5,5'-Dithiobis (2-nitrobenzoic acid)
DTT	Dithiothreitol
EDTA	Ethylene diamine tetracetic acid
ES cell	Embryonic stem cell
Fe^{2+}	Ferrous iron
Fe^{3+}	Ferric iron
G418	Geneticin sulphate
GANC	Gancyclovir
γGCS	gamma glutamylcysteine synthetase holoenzyme
γGCSh	gamma glutamylcysteine synthetase heavy subunit
γGCSl	gamma glutamylcysteine synthetase light subunit
γGT	gamma glutamyl transpeptidase
GMEM	Glasgow's modified eagle's medium
GPx	Glutathione peroxidase
GR	Glutathione reductase
GS	Glutathione synthetase
GSH	reduced Glutathione
GSH-MEE	Glutathione monoethyl ester
GSSG	Glutathione disulphide
H_2O_2	Hydrogen peroxide
HO•	Hydroxyl radical
HR	Homologous recombination
kb	1000 base pairs
λ	phage lamdba

LIF	Leukaemia inhibitory factor
$MgCl_2$	Magnesium chloride
MQ	2-Methyl-1,4-naphthoquinone
mRNA	messenger ribonucleic acid
MRP	Multi-drug resistance protein
NAC	N-acetylcysteine
NaCl	Sodium chloride
NADP	Oxidised nicotinamide adenine dinucleotide phosphate
NADPH	Reduced nicotinamide adenine dinucleotide phosphate
Neo	Neomycin phosphotransferase
NER	Nucleotide excision repair
NF-kβ	Nuclear factor kappa β
O_2	Oxygen
$O2^{\bullet -}$	Superoxide anion
ONOO•	Peroxynitrite radical
ORF	Open reading frame
PAGE	Polyacrylamide gel electrophoresis
PBS	Phosphate buffered saline
PCR	Polymerase chain reaction
PIG	p53-inducible genes
PGK	Phospho
PK-A	Phosphokinase-A
PK-C	Phosphokinase-C
Poly A	Polyadenosine
PNS	Positive-negative selection
PT	Permeability transition pore
Rb	Retinoblastoma
Ref-1	Redox-factor 1
RNA	Ribonucleic acid
ROS	Reactive oxygen species
RS•	Thiyl radical
RT-PCR	Reverse transcription-polymerase chain reaction
SF	Serum free
SH3	Src homology 3
SOD	Superoxide dismutase
SSA	Sulphosalicyclic acid
SSC	Saline, sodium citrate buffer
TBE	Tris/Borate EDTA buffer
TBF	TATA-binding protein
tBHQ	*tert*-butylhydroquinone
TEMED	N',N',N',N',Tetramethylethylenediamine
TFII	transcription factor II
TGF-β	Transforming growth factor-β
tk	Thymidine kinase
TNF-α	Tumour necrosis factor α
UV	Ultraviolet light
$X^{-}c$	Sodium- and energy-independent transport system for dibasic amino acids

Abstract

The response to oxidative stress, a process that can lead to genotoxic injury, is thought to involve the abundant cellular antioxidant, glutathione, and the stress response transcription factor, p53. Glutathione (GSH) biosynthesis occurs through a two-step pathway, the first reaction of which is rate limiting and is catalysed by the enzyme gamma glutamylcysteine synthetase (γGCS). γGCS is a heterodimer, composed of a heavy (γGCSh) and a light (γGCSl) subunit. The heavy subunit contains the active site, whereas the light performs a regulatory function on the heavy by means of a redox-sensitive inter-subunit disulphide bridge.

The hypothesis that GSH mediates protection against oxidative stress was investigated by gene targeting of *γGCSh* in murine embryonic stem (ES) cells. Mouse *γGCSh* cDNA sequence was isolated by RT-PCR, cloned, characterised and used to screen a mouse genomic λ library. Characterisation of the resultant clone confirmed that it contained *γGCSh* gene sequences. This information was used to design and construct a replacement targeting vector which was subsequently electroporated into ES cells to delete a segment of the endogenous locus. A total of 285 clones were isolated and analysed for a correct gene targeting event. Unfortunately, no positive clones were identified.

The role of GSH and p53 in the response of ES cells to oxidative stress was also examined via a series of *in vitro* assay strategies measuring cellular viability, apoptosis and intracellular GSH levels. ES cells were shown to express *γGCSh*. Agents known to induce oxidative stress or lower GSH levels in other cell lines were then tested for toxicity and their potential to modulate GSH levels in ES cells. On the basis of these experiments, the quinone menadione (MQ) and the γGCS inhibitor, buthionine sulphoximine (BSO), were investigated further. Treatment with MQ was associated with a transient elevation of GSH, a strong apoptotic response and reduced clonogenic survival. Addition of BSO depleted GSH levels and prevented the MQ-induced increase in GSH, sensitising cells to oxidative insult. In order to

address the role of p53 in the response to oxidative stress, karyotypically normal p53-/- ES cells were compared to wild-type cells. This showed that both maintenance of basal GSH levels and MQ-induction of GSH were independent of p53 status. However, a role for p53 in this response was demonstrated as the kinetics of MQ-induced apoptosis were delayed in the absence of p53. Taken together, these findings suggest that the pathways involving p53 and GSH act independently to protect against the deleterious effects of oxidative damage.

Consistent with studies using a wide spectrum of other DNA damage inducing agents, loss of p53 conferred an immediate survival advantage post oxidative stress. However, the long-term clonogenic survival of p53-/- ES cells was found to be lower than cells with an intact p53 pathway. This suggests that compensatory mechanisms exist to ensure that, in the absence of functional p53, cells bearing genetic lesions are less likely to be propagated, and furthermore that the ability to engage apoptosis does not necessarily predict long term clonogenic survival.

In summary, an attempt was made to address the *in vivo* significance of GSH by creating a *γGCSh* null strain of mice. To this end a targeting vector was generated and used in ES cells, but unfortunately this failed to produce a mutant *γGCSh* allele. This thesis has also explored the relationship between oxidative damage and the cellular responses of GSH and p53 *in vitro*. Evidence is presented to demonstrate that, within embryonic tissues, multiple pathways operate in response to oxidative stress, and that in the absence of p53 cells are prevented from propagating.

Chapter 1

Introduction

1.1 ROS and Oxidants

Oxygen is essential to aerobic life, though respiration of oxygen to water gives rise to reactive, toxic intermediates. These oxidants, or free radicals, are defined chemically as molecules that can lose electrons. Such umbrella descriptions cover a kaleidoscope of structurally heterogeneous pro-oxidative compounds that have in common an ability to exist independently for a period of time with one or more unpaired electrons in their outer orbital. Molecular oxygen can be considered as a bi-radical, because it has two unpaired electrons. They are relevant to the spheres of biology and medicine, since they are tissue damaging molecules implicated in a variety of human conditions ranging from developmental abnormalities to natural ageing.

The term reactive oxygen species (ROS) was originally employed to designate a group of oxygen-centred radicals and several non-radicals derived from oxygen such as hydrogen peroxide (H_2O_2) (Halliwell et al., 1992). However sulphur or nitrogen-based radicals are also referred to as ROS by many researchers (table 1.1), as long as they exist with an incomplete or excessive electron quota.

ROS and free radicals can be harmful due to their reactivity towards nearby cellular molecules. To complement the unpaired electron in their outer orbit a ROS may remove an electron from a cellular molecule, or join that molecule to form a stable bond. Alternatively, a ROS may donate its unpaired electron to a biological nonradical. A nonradical with an additional electron becomes a radical, thus ROS chemistry can, on such occasions, proceed as chain reactions. Only when two radicals meet, or when an electron is donated from an external system does the reaction terminate. Highly reactive radicals, such as the hydroxyl radical ($OH\bullet$) frequently attack cellular components. Peroxynitrite ($ONOO\bullet$), superoxide ($O_2\bullet^-$) and

Table 1.1 Types of endogenously produced radicals

An example of biologically relevant ROS, adapted from (Woods et al., 1998). The dot designates the presence of unpaired electrons, nomenclature recommended by (Pryor and Davies, 1993). * Indicates reactive non-radicals derived from oxygen.

Chemical symbol	Chemical name
$O_2^{\cdot-}$	Superoxide
HO·	Hydroxyl radical
RS·	Sulphur-centred radical (thiyl)
CCl_3·	Carbon-centred radical (trichloromethyl)
NO·	Nitrogen-centred radical (nitric oxide)
ONOO·	Peroxynitrite
HOCl	* Hypochlorous acid
$^1O_2$	* Singlet oxygen
H_2O_2	* Hydrogen peroxide

H_2O_2, although less reactive, still have biologically sensitive targets (Halliwell et al., 1992).

1.1.1 The generation of ROS

Radicals are produced by accepting or losing an electron. Within cells this can occur, for the most part, by four major processes. (1) By normal aerobic respiration. The sequential reduction of oxygen to water in the mitochondrial electron transport chain generates ROS by-products (figure 1.1a), of which approximately two per cent leak to the cytosol. During infection, exposure to X-rays, irradiation, exogenous toxins or other stress-inducing factors, mitochondrial respiration accelerates, oxygen consumption and leakage of ROS to the cytoplasm escalates (Ames et al., 1993; Park et al., 1998; Woods et al., 1998). (2) By degradation of fatty acids in peroxisomes. Degradation products include H_2O_2 that, under certain conditions, may leak from the organelle to other cellular compartments. (3) By cytochrome P450 activation. While many toxins are directly harmful, the toxicity of others is due to activation by metabolic conversion. The induction of P450 enzymes constitutes a primary defence system against naturally occurring toxins, but it can also yield metabolic intermediates bearing defective electronic arrangements (Ames et al., 1993). (4) By the actions of polymorphonuclear cells as they engulf and consume bacteria. Although the exact mechanism is not clear, phagocytes are thought to employ an oxidative burst of $NO\bullet$, $O_2\bullet^-$, H_2O_2 and $OCl\bullet^-$ to help destroy bacteria or virus-infected cells. This potent bactericidal cocktail protects against death from infection at the expense of localised oxidative injury (Ames et al., 1993; Woods et al., 1998).

Whilst these endogenous processes routinely generate ROS, exogenous sources of ROS are the predominant mediators of oxidative injury. Two exogenous sources may increase the endogenous oxidant burden: (1) ROS-generating chemical and physical agents that cause oxidation of macromolecules and depletes antioxidant levels, and (2) dietary iron salts which promote release of hydroxyl radicals (Ames et al., 1993).

The mechanism of oxidant production varies between the mode of induction. Ionising (γ) and ultraviolet (UV) irradiation initiate an ROS burden through direct,

Figure 1.1 Generation of ROS

A, Normal metabolism produces of ROS. Electrons (e^-) are sequentially added by mitochondrial oxidases in the aerobic respiration of oxygen to water (de Groot and Littauer, 1989). *B*, Under circumstances of excess H_2O_2 production, H_2O_2 can be cleaved in transition metal (iron or copper) ion-catalysed reactions to produce the hydroxyl radical. (1) The Fenton reaction and (2), the Haber-Weiss reaction.

A

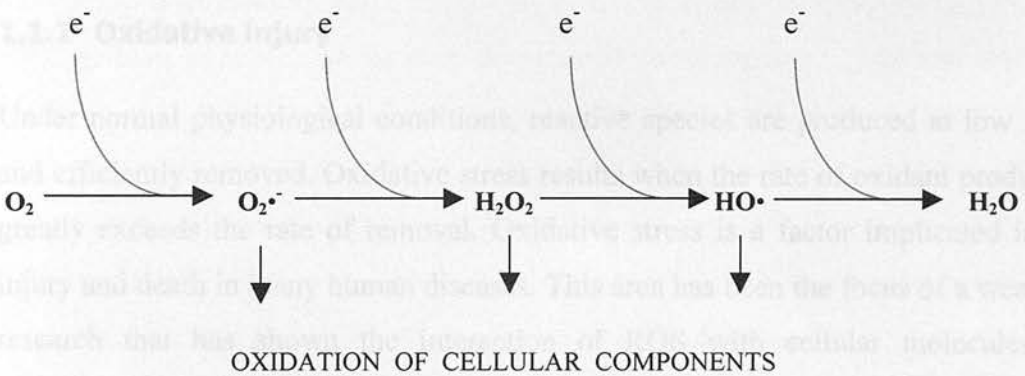

B

(1) $Fe^{2+} + H_2O_2 \rightarrow Fe^{3+} + HO^- + HO\bullet$

(2) $O_2\bullet^- + H_2O_2 \xrightarrow{Fe} O_2 + HO^- + HO\bullet$

high-energy electron displacement from cellular molecules (Stadtman and Levine, 2000), while many phenolic compounds and quinones are thought generate radicals by "redox cycling". In this process, radicals typically transfer their extra electron to oxygen, forming a superoxide anion radical and regenerating the parent donor, which is ready to gain a new electron (Figure 1.2). Through this "redox-cycling", one electron acceptor molecule can generate many superoxide anions (Klassen, 1996).

H_2O_2 and alkylperoxides are the most common end products of oxidative stress. These peroxides by themselves are relatively unreactive compounds. However, in the presence of transition metals ions, at physiological concentrations, a limited amount of H_2O_2 is converted to the highly reactive hydroxyl radical (Stadtman and Levine, 2000). The reactivity of HO• is such that it does not diffuse more than two molecular diameters before reacting with a cellular molecule (Pryor, 1986).

1.1.2 Oxidative injury

Under normal physiological conditions, reactive species are produced at low levels and efficiently removed. Oxidative stress results when the rate of oxidant production greatly exceeds the rate of removal. Oxidative stress is a factor implicated in cell injury and death in many human diseases. This area has been the focus of a wealth of research that has shown the interaction of ROS with cellular molecules can precipitate both their dysfunction and destruction. Biomolecules subject to reactivity with ROS include lipid, protein, carbohydrate and nucleic acids.

ROS can activate proteins or, more commonly, inhibit their function. These processes are predominantly localised to the iron- or copper-binding sites on proteins, resulting in localised OH• generation which selectively modifies adjacent amino acids residues (Levine et al., 1981; Stadtman, 1990; Neuzil et al., 1993; Stadtman and Levine, 2000). Therefore, it is thought that protein oxidation is, under physiological conditions, a site-specific process. Reaction with critical protein sulfhydryls (SH-groups) usually impairs catalytic activity of enzymes, especially those dependent on metal ions for activity (Fucci et al., 1983). A similar end result can occur through arylation of protein sulfhydryls (van Ommen et al., 1988; Brown

et al., 1991). With particular compounds, including many quinones, this direct covalent binding between ROS and sulfhydryl groups is considered as toxic as the effects of oxidation (Nicotera et al., 1990b; Stone et al., 1996; Qiu et al., 1998). Arylation of cellular SH-groups results in the deleterious formation of MQ-protein adducts (Qiu et al., 1998). ROS can also generate conformational changes that inhibit assembly into macromolecular complexes (Stadtman and Levine, 2000), and fragment carbohydrate groups (Woods et al., 1998). Through both oxidation and arylation mechanisms ROS are thought to block receptors, ion channels and ablate the catalytic activity of enzymes.

The sensitivity of biolipids to oxidation resides in their esterified lipid residue (Porter, 1986). This group, found at the tip of polyunsaturated fatty acid tails, has an unpaired electron that represents a prime target for reaction with ROS. This phospholipid species is present in very high concentrations in all cell membranes and enables them to participate in long free radical chain reactions (Marnett, 2000). A single reaction with the lipid bilayer can initiate a cascade that consumes up to 200 molecules of fatty acid (Awad et al., 1993). The major products of lipid peroxidation are malondialdehyde (MDA) and 4-hydroxynonwnol (HNE) (Schauenstein and Esterbauer, 1978). MDA is directly mutagenic, while HNE has powerful effects on signal transduction pathways, the phenotypic effects of which appear independent of DNA damage (Basu and Marnett, 1983).

Though ROS can attack most biomolecules, DNA probably represents the most important biological target (Berlett and Stadtman, 1997; Henle and Linn, 1997). The injuries inflicted by ROS on DNA are almost exclusively small, but their accumulation is suspected to be carcinogenic (Bohr and Dianov, 1999; Akman et al., 2000; Marnett, 2000) and represent a major contribution to the development of a variety of other pathologies. Intercalation of compounds in the double helix push adjacent bases apart causing shifts in reading frame (Klassen, 1996), whilst covalent binding of oxidants to DNA can cause nucleotide mispairing during replication (especially the G→T transversion) (Wang et al., 1998a; Marnett, 2000). Some ROS-inducing compounds, including quinones, can also arylate DNA to produce modified

Figure 1.2 Quinone-based redox-cycling

Quinones (Q) can be metabolised intracellularly (within circle) by either a one or a two step reaction. One-step reaction: $2e^-$ are donated by quinone oxidoreductase NQO1 (b) to directly form a less reactive hydroquinone (HQ) product. Two step reaction: sequential addition of single electrons by individual flavoenzymes (a) generates a semiquinone (SQ•) intermediate that readily reacts with cellular oxygen to produce $O_2^{\bullet -}$, regenerating the parent molecule. Subsequent production of H_2O_2 and OH• occurs as indicated (adapted from Thor et al., 1982).

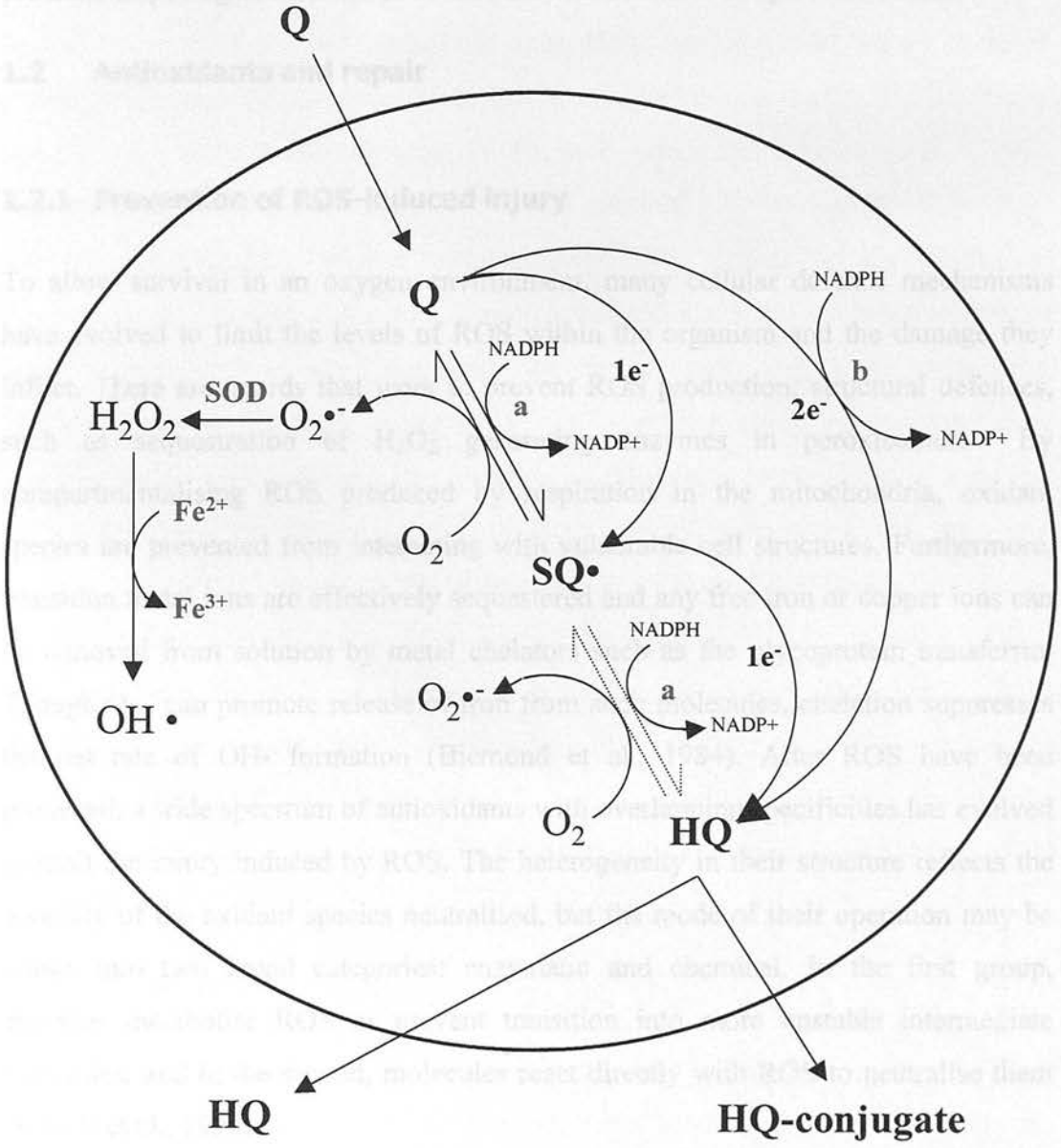

bases known as adducts. Adducts slow replication, which can arrest cell division or generate chromosomal alterations (Woods et al., 1998; Sharma and Slocum, 1999). Quinones can also initiate single-strand breaks, the effects of which may be compounded by the incorporation of damaged nucleotides during DNA repair (Zastawny et al., 1998). The reaction of OH• radicals with DNA can induce depurination, as well as strand scission caused by interaction with the phosphodiester bond (Klassen, 1996). Tissue culture data regarding ROS-inflicted DNA damage indicates that the lesions induced are mutagenic and reflect mutations commonly observed in human genes (Marnett, 2000). Last, and in addition to reaction with individual classes of biomolecules, ROS can cross-link proteins, DNA, or DNA with proteins: imposing structural and functional constraints on coupled molecules.

1.2 Antioxidants and repair

1.2.1 Prevention of ROS-induced injury

To allow survival in an oxygen environment, many cellular defence mechanisms have evolved to limit the levels of ROS within the organism and the damage they inflict. There are guards that work to prevent ROS production: structural defences, such as sequestration of H_2O_2 generating enzymes in peroxisomes. By compartmentalising ROS produced by respiration in the mitochondria, oxidant species are prevented from interacting with vulnerable cell structures. Furthermore, transition metal ions are effectively sequestered and any free iron or copper ions can be removed from solution by metal chelators such as the glycoprotein transferrin. Though $O_2^{\bullet -}$ can promote release of iron from such molecules, chelation suppresses the net rate of OH• formation (Biemond et al., 1984). After ROS have been produced, a wide spectrum of antioxidants with overlapping specificities has evolved to limit the injury induced by ROS. The heterogeneity in their structure reflects the diversity of the oxidant species neutralised, but the mode of their operation may be drawn into two broad categories: enzymatic and chemical. In the first group, enzymes metabolise ROS or prevent transition into more unstable intermediate molecules, and in the second, molecules react directly with ROS to neutralise them (Woods et al., 1998).

Catalysed removal of ROS includes the structurally unrelated and intracellular enzymes superoxide dismutases (SOD), catalase, thioredoxin reductase and glutathione peroxidases (GPx) glutathione *S*-transferases (GST). Different isoforms of SODs are found in cytosol, nucleus, mitochondria and plasma though all eliminate ROS by reducing (adding an electron to) superoxide to form hydrogen peroxide, which in turn is removed by other enzymes (editorial, 1993). Catalase and GPx are responsible for reducing H_2O_2 to H_2O and O_2 (Warner, 1994), while thioredoxin reductases maintain proteins in their reduced state (Mustacich and Powis, 2000) and GSTs eliminate a wide variety of foreign compounds.

In addition to the major antioxidant enzymes, many low molecular weight chemical antioxidants such as ascorbate (vitamin C), α-tocopherol (vitamin E), β-carotene (vitamin A), thioredoxin (Deneke, 2000), uric acid, urate (Ames et al., 1993), carnosine, ubiquinol (Podda et al., 1998) and possibly bilirubin operate to preserve cellular redox balance (Stocker and Peterhans, 1989; Minetti et al., 1998). α-tocopherol, an essential vitamin, is lipid soluble and can integrate into membranes where it is thought to break the chain reaction of lipid peroxidation. β-carotene, another dietary antioxidant, is also lipid soluble and can scavenge $O_2\bullet^-$. Ascorbate also neutralises $O_2\bullet^-$ and H_2O_2, but is water soluble and is located both in intra and extracellular spaces. Interestingly, both ascorbate and β-carotene can have pro-oxidant capability. However, the most abundant intracellular antioxidant is the tripeptide glutathione (GSH), L-γ-glutamyl-L-cysteinylglycine. GSH carries a reduced SH-group (termed "thiol", to distinguish it from protein SH- "sulfhydryl" groups) that acts as a non-specific reducing site with either free ROS or cellular compounds with an incomplete electron compliment. In both cases a hydrogen atom, which has a single unpaired electron, is transferred from the thiol group to the recipient radical (Bergendi et al., 1999).

1.2.2 Repair of ROS damage

These elaborate antioxidant defences do not provide complete protection from oxidative stress however, as residual ROS are often free long enough to interact with

cellular architecture. As such, other systems are dedicated to the removal of damaged cellular components.

Toxic lipid by-products are removed by glutathione peroxidase and oxidised proteins are degraded by proteases. Most oxidised base damage in DNA is repaired rapidly, within several hours of oxidant exposure, though repair of single or double strand breaks is considerably slower (Akman et al., 2000). Repair of the majority of ROS-induced DNA damage occurs via the BER (*b*ase *e*xcision *r*epair) system, a conserved and intricate process. This utilises DNA glycosylases to excise oxidised base residues (Bhagwat and Gerlt, 1995), which are then excreted in the urine. The resulting nucleotide gap is filled by synthesis with DNA polymerase β and concludes with a complex assembly including DNA Ligase III to complete repair (Cappelli et al., 1997). To assist in the annealing of complimentary strands, the stress response regulator p53 (section 1.5) is thought to bind single-stranded DNA ends (Yokote et al., 1998). More recently, *in vitro* studies showed nuclear extracts overexpressing p53 exhibited an augmented BER activity, whilst p53 depletion abolished this enhanced activity (Offer et al., 1999). To a lesser extent, oxidative DNA damage is repaired by restitution via hydrogen donation from an SH-group (section 1.3), nucleotide excision (section 1.5.4.3), and recombination (Henle and Linn, 1997).

In the absence of cell division, oxidative lesions are removed quite rapidly and the mutation rate effectively repressed. However, from a cellular perspective the optimum strategy would be to neutralise ROS prior to damage infliction, and in this regard GSH plays a central role.

1.3 Glutathione

GSH was originally discovered in 1888 and the structure resolved in 1929 (figure 1.3). The peptide has a stable structure, resistant to most peptidases due to the strong glutamyl-cysteine bond (Anderson et al., 1989). GSH is synthesised by virtually all eukaryotic cells and participates in a myriad of biological processes, including cellular defence against oxidative stress by scavenging ROS or by reducing disulphide linkages in proteins and other cellular molecules. GSH also protects

Figure 1.3 Structure of GSH and GSSG

Source: Http://www.sigma-aldrich.com.

GSH

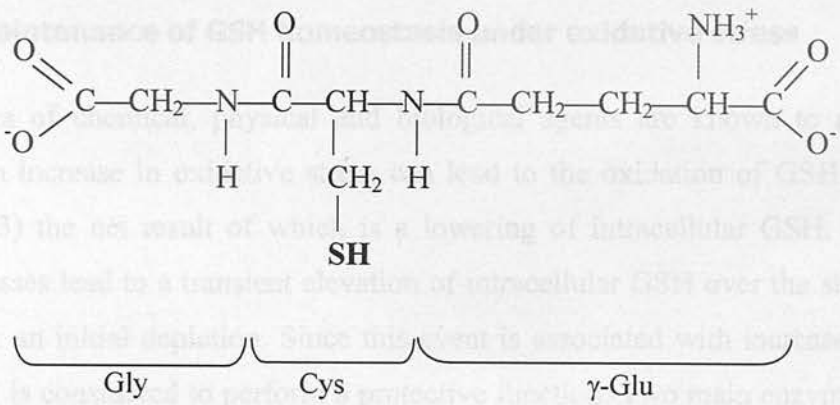

GSSG

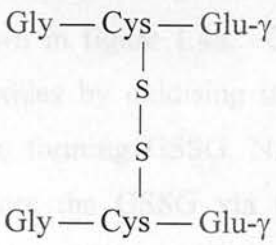

against other toxic insults such as heavy metals, xenobiotics and radiation either through direct conjugation or in enzyme-catalysed reactions as a co-factor for GPx and GST (Rahman et al., 1996; Sagara et al., 1998; Shimizu et al., 1998). Image analysis with the fluorescent compound monochlorobimane, which binds specifically with GSH, has shown GSH is concentrated in the cell nucleus of hepatocytes. This pool of GSH is more resistant to GSH depletion agents and reinforces the hypothesis that GSH is important in guarding against oxidative damage to nuclear components (Bellomo et al., 1992). The physiological role of GSH as an antioxidant has been described in numerous disorders reflecting increased oxidation as a result of abnormal GSH metabolism.

1.3.1 Maintenance of GSH homeostasis under oxidative stress

A plethora of chemical, physical and biological agents are known to alter GSH levels. An increase in oxidative stress can lead to the oxidation of GSH to GSSG (figure 1.3) the net result of which is a lowering of intracellular GSH. However, many stresses lead to a transient elevation of intracellular GSH over the steady-state level after an initial depletion. Since this event is associated with increased cellular survival it is considered to perform a protective function. Two main enzyme systems mediate this elevation and sustain intracellular GSH in its reduced form within normal physiological concentrations. One route is through a recycling of GSSG and the other *de novo* biosynthesis of GSH.

1.3.1.1 Cyclical regeneration

The levels of reduced (GSH) and oxidised glutathione (GSSG) are regulated, in part, by a series of reactions shown in figure 1.4a. GSH can reduce oxidised protein residues, ROS or lipid peroxides by oxidising its own thiol group via the GSH peroxidase-catalysed reaction, forming GSSG. NADPH is the ultimate source of reduced hydrogen and reduces the GSSG via the glutathione reductase (GR)-catalysed reaction, reconstituting GSH. NADPH is re-supplied by a reduction of NADP+ via the pentose phosphate pathway. Under normal conditions the balance of the equation is far in the direction of maintaining cellular glutathione (>90%), however, GSSG can accumulate in situations of rapid GSH oxidation or limited

Figure 1.4 Regeneration and synthesis reactions of GSH

Enzymes catalysing each stage are highlighted in grey. *A*, Cyclical depletion and regeneration of GSH. Glutathione peroxidase uses GSH as a co-factor to convert H_2O_2 to water and oxygen. This reaction and spontaneous ROS scavenging oxidises GSH to GSSG: the substrate for glutathione reductase to reform GSH. The hydrogen ion used for this reaction is abstracted from NADPH, in turn maintained by conversion of G-6-P (glucose-6-phosphate) to 6-P (6-phosphoglucono-lactone) via the pentose phopsphate shunt (Deneke et el., 1989). *B*, *De novo* biosynthesis of GSH from its constituent amino acids. The two sequential reactions are catalysed by gamma-glutamylcysteine synthetase (γGCS) and glutathione reductase (GR).

A

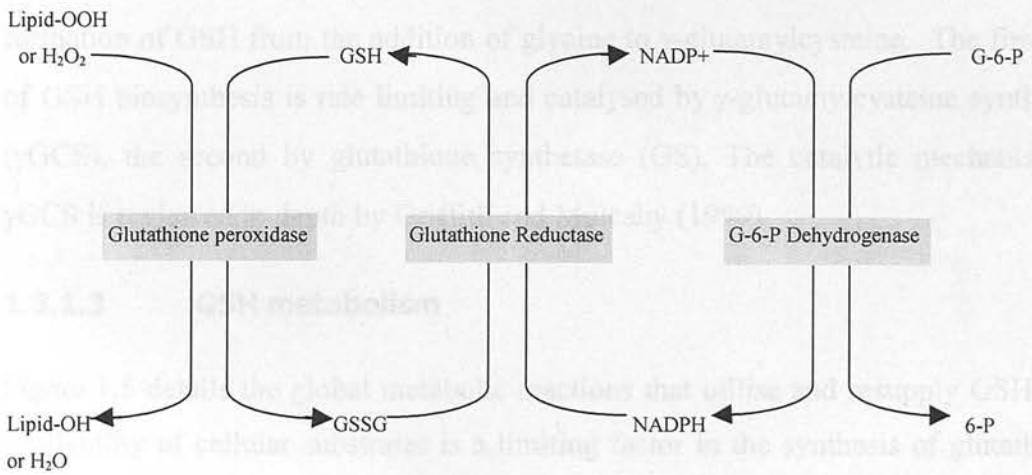

B

1 GLUTAMIC ACID + CYSTEINE —— γGCS ——→ γ -GLUTAMYLCYSTEINE

2 γ-GLUTAMYLCYSTEINE + GLYCINE —— GS ——→ GLUTATHIONE

NADPH availability. GSSG generated has several possible fates, namely intracellular regeneration back to GSH or ATP-dependent exportation from the cells. If not removed by regeneration or efflux, GSSG may react with protein sulfhydryls according to the following reaction (Thomas and Sies, 1991):

$$GSSG + Protein\text{-}SH \rightleftharpoons Protein\text{-}S\text{-}SG + GSH.$$

Formation of protein-GSH mixed disulfides (PrSSG), though reversible, is thought to impair protein function (Bannai, 1984; Rahman et al., 1995).

1.3.1.2 *de novo* biosynthesis

The second mechanism to maintain GSH homeostasis involves endogenous synthesis of GSH from its three constituent amino acids, shown in figure 1.4b. The production of GSH involves two ATP-dependent and Mg^{2+}-sensitive enzymatic reactions: the formation of γ-glutamylcysteine from addition of glutamate to cysteine and formation of GSH from the addition of glycine to γ-glutamylcysteine. The first step of GSH biosynthesis is rate limiting and catalysed by γ-glutamylcysteine synthetase (γGCS), the second by glutathione synthetase (GS). The catalytic mechanism of γGCS is reviewed in depth by Griffith and Mulcahy (1999).

1.3.1.3 GSH metabolism

Figure 1.5 details the global metabolic reactions that utilise and resupply GSH. The availability of cellular substrates is a limiting factor in the synthesis of glutathione. Although a few epithelial cell lines can uptake intact GSH directly from plasma, most cell types rely on importing the constituent amino acids of GSH prior to intracellular synthesis. This occurs by direct transport into cells. Cysteine is the most limiting substrate, is present in very low concentrations in plasma and is imported by multiple transport systems (Bannai, 1984; Deneke and Fanburg, 1989). However, the oxidising environment of plasma favours the oxidised form of cysteine, termed cystine. Cystine is imported predominantly through the X^-c transport system, whereupon the reduction reforms cysteine and generates an intracellular equilibrium. Another route for cells to obtain the substrates for GSH synthesis is via the

Figure 1.5 Global metabolism of glutathione

Pathways catalysed by enzymes are indicated by a yellow circle. Letters refer to the following enzymes: (A) γ-glutamyl transpeptidase; (B) γ-glutamyl cyclotransferase; (C) oxoprolinase; (D) γ-glutamylcysteine synthetase; (E) glutathione synthetase; (F) glutathione peroxidase; (G) glutathione S-transferase; (H) glutathione reductase; (I) dipeptidase and (K) X^-c transporter. Red circles correspond to spontaneous pathways: (*1*) scavenging free ROS. Excess GSSG is either transported from the cell or reacts with reduced sulphydryl groups of cellular proteins to generate PrSSG (*2*). PrSSG not reduced by GSH is targeted for degradation (adapted from Griffith et al., 1999, and Deneke et al., 1989).

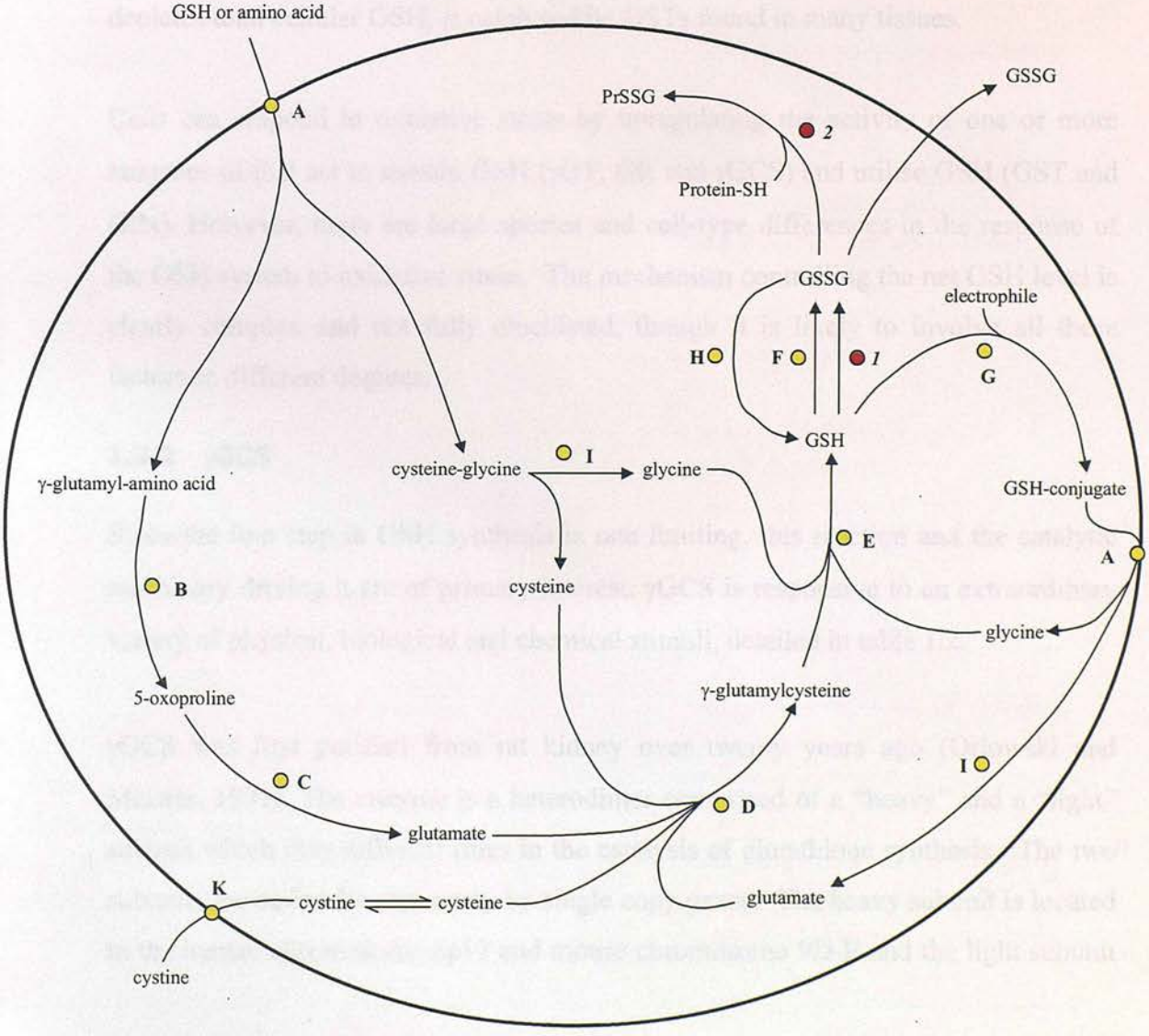

breakdown of circulating GSH. Liver is the main source of plasma GSH and its half-life is less than two minutes (Morris and Bernard, 1994). γ-glutamyl transpeptidase (γ-GT) is a transmembrane enzyme which transfers the γ-glutamyl moiety from extracellular GSH to an amino acid, which is then imported into the cell. If resulting the dipeptide is γ-glutamylcysteine, it could be utilised directly for GSH synthesis in reaction E. Other γ-glutamyl-amino acid complexes can be converted by γ-glutamylcyclotransferase to glutamate by reactions B and C.

GSH interacts non-enzymatically with free ROS or as a co-factor in GPx-catalysed hydrolysis of H_2O_2. GSH is also utilised via the GSH transferase reaction (GST). GSH is a strong nucleophile (a molecule containing an extra electron in its outer orbit), and conjugation of GSH with a large number of unstable foreign compounds with electrophilic (electron deficient) centres stabilises them. This reaction, which depletes total cellular GSH, is catalysed by GSTs found in many tissues.

Cells can respond to oxidative stress by upregulating the activity of one or more enzymes of that act to sustain GSH (γGT, GR and γGCS) and utilise GSH (GST and GPx). However, there are large species and cell-type differences in the response of the GSH system to oxidative stress. The mechanism controlling the net GSH level is clearly complex and not fully elucidated, though it is likely to involve all these factors in different degrees.

1.3.2 γGCS

Since the first step in GSH synthesis is rate limiting, this reaction and the catalytic machinery driving it are of primary interest. γGCS is responsive to an extraordinary variety of physical, biological and chemical stimuli, detailed in table 1.2.

γGCS was first purified from rat kidney over twenty years ago (Orlowski and Meister, 1971). The enzyme is a heterodimer comprised of a "heavy" and a "light" subunit which play different roles in the catalysis of glutathione synthesis. The two subunits are coded for separately by single copy genes. The heavy subunit is located in the human chromosome 6p12 and mouse chromosome 9D-E and the light subunit

Table 1.2 Stimuli known to modulate γGCS and GSH levels

Abbreviations: H_2O_2 (hydrogen peroxide); LDL (low density lipoprotein); CSC (cigarette smoke condensate); MQ (menadione); DMNQ (dimethoxy naphthoqunione); tBHQ (*tert*-butylhydroqunione); ACNU (aminomethylpyrimidinyl-methylchloroethyl nitrosourea); TNF-α (tumour necrosis factor); IL-1 (interlukin-1); TGF-β (transforming growth factor); BHT (butylated hydroxytoluene); BSO (buthionine sulphoximine); DEM (diethyl maleate) and NO (nitric oxide). * This information refers to the levels of GSH during the response phase (post any initial GSH depletion), except the GSH-depleting factors BSO, DEM and dexamethasome, which refer to the time at which those agents were withdrawn from cells.

Stimuli	Effect on GSH levels *	Effect on γGCS levels	References
Physical shock			
ionizing radiation	↑	↑	(Morales et al., 1998; Iwanaga et al., 1998)
γ-irradiation	↑	↑	(Kojima et al., 1998a; Kojima et al., 1998b)
Pro-ROS and alkylating agents			
H_2O_2	↑	↑	(Rahman et al., 1996)
LDL	↑	↑	(Cho et al., 1999)
CSC	↑	↑	(Rahman et al., 1998; Rahman et al., 1996)
MQ	↑	↑	(Shi et al., 1994; Rahman et al., 1998)
DMNQ	↑	↑	(Shi et al., 1994b; Shi et al., 1994a)
tBHQ	↑	↑	(Galloway et al., 1997)
ACNU	↑	↑	(Gomi et al., 1997b)
cytokines			
TNF-α	↑	↑	(Urata et al., 1996; Morales et al., 1997a)
IL-1	↑	↑	(Urata et al., 1996)
TGF-β	↓	↓	(Arsalane et al., 1997)
hormones			
Insulin	↑	↑	(Cai et al., 1995)
hydrocortisone	↑	↑	(Cai et al., 1995)
antioxidants			
BHT	↑	↑	(Borroz et al., 1994; Tu and Anders, 1998c)
Glutamine analogues			
BSO	↓	↑	(Aliosman et al., 1996; Tanaka et al., 1998)
GSH conjugating agents			
Dexamethasone	↓	↓	(Rahman et al., 1998; Rahman et al., 1999)
DEM	↓	↑	(Kitteringham et al., 2000)
NO	↑	↑	(Moellering et al., 1998; Moellering et al., 1999)

gene in human chromosome 1p21-p22 and mouse chromosome 3H1-3 (Tsuchiya et al., 1995; Walsh et al., 1996). The heavy subunit, γGCSh, has a molecular weight of 73 kDa. Data on the macromolecular structure is limited, although it is known the heavy subunit contains the sites for catalysis which harbour a vital sulfhydryl moiety (Simondsen and Meister, 1986; Tu and Anders, 1998b; Tu and Anders, 1998a). The recent discovery of sequence homology between γGCS and GS led to the identification of two candidate γGCS metal biding sites, each chelated by three amino acids (Abbott et al., 2001). Replacement of these residues by site-directed mutagenesis indeed lead to a large reduction in γGCS catalytic efficiency, confirming a critical role in the γGCSh active site. Furthermore, mutation of ligands individually suggests one site is involved in binding glutamic acid and stabilisation of its transition state, while the other is responsible for binding and orienting MgATP (Abbott et al., 2001).

The human light subunit, γGCSl, migrates at 31 kDa (Gipp et al., 1995). Alignments between light subunit cDNA and amino acid sequences from rat, human and mouse reveal extensive homology among these species. Mouse cDNA shares 95% (rat) and 91% (human) identity, while mouse amino acid sequence is 99% and 96% similar to rat and human sequences, respectively (Reid et al., 1997). However, there are species differences. For example, rat kidney and *E. coli* γGCS have very similar Km, turnover and specificity, but *E. coli* GCS is composed of a single polypeptide (Huang et al., 1993b).

1.3.2.1 Regulation of holoenzyme activity

The activity of γGCS is regulated at multiple levels. In 1975 it was shown that GSH inhibited rat γGCS in a competitive fashion with glutamate (Richman et al., 1975). Later experiments with GSH analogues such as ophthalmic acid suggest that this is mediated via the GSH glutamyl moiety while, for optimal inhibition, the GSH thiol group interacts with the enzyme at a site distinct from the glutamate binding domain, reviewed in Griffith and Mulcahy (1999). These studies lend support for the concept that feed back inhibition of γGCS occurs by an excess of GSH. This theory certainly fits with a transient decrease in GSH often observed prior to an increase.

Another fundamental level of regulation is the generation of the holoenzyme. While the heavy subunit contains all the substrate binding and catalysis sites, it is now widely accepted that the light chain exerts an important regulatory function on the catalytic activity of the heavy chain, in two ways. First, the recombinant holoenzyme and isolated holoenzyme show similar Km values for γGCS substrates, whereas the heavy subunit alone shows a markedly increased Km value for glutamate (table 1.3). Hence formation of the holoezyme is held to elevate catalytic activity. Second, association of the subunits raises the apparent K*i* for GSH. Such is this effect Huang *et al* argue that, under physiological conditions, the catalytic activity of the heavy chain alone is effectively zero due to binding GSH (Huang et al., 1993b; Huang et al., 1993a). In these respects, the ratio of the heavy: light subunit represents an important level of control in the overall GSH-synthetic capability of a cell.

In addition to the feedback loop and generation of the holoenzyme, it is possible the enzyme is controlled by the reversible formation of redox-sensitive disulphide bonds between cysteine residues (Ochi, 1995; Tu and Anders, 1998b; Soltaninassab et al., 2000). In 1993 Huang et al. proposed that intersubunit di-sulphide bridge formation produces a steric alteration that increases the affinity between glutamate and the binding site (Huang et al., 1993b). In this model, γGCS "senses" oxidative stress and "reacts" to increase GSH synthesis. However, anomalies that are inconsistent with this model should be noted. In particular, inhibition of γGCS by the GSH analogue ophthalmic acid occurs via a non-competitive route. Further, the K*i* value measuring γGCS inhibition is 1.8 mM for GSH, whilst ophthalmic acid is 12.5 mM. Such conspicuously distinct properties between these related compounds suggests regulation may not be a simple as previously imagined. Nevertheless, a similar system of control has become apparent in the regulation of tyrosine phosphatases, receptor tyrosine kinases, NF-κB (see section 1.3.5), GSTs, thioredoxin and PKC (Bauskin et al., 1991; Knebel et al., 1996; Gopalakrishna et al., 1997a; Denu and Tanner, 1998). For example, under oxidative conditions, disulphide bridge formation in an autoinhibitory domain of PKC is associated with enhanced activity, whereas antioxidant activity upon catalytic cysteine residues correlates with depressed activity (Gopalakrishna et al., 1997b; Gopalakrishna and Jaken, 2000). Huang and

Table 1.3 Comparative affinity of substrates and GSH for γGCSh and holoenzyme

All kinetic values are expressed as mM. Data derived from rat (Huang et al., 1993; Tu and Anders, 1998).

Enzyme status	Km L-Glu	Km L-Cys	Ki GSH
γGCS holoenzyme	~1.6	0.2	8.2
γGCSh alone	~18	0.2	1.8

Figure 1.6 Proposed redox structures of the γGCS holoenzyme

Scheme to account for the reversible regulation of γGCS holoenzyme activity, by the redox environment of the cell. Blue indicates γGCSh; green γGCSl. γGCS contains 20 protein sulfhydryl groups (SH). Under conditions of GSH depletion, at least one intra- and one inter-disulphide bridge (S-S) form. This correlates with an optimal affinity between glutamate (Glu) and its binding site, possibly via alteration of γGCS tertiary conformation. Upon re-establishing physiological concentrations of GSH, S-S linkages are reduced back to individual SH groups. Text and figure based on propositions and data of (Huang et al., 1993; Tu and Anders, 1998; Soltaninassab et al., 2000).

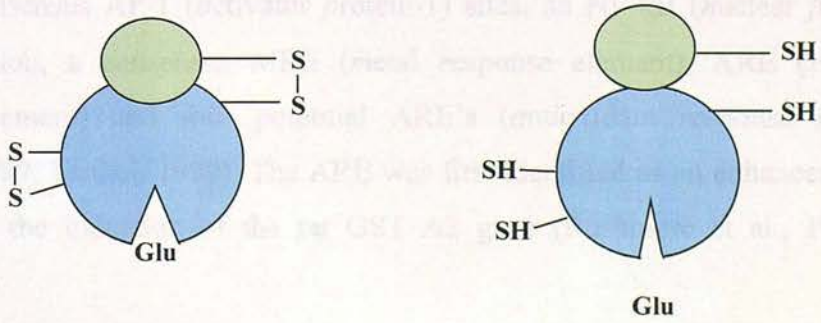

colleagues' proposal, modified in light of recent data, is outlined in figure 1.6.

In addition to disuphide regulation, the activity of γGCS may be under phosphorylation control. Three serine-threonine residues in the heavy subunit are subject to reversible phosphorylation by protein kinase (PK-A), protein kinase (PK-C) Ca^{2+}/Calmodulin-dependent kinase *in vivo* (Sun et al., 1996) and the enzyme can autophosphorylate (Sekhar and Freeman, 1999). The degree of phosphorylation correlated with loss of γGCS activity without altering gross structure of the holoenzyme, so inactivation occurs by unidentified mechanism. Treatment with agonists of signal transduction pathways, such as cAMP (*c*yclo *a*denosine *m*ono*p*hosphate), significantly increased the phosphorylation suggesting a tentative physiological role where phosphorylation status may regulate GCS activity (Sun et al., 1996). However, PKC activation in a neuronal cell line prevents, rather thanenhances oxidative-induced cytotoxicity (Davis and Maher, 1994), and others show many oxidative-stress inducing agents do not activate PKC (Devary et al., 1992). Clearly, further work is needed to confirm whether this potential mechanism of mammalian regulation is relevant *in vivo*.

1.3.2.2 Transcriptional regulation

γGCSh and *γGCSl* can be induced by a striking variety of external stumuli, though the majority of studies have tended to focus upon *γGCSh* regulation. Detail of *cis*-acting componentry helped to identify putative *trans*-acting factors that execute expression.

Sequencing the human γGCSh 5' regulatory region (-3802 to +547) has revealed multiple promoter motifs and transcription start sites, the former shown in figure 1.7. In addition to a variety of standard regulatory motifs, the γGCSh upstream sequence contains consensus AP-1 (*a*ctivator *p*rotein-1) sites, an NF-κB (*n*uclear *f*actor-*κB*) binding region, a consensus MRE (*m*etal *r*esponse *e*lement), XRE (*x*enobiotic *r*esponse *e*lement) and four potential ARE's (*a*ntioxidant *r*esponse *e*lements) (Griffith, 1999; Tsuboi, 1999). The ARE was first identified as an enhancer element involved in the induction of the rat GST A2 gene (Rushmore et al., 1991) and

Figure 1.7 Potential transcription control elements in *γGCSh*

Schematic map of 5' flanking region of human *γGCSh* gene (orange) showing some identified nuclear protein binding sites and transcription start site (bent arrow). Numbers indicate distance from ATG in bp. Sequences thought to play vital roles in *γGCSh* transcription are highlighted in red.

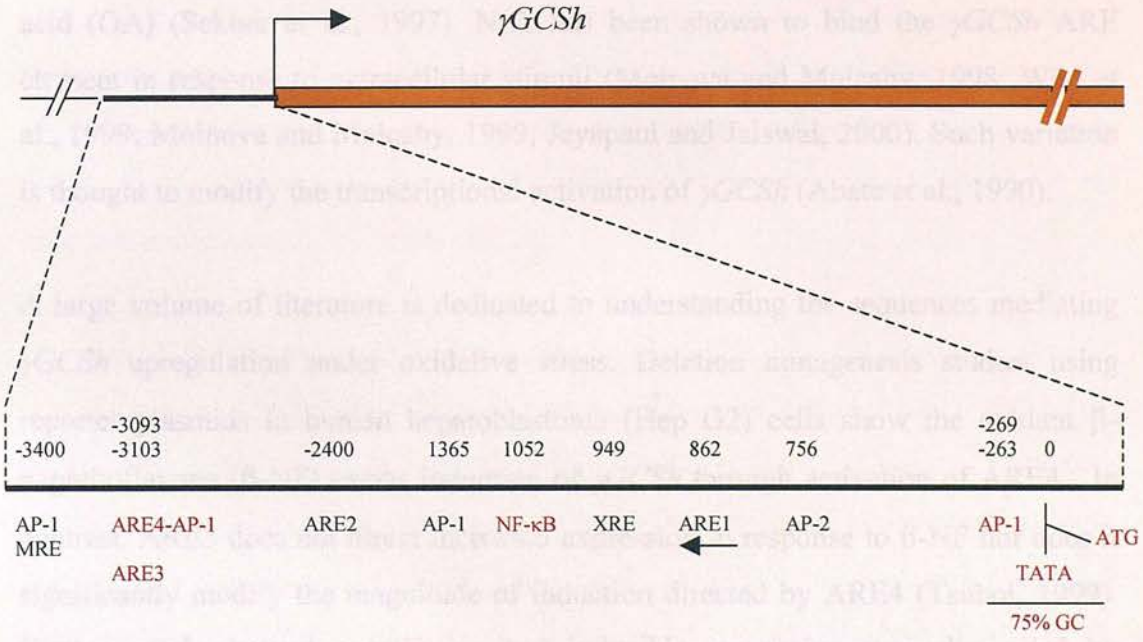

consists of a core sequence 5'-RTGACnnnGC-3' that can contain an internal AP-1 and/or an adjacent AP-1 motif. An AP-1-like sequence is located adjacent to the *γGCSh* ARE4 sequence, and is thought to regulate *γGCSh* similar fashion to others detected in the promoter region of several P450 phase II and antioxidant enzymes (Li and Jaiswal, 1994; Mulcahy and Gipp, 1995; Xie et al., 1995).

The AP-1 transcription factor is a dimeric complex, usually composed of Fos and Jun proteins, though other transcription factors, including Fra, Maf, Nrf1 and Nrf2 may form heterogeneous complexes with Jun proteins. Induction of mRNA for the components of AP-1 (c-fos and c-jun) has been described in cells exposed to CSC (Muller, 1995; Rahman et al., 1996). AP-1 indeed mediates, at least in part, *γGCSh* upregulation induced by cadmium (Wu and Moye-Rowley, 1994), cisplatin (Yao et al., 1995), phenolic antioxidants (Choi, 1993) and phosphatase inhibitor, okadaic acid (OA) (Sekhar et al., 1997). Nrf2 has been shown to bind the *γGCSh* ARE element in response to extracellular stimuli (Moinova and Mulcahy, 1998; Wild et al., 1999; Moinova and Mulcahy, 1999; Jeyapaul and Jaiswal, 2000). Such variation is thought to modify the transcriptional activation of *γGCSh* (Abate et al., 1990).

A large volume of literature is dedicated to understanding the sequences mediating *γGCSh* upregulation under oxidative stress. Deletion mutagenesis studies using reporter plasmids in human hepatoblastoma (Hep G2) cells show the oxidant β-naphthoflavone (β-NF) exerts induction of *γGCSh* through activation of ARE4. In contrast, ARE3 does not direct increased expression in response to β-NF nor does it significantly modify the magnitude of induction directed by ARE4 (Tsuboi, 1999). Further work showed constitutive and inducible expression was eliminated by introduction of a single base mutation in the either the ARE4 core sequence (Mulcahy et al., 1997) or terminal GC box (Wild et al., 1998). This contrasts with the dependency of γ-irradiation-induced upregulation of *γGCSh* by NF-κB in the malignant glioblastoma cell line T98G. Moreover, the GC-rich fragment –108 to +91 (containing only housekeeping promoter elements) is sufficient for cisplatin-induced *γGCSh* upregulation in lung cancer SBC-3 (Tomonari et al., 1997b). Heterogeneity in *cis*-acting factors employed for *γGCSh* induction suggests multiple

signalling pathways may operate to elicit a GSH-mediated response to diverse sources of stress.

Deletion and binding studies have also revealed that the constitutive expression of the human heavy subunit gene is mediated by the TATA box-containing fragment –202 to +22, and both distal ARE3 and ARE4 sequences at –3093 to –3103 in Hep G2 cells (Tomonari et al., 1997a). Full basal expression also requires the embedded AP-1 site be intact (Wild et al., 1998). As in inducible expression, AREs are not a ubiquitous requirement for constitutive expression of the *γGCSh* gene. COS7 cells require only a proximal –108 to –28 GC-rich region (containing multiple promoter elements but lacking any AP-1 consensus) for basal transcription (Tomonari et al., 1997a), although the –269 to –263 AP-1 site also has a marginal positive regulatory effect, whereas the critical site in lung epithelial cells is the same –269 to –263 AP-1 motif (Rahman et al., 1998). The biological importance of such heterogeneous sequences controlling basal transcription is also unclear. It is possible that exposure of particular tissues to high levels of oxidative stress, such as liver and lung, may require local variations in the strength of basal expression may account for the differences in promoter elements utilised.

In addition to these elements driving expression, *γGCSh* contains a putative silencer region containing NF-1 sites (Imagawa et al., 1991; Osada et al., 1997). Interaction of the NF-1 transcription factor with similar motifs in the GST-P gene suppresses transcription. Whether this system is functional in the γGCS genes remains to be resolved. Of note however, NF-1 - like γGCS, contains redox-sensitive cysteine residues which modulate its activity (Novak et al., 1992; Bandyopadhyay et al., 1998).

Analysis by Galloway *et al* and Moinova *et al* revealed many potential promoter elements in the human light subunit promoter region, shown in figure 1.8 (Galloway et al., 1997; Moinova and Mulcahy, 1998). *γGCSl* can also be repressed by transforming growth factor (TGFβ) (Arsalane et al., 1997). Moinova *et al.*, 1998, investigating 3.3Kb of known upstream sequence in HepG2 cells, demonstrated a

Figure 1.8 Potential transcription control elements in *γGCSl*

Schematic map of 5' flanking region of human *γGCSl* gene showing identified nuclear protein binding sites (not to scale). The area covered indicates the total area analysed to date, numbers indicate approximate distance from ATG in bp. Sequences thought to play vital roles in *γGCSl* transcription are highlighted in red.

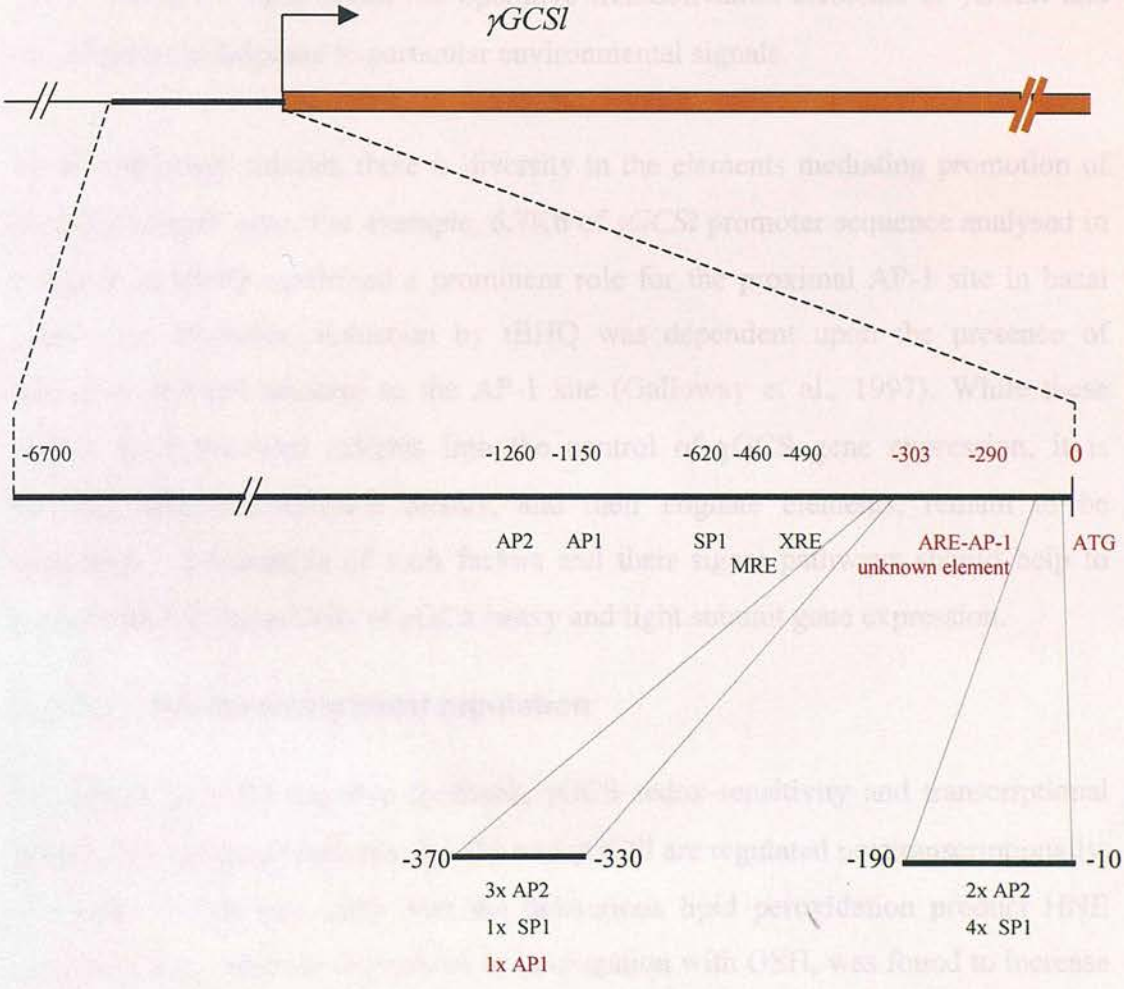

fragment only –344 to –242bp 5' of the transcription initiation start site is required for constitutive and β-NF induced expression. This DNA contains a consensus ARE with internal AP-1 site and an adjacent AP-1 site. Subtle deletion studies demonstrate the adjacent AP-1 site alone is capable of driving full basal *γGCSl* transcription in HepG2 cells, and contributes to and β-NF induction. However, removal of both ARE and adjacent AP-1 is necessary to eliminate *γGCSl* upregulation (the embedded AP-1 motif performs no function here). Cloned ARE, isolated from native promoter sequence, is sufficient to drive β-NF-mediated *γGCSl* induction, so represents the dominant enhancer element (Moinova and Mulcahy, 1998). Table 1.4 summarises the operative transactivation elements of *γGCSh* and *γGCSl* genes in response to particular environmental signals.

As for the heavy subunit, there is diversity in the elements mediating promotion of the light subunit gene. For example, 6.7Kb of *γGCSl* promoter sequence analysed in response to tBHQ confirmed a prominent role for the proximal AP-1 site in basal expression. However, induction by tBHQ was dependent upon the presence of unknown element adjacent to the AP-1 site (Galloway et al., 1997). While these studies have provided insights into the control of γGCS gene expression, it is possible other transcription factors, and their cognate elements, remain to be identified. Elucidation of such factors and their signal pathways should help to unravel the full complexity of γGCS heavy and light subunit gene expression.

1.3.2.3 Posttranscriptional regulation

In addition to GSH negative feedback, γGCS redox-sensitivity and transcriptional control of constituent subunits, γGCSh and γGCSl are regulated posttranscriptionally. Incubation of rat lung cells with the deleterious lipid peroxidation product HNE (section 1.1.2), which is neutralised by conjugation with GSH, was found to increase the half-life of *γGCSh* mRNA (Liu et al., 1998). Similarly human glioma cells exposed to a pro-oxidant induced *γGCSh* via an increase in message stability (Gomi et al., 1997) and, interestingly, the presence of ROS also initiates the stabilisation of

References for Table 1.4

(1) (Mulcahy et al., 1997; Wild et al., 1998)

(2) (Sekhar et al., 1997)

(3) (Morales et al., 1998)

(4) (Morales et al., 1997b)

(5) (Tomonari et al., 1997)

(6) (Rahman et al., 1996)

(7) (Rahman et al., 1998)

(8) (Cho et al., 1999)

(9) (Rahman et al., 1999)

(10) (Morales et al., 1997a)

(11) (Cai et al., 1997)

(12) (Kitteringham et al., 2000)

(13) (Urata et al., 1999)

(14) (Urata et al., 1996)

(15) (Iwanaga et al., 1998)

(16) (Moinova and Mulcahy, 1998)

(17) (Galloway and McLellan, 1998)

Table 1.4 Comparison of promoter elements controlling induced and constitutive *γGCSh* and *γGCSl* transcription

γGCSh expression

INDUCED			CONSTITUTIVE	
Stimuli	*Promoter element*	*Cell type & Ref. No.*	*Promoter*	*Cell Type & Ref.No.*
β-NF	ARE4/ AP-1	HepG2 (1)	ARE4 and TATA	HepG2 (1)
OA (H_2O_2)	AP-1	HepG2 (2)	AP-1	A549 (7)
γ irradiation	AP-1	HepG2 (3)	Proximal GC-rich	COS 7 (5)
TNF-α	AP-1	HepG2 (4)		
Cisplatin	AP-1	Lung tunour SBC3 (5)		
CSC	AP-1	A549 (6)		
MQ/ H_2O_2	AP-1	A549 (7)		
LDL	AP-1	Endothelial: Human vascular (8)		
Melatonin	AP-1	Endothelial: Human vascular (13)		
DEM	AP-1	Mouse liver (12)		
TNF-α	AP-1	A549 (9)		
TNF-α	AP-1/MRE	Rat hepatocytes (10)		
Insulin	not NF-kB	Rat hepatocytes (11)		
tHBQ	NF-kB	Rat hepatocytes (11)		
DEM	NF-kB	Mouse liver (12)		
TNF-α/ IL-β	NF-kB	Endothelial: Mouse glycemic (14)		
Ionizing radiation	NF-kB	Glioblastoma: Human, T98G (15)		

γGCSl expression

INDUCED			CONSTITUTIVE	
Stimuli	*Promoter element*	*Cell type & Ref. No.*	*Promoter*	*Cell Type & Ref.No.*
β-NF	ARE-AP-1	HepG2 (16)	AP-1	HepG2 (17)
tBHQ	unknown element	HepG2 (17)		

a GST transcript (Chen et al., 1995; Ming et al., 1998). However, the mechanism mediating these increases in message stability is presently unclear.

1.3.3 Co-ordination of *γGCSh* with other genes

Cells co-ordinate *γGCSh* expression with other proteins under particular conditions. *γGCSl* is one obvious and important candidate. Comparison of the light with the heavy chain promoter region has revealed several common putative enhancer elements: ARE, XRE, AP-1 and AP-1-like sites, each of which could initiate γGCS transcription in response to chemical and oxidative stress (Galloway et al., 1997). Clearly, it is conceivable that common *cis*-acting sequences between light and heavy subunit promoters co-ordinates expression to maximise holoenzyme formation. However, northern analysis of *γGCSh* and *γGCSl* in multiple tissues indicates this is not always the case (Gipp et al., 1995). Indeed, many stimuli increase only the heavy subunit, while others do advance a dual response. Thus the two genes can be subject to co-ordinate or independent regulation. In addition to *γGCSl*, GSH-cycle components, the transmembrane MRP (*m*ultidrug *r*esistance *p*rotein) and detoxification enzymes such as SOD and catalase are documented examples (table 1.5).

Constitutive upregulation of γGCS activity has been previously noted in many drug-resistant tumour cell lines. The relevance of this to carcinogenesis has been attributed to a protective effect either mediated by an enhanced detoxification capacity or resistance to cell death, reviewed by (Hall, 1999). Since GSTs are dependent on GSH as a co-factor, it is perhaps not surprising that γGCS is jointly upregulated with GSTs in cisplatin-resistant bladder cancer cells (Kotoh et al., 1997). Indeed, a variety of transformed cell lines (Ishikawa et al., 1996; Kuo et al., 1996) and normal mouse tissue (Kuo et al., 1998) co-ordinate transcriptional upregulation of *γGCSh* with MRP. Individual stimuli upregulate a pattern of enzymes from a bank of detoxification genes, the permanent over-expression of which may confer a survival advantage.

Table 1.5 Co-ordination of γGCSh with GSH-metabolism and antioxidant enzymes

Summary of a representative cross-section of literature regarding the co-expression of γGCSh with related GSH factors and antioxidants. Abbreviations: TRX (thioredoxin) and CTX (catalase). For other compounds, refer to table 1.3.

Cell type	Conditions	Increased activity /transcription	Decreased activity /transcription	References
Hep G2	tBHQ	γGCSl	-	(Galloway et al., 1997)
Hep G2	β-NF	γGCSl	-	(Wild et al., 1999)
Hep G2	PDTC	γGCSl	-	(Wild et al., 1999)
Rat lung L2	DMNQ	γGCSl	-	(Li et al., 1996)
Rat retinal rMC-1	tBHQ	γGCSl	-	(Lu et al., 1999)
Rat fibroblasts	Ionizing radiation	γGT	-	(Sierra-Rivera et al., 1994)
Mouse liver	γ-rays	GPx, GR, TRX	-	(Kojima et al., 1998a)
Human lung	Heavy metals	MRP	-	(Ishikawa et al., 1996)
Mouse Nerve HT-22	Glutamate-resistant	GR, GST, CTX GST	-	(Sagara et al., 1998)
Bladder cancer	Cisplatin-resistant	GST	-	(Kotoh et al., 1997)
Mouse liver	CCl4	GPx, GR	-	(Kojima et al., 1998b)
Leukaemia	Cisplatin	MRP	-	(Ishikawa et al., 1996)
Colorectal cancer	none	γGCSl, MRP	-	(Kuo et al., 1996)
172 Glioblastoma	ACNU	MRP	-	(Gomi et al., 1997)
Hep G2	DEM	γGCSl	-	(Sekhar et al., 1997)
Lung carcinoma, A549	TGF-β	-	GR, CTX	(Arsalane et al., 1997)
Rat lung, freshly isolated	BSO	-	GPx, CTX, SOD, ascorbic acid, a-tocopherol	(Thanislass et al., 1995)
Lung carcinoma, A549	Dexamethasone	-	γGT	(Rahman et al., 1998)

1.3.4 ROS and GSH in gene activation and cell cycling

GSH is thought to be intimately involved in the regulation of stress-induced gene expression. Shifts in the intracellular redox potential, largely initiated by excess production of ROS, are increasingly correlated with a change in the activity of signal transduction and transcription components (Choi, 1993; Yao et al., 1995; Rahman et al., 1996; Sekhar et al., 1997; Arsalane et al., 1997). GSH, by its capacity to scavenge ROS and regulate the redox status of cellular proteins, was therefore proposed to regulate the activity of such redox-sensitive factors (Gipp et al., 1995).

One response of mammalian cells to diverse chemical and physical agents is the activation of a global regulon known as the UV or stress response. To date, all stimuli that elicit the stress response share in common the ability to alter the balance of the intracellular redox potential, reviewed in Adler *et al.*, 1999. The response includes activation of a battery of genes involved in repair and ROS scavenging that include, amongst others, genes regulating GSH metabolism. This transactivation is dependent, at least in part, on the transcription factors AP-1 and NF-κB. NF-κB normally resides in the cytosol as an inactive dimer bound to the inhibitory subunit I-κB. Activation requires phosphorylation of I-κB to dissociate the NF-κB:I-κB complex. Devary *et al.*, 1993, showed NF-κB activation, when by stimulated by UV, depends upon a redox-sensitive tyrosine kinase to recognise and to initiate transduction of the stress signal. Indeed, oxidative stress induced by H_2O_2, diamide and IL-1 has also been shown to activate tyrosine kinases (Heffetz et al., 1990; Bauskin et al., 1991; Munoz et al., 1992). This is thought to occur via modifications to kinase conformation enforced by the formation of di-sulphide bridges between native sulfhydryl groups. This regulatory mechanism, introduced in section 1.3.2.1, is well characterised for the bacterial transcription factors OxyR and SoxR (Bessette et al., 1999; Gonzalez-Flecha and Demple, 2000; Zheng and Storz, 2000).

ROS also activate NF-κB by inhibiting the activity of tyrosine phosphatases (Knebel et al., 1996). Dephoshorylation enzymes all share a common amino acid motif at the active site. This includes a catalytically important cysteine (Barford et al., 1995), the

reversible oxidation of which is thought to lead to a loss of function (Denu and Tanner, 1998; Herrlich and Bohmer, 2000). A last mode of NF-κB oxidoreductive control is the direct interaction of ROS with NF-κB peptides. This redox sensitivity is also attributed to the reversible oxidation of cysteine residues in NF-κB DNA binding site, an event purported to modulate DNA recognition (Hayashi et al., 1993; Galter et al., 1994).

The antioxidant N-acetylcysteine (NAC), a precursor of GSH, can inhibit tryosine kinase-dependent UV-triggered induction of NF-κB (Devary et al., 1993). GSH depletion has also been implicated in the regulation of stress kinases JNK (c-*J*un *N*-terminal *k*inase), p38 (Wilhelm et al., 1997) and PKC (Gopalakrishna et al., 1997a; Gopalakrishna et al., 1997b). Indeed, a variety of antioxidants can suppress NF-κB activation by a great variety of pathogenic stimuli, including H_2O_2, cytokines, TNF, viruses, double stranded RNA, endotoxins, phorbol esters, UV and ionising radiation (Schreck et al., 1992). That antioxidants can prevent NF-κB activation by a wide repertoire of agents is further evidence that ROS are intracellular messengers that channel disparate stresses into a common cellular response (Schreck et al., 1991).

Reprogramming of stress-response genes by factors that modulate the redox potential can conclude in cellular consequences that include mitotic arrest, cell death and division. Recently, low level oxidation induced by H_2O_2 in human lymphoid cells reversibly activated p38 cascade, an event that directly induced an aberrant cell cycle (Kurata, 2000). This stimulus did not produce NF-κB activation, though different levels of oxidation appears to activate discrete signal transduction pathways and nuclear factors (Su and Karin, 1996). In agreement with this, other oxidants can induce apoptosis or necrosis- depending on the concentration of the oxidant (Dypbukt et al., 1994; Sata et al., 1997; Vayssier et al., 1998), or the level of cellular GSH (Fernandes and Cotter, 1994). In contrast, the presence of other pro-oxidants can induce cell proliferation (Duhe et al., 1998). These effects of ROS on cell behaviour points toward an oxidant-effect dependency on dose, antioxidant status and cell type.

1.3.5 Role of GSH in Development

The blood in the decidua surrounding the early mammalian embryo contains 5% oxygen (New et al., 1976). Low oxygen is necessary for normal development of the neural tube, whereas atmospheric oxygen concentrations (20%) are essential for subsequent development (Akazawa et al., 1994). The levels of GSH and ROS vary in a dramatic and controlled fashion during embryogenesis. The GSH content of mouse oocytes falls by nearly a quarter at fertilisation, nearly by half between the two- and four-cell stages (days 1-2.5) and ten-fold at the stage of the blastocyst (day 4) (Nasr-Esfahani and Johnson, 1992; Gardiner and Reed, 1994; Gardiner and Reed, 1995b).

Several studies have attributed the cause of drug-induced birth defects to oxidative DNA damage (Slott and Hales, 1987; Winn and Wells, 1995; Winn and Wells, 1997; Baek et al., 2000). Indeed, at both the two-cell and blastocyst stages, incubation with the pro-oxidant tBHQ depletes the embryo of GSH and reduces the number of embryos with normal developmental features. The loss of GSH was accounted for by increases in GSSG and PrSSG, indicating that the embryo was undergoing oxidative stress (Gardiner and Reed, 1994). Recently, γGCS was shown to be expressed throughout development to adult tissues (Levonen et al., 2000). However, recovery of basal GSH levels in two-cell embryos is dependent upon cyclical regeneration with GR, although blastocyst recovery is dependent upon a combination of regeneration and *de novo* synthesis (Gardiner and Reed, 1995a).

At day 5 of mouse development, a burst of $O_2^{\bullet -}$ correlates with hatching from the zona pellucida. This is thought to be vital since hatching was successfully induced *in vitro*, without loss of viability, by treatment of embryos with $O_2^{\bullet -}$ (Thomas et al., 1997). At neuralation (9-10 days), embryos remain entirely dependent on anaerobic glycolysis. When efficient oxygen delivery is established on day 11, the TCA cycle begins and mitochondrial morphology matures. In rat embryos exposed to 20% oxygen at day 9-10, prematurely developed mitochondria are visible and ROS production is increased, indicating the initiation of the tricarboxylic acid cycle. This correlated with a subsequent manifestation of an array of embryonic defects,

including stunted growth and a reduction in GSH. Culturing embryos in 2mM GSH reduced H_2O_2 formation, prevented the acquisition of embryonic malformations and restored growth (Ishibashi et al., 1996). Neuralation-stage rat embryos derived from streptozotocin-induced diabetic rats or embryos exposed to hyperglycemic conditions (66.7mM glucose) displayed similar lesions, also reversible by GSH (Trocino et al., 1995; Sakamaki et al., 1999).

In consideration of the total developmental data, it was predicted GSH has a central role in normal embryogenesis and in the embryonic response to oxidative stress. The former proposition was recently verified by the lethal phenotype of *γGCSh* null (*γGCSh*-/-) mice. These mice die at E 8.5, associated with a massive increase in apoptotic cell death in distal regions, suggesting GSH may also be involved in the signal transduction of embryonic remodelling events (Shi et al., 2000). A further study showed (*γGCSh*-/-) embryos die before day 13 post gestation (Dalton et al., 2000). This work also revealed that heterozygotes show an approximate 30% increase in ascorbate levels, showing a role of GSH in modulating alternative antioxidants.

1.4 Apoptosis

The removal of specific cells from the surrounding population is a biologically essential and highly controlled process. The first recognition of it, then termed "necrobiosis", was in 1858 and was described as "a shrinkage being where the cell vanishes and can no longer be seen in its previous form" (Virchow and Chandler, 1859). This was also the first differentiation from necrosis, later shown as a predominantly uncontrolled process of cell death where, after membrane collapse, the cellular content is dispersed into the extracellular mileu. In humans a local discharge of the cellular content causes unfavourable inflammation, though recent work shows necrosis sometimes has important functions in the normal life cycle of lower organisms (Cornillon et al., 1998). Over a century later, ultrastructural detail of the controlled process was revealed by electron microscopy and in 1972 the term apoptosis was coined (Kerr et al., 1972). More recently, an explosion of biochemical and genetic information has led to an appreciation of the mechanisms underlying the

original morphological observations. Apoptosis is a phenomena now observed universally in both the plant and animal kingdoms, and dysfunction of it is recognised as a major contributory factor in many human diseases.

Reflecting the occurrence of its dysregulation in disease, apoptosis is critical in the implementation of many normal physiological processes. In addition to a host of functions throughout development (section 1.4.1), apoptosis is critical for immune system turnover and killing. Apoptosis mediates T- and B-cell removal once their purpose has been served (Miller and Heath, 1993; Russell et al., 1995), whilst cytotoxic T lymphocytes and natural killer can destroy target cells by initiating their apoptosis via CD95 (*s*urface *d*eterminant 95) receptor signalling (Rouvier et al., 1993; Darmon et al., 1995). Other prominent roles include involution of the mammary gland during lactation (Walker et al., 1989; Strange et al., 1992), regression of the adrenal cortex following adrenocorticotrophic hormone withdrawal (Wyllie et al., 1973) and breakdown of the uterine endometrium during the menstrual cycle (Hopwood and Levison, 1976).

The apoptotic process can be broken into four discrete stages, the first of which is receipt of a potentially lethal stimulus. Second, this signal is internalised by binding of external ligands to specific cell receptors and relayed to a checkpoint where, third, the information is "processed" to decide whether to proceed or not. If the decision is to terminate the cell, the final stage is effecting the apoptotic programme.

1.4.1 Apoptosis in development

From the earliest stages, apoptosis has a role in development. For example, ovulated eggs in the mammalian oviduct are destined for apoptosis if unfertilised (Morita and Tilly, 1999). After fertilisation, it is thought embryos that fail to achieve early developmental progression undergo apoptosis by default (Jurisicova et al., 1996; Jurisicova et al., 1998a; Jurisicova et al., 1998b). Later, at the blastocyst stage, apoptosis occurs as a normal part of development (Mohr and Trounson, 1982; Brison and Schultz, 1997), though the function of this is presently unknown.

A study of apoptosis throughout embryogenesis was undertaken in the nematode worm *Caenorhabditis elegans,* revealing the striking control of the process. During development, 131 cells die by apoptosis in a precise temporal fashion, leaving a mature worm of 1090 cells (reviewed in Metzstein et al, 1998). In higher organisms apoptosis is not so defined but appears essential in many developmental processes. For example, apoptosis mediates digit and palette formation by deleting interdigital membrane and midline epithelium, respectively (Pratt and Greene, 1976; Garcia-Martinez et al., 1993; Mori et al., 1994).

1.4.2 Apoptosis in cellular injury

In addition to the role of apoptosis in mediating physiological processes in development and adult life, apoptosis can be vital in the response to pathological stimuli. Apoptosis triggered by physical or chemical insults is not reliant upon cell-surface ligand-receptor binding, though some in systems transmembrane receptors are activated internally (Caricchio et al., 1999; Gonin et al., 1999). The majority of cytotoxic agents enter the cell directly, causing internal damage, which activates the apoptotic pathway in the absence of specific cell-surface receptors. Examples of such agents include heat shock (Thompson, 1995), UV light, γ-irradiation (Corbet et al., 1999), numerous drugs, synthetic peptides (Schwall et al., 1993) and toxins (Sachs and Lotem, 1993).

1.4.3 Biochemical and morphological changes

After commitment to the apoptotic programme, cells complete a repertoire of defined structural changes that are mediated by particular biochemical effectors. A pivotal intracellular event prior to the physical manifestation of apoptosis is an alteration in the function of the mitochondrial membrane. Escalation of mitochondrial activity precedes collapse of the transmembrane potential. This correlates with leakage of mitochondrial cytochrome c, AIF (*a*poptosis-*i*nducing *f*actor), calcium ions and a cellular depletion of ATP (Fernandez-Checa et al., 1997). This is probably mediated by opening of the mitochondrial transmembrane megachannel PT (*p*ermeability *t*ransition) pore (Kroemer et al., 1995; Zamzami et al., 1995; Zamzami et al., 1996), which allows free passage of solutes <1500 Da (Zoratti and Szabo, 1995). In

agreement with this, inhibition of the PT pore prevents apoptotic activation (Kroemer et al., 1997; Kroemer, 1997). Loss of mitochondrial membrane integrity is an event widely accepted to have critical and irreversible downstream effects on the process of cell death.

Morphologically, an apoptotic cell initially retreats from neighbouring cells and an involution of the plasma membrane, termed blebbing, occurs. Next, chromatin condense and migrate towards the nuclear envelope. This is usually associated with disintegration of nuclear DNA into 50-300kb fragments by the action of specific endonucleases (Bustamante et al., 1997). Finally, the plasma membrane begins to bud off to form a cluster of cytoplasmic apoptotic bodies that encapsulate degenerated organelles. This event parallels an increase in transglutaminase activity, which cross-links adjacent cytoplasmic proteins (Piacentini et al., 1992). Remarkably, the entire process of apoptosis is completed within a few hours (Kerr, 1971; Wyllie et al., 1980; Allen, 1987; Lazebnik et al., 1993).

An important phase of apoptosis not formally included in the morphological definition is the ensuing phagocytosis of apoptotic bodies. Apoptotic cells, if not consumed by surrounding cells or the immune system, can eventually assume necrotic morphology *in vivo* (Dong et al., 1997). In agreement with this, apoptosis can be triggered by low concentrations of a pro-oxidant, whilst the same compound at higher concentrations causes necrosis (Sata et al., 1997) (and expanded in section 5.8.3). In consideration of this and other data, it is argued there is more crossover between apoptosis and necrosis than previously imagined (reviewed in Kroemer et al, 1997).

1.4.4 Genetic regulation of apoptosis

Each cell of the *C. elegans* that dies by apoptosis during development does so under the command of genetically pre-determined programme. Investigation of this pathway has lead to the identification of a host of factors that encode the apoptotic machinery. Because the process of apoptosis appears highly conserved between

disparate cell types (Frade and Michaelidis, 1997), mammalian homologs of many of these and other factors have been isolated, summarised in table 1.6.

The first family to be characterised was the Caspases, a group currently comprising 13 individual members. These encode cysteine proteinases that differ in size and substrate specificity though appear essential effectors of the apoptotic cascade. Activated caspases execute apoptosis by cleaving factors involved in cellular homeostasis, repair and the maintenance of cell structure (reviewed in Wolf et al, 1999). By forming a signalling cascade that activates transcription factors caspases are also thought to play a role in the initiation of apoptosis (Hofmann et al., 1997; Buckley et al., 1999).

The Bcl-2 superfamily represents a critical apoptosis-regulating family, encoding proteins that promote or suppress cell survival. Bcl-2 forms heterodimers with other bcl-2 superfamily members, including Bax (Oltvai et al., 1993), Bcl-xl, Bcl-xs (Boise et al., 1993), Bad (Yang et al., 1995) and Bak (Chittenden et al., 1995), which differ in their structure and pattern of expression. This heterodimer acts as an inhibitor or promoter of apoptosis. The bcl-2 protein co-localises with the PT pore in the outer mitochondrial membrane (Zoratti and Szabo, 1995; Kroemer et al., 1997), a site that appears necessary for bcl-2 function (Tanaka et al., 1993; Hockenbery et al., 1993). Gene knock-out studies have shown some bcl-2 members are essential for early development, by repressing excessive thymus, spleen, nervous and haemopoetic apoptosis. Consistent with this, over-expression of bcl-2 protects most cells from apoptosis induced by a variety of stimuli (Okazawa et al., 1996).

The Bax subfamily, comprising the Bak, Bax and Bok proteins appear to promote cell death. The BH3 subfamily, a group of posttranslationally activated proteins that include Bad, Bik, Bid and Blk, share a motif common to bcl-2 members. Bid can modify the conformation of Bax, an event correlating with apoptosis (Wang et al., 1996) and cytochrome c release (Desagher et al., 1999). BH3 peptides can also interact with death suppressers such as Bcl-xL to block their activity (Sattler et al., 1997).

Table 1.6 Genes that regulate apoptosis

Adapted from Afford et al., 1999.

Genes	Effect on cell survival
Bcl-2 family	
Bcl-2	Positive
Bcl-xl	Positive
Bcl-w	Positive
Bcl-xs	Negative
Bax family	
Bax	Negative
Bak	Negative
Bok	Negative
BH3 family	
Bad	Negative
Bik	Negative
Bid	Negative
Blk	Negative
Bim	Negative
Caspases 1-13	Initiate and execute vital aspects of the apoptosis programme
p53	Effects bcl-2 and Bax directly, has a critical role in determining either growth arrest or apoptosis.
IRF-1	critical role in determining either growth arrest or apoptosis.
Rb	Modulates exit from cell cycle- inhibition causes apoptosis

Once the mitochondrial gradient is lost and cytochrome c released, the caspase effector pathway may be activated via the Apaf1 (*a*poptotic *p*rotease *a*ctivating *f*actor 1) gene product (Zou et al., 1997). This molecule, with ATP and a caspase cofactor, can bind cytochrome c and activate the caspase cascade. Bcl-2 is thought to regulate the activity of Apaf1 by controlling the flow of mitochondrial cytochrome c through the PT pore (reviewed by (Morita and Tilly, 1999). In agreement with this, release of cytochrome c in response to pro-apoptotic stimuli is blocked in cells over-expressing bcl-2 (Kluck et al., 1997; Yang et al., 1997). Thus, the members of the Bcl-2 superfamily appear to fit into the apoptotic sequence upstream from caspase activation but downstream from initial signalling molecules, and are thought to integrate cell survival and death signals (Lutz, 2000).

Other important apoptotic genes include genes implicated in cell cycle progression. The tumour suppressor genes p53 and IRF1 can signal either growth arrest or apoptosis (Canman et al., 1995; Tamura et al., 1995). P53 is known to transactivate a variety of apoptotic factors and directly modulate bcl-2 and bax activity (see section 1.5.3). Rb (*R*etino*b*lastoma), another tumour suppressor gene, encodes a product that determines exit for the cell cycle into G_0. Inactivation of Rb by a variety of different factors prevents cell cycle exit and causes apoptosis (Debbas and White, 1993; Slebos et al., 1994). Ultimately, the fate of the cell is controlled by a complex balance of pro- and anti-apoptotic factors that is poorly understood.

1.4.5 Role of ROS in apoptosis

ROS are implicated in the initiation the implementation of the apoptotic programme (Buttke and Sandstrom, 1994). Radicals themselves, including H_2O_2 and lipid peroxides induce apoptosis (Bladier et al., 1997; Hockenbery et al., 1993; Ratan et al., 1994). Furthermore, cytotoxic physical and chemical agents that exert oxidative stress activate apoptosis in manifold cell types. Similarly apoptosis induced by physiological stimuli, such as TNF-α or glucocorticoid, also induces an alteration in the redox state prior to the morphological features of apoptosis becoming apparent (Bustamante et al., 1997; Pierce et al., 2000; Jiang et al., 2000). Consistent with this,

Laster and collegues observed that culture in oxygen-free conditions can inhibit TNF-α-induced death (Laster et al., 1988).

There is evidence that ROS are also required for the execution phase of apoptosis. For example, after the apoptotic signal is triggered many cells sustain lipid peroxidation (Amstad et al., 1994; Czene et al., 1997; Dimmeler et al., 1998). Since antioxidants (Johnson et al., 1996), including NAC, GSH (Jiang et al., 2000) and γGCS (Manna et al., 1999) can rescue cells from apoptosis ROS are, in some circumstances, implicated as downstream effectors in the execution phase of cell death. However, caution should be exercised in interpreting the effects of multifunctional antioxidants.

Other evidence for a role of ROS in the regulation of apoptosis comes from a comparison of apoptosis-resistant (LYar) and apoptosis-sensitive (LYas) mouse lymphoma lines. Voehringer and colleagues initially demonstrated that LYar cells have elevated bcl-2 and GSH levels (Voehringer et al., 1998). Subsequent gene microarray analysis of 11,000 mRNA transcripts revealed LYar cells constitutively upregulate two genes thought to boost the level of GSH, via the GR-catalysed GSSG-recycling reaction and γGT-catalysed GSH-scavenging reaction (Voehringer et al., 2000).

Interestingly, over expression of bcl-2 can abrogate lipid peroxidation (Hockenbery et al., 1993) and block apoptosis- at least in part by inhibiting the production or effects of ROS (Kane et al., 1993). Thus, Bcl-2 is thought to function in an anti-oxidant pathway. Since depletion of LYar GSH levels reverses the bcl-2-mediated block of apoptosis, the redox state and not bcl-2 *per se* has been proposed to account for the resistance to apoptosis (Voehringer et al., 1998; Voehringer et al., 2000). Consistent with this, the PT pore has redox-sensitive sulfhydryl groups that may regulate its activity (Petronilli et al., 1994; Chernyak and Bernardi, 1996), a mechanism thought to override the effect of bcl-2 (Zamzami et al., 1998).

However, there are some contradictory observations regarding the importance of ROS in apoptosis. Of particular note, some cell types under anaerobic conditions can undergo apoptosis (Shimizu et al., 1995). This casts some doubt over a universal role for ROS in apoptosis. Within this study, expression of bcl-2 prevented hypoxia-induced apoptosis, a phenomenon associated with no increase in oxidation of lipid, DNA or protein. This opens a potential mechanism of bcl-2 action that does not depend upon the modulation of ROS. It should be borne in mind that multiple divergent pathways leading to cell death exist and further work is required to clarify the significance of ROS in the execution phase.

1.5 p53

Unlike γGCS, which is primarily monofunctional, the 53kDa nucleoprotein p53 is highly pleiotropic. P53 is a stress-surveillance factor and tumour suppressor, drawing international attention since the finding that it is the gene most commonly mutated in human cancer (Caron and Soussi, 1992; Hollstein et al., 1994; Hollstein et al., 1996). In response to a variety of stress signals, including oxidative stress, p53 co-ordinates the cellular processes of cell cycle arrest, DNA repair and apoptosis (Lane, 1992; Clarke et al., 1993; Smith et al., 1995) (Levine, 1997).

1.5.1 Functional domains and structure

The p53 protein is divided into five functional domains, *I-V*, which display a high level of sequence conservation (Soussi et al., 1990). The N-terminal region, spanning amino acids 1-42, embodies the activation (*I*) domain (Fields and Jang, 1990; Unger et al., 1992), though neighbouring sequences are probably required for optimal performance (May and May, 1999). As with all transactivators, p53 binds both DNA sequences and other components of the transcription machinery. Currently, these include the TBP (*T*ATA box *b*inding *p*rotein), TBP-associated proteins of the transcription factors TFIID (*t*ranscription *f*actor IID) (Lu and Levine, 1995; Thut et al., 1995), TFIIH (He et al., 1993), TFIIIB (Chesnokov et al., 1996), Sp-1 (Borellini and Glazer, 1993) and the single-stranded DNA-binding protein RP-A (Dutta et al., 1993). The amino-terminal region also mediates interaction with the p53 negative

regulator, mdm2 (discussed in section 1.5.2.3) and various viral proteins all of which repress p53 transcriptional activation (May and May, 1999).

Adjacent to the N-terminus resides a proline-rich linker region (amino acids 63-97), containing a motif found in the SH3 (*S*rc *h*omology 3) domain. This sequence is thought necessary for interaction with SH3-containing regulatory proteins, for example the gas-1 (*g*rowth *a*rrest *s*pecific) which blocks G0/S phase transition (Del Sal et al., 1995; Ruaro et al., 1997). The proline-rich region has been shown to play a role in growth suppression by influencing p53-mediated apoptosis (Sakamuro et al., 1997). Subsequent deletion of it appears not to affect p53 transactivation, though it can release transrepression (Venot et al., 1998).

The p53 core, covering amono acids 102-292, contains the functional domains *II-V*. These areas comprise the DNA binding region (el-Deiry et al., 1992) which permit interaction with target DNA motifs, and the transcriptional activity associated with p53 activation in response to a stimulus. Consistent with the importance of this function, this area is highly conserved and is also the site in which 80-90% of p53 tumour mutations occur (Hollstein et al., 1994). The crystal structure of the core domain bound to its promoter sequence has revealed a 4 loop arrangement that binds a major and minor DNA groove (Cho et al., 1994). The tertiary configuration is stabilised by a zinc ion, chelation of which alters the structure and reduces DNA binding *in vitro* (Hainaut and Milner, 1993b). The valence of the zinc ion is dependent on the prevailing redox potential and this bestows a degree of ROS sensitivity on p53, expanded in section 1.5.2.3. In addition to DNA binding, the core domain mediates a limited protein binding function and 3'-5' exonuclease activity associated with the "latent" form of p53 (Mummenbrauer et al., 1996), outlined in section 1.5.2.1.

The principal provinces of the carboxy terminus are the oligmerisation and regulatory domains (amino acids 363-393 and 323-356, respectively). The former region permits aggregation into di- or tetrameric complexes (Stenger et al., 1992), partial deletion of which prevents tetramer formation and reduces the affinity of p53

for cognate DNA sequences (Milner et al., 1991; Hainaut et al., 1994). The latter domain, though relatively short, has several distinct functions assigned it. In particular, three nuclear localisation signal have been discovered within, mutagenesis of which can generate either an entirely cytoplasmic protein, or one that resides in both the cytoplasm and nucleus (Dang and Lee, 1989; Shaulsky et al., 1990). In addition an autoinhibitory function has been ascribed to this domain, discussed in the next section.

1.5.2 Regulation of p53 function

One theory advanced to explain the regulation of p53 activity advocates an interaction between the carboxy terminus and another region in the p53 tetramer which prevents sequence specific binding of DNA (Hupp and Lane, 1994; Hainaut et al., 1994). This inactive, or "latent" form is the predominant species within normal cells and is now widely accepted to have a discrete function from activated p53. In particular, latent p53 is implicated in proofreading and repair of low-level DNA damage (see section 1.5.4.3). Latent p53, present at low concentrations, is subject to highly efficient degradation via the ubiquitin-dependent pathway and has a half-life measured in minutes (Haupt et al., 1997; Kubbutat et al., 1997). Upon DNA damage the latent form switches to the active form, capable of transactivating target genes.

Activation is predicted to require a steric modification of the tetramer that releases the association between the autoinhibitory C-terminal domain from its partner(s). This view is supported by the finding that deletion of the C-terminus (Okorokov et al., 1997) or the C-terminal recognising monoclonal anitobody, Pab421, can activate specific DNA binding (Hupp and Lane, 1995; Abarzua et al., 1996; Shaw et al., 1996; Selivanova et al., 1999). Physiologically, p53 activation is associated with C-terminal phosphorylation (Ko and Prives, 1996) and acetylation (Sakaguchi et al., 1998) (enlarged in section 1.5.2.2). Activation also correlates with an extension of the half-life, elevating p53 protein levels (see next section). Thus, activation-stabilisation events are critical in the p53 response to stress, and occur via a series of highly regulated, predominantly posttranscriptional pathways that modify the p53 protein.

1.5.2.1 Protein-protein associations

p53 is regulated by interactions with cellular and non-cellular peptides. In particular, the mdm2 protein was demonstrated to bind p53 *in vitro* and *in vivo* (Barak and Oren, 1992; Oliner et al., 1992), a consistent event that inactivates p53 (Momand et al., 1992; Oliner et al., 1993). This p53 inhibitor appears to function in two ways. First, mdm2 binds the N-terminal transactivation domain which prevents p53-dependent transcription (Momand et al., 1992; Oliner et al., 1993) and second, mdm2 targets nuclear p53:Mdm2 complexes to the cytoplasm for rapid ubiquitin degradation (Haupt et al., 1997; Kubbutat et al., 1997). Disruption of the p53:mdm2 complex is the principle mechanism for p53 stabilisation (Ashcroft and Vousden, 1999b). Immediately after genotoxic damage, for example UV irradiation, Mdm2 messenger RNA and protein levels fall in a p53-independent fashion and free p53 levels rise (Arriola et al., 1999; Blattner et al., 1999). Subsequent posttranslational modifications further adjust p53 activation. With increasing p53 levels, mdm2 becomes induced and re-establishes the repression of p53, forming a well characterised autoinhibitory loop, reviewed by Freedman *et al.*, 1999.

However, the feedback pathway to promote p53 stabilisation in response to DNA damage would require interruption to permit p53 time to complete its functions, thus invoking additional control features to regulate the inhibitory effect of mdm2. Both phosphorylation of p53:mdm2 and interaction of mdm2 with other factors are candidate mechanisms. Indeed, mdm2 can be phosphorylated (Mayo et al., 1997) and the tumour suppressor gene product p19ARF can prevent mdm2-mediated inhibition of p53. This occurs through direct mdm2 binding and sequestration in the nucleolus, preventing the nuclear export necessary for p53 proteolysis (Honda and Yasuda, 1999; Weber et al., 1999).

Furthermore, a p53-binding protein with homology to mdm2, mdmX, has been identified (Shvarts et al., 1996). MdmX has also been shown to inhibit p53 transactivation upon binding though, in contrast to mdm2, it cannot signal nuclear export or induce proteolysis. On this basis Jackson and co-workers have proposed

that mdmX may function to maintain a nuclear pool of p53 in undamaged cells (Jackson and Berberich, 2000).

p53 can also be modulated by non-cellular proteins. p53 is bound and functionally repressed, through different mechanisms, by viral factors such as SV40 T antigen (Jenkins et al., 1988; McCarthy et al., 1994), adenovirus E1B (Yew et al., 1994) and HPV E6 (Thomas et al., 1995).

1.5.2.2 Phosphorylation and acetylation

Eleven major phosphorylation sites have been identified on the p53 protein, clustered mostly in the C- and A-terminal regions. Phosphorylation is thought to modulate different aspects of p53 activity, namely protein stability (Shieh et al., 1997), DNA binding (Takenaka et al., 1995) and transactivation (Jamal and Ziff, 1995) via subtle alterations in tertiary structure. Dephosphorylation, induced by ionising irradiation, generates a binding site that permits association with other factors that activate sequence specific DNA binding (Waterman et al., 1998). In addition, Chernov *et el* report that the stability and activity of p53 are likely to be regulated independently by phoshorylation of discrete sites (Chernov et al., 1998). However, mutation of all phosphorylation sites does not significantly prevent the ability of DNA damage to activate p53 (Ashcroft et al., 1999a). Further, attempts to understand the specific biological effects of individual phosphorylation events are limited by the fact that, *in vivo*, p53 may be subject to multiple kinase and phosphatase activities simultaneously.

Acetylation of the p53 molecule also appears to control p53 activity in response to DNA damage. An early response to UV or ionising radiation is p53 phosphorylation (Shieh et al., 1997), which is then preferentially and acetylated in a site-specific manner (Sakaguchi et al., 1998). Furthermore, the acetyl transferase p300 acetylates the C-terminus of p53, which enhances sequence-specific DNA- recognition (Gu and Roeder, 1997). This may operate by inhibiting the random DNA-binding activity associated with latent p53 (Anderson et al., 1997), a theory yet to be tested. Recently, the small ubiquitin-like protein SUMO-1 has also shown to interct with p53 in a

specific and regulatory manner. SUMO-1 ubiquinates a lysine residue at position 386 on the C-terminus, initiating transcriptional activation (Gostissa et al., 1999; Rodriguez et al., 1999; Muller et al., 2000).

1.5.2.3 ROS and Ref-1

In addition to mechanisms controlling p53 activity previously outlined, the redox environment appears to a have a significant regulatory effect on p53. First, a host of ROS-generating physical and chemical agents induce p53, an event blocked in the presence of GSH or NAC (reviewed by Hainaut et al, 2000). Oxidative damage to DNA, in particular single and double strand breaks, is thought the major mediator of such p53 activation (Nelson and Kastan, 1994).

Second, the functional capability of p53, like that of an increasing number of stress-response transcription factors (such as AP-1 and NF-κB), is subject to the surrounding redox milieu. Site specific DNA-binding of p53 requires the central domain that holds a zinc ion (Bargonetti et al., 1993; Pavletich et al., 1993; Wang et al., 1993) and contains highly conserved cysteine residues at positions 176, 238 and 242 (Cho et al., 1994). Mutation of these residues abolishes or reduces the sequence-specific DNA-binding activity *in vitro* (Rainwater et al., 1995).

Oxidising agents and metal chelators were shown to disrupt p53 conformation and render p53 incapable of DNA-binding, whereas reductants restored conformation and enhanced DNA-binding *in vitro* (Hainaut and Milner, 1993b; Hainaut and Milner, 1993a). This effect of metal chelation on p53 conformation and DNA binding were later shown reversible *in vivo* (Verhaegh et al., 1998). Within cells, hydrogen peroxide (Parks et al., 1997) or diethyl maleate (Russo et al., 1995) depressed the ability of p53 to bind and transactivate, whereas binding to non-specific DNA was not altered. Subsequently, residues 176, 238 and 242 were shown to be oxidised *in vivo*, an event that dampened p53 transactivation (Wu and Momand, 1998).

However, in some instances metal chelation can lead to an increase in p53 DNA-binding *in vivo* (Sun et al., 1997; Chandel et al., 2000). Sun *et al* propose that metal

chelation may release p53 from binding cellular inhibitory proteins. Consistent with this, zinc was required for formation of stable p53-large T antigen complex *in vitro* (Kernohan et al., 1996). Clearly, the conformation, DNA-binding and transactivation capacity of p53 is regulated to some degree by ROS and the availability of zinc or copper ions. In light of these discoveries, Meplan *et al* postulate redox events may play a role in the "fine tuning" of DNA binding (Meplan et al., 2000).

Regulators of the intracellular redox and protein cysteine state may then have a significant regulatory effect on p53. Ref-1 (*re*dox *f*actor-1) is a potent activator of latent p53 that acts via redox dependent and independent mechanisms (Jayaraman et al., 1997; Meira et al., 1997). Oxidised Ref-1 is regenerated by direct association with the antioxidant thioredoxin, which augments Ref-1-enhanced p53-dependent expression of p21 (Ueno et al., 1999). Ref-1, also implicated in BER repair of oxidised DNA (section 1.2.2), enhances p53 transactivation when over-expressed *in vivo*. Antisense Ref-1 downregulates p53 induction and correlated with attenuated apoptosis (Gaiddon et al., 1999). Interestingly, Ref-1 is co-activated with AP-1 in colon cancer cells in response to hypoxia (Yao et al., 1994).

1.5.2.4 p53 homologues

A final possible mechanism of control of p53 was revealed when the presence of new family members were reported. P73 and p63 both have striking similarity to p53 in all domains bar the C-terminus, which is considerably longer (Kaghad et al., 1997; Schmale and Bamberger, 1997). Some isoforms of p73 can transactivate p53 targets and initiate cell cycle arrest (May and May, 1999) or apoptosis when overexpressed (Jost et al., 1997). Therefore, it seemed possible that p73 and p63 compensate for p53 in p53-/- mice. Recently however, functional differences between family members are emerging. Notably and unlike p53, p73 cannot interact with oncogenic viral proteins, is unresponsive to genotoxic injury (Kaelin, 1999) and shows no clear tumour suppressor activity (Lohrum and Vousden, 1999). Moreover, the strikingly different phenotypes of the p73-/- and p63-/- mice compared to p53-/- animals would suggest the p53 homologues fulfil distinct physiological purposes (Mills et al., 1999; Yang et al., 1999; Yang et al., 2000).

1.5.3 Molecular outcomes of p53 activation

After receipt of genetic injury or other cellular stress, p53 becomes stabilised and activated by release from inhibitory proteins such as mdm2 (figure 1.9). Subsequently, p53 activity may be further adjusted via phosphorylation, acetylation and redox processes. Activated p53 performs a variety of functions that have, in combination with other molecular responses, defined molecular consequences. The characteristic events activated p53 causes are referred to as the "p53 response", the most prominent aspect of which is the impact on gene expression and influence on interaction with other proteins.

1.5.3.1 Increased transcription

Genes induced by p53 broadly fall into functional categories. In addition to genes of uncertain function, p53 upregulates genes directly involved in cell cycle arrest; apoptosis; angiogenesis and p53 autoregulation.

The most characterised p53-transactivated mediator of the cell cycle arrest is p21. Elevated p21 levels inhibit G1-active members of the cell-cycle regulatory family, CDKs (*c*yclin-*d*ependent *k*inases) (Xiong et al., 1993) (Harper et al., 1993) (see also section 1.5.4.2). Other genes involved in cell cycle arrest are also transcriptional targets of activated p53. These are cyclin G1 (Okamoto and Beach, 1994); cyclin D1 (Chen et al., 1995); the DNA replication protein, PCNA (*p*roliferating *c*ell *n*uclear *a*ntigen) (Morris et al., 1996); GADD45 (*g*rowth *a*rrest and *D*NA *d*amage-inducible protein) (Kastan et al., 1992); IGF-BP3 (*i*nsulin-like *g*rowth *f*actor *b*inding *p*rotein 3), a factor that suppresses mitogenic stimuli (Buckbinder et al., 1996); the signal transduction protein 14-3-3σ (Hermeking et al., 1997); Siah (Matsuzawa et al., 1998) and Rb (*r*etino*b*lastoma) (Osifchin et al., 1994).

A second superfamily of genes upregulated by active p53 are those involved in promoting apoptosis. The expression of the pro-apoptotic factor bax is elevated in a p53-dependent fashion (Miyashita and Reed, 1995). In addition, the Fas gene, which encodes a cell surface receptor that internalises an apoptosis signal upon ligand

Figure 1.9 Modifications to p53 and the cellular consequences

Indicated: Latent p53 (asymmetric green tetramer) is bound by mdm2 (purple oval), repressing sequence specific DNA binding and targeting p53 for rapid cytoplasmic degradation. Receipt of a stress signal (indicated by red explosion), such as DNA strand breakage, activates p19ARF which blocks nuclear export of p53. Dissociation of the p53:mdm2 complex follows, possibly by phosphorylation of p53 or mdm2, freeing the transactivation domain from mdm2 occlusion. Final activation is achieved by the divergent actions of families of kinases, acetyl transferases and redox modulators. Active p53 (symmetric green tetramer) mediates molecular changes such as altered gene expression and protein-protein interactions. The outcome of these, dependent on the level of damage incurred, can be cell cycle arrest, DNA repair or apoptosis. Not indicated: Rising levels of active p53 increases mdm2 transcription, which shuts down the response.

Figure 1.9 Pathways mediating the p53 response to genotoxic stress

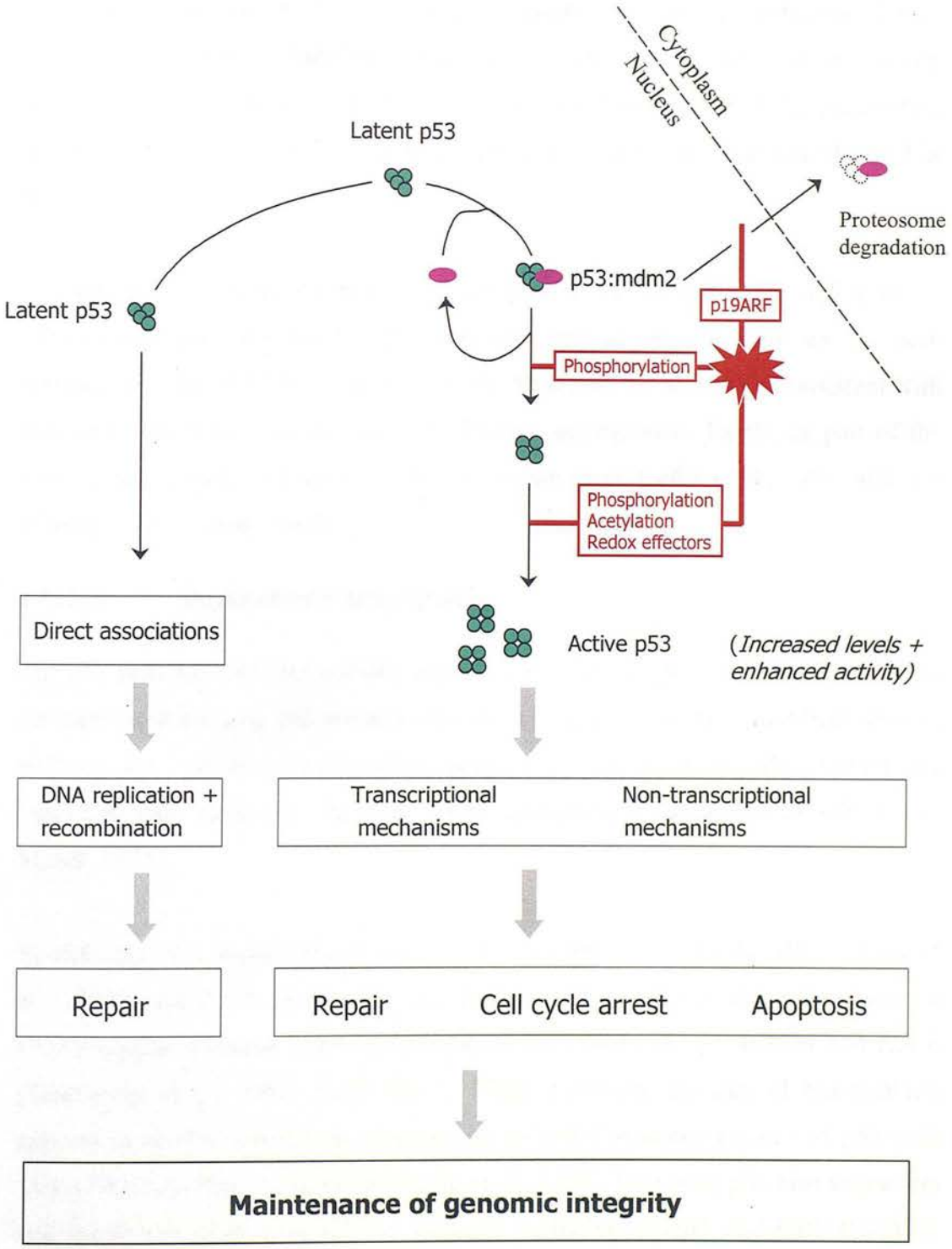

binding, is also transcribed by p53 *in vitro* and *in vivo* (Owen-Schaub et al., 1995; Reinke and Lozano, 1997). The SH3-containing kinase regulator, p85 (Yin et al., 1998) and a novel gene PAG608 (Israeli et al., 1997) may also represent points of control. Using differential display, Polyak *et al.* revealed a battery of genes preferentially transactivated by p53 in early apoptosis. Many of the fourteen PIG's (*p*53 *i*nducible *g*enes) identified encode factors related to, or known to be directly involved in the maintenance of the redox potential. This has led to the proposition that the transactivation of PIG's induces apoptosis by ROS production (elaborated in section 1.5.4.1).

A third class of genes expressed by p53 play a role in impeding angiogenesis. Thrombospondin-1 and BAI1 both encode inhibitors of vascularisation and are both transactivated by p53 (Dameron et al., 1994; Nishimori et al., 1997). Consistent with this, p53 deficiency is correlated with elevated angiogenesis. Lastly, as part of the autoregulatory loop, p53 can transactivate its own gene (Deffie et al., 1993) and that of mdm2 (Juven et al., 1993).

1.5.3.2 Depressed transcription

The p53 response can also embody abated expression of specific genes. Though the mechanism underlying this remains obscure, a cellular significance has been shown: proteins that inhibit p53-dependent apoptosis, such as bcl-2, also inhibit the transcriptional repression function while unaffecting transactivation (Shen and Shenk, 1994).

Specifically, p53 transrepresses cyclin A (Yamamoto et al., 1994), MRP (Wang et al., 1998b), the AP-1 component *c-fos* (Ginsberg et al., 1991), the pro-antioxidant COX2 (*c*yclo*ox*ygenase 2) (Subbaramaiah et al., 1999) and interleukins 2, 4 and 6 (Santhanam et al., 1991; Pesch et al., 1996). Lowering the rate of transcription appears to involve interaction between the N- and C-terminal regions of p53 with TBP (*T*ATA-*b*inding *p*rotein) (Horikoshi et al., 1995). However, p53 also sequesters and inactivates other transcription apparatii, including TFIIIB, and CBF (CCAAT

binding factor) (Cairns and White, 1998) and probably operates via other unidentified routes.

1.5.3.3 Translational control

In addition to modulating transcription, p53 can influence translation of specific transcripts. In response to treatment with TGFβ, polysomes fail to associate with CDK4 mRNA in a p53-dependent manner (Ewen et al., 1995). The mechanism underlying this translational block is currently unknown.

1.5.4 Cellular outcomes of p53 activation

1.5.4.1 Apoptosis

An enormous volume of evidence supports a role of p53 in the controlled deletion of cells in response to a bewildering variety of stimuli. Exogenous p53, when introduced to tumour cell lines activates apoptosis (Shaw et al., 1992; Yonish-Rouach et al., 1994). Moreover, a spectra of p53-/- cell types treated with DNA damaging agents display a markedly attenuated level of apoptosis (Clarke et al., 1993; Strasser et al., 1994; Ziegler et al., 1994; Clarke et al., 1994). The p53-dependent apoptotic response also shows a gene-dose effect, with p53 heterozygotes exhibiting intermediate levels of apoptosis between that shown by wild-type and p53 homozygotes (Clarke et al., 1993; Lowe et al., 1993).

However, in some cell types p53 deficiency results only in an alteration of the kinetics of apoptosis (Xia et al., 1995; Aladjem et al., 1998; Frenkel et al., 1999), and others contain pathways to apoptosis not dependent on p53. For example, treatment of thymocytes with dexamethasome results in p53-independent apoptosis (Clarke et al., 1993).

While the effectors of apoptosis are now quite well understood, the regulation of those effectors has been the subject of controversy. Recently, mechanisms of p53-dependent apoptosis have become clearer. In one pathway, the transactivation of p53-responsive genes is critical for p53-dependent apoptosis (Sabbatini et al., 1995).

Intriguingly, many of the p53-inducible genes (PIG) induced prior to the onset of apoptosis are involved in the regulation of ROS and include pro-oxidative factors (Polyak et al., 1997). Polyak *et al* postulate that the PIGs, upregulated by a similar degree as p21, collectively generate ROS that damage mitochondrial components. This, in turn, causes leakage of cytochrome c and pro-apoptotic factors to the cytosol which activate the caspase cascade. Indeed, p53 specifically represses expression of the antioxidant and anti-apoptotic factor, bcl-2 (White, 1996), the adenovirus-mediated forced expression of which inhibits p53-dependent apoptosis (Chiou et al., 1994). This pathway can be inhibited by the kinase c-KIT, which stabilises the mitochondrial electrochemical gradient and inhibits ROS production, suggesting redox processes may be critical in p53-dependent apoptosis (Lee, 1998). Consistent with this model, p53 sensitises TNF-resistant tumour cells to TNF by increasing ROS and depleting GSH (Shatrov et al., 2000).

In other circumstances, transcriptional activation by p53 is dispensable for the initiation of the death program. For example, p53-dependent apoptosis can occur in the presence of RNA and protein synthesis inhibitors (Caelles et al., 1994; Wagner et al., 1994) and p53 transactivation-mutants are capable of apoptosis, albeit at a slower rate than wild type p53 (Haupt et al., 1995; Chen et al., 1996). It is now clear that p53 can activate apoptosis via either pathway, and that the route taken is determined by the origin of the cell (Haupt et al., 1996).

Since p53 is able to initiate growth arrest or apoptosis, the question arises over how the cell decides its fate. As the level of injury is known to regulate the cellular outcome, with minor injuries inducing cell cycle arrest and extensive injuries triggering apoptosis, the degree of damage sustained by p53 gene is a candidate mechanism (Chen et al., 1996). This model could operate via injury to or mutations in the sequence-specific DNA-binding region, yielding a molecule capable of transactivating genes only containing strong promoter motifs. Examination of p53 point mutants showed they were indeed able to differentiate between p53 target promoters, remaining active toward p21 (favouring G1 arrest) but became inactive

towards bax and IGF-BP3 (disfavouring apoptosis) (Friedlander et al., 1996; Ludwig et al., 1996). In support of this, the preferential transactivation of particular genes has been reported for wild-type p53 in some instances (Nakano et al., 2000), with a tentative role for phosphorylation (Wang et al., 1995; Bouvard et al., 2000). Whether this system is responsible for making critical cellular decisions remains to be shown.

Of note, p21 seems to be transactivated irrespective of the cellular outcome. Inhibition of cell death in a variety of cell types leads to G1 arrest, suggesting that without downstream prevention, the default outcome is growth arrest.

1.5.4.2 Reversible or irreversible cell cycle arrest

The p53-transactivated p21 gene plays a prominent role in the initiation of growth arrest following DNA damage. At high concentrations, such as those provoked by p53, p21 complexes with and potently inhibits several members of the cdk family, including cyclin E/CDK2, cyclinD/CDK4/6 and cyclinA/CDK2 (Dulic et al., 1994), which prevents entry to S-phase via Rb (Slebos et al., 1994). However, fibroblasts isolated from p21-/- embryos have only a partial attenuation of G1 arrest following DNA damage (Deng et al., 1995; Brugarolas et al., 1995). Thus arrest of the cell cycle is not always wholly dependent on p21. In line with this, p53 has been shown to play a role in inhibiting G1/S transition via direct association with cyclin H/CDK7 (Schneider et al., 1998). Interestingly, oxidant-induced growth arrest that is independent of p53 but directly dependent on p21 has been noted in lung epithelial cells (Corroyer et al., 1996; O'Reilly, 2001; Rancourt et al., 2001).

P53 is also thought to have a limited function in the G2 checkpoint (Guillouf et al., 1995), G2/M phase transition (Agarwal et al., 1995; Stewart et al., 1995), centrosome regulation (Fukasawa et al., 1996) and possibly the mitotic spindle checkpoint in cells bearing spindle damage (Lanni and Jacks, 1998).

Originally, it was believed that the p53-dependent arrest of the cell cycle opened a temporal window for DNA repair to occur. However, distinct from transient G1 arrest or apoptosis, the response of some cells to genotoxic stress can be an

irreversible G1 growth arrest (Toussaint et al., 2000). Non-neoplastic cells naturally lose replicative potential after a certain number of cell divisions (Hayflick and Moorhead, 1961; Hayflick, 1991), whereby they assume a stable metabolic condition, known as replicative senescence, for a period which can run into years. Senescent cells are further characterised by an enlarged cell volume (Smith and Lincoln, 1984), elevated activity of a unique β-galactosidase (Dimri et al., 1995), upregulated p21 levels (Cristofalo et al., 1992; Campisi, 1992) and resistance to physiologic mitogenic (Goldstein, 1990; Campisi, 1996; Smith and Pereira-Smith, 1996) or apoptotic stimuli (Wang et al., 1995). These characteristic morphological and biochemical alterations may, after exposure to oxidants or other cytotoxic compounds, be prematurely induced well below the normal number of cell divisions, reviewed in Chen *et al.*, 2000.

Work to elucidate whether p53 functions in senescence has shown that enhanced p53 proteolytic degradation in normal HDFs (*h*uman *d*iploid *f*ibroblasts) can delay replicative senescence (Shay et al., 1991). In addition, embryonic fibroblasts derived from p53-/- animals can proliferate for over 50 passages *in vitro*, whereas heterozygote and wild-type fibroblasts enter senescence around passage 20 (Harvey et al., 1993). Senescence has also been correlated with increased p53 activity (Atadja et al., 1995) and re-introduction of p53 to a previously immortal cell line (Sugrue et al., 1997). However, there is contradictory evidence. For example, SV40 large T antigen-mediated inactivation of p53 in senescent cells permits some cells to initiate DNA synthesis, but these cells fail to replicate (Ide et al., 1983; Gorman and Cristofalo, 1985). Furthermore, HDFs cultured in the presence of p53 antisense oligonucleotides had a lifespan similar to untreated HDFs (Hara et al., 1991). Clearly further research is required to elucidate the role of p53 in senescence.

1.5.4.3 DNA repair

Activation of p53 after genotoxic stress leads to transitory cell cycle arrest, senescence or apoptosis. While initiation of the death programme circumvents the requirement to maintain the fidelity of the genome, transient growth arrest exists to permit the repair of damaged DNA. Logically, p53-dependent transactivation of

DNA repair genes could therefore follow. Until recently, no such genes were known. However, using differential display, Tanaka *et al* identified the p53R2 gene as a transcriptional target for p53. This encodes a protein closely related to ribonucleotide reductases, which are important in DNA repair by providing a supply of deoxyribonucleotides (Jordan and Reichard, 1998). p53R2 is upregulated in response to diverse stress stimuli (Nakano et al., 2000) and p53R2 inhibition during genotoxic stress results in reduced DNA reduced repair and cell survival (Tanaka et al., 2000). This data is evidence for a direct link between p53 and the repair of damaged DNA. However, other data regarding the involvement of p53 in DNA repair is contradictory. Different groups conclude p53 deficiency results in reduced DNA repair (Ford and Hanawalt, 1995; Ford and Hanawalt, 1997), no alteration in the rate of repair (Ishizaki et al., 1994; Sands et al., 1995) and increased rate of repair (Prost et al., 1998).

In addition to the transcription of genes involved in DNA repair, p53 can directly interact with pre-existing DNA repair proteins. In particular, an association between p53 and helicase members of the multiprotein TFIIH, which initiates basal transcription of RNA polymerase II and couples transcription with NER (*n*ucleotide *e*xcision *r*epair) has been reported (Xiao et al., 1994; Wang et al., 1995; Leveillard et al., 1996). The effect of this interaction is inhibition of helicase activity. Furthermore, p53 is known to bind DNA strand breaks (Bakalkin et al., 1995), mismatches (Lee et al., 1995) and the Rad51 protein, a RecA homolog purported to constitute part of the cellular recombination machinery (Buchhop et al., 1997) (discussed in section 4.2.2). Consistent with this, p53 is also known to catalyse DNA renaturation and strand transfer (Brain and Jenkins, 1994; Yokote et al., 1998).

Even in its latent form, p53 may have a role to play in DNA repair. P53 can bind single strand nucleotides, anneal DNA or RNA (Oberosler et al., 1993) and recognise 1-3bp mismatches (Lee et al., 1995). Exonuclease activity is central to the recognition of damage prior to restoration via the mismatch repair pathway. The intrinsic 3'-5' exonuclease activity of unactivated p53 may link it with the tumour suppressor Msh2 (Janus et al., 1999). Circumstantial evidence to support this comes

from mouse models: loss of either p53 or msh2 results in increased incidence of colon carcinomas (reviewed in (Bodmer et al., 1994), and Msh2-/- p53-/- mice develop tumours significantly earlier than either of the single mutants (Cranston et al., 1997).

Furthermore, overexpression of p53 with nuclear extracts *in vitro* enhanced the BER pathway (outlined in section 1.2.2), an effect nullified by p53 depletion (Offer et al., 1999). Lastly, p53 has been demonstrated to bind RPA (*r*eplication *p*rotein A) *in vitro* and *in vivo*, a DNA unwinding and synthesis factor required for NER (Li and Botchan, 1993). Formation of the p53-RPA complex also inhibits p53 sequence specific DNA binding (Miller et al., 1997) by effectively sequestering p53, though UV treatment has been demonstrated to dissociate the p53-RPA complex *in vivo*. Via this route DNA damage can increase the levels of free p53 (Abramova et al., 1997), then able to participate in transactivation and protein-protein associations. Further investigation should reveal whether these are important events in the repair of genome injury.

1.5.5 Role of p53 in development

Considerable attention has been focused on the contribution of p53 in embryonic development. Undifferentiated ES (*e*mbryonic *s*tem) cells express high levels of p53 and respond to UV-induced damage by undergoing apoptosis, whereas differentiated cells have lower levels of p53 and are relatively UV resistant. Indeed, a number of studies closely correlate p53 activity with the degree of differentiation (Louis et al., 1988; Sabapathy et al., 1997).

The generation of p53-/- mice permitted analysis of p53 function throughout embryogenesis. Unexpectedly these mice were viable, though close inspection revealed an increased incidence of exencephaly and associated defects in neural tube closure. This suggests a role for p53 in neural tube development (Armstrong et al., 1995; Sah et al., 1995). p53 also functions in the reproductive potential of offspring, as male mice show defective spermatogenesis (Rotter et al., 1993) and females a lower fertility than wild-type littermates (Armstrong et al., 1995; Donehower, 1996).

Finally, delayed cartilage maturation is observed in p53-/- embryos, identifying a p53 function in skeletal regulation (Ohyama et al., 1997).

In contrast to p53, embryos deficient for the p53 negative regulator, mdm2, are non-viable at an early stage. Significantly, viability of mdm2 null mice is fully restored in the absence of p53. P53 overexpression is similarly detrimental to development (Li and Jaiswal, 1994; Jones et al., 1995; Nakamura et al., 1995; Godley et al., 1996). Together these findings suggest that a correct balance of p53 activity is critical for embryogenesis.

Finally, p53 is implicated in the embryonic response to genotoxic stress. A role for p53 as a teratological suppressor was suggested on the basis of the ability of p53 to inhibit the effects of the teratogens benzo[a]pyrene or γ-irradiation on mouse embryonic development (Nicol et al., 1995; Norimura et al., 1996), possibly by protection against ROS-induced DNA damage (Winn and Wells, 1995; Liu and Wells, 1995). As with most other aspects of p53 function, there are exceptions. Wubah and colleagues demonstrated the genotoxic agent 2-chloro-2-deoxyadenosine caused a 73% incidence of eye abnormalities in wild-type embryos, compared with 52% and 2% in p53+/- and p53-/- embryos, respectively (Wubah et al., 1996). Overall however, there is robust evidence that p53 efficiently deletes embryo cells with DNA-damage. Indeed, it has been predicted over 50% of foetuses do not survive to childbirth due to p53-dependent mechanisms resulting in unrecognisable spontaneous abortions (Boue et al., 1985; Gilbert, 1991; Hall and Lane, 1997). This would make good evolutionary sense, if failure to abort foetuses bearing DNA damage generated progeny with compromised reproductive potential (Choi and Donehower, 1999).

1.6 Rationale of the thesis

Many disparate factors are orchestrated to protect mammalian cells from endogenous and exogenous oxidative injury. The GSH-mediated response constitutes a broad, potent and inducible antioxidant screen that is likely to play a pivotal role in protecting against oxidative injury and maintaining cellular redox homeostasis. It is

primarily executed through the transcriptional control of *γGCSh* and related genes, to effect an increase in GSH, though the mechanisms underlying this response are complex and only partly elucidated. A variety of studies point toward a critical role for GSH during normal development (Nasr-Esfahani and Johnson, 1992; Gardiner and Reed, 1995a; Shi et al., 2000), in addition to protecting the foetus from stress-induced oxidative damage (Trocino et al., 1995; Ishibashi et al., 1996; Sakamaki et al., 1999). Despite being implicated in the earliest stages of embryogenesis, the functional consequences of a constitutive GSH depletion on development were not conclusively known at the outset of this project.

The correct kinetics of cell death, in addition to growth, are central to normal development. It is here hypothesised that absence of the GSH-system would impact upon the capacity to recover and continue cycling. Additionally it is proposed that, subsequent to redox alterations within cells caused by GSH loss, the ability to enter apoptotic pathways will be affected. If either of these processes were disrupted, subsequent analysis of the mechanism underlyling them may yield information on how to limit abnormalities arising *in utero*.

To test these hypotheses, two strategies were employed. First, a gene targeting strategy was adopted to generate a murine ES (*e*mbryonic *s*tem) cell line bearing a deleted *γGCSh* allele. Prior to attempting to complex tissue specific or inducible targeting technology, a replacement approach was chosen to constitutively delete *γGCSh* in all tissues.

To understand the effects of constitutive *γGCSh* and GSH deficiency, it is necessary to first understand the normal situation. To date, the majority of studies investigating the cytotoxicity of oxidative stress have utilised the culture of primary or transformed cell lines for limited periods of time (<48 hours). ES cells, the pluripotent progenitors of all subsequent development, proliferate continuously in culture (section 4.4). However, ES cells are non-transformed and exhibit normal growth and responses to damage characteristic of that in vivo. These traits permit analysis of the long-term effects of oxidative stress on healthy mammalian cells.

Second, therefore, unmodified ES cells - a cell type in which very little oxidative stress work has been carried out, were used to investigate the response to oxidative stress induced by the pro-oxidant menadione (MQ). MQ can introduce DNA strand breaks, though this damage has been dissociated from immediate cell death in hepatocytes (Coleman et al., 1989) and fibroblasts (Renzing et al., 1996). In embryonic development, however, such damage to DNA propagated through successive rounds of replication may accumulate to the long-term detriment of the organism.

Factors involved in the maintenance of cellular integrity ultimately act to preserve the well being of the organism. p53, by delaying DNA replication until DNA repair is complete and eliminating heavily damaged cells from the population, similarly acts to safeguard the integrity of the cell. In addition to its role as a tumour suppressor gene there is evidence that p53 also plays a significant role in promoting normal embryogenesis. How p53 performs this function is unclear. Several studies have attributed the cause of drug-induced birth defects to oxidative DNA damage (Winn and Wells, 1995; Baek et al., 2000; Liu and Wells, 1995) and here it is proposed that p53 is a major factor in deleting cells injured by oxidative stress during development.

Oxidative stress can activate the p53 response in a wide repertoire of cell lineages of normal and neoplastic origin. ROS can also operate as downstream effectors in apoptosis, via p53-dependent upregulation of redox-related genes. In light of this, a possible functional relationship between GSH and p53 is hypothesised. If p53 modulates the GSH response directly via γGCS transactivation or indirectly by other mechanisms, then p53 deficiency would attenuate the GSH response. Furthermore, if embryonic cell death is indeed due to oxidative stress-induced p53-dependent apoptosis, then a deficiency in p53 would be expected to increase resistance against oxidative injury. These suppositions are directly tested in this thesis by the use of gene targeted p53-/- cells.

This thesis explores the relationship between oxidative stress, p53 status and glutathione levels, and directly tests whether p53 mediates resistance to oxidative stress through regulation of GSH levels in ES cells.

1.6.1 Specific aims

This thesis sets out three main objectives. (1) To isolate, clone and characterise both novel mouse *γGCSh* cDNA, and a large (10-20kb) portion of mouse gene sequences. (2) Analyse the impact of a permanent GSH deficiency, using gene targeting technology. To achieve this, the gene sequences generated will be used for the design and construction of a targeting vector. Electroporation of this plasmid into mouse ES cells is anticipated to deactivate the endogenous *γGCSh* gene. Culture of heterozygotes in high G418 is a technique used routinely to render cells homozygous. Comparison of the survival, GSH levels and apoptotic rates between *γGCSh-/-* and unmodified ES cells would show the impact of GSH loss (3) To characterise the role of GSH and p53 in response of ES cells to oxidative stress. Initially, to determine baseline responses of genetically normal ES cells to GSH depleting agents and pro-oxidative compounds to isolate suitable agents for further study. Use of the selected compounds will allow investigation of the cellular responses of cell proliferation, death and GSH levels to redox imbalance. Comparison of the responses made by wild-type and p53-/- ES cells will reveal any role of p53 in these parameters, and show whether a causal association between these factors and viability exist in early embryogenesis.

Chapter 2

Materials and Methods

2.1 Manipulation of RNA

2.1.1 Extraction of RNA from fresh tissue

Following removal from the host animal, samples of fresh tissue were immediately frozen in liquid nitrogen, then rapidly transferred to -80°C storage prior to use. 1ml TRIZOL was added per 100mg fresh tissue and homogenised thoroughly using a "drill-bit" homogeniser. For subsequent treatment, see section 2.1.2.

2.1.2 Extraction of RNA from cultured cells

Cell cultures had media aspirated and were washed x1 in PBS. 1ml of TRIZOL Reagent (Gibco-BRL) was added per $10cm^2$ of culture dish and left at room temperature for approximately 2 minutes. The resulting whole cell lysate was passed several times through a blue (p1000) pipette tip, transferred to a RNase-free eppendorf tube and the RNA cleaned as described (section 2.2.4).

RNA was washed by removal of supernatant from the pellet, and addition of 1ml 70% ethanol per 1ml of TRIZOL reagent used. Samples were vortexed thoroughly and centrifuged at 10,000 rpm for 5 minutes at 4°C. Ethanol supernatant was discarded and the RNA pellet briefly air-dried for 5 to 10 minutes. Pellets were resuspended in an appropriate volume of RNase-free water by passing the solution several times through a yellow (p200) tip and incubating at 55°C for 10 minutes.

2.1.3 Generation of cDNA from RNA template with reverse transcriptase

For first strand cDNA synthesis 1µl Oligo $(dT)_{15}$ at 100ng, 1-5µg total RNA and 12µl DEPC treated dH_2O were added to PCR tubes. Samples were mixed, incubated at 70°C for 5 minutes and left to slowly cool to ambient temperature. The contents of

tubes were collected by centrifugation and placed on ice. 4µl 5X First Strand Buffer (Gibco BRL; supplied with enzyme), 2µl 0.1M, DTT1µl, 10mM and dNTP mix1µl (200 units) of Superscript II (Gibco BRL) were added to the tubes. The contents were mixed and subjected to the following cycle: 37°C for 10 minutes; 42°C for 60 minutes and 50°C for 10 minutes. 80µl sterile H_2O was added and the reaction inactivated by incubation at 94°C for 10 minutes. 5-20µl of the sample was used as template in conventional PCR reactions (see section 2.2.1).

2.2 Manipulation of DNA

2.2.1 PCR amplification of DNA

Two types of PCR reactions were employed, "standard" and "Hi-Fidelity", distinguished by the type of polymerase and contents of reaction buffers. All standard and high Hi-Fidelity PCR reactions were performed in a Hybaid Omni Gene DNA thermocycler and only cycle conditions were varied to enable optimisation of specific template amplification for each individual primer pair (detailed at each relevant section throughout thesis).

Primers and PCR conditions used for the amplification of γGCSh sequences are shown in table 2.1. All reactions were subject to an initial cycle of 3 minutes at 94°C; 1 minute at 57°C and 72°C for 2 minutes. A final extension step of 72°C for 10 minutes was also included. For intermediate cycle conditions refer to relevant PCR reaction in table 2.1.

Once prepared, individual standard or Hi-Fidelity PCR reaction tubes were transferred to a dedicated template loading area where 1µl of template was added to each sample, excepting negative control (approx. 300ng genomic DNA or 1µl of a 10^{-6} plasmid dilution). 60µl of paraffin oil was overlaid to reduce sample evaporation during thermocycling.

Table 2.1 Amplification of γGCSh sequences

Up- indicates upstream primer, Rev-indicates downstream primer. The same conditions were applied for standard and High Fidelity PCR.

Reaction and product size	Primer sequence 5'-3'	Cycle conditions	Parameters
5' RT-PCR no product	5' Up – ATGGGGCTGCTGTCCCAGG Rev 3– CATTTTGAGAATATTCAGTC	94°C 30s 57°C 30s 72°C 120s	Mg^{2+} @ 1, 1.5 and 2mM Annealing @ 59, 55 and 53°C
Central RT-PCR (Mouse liver/ES cell)			
130bp	Up2 – AGGAGAAAAGGTTGTCATCA Rev2 – ATGTACCTACGGTACCCTA	94°C 30s 57°C 30s 72°C 30s	Mg^{2+} @ 1.5Mm
98bp	Up3– TGCTCATCTCTTTATTAGAGA Rev3- TCGAGTAGAGAAATAATCTCT	as above	Mg^{2+} @ 1.5mM
108bp	Up4 - ATCCTGACTACAAGCAAGACA Rev4 – TAGGACTGATGTTCGTTCT	as above	Mg^{2+} @ 1.5mM
1321bp	Up2+Rev4	94°C 30s 57°C 30s 72°C 90s	Mg^{2+} @ 1.5mM
Genomic PCR 230bp	Up2+Rev2	94°C 30s 57°C 30s 72°C 90s	Mg^{2+} @ 1.5mM
no product	Up2+Rev3	as above	Mg^{2+} @ 1, 1.5 and 2mM Extension @ 1, 3, 5 and 10mins
no product	Up3+Rev3	as above	
no product	Up3+Rev4	as above	
no product	Up4+Rev4	as above	
Characterisation PCR 178bp	Up2+ RevB- CTTTTCTCCT CTCCGATGCC	94°C 30s 57°C 30s 72°C 90s	Mg^{2+} @ 1.5mM

All PCR reactions were "hot-started" to reduce the potential amplification of background templates. Samples were pre-heated to 94°C for 1 minute prior to 1st cycle and 1µl respective *Taq* DNA polymerase (Life technologies or ClonTech) was added to each sample tube below the paraffin oil.

Standard PCR

The following reaction mix was prepared:10µl 10X PCR reaction buffer (Life technologies), 6µl 50mM $MgCl_2$ (Life technologies), 8µl 1.25mM dNTP stock mix (Pharmacia Biotech), 1µl 100pmol/µl each primer A and B (Genosys) and ddH_2O to 98µl.

Hi-Fidelity PCR

The following reagent mix was prepared: 2µl 50X polymerase buffer with 15mM $MgCl_2$ (ClonTech), 2µl 50X dNTP mix (ClonTech), 10µl 10X High Fidelity PCR, reaction buffer (ClonTech), 1µl 100pmol/µl each primer A and B (Genosys), and ddH_2O to 98µl.

2.2.2 Restriction endonuclease digestion of DNA

Examples of typical restriction digest reaction volumes are detailed in table 2.2. These include routine volumes for the analysis of plasmid DNA, for the cloning of plasmid DNA and for the analysis of genomic DNA. Although total reaction volumes and incubation times differed for each application of this technique, the relative volume of restriction enzyme(s) were consistent and never exceeded 10% of the total reaction volume. To ensure complete cleavage, restricted DNA was electrophoresed through an agarose gel containing 0.1mg/ml ethidium bromide and visualised using ultra-violet light. Molecular weight markers were loaded to determine size of fragments. The concentration of agarose in the gels was varied between 0.7 and 3% depending on the size of the fragments to be separated.

Table 2.2 Restriction analysis of DNA

Conditions	PCR DNA	Plasmid DNA	Cloning of plasmid DNA	GENOMIC DNA
NEB 10X buffer, µl	2	1	5	3
DNA, µg	0.2/PCR	~1	~15	10
RNAase A, µl	0	0.5	0	0
dH_2O to increase total reaction volume to, µl	20	10	50	30
Restriction enzyme, µl	2	1	5	3
Incubate at appropriate temperature for, hrs	3	3	3	12

2.2.3 Extraction of DNA fragments from agarose gels

DNA fragments were isolated from agarose gels using the Qiaex II gel extraction kit (Qiagen). Appropriate fragments were excised from the gel using a sterile scalpel blade and placed into a pre-weighed 1.5ml microfuge tube. The microfuge tube was re-weighed to determine the weight of the gel slice. 300µl of QX1 buffer was added per 100mg of gel slice to solubilise the agarose, dissociate DNA binding proteins from the DNA fragment and give a suitable pH to allow absorption of the DNA fragment to the QiaexII silica particles. QiaexII particles were vortexed, 10µl of the solubilised sample added and incubated at 50^0C for 15 minutes. Particles were washed with QX1 buffer and 80% ethanol. Pelleted particles were vacuumed dry and DNA eluted with 20µl of sterile dH_2O.

2.2.4 Purification of DNA

An equal volume of phenol:chloroform:isoamyl alcohol was added to the sample volume and mixed to form an emulsion. This was centrifuged at 12,000rpm for 5 minutes at room temperature. The clear aqueous phase was pipetted to a new tube, exactly two volumes of ice-cold absolute ethanol added to the aqueous phase and

mixed to form a visible DNA precipitate. The DNA mix was placed at –20°C for 15-30 minutes, then centrifuged at 12,000rpm for 10 minutes at 4°C. Pellets were washed and dried in air or under vacuum. Dry pellets were dissolved in the desired volume of dH_2O or TE and stored at –20°C until required for use.

2.2.5 Dephosphorylation of vectors

Following restriction, the intended vector sequence was added to the digests and incubated with 1µl appropriate 10x reaction buffer, 8µl dH_2O and 1µl Shrimp Alkaline Phosphate (SAP). Samples were vortexed and the reaction incubated at 37°C for 1 hour. SAP was heat inactivated by incubation at 65°C for 10 minutes. This step, though optional, reduces the frequency of background cloning products considerably by preventing the recircularisation of vector sequences in the absence of insert. Enzymatic treatment with SAP removes the 5' terminal phosphate groups from linearised vector sequence and thus prevents the ligation of free vector ends in the absence of insert sequence.

2.2.6 Rapid ligation of DNA fragments

This section details protocols used to clone fragments of DNA into plasmid vector backbones. This technique is applicable when the restriction enzyme(s) used in the preparation of DNA vector and insert are either identical and thus generate identical 5' or 3' overhangs, or are different but generate compatible 5' or 3' overhangs.

Both insert and dephosphorylated vector were cut with the appropriate restriction enzyme(s), as described (section 2.2.2). DNA was run in a 0.7% agarose gel (or appropriate) to separate desired DNA fragments from all non-required or undigested sequences present in the sample. The appropriate digested vector and insert bands were excised from the gel with a scalpel blade and purified using QIAquick Gel extraction kit (Qiagen): see section 2.2.3. 10% of the gel-purified vector and insert fragments were run on a 0.8% agarose gel beside known DNA standards. This step enabled evaluation of the integrity of the purified DNA fragments. DNA bands that appeared slightly diffuse or "smeary" were not used to attempt cloning, since this indicates poor integrity and/or degradation of the desired DNA fragment. The

concentrations of both vector and insert were determined using ethidium bromide plates. Plates contained 1% agarose in 1x TBE buffer with 0.1mg/ml of ethidium bromide. Both 1µl of samples and 1µl standard DNA of known concentration ranging from 3ng/µl to 125ng/ul were pipetted onto the plate. Plates were left at room temperature for 25 minutes and viewed under ultraviolet light to estimate the concentration of unknown samples against the standards. Ligations using 50ng of vector and a vector to insert molar ratio of 1:3 were prepared. This was calculated by the conversion of molar ratio to mass ratio using the following equation:

$$\frac{100\text{ng of vector x Kb size of insert}}{\text{Kb size of vector}} \text{ x molar ratio of } \frac{\text{insert}}{\text{vector}} = \text{ng of insert}$$

The following preparatory ligation reaction was set up: 10µl 2x T4 DNA ligation buffer and 10µl DNA (vector to insert in 1:3 ratio) in 1x DNA dilution buffer. This was thoroughly mixed, and 1µl T4 DNA ligase (Boehringer Mannheim) added, mixed again thoroughly prior to incubattion at room temperature for 10 minutes. Competent bacteria were subsequently transformed with ligation reaction as described (section 2.2.7).

2.2.7 Heat-shock transformation of competent *E. coli* with plasmid DNA

100µl aliquots of competent XL-1 blue *E. coli* (Stratagene) were removed from –70^{0}C and thawed in a pre-chilled Falcon tubes on ice. β-mercaptoethanol was added to give a final concentration of 25mM. Either 50ng of supercoiled plasmid DNA, or 10% volume of a plasmid DNA ligation mixture was added to the thawed cells. Samples were gently mixed by stirring with a p200 pipette tip, maintained on ice for a further 30 minutes then heat-shocked at 42°C for 45 seconds, before being replaced on ice for 2 minutes. 950µl of preheated (37°C) LB broth was added to each sample tube and incubated at 37°C shaking at 225 rpm for 1 hour. Routine transformation of supercoiled plasmid DNA was achieved by plating 200µl of each transformation onto LB-agar plates containing the antibiotic ampicillin. Plates were inverted and incubated at 37°C overnight. The L-broth supports the growth of *E. coli* cells and the

ampicillin selects for bacterial colonies that have successfully been transformed with the plasmid, as the plasmid contains the ampicillin resistance gene.

2.2.8 *E. coli* cultures and plasmid isolation

Miniprep (small scale preparations)

The preparation of plasmid DNA by this method produced between 20-50μg DNA. This method was routinely used to provide sample DNA for the analysis of cloning steps involved during the construction of all vectors detailed within this thesis. For all buffer compositions, refer to Appendix II.

5ml of LB media (supplemented with appropriate antibiotic) in a white-capped universal tube (Griener) was inoculated with a single bacterial colony previously grown on a LB-agar plate. Samples were incubated at 37°C overnight with vigorous shaking (225rpm). To promote efficient growth of bacterial culture, lids of universal sample tubes were left slightly loose to enable good oxygenation of sample.

The Following Day

1.5ml of each turbid sample was removed, spun at 4,000rpm for 5 minutes on a desktop microfuge (Sanyo) and all LB supernatant carefully removed and discarded. 100μl of ice cold resuspension buffer was added to remaining pellet and vortexed vigorously to ensure complete resuspension of pellet. 250μl of lysis buffer was added and the tubes gently inverted 4-6 times to mix the sample. Bacterial suspensions should have become viscous and slightly clear. 350μl of neutralisation buffer was added, the tubes again gently inverted 4-6 times to mix the sample which forms a cloudy white precipitate. To prevent shearing of bacterial genomic DNA and subsequent contamination of final plasmid DNA preparation, sample tubes were not vortexed at these two latter stages. Samples were incubated on ice for 5 minutes before centrifugation at full speed (13,000 rpm) on a desktop microfuge for 10 minutes.

Plasmid DNA was purified using the Qiaprep Spin System (Qiagen). The supernatant was carefully transfered to a QIAprep spin column in a 2ml collection tube, spun for

1 minute and the flow-through discarded. Spin columns were washed by adding 0.5ml of 95% ethanol and centrifugation for 1 minute. Flow-throughs were discarded and to completely remove residual ethanol, which may inhibit subsequent enzymatic reactions, spin columns were centrifuged for an additional 1minute and residual wash buffer removed.

Maxiprep (large scale preparations)

The preparation of plasmid DNA by this method produced between 200-500μg DNA. The method employed used QIAGEN columns to produce very high quality plasmid DNA in large quantities, suitable for the purposes of mammalian cell transfection and DNA sequencing.

Sterile 500ml conical flasks containing 100ml of LB media (supplemented with appropriate antibiotic) were inoculated with with a single bacterial colony previously grown on a LB-agar plate. The top of the conical flask was loosely covered the with tinfoil and samples incubated at 37°C overnight with vigorous shaking (225rpm).

The Following Day

Plasmid isolation from bacterial cultures of 100ml or more were carried out using the QIAGEN plasmid maxi prep kit. This is a scaled up version of the miniprep technique with the following alternative steps. Following addition of neutralisation buffer, mixtures were on ice for 20 minutes prior to centrifugation at 20,000 g for 30 minutes at 4°C. Supernatents were removed promptly and the supernatent applied to the QIAGEN-tip to allow it to enter the resin by gravity flow. QIAGEN-tips were washed with 2x 30ml 95% ethanol and the DNA eluted with 15ml elution buffer. DNA was precipitated by the addition of 10.5ml (0.7 volumes) isopropanol to the eluted DNA, mixing and immediate centrifugation at 15,000 g for 30 minutes at 4°C. Supernatent was carefully decanted, the DNA pellet washed with 5ml 70% ethanol and centrifuged at 15,000 g for 10 minutes. Supernatent was carefully decanted to prevent disturbing the pellets, which were air-dried for 10 minutes and the DNA re-dissolved in 50ml TE, pH 8.0.

2.2.9 Dideoxy-sequencing of plasmid DNA

To optimise sequencing results, plasmid DNA of the highest quality was used and prepared with a QIAGEN Maxiprep column. dH_2O was added to 10µg of plasmid DNA to make a final volume of 45µl and DNA denatured by the addition of 5µl of 2M NaOH, 2mM EDTA. Samples were thoroughly mixed by inversion and kept at room temperature for 5 minutes, and this strong alkali neutralised by addition of 5µl of 2M ammonium acetate, pH 4.6 and vortexing. To precipitate DNA, 185µl of ice-cold absolute ethanol was added, the tube vortexed and placed at -70°C for 30 minutes. Sample tubes were spun at 13,000 rpm for 10 minutes at 4°C and the supernatant decanted. Pellets were washed X1 with 200µl ice-cold ethanol, dried under vacuum for approximately 15 minutes before resuspension in 6µl of dH_2O.
Sequencing primers were annealled by addition of 2µl 5X Annealing Buffer (USB) and a 2µl volume (0.5pmol) of primer to resuspended DNA. Samples were heated to 65°C for 2 minutes, the temperature then allowed to drop slowly (approx. 30 minutes) to room temperature before chilling on ice. 2.5µl of each dideoxy termination mix (USB) was added to 4 eppendorfs and pre-warmed to 37°C. To the annealed reaction tube 1µl of 0.1M DTT, 2µl Labelling Nucleotide Mix (USB), 0.5µl or 5µCi radio-labelled dATP (α-S^{35}) and 2µl of a 1:8 diluted stock of Sequenase Enzyme (USB) was added. Where sequencing of DNA close to primer was required, 1µl 0.1M $MnCl_2$, 0.15M sodium isocitrate further added. The total volume (approx. 15µl) was mixed and incubated at room temperature for between 2 to 5 minutes, depending on requirement to read sequence either close or increasingly distant from the primer. 3.5µl of labelling reaction was transfered to each of the four pre-warmed dideoxy termination mixes, the termination reactions incubated at 37°C for between 2-5 minutes before addition of 4µl of Stop Solution (USB). The sample was mixed and either kept on ice prior to running on a sequencing gel (see below), or stored at -20°C.

Preparation of a Polyacrylamide Sequencing Gel

Two large sequencing plates were washed once with water and detergent, then washed once with acetone. The inner side of one plate was coated with "Gel-slick" (FMC BioProducts, USA) to facilitate the separation of both plates following electrophoresis of samples. The following were mixed in a 500ml beaker: 80ml 6%Acrylamide, 6M Urea, 1X TBE, 80µl 25% Ammonium Persulphate and 80µl TEMED. Immediately following the addition of TEMED, the gel-mix was poured between the plates, an inverted sharks-tooth combs placed at the top of gel (to form a single large well) and left to polymerise at room temperature for between 45 to 60 minutes. Following removal of comb, the gel was immediately transfered to an electrophoresis rig and positioned in the apparatus. Buffer tanks were filled with 1X TBE, and the single well rinsed out with buffer using a 50ml syringe to ensure that all non-polymerised gel was washed out. Sharks tooth combs were replaced in the opposite orientation and pressure applied until the tips of the teeth penetrate about 2-3mm into the gel, forming individual wells in which to load samples.

Denaturing PAGE of Sequencing Reactions

Immediately prior to the loading of the sequencing reactions, the sequencing gel was pre-run at 40W, or 1.7kV for 20 minutes or until the temperature of the outer glass plate reaches approximately 50°C. Samples were heated to 80°C for 10 minutes and immediately placed on ice. 2µl of each reaction was loaded into wells, ensuring that the loading order of reactions is consistent (e.g. G, A, T, C from left to right) to enable subsequent interpretation of sequencing results. Samples were run at 40W or 1.7kV until the bromophenol blue dye front from the samples reached the foot of the gel. If free wells were available, the current was stopped, samples reloaded in spare wells and the electrical current re-applied. Gels were run until either the bromophenol blue dye front of the newly loaded samples, or the cyanol blue of the original samples reached the foot of the gel. The electrophoresis rig was dismantled, taking great care since the bottom TBE buffer reservoir then contains S^{35} nucleotide. The glass plates were separated and one removed to expose the gel. The base plate was rested in a completely horizontal position, Gel Fix Solution poured over the entire surface area of the gel and left in contact with the gel for 10 minutes. The gel

was drained by carefully tipping the base plate, then removed by placing a piece of Whatmann 3MM paper on the gel surface, and peeling it away from the glass plate in one rapid and constant movement. The gel surface was covered in cling film and dried in a vacuum dryer at 80°C for 2 hours, or until completely dry. The dried gel was placed in an autoradiography cassette, overlaid with a piece of Bio-Max MR-1 film (Amersham) and sealed. Film was exposed to the gel at room temperature overnight and developed the following day.

2.2.10 Southern transfer of plasmid and genomic DNA

Genomic or plasmid DNA was digested overnight as described (section 2.2.2). Digests were run out on a 0.8% agarose gel until the 500bp DNA marker reached the foot of the gel, where upon the gel was photographed beside a ruler to enable accurate sizing of bands which subsequently hybridised to P^{32} radiolabelled probe. In instances where the fragment of interest was greater than 10Kb, depurination of DNA *in situ* was carried out prior to denaturation to increase the efficiency of DNA migration from the gel. The gel was transfered to a tray containing several volumes of depurination solution and soaked, with gentle agitation, for 10 minutes. After briefly rinsing with dH_2O, the gel was placed in a tray containing several volumes of denaturation solution and gently agitated for 45 minutes. Subsequently the gel was rinsed with dH_2O, transferred into a tray containing several volumes of neutralisation solution and left to soak, with gentle agitation, for 30 minutes before rinsing briefly with dH_2O.

Capillary transfer of DNA from gel to nylon filter

A tray was filled with 10x SSC and a piece of plastic rested between the sides to form a platform over the 10 x SSC bath. the platform was wrapped with a piece of Whatmann 3MM filter paper soaked in 2 x SSC, ensuring that all trapped air bubbles that arise between paper and platform were removed and that the edges of the 3MM paper rest within the 10 x SSC solution. The neutralised gel was placed on top of the 2 x SSC soaked 3MM paper. Strips of para-film were cut to cover all wet areas of the 2 x SSC soaked 3MM paper not already covered by the gel, and a piece of Hybond-N+ (Amersham) nylon filter cut to size, was submersed in dH_2O and placed on top of

was drained by carefully tipping the base plate, then removed by placing a piece of Whatmann 3MM paper on the gel surface, and peeling it away from the glass plate in one rapid and constant movement. The gel surface was covered in cling film and dried in a vacuum dryer at 80°C for 2 hours, or until completely dry. The dried gel was placed in an autoradiography cassette, overlaid with a piece of Bio-Max MR-1 film (Amersham) and sealed. Film was exposed to the gel at room temperature overnight and developed the following day.

2.2.10 Southern transfer of plasmid and genomic DNA

Genomic or plasmid DNA was digested overnight as described (section 2.2.2). Digests were run out on a 0.8% agarose gel until the 500bp DNA marker reached the foot of the gel, where upon the gel was photographed beside a ruler to enable accurate sizing of bands which subsequently hybridised to P^{32} radiolabelled probe. In instances where the fragment of interest was greater than 10Kb, depurination of DNA *in situ* was carried out prior to denaturation to increase the efficiency of DNA migration from the gel. The gel was transfered to a tray containing several volumes of depurination solution and soaked, with gentle agitation, for 10 minutes. After briefly rinsing with dH_2O, the gel was placed in a tray containing several volumes of denaturation solution and gently agitated for 45 minutes. Subsequently the gel was rinsed with dH_2O, transferred into a tray containing several volumes of neutralisation solution and left to soak, with gentle agitation, for 30 minutes before rinsing briefly with dH_2O.

Capillary transfer of DNA from gel to nylon filter

A tray was filled with 10x SSC and a piece of plastic rested between the sides to form a platform over the 10 x SSC bath. the platform was wrapped with a piece of Whatmann 3MM filter paper soaked in 2 x SSC, ensuring that all trapped air bubbles that arise between paper and platform were removed and that the edges of the 3MM paper rest within the 10 x SSC solution. The neutralised gel was placed on top of the 2 x SSC soaked 3MM paper. Strips of para-film were cut to cover all wet areas of the 2 x SSC soaked 3MM paper not already covered by the gel, and a piece of Hybond-N+ (Amersham) nylon filter cut to size, was submersed in dH_2O and placed on top of

the gel. One side of the nylon filter was trimmed with a scalpel to facilitate subsequent orientation of the autoradiogram to the filter. Two pieces of Whatmann 3MM paper were cut to the size of the gel, wet in 2x SSC and placed on top of Hybond-N+ filter. A stack of dry paper towels were placed on top of the wet 3MM paper, a glass plate was positioned over the top of the paper towel stack and weighed down with a heavy object. The edges of the tray were covered with cling-film to minimise the evaporation of 10 x SSC and left to transfer overnight. This procedure sets up a flow of liquid from the reservoir into the tray, through the gel and into the paper towels, transferring the digested DNA fragments from within the gel onto the nylon membrane.

The following day, the stack was dismantled and Hybond-N+ filter completely dried between two sheets of 3MM Whatmann filter paper to ensure fixation of the DNA to the nylon membrane.

2.2.11 Radiolabelling DNA probes with P^{32} by random priming

All probes were labelled with the "High Prime" labelling kit (Boehringer Mannheim). 25ng of probe DNA and dH_20 were combined in a single reaction tube to a volume of 11µl. The sample tube was boiled for 10 minutes, before briefly centrifuging to collect condensation and chilling on ice. 4µl of High Prime and 5µl of P^{32} labelled dCTP (ICN) was added, mixed thoroughly and the reaction tube placed at 37°C for a minimum of 10 minutes. At end of labelling reaction 2µl of 0.2M EDTA pH8.0 was added.

Determination of radio-nucleotide incorporation

The contents of a Sephadex G50 column (Amersham) was emptied and resin washed by allowing a minimum of 1ml TE buffer to pass through the column. 2µl 0.2M EDTA and 20µl 10mg/ml Salmon sperm DNA were added to the sample, mixed thoroughly to stop the probe labelling reaction, and the total volume transferred directly onto Sephadex resin. 400µl TE was added directly onto the resin, and through flow collected. A second 400µl of TE was added to the resin, the probe-containing discharge secured in a screw-top eppendorf. Residual counts in the

Sephadex column were compared with those present in the fraction of TE containing labelled probe. 50% label incorporation was assumed if counts from both sources are approximately equal, which was the minimum radio-nucleotide incorporation efficiency that was used for subsequent experimentation.

2.2.12 Hybridisation of probe to DNA immobilised on nylon membrane

The dry DNA-bound nylon membrane was rinsed in 2 x SSC solution. This was placed on top of a piece of dH_2O-wetted nylon gauze, to ensure even distribution of probe over the entire surface of the DNA bound nylon membrane. The two pieces were rolled together to form a tube and placed inside of a Hybaid hybridisation tube. 25ml of pre-hybridisation solution (with 500µl boiled 10mg/ml Salmon sperm DNA, Sigma) was added to the hybridisation tube and incubated with the membrane at 65°C in a rolling incubator for 3 hours. The P^{32} radiolabelled probe was boiled in a screw-top eppendorf (see section 2.2.10) for 10 minutes and pipetted into a blue-capped Falcon tube. The pre-hybridisation solution was immediately decanted into a Falcon tube containing the probe, inverted to mix, then quickly poured back into the Hybaid tube containing the membrane. The probe was incubated with the membrane at 65°C, in a rolling incubator, overnight. The following morning, the probe/hybridisation solution was decanted from the Hybaid tube and rinsed twice with 2 x SSC. 100ml Wash Solution I (pre-warmed to 65°C) was added to the hybaid tube and incubated at 65°C in the rolling incubator for 20 minutes before decanting. This step was repeated a further four times by sequentially adding 100ml pre-warmed Wash Solution II through to V. This step removes non-hybridised and non-specifically hybridised probe from the nylon filter membrane. Following the last wash, the filter membrane was removed from the Hybaid tube, gently blot dried with a piece of Whatmann 3MM paper, sealed into a polythene bag and taped securely into an auto-rad cassette (with enhancer screens). A piece of KODAK Biomax MS film (Amersham) was laid onto the hybridised filter membrane and placed at -70°C for between 1- 4 days prior to developing.

2.2.13 Plating λ–PS genomic library

The λ–PS library was obtained from Molecular Biologische Technologie GmbH, Wagenstieg 5, D-37077 Gottingen, Germany. All recombinant DNA libraries contain a large number of bacteriophage plaques, each containing a relatively large amount of insert DNA. The technique of *in situ* plaque hybridization, originally described by Benton and Davis 1997 (Benton and Davis, 1977), identifies the location of specific DNA sequences of interest. The first step in the nucleic acid hybridization screening procedure is to grow large numbers of plaques on normal agarose plates. Replica copies of these colonies are transferred to nylon filters, where they can be screened. In this section the techniques for producing large numbers of plaques are outlined.

To prepare plating bacteria (C600), a single colony of the bacterial strain C600 was grown in 50 ml of LB++ (see appendix II) in a 250 ml flask, with vigorous agitation (250 cycles/minute in a rotatory shaker at 37°C overnight). 50 ml was transferred into a sterile plastic tube, centrifuged at 2500g for 10 minutes, the supernatant decanted and the bacterial pellet resuspend in 25ml 20mM $MgSO_4$. Plating bacteria were used up to five days hence if stored at 4°C. To determine the titer a serial dilution of the library in SM was prepared as follows. 300µl of the C600 plating bacteria were infected with 1µl of a 10^{-2}, 10^{-3}, 10^{-5}, 10^{-6} dilution and incubated for 30 minutes at 37°C. In the meantime LB/$MgSO_4$ 8 cm diameter plates were warmed to 37°C and the LB/top agar cooled to 55°C, after melting in a boiling water bath. 4.5ml of the LB/top agarose was added to infected bacteria and poured onto the prewarmed plates, which were left at room temperature until solid before incubated in an inverted position at 37°C overnight. The following day, the plaques were counted and the exact titer of plaque forming units (pfu's) of the library stock calculated.

To plate the library to guarantee complete representation of the genome, $2x10^6$ pfu's were used for one library plating. 3 ml of C600 infected plating bacteria and 9ml LB/top agarose (kept at 55°C) were poured onto prewarmed LB/$MgS0_4$ plates (12cm x 12cm). To plaque blot, circular Hybond-N+ nylon filters (Amersham), pre-wetted in 2X SSC, were carefully laid on the agar surface. The membrane and agar were

marked using a sterile needle to ensure correct orientation of plaques. Using forceps, the filter was removed after 1 minute and placed, plaque side up, on sterile filter paper. The replica blots were treated as described (section 2.2.10).

2.2.14 Isolation of genomic DNA by screening λ–PS filters

λPS is a replacement vector of lambda phage origin, containing DNA sourced from the mouse 129 Sv D3 strain. The linear vector contains two loxP sites in direct orientation flanking a high copy plasmid backbone (pBluescript) and approximately 13kb of insert (Nehls et al., 1994). Recombination between these two sites is mediated by Cre recombinase, leading to the excision of the insert and multi-copy plasmid from the phage genome (see figure 3.11). Hence, this is termed automatic subcloning. It can be achieved simply by transferring the phage into the constitutively Cre-expressing *E. coli* strain BNN132. The process used to isolate genomic γGCSh sequences is outlined below.

First, filter hybridization - as carried out as described previously (section 2.2.12). Any positive plaques were purified by 3 additional rounds of plating and hybridization. Plaques were picked using a glass pipette and transferred into a reaction tube containing 500µl SM/ 20µl Chloroform. The tube was vortexed and centrifuged briefly, then keep at 4°C for further processing. Second, plating bacteria (BNN 132) were prepared. From BNN 132 cells grown on kanamycin plates (25µg/ml), a single colony was transfered into LB++ medium and plating bacteria prepared as described for C600. Third, infection with purified phage. 20µl of the purified phage stored in SM/Chloroform were added to 100µl of the BNN132 plating bacteria. Phage-bacteria mixes were then incubated at 37°C for 30 min, plated onto ampicillin plates (50µg/ml) and incubated overnight at 37°C. Single colonies were picked and separately grown to saturation by vigorous agitation (250 cycles/ minute) in rotary shakers at 37°C. Forth, plasmid DNA was isolated using standard protocols (section 2.2.8).

2.3 ES cell culture techniques

2.3.1 Routine culture of ES cells

ES cells were maintained in GMEM BHK-21 supplemented with non-essential amino acids, sodium pyruvate, L-glutamine, 10% foetal calf serum (Life Technologies) β-mercaptoethanol (Sigma) and leukaemia inhibitory factor. $0.3x10^6$ cells/well were seeded in gelatinised 6 well plates (Greiner Laboratories) and propagated at 37°C in 5% CO_2, in a humidified atmosphere of 5% O_2, 95% air. Medium was changed every day or every other day.

Gelatinisation of tissue culture plates

Swine skin gelatin (Sigma) was made up to 1% in dH_2O, double autoclaved and stored at 4°C (equivalent to a 10x stock solution). A sufficient volume to cover the entire base of tissue culture plate/wells was added and left for a minimum of 10 minutes at room temperature to gelatinise the tissue plates, which were then ready for plating with ES cells.

Passaging ES cells

ES cells were routinely passaged 1 in 5 upon reaching approximately 70-80% confluency. Culture media was refreshed approximately 3 hours prior to passaging cells by aspiration of medium and washing with an equal amount of warm PBS (Life Technologies). PBS was subsequently aspirated, pre-warmed 1% trypsin/EDTA (Gibco-BRL) added to cover the entire base of the tissue culture plate, and plates incubated for 2-3 minutes at 37°, with occasional agitation. The side of the flasks/plates were tapped to confirm, under magnification, that cells have detached from the gelatin to form a cell suspension. The trypsin was neutralised by promptly adding a minimum of 2 volumes of media, the cells diluted with medium as appropriate and transferred to a freshly gelatinized flask. Media was refreshed 3 hours after passaging to remove any debris from the trypsinisation process.

Freezing ES cells

Following trypsinisation, ES cells were centrifuged at 1,100 rpm for 3 minutes. Media was aspirated and the pellet resuspend in an appropriate volume of Freezing Media (FM). 1ml of FM-ES cell suspension was aliquoted into an appropriate number of Cryovials, as detailed in table 2.3, that were subsequently placed at -80°C overnight. The following day, cryovials were transferred to liquid nitrogen storage.

Table 2.3

Plate area	Volume of FM	To Fill No. of Cryovials	Area to Re-thaw Into
24-well	800µl	1	24-well
6-well	800µl	1	6-well
25cm^2	1.6µl	2	6-well
75cm^2	6.5µl	8	6-well
175cm^2	13µl	16	6-well

Thawing frozen stocks of ES cells

Cryovials containing cells were removed from liquid nitrogen or -80°C storage and thawed rapidly (with agitation) in a 37°C waterbath. The cryovial contents were diluted in 10x volume of culture medium and spun immediately at 1,100 rpm for 3 minutes. The medium was aspirated and the pellet gently resuspended in 1-2ml medium, using a pastette. Resuspended cells were diluted in a volume of culture medium appropriate to the area of tissue culture plate to be used (1ml=24-well plate; 3ml=6-well plate; 5ml=25cm^2 flask), and the media refreshed 3 hours post plating.

Estimating ES cell concentration

To ensure equal numbers of wild-type and p53-/- ES cells was plated prior to experimental treatments, the approximate concentration of cells were estimated using

a rinsed, dried hemocytometer with an added cover slip. ES cells were trypsinised, neutralised with 10ml medium and transferred to a Universal tube. 10µl trypsinised cell suspension was removed and added to a cryotube containing 80 µl PBS, 10µl tryphan blue (Sigma). The suspension was mixed by pipetting, and 10µl of the tryphan blue-cell suspension mixture transferred to the underside of the coverslip. Under magnification, the total number of cells in each of the central and four corner squares was recorded - the mean of these five values was taken to represent the number of cells $x10^5$ / ml.

2.3.2 Vector preparation and electroporation of ES Cells

Targeting vectors were linearised and confirmed by gel electrophoresis. The DNA was precipitated (section 2.2.4) and the pellet dried under sterile conditions. 0.6ml sterile PBS was added and the pellet resuspended by tapping the tube and incubating at 55°C. Following trypsinisation, ES cells were centrifuged in a volume equivalent to 10^8 cells at 1,100 rpm for 3 minutes. The medium was aspirated, making sure the pellet was not disturbed, which was then carefully resuspended in 0.6ml of the vector in PBS, and transferred to an electroporation cuvette (Bio-Rad). The cuvette was capped and pulsed with a charge of 0.8kV, 3µF capacitance, which resulted in a time constant of 0.1 seconds (Bio-Rad Gene-Pulser). Electroporated cells were added to 100ml of non-selective culture medium, mixed and 10ml cells plated on ten 10cm gelatinised plates (resulting in a density of $1x10^6$ cells per plate which is appropriate to permit selection the following day with G418 and gancyclovir).

2.3.3 Selection and picking of ES cell clones

24 hours after electroporation, the non-selective CM was replaced with selective CM containing 1x gancyclovir and 200µg/ml G418 (Gibco-BRL). Selective media was refreshed every 3 or 4 days until colonies of G418 and gancyclovir-resistant clones became visible to the eye (usually within 12-13 days post-electroporation). A 96 well plate containing 100µl of trypsin-EDTA in each well was prepared. Selective media was aspirated from the 10cm plates, cells washed with 1x in PBS and partially aspirated to leave a residual volume of PBS sufficient to cover the base of the tissue culture plate. This measure prevented dehydration of clones during picking. A p200

tip was placed over a single G418 and gancyclovir resistant ES cell clone, and gentle suction applied to take the clone up into the pipette. Clones were pipetted into a trypsin-EDTA containing well of a 96-well plate and left for 2-5 minutes at room temperature. Full resuspension of clones was confirmed under phase contrast microscopy, prior to transfer into a single gelatinised well of a 24-well plate containing 1ml of non-selective CM. Clones were subsequently refreshed with non-selective CM on a daily basis.

2.3.4 Preparation of ES cell DNA for analysis

This protocol is essentially identical to that published (Laird et al., 1991). Following trypsinisation, ES cells were centifuged at 1,100 rpm for 3 minutes, washed x1 in PBS and re-centrifuged at 1,100 rpm for a further 3 minutes. PBS was partially aspirated leaving sufficient residual PBS to cover the pellet. The side of the tube was flicked until the pellet was resuspended in this volume. 500µl Lysis Buffer was added, incubated at 55°C for 3 hours prior to addition of 500µl isopropanol. DNA was precipitated by agitation on an orbital shaker for 30 minutes and carefully removed using a fine glass hook made from a Pasteur pipette. DNA was washed once in 70% ethanol, transferred to an eppendorf tube containing 100µl TE buffer and incubated at 60°C for 30 minutes to achieve evaporation of any trace residual ethanol. DNA was resuspended by adding 30µl dH_2O and incubating at 50°C overnight, before storage at 4°C.

Derivation of p53-null embryonic stem cells by high G418 selection

The p53-/- ES cell line HG287 was derived from the hemizygous line R72 by high G418 selection (Mortensen et al., 1992) R72 cells were previously derived from E14 (Hooper et al., 1987a) by targeting the p53 locus with a neomycin resistance cassette (Clarke et al., 1993).

2.4 Experimental treatment of ES cell cultures

The different treatments used in this study to modulate intracellular GSH levels and cause oxidative stress are prepared and administered as described (sections 2.4.1 and 2.4.2).

2.4.1 Pre-treatments of ES cell cultures

2.4.1.1 BSO

50mM stock solutions of BSO (DL-Buthionine -[S,*R*]-sulfoximine, Sigma) were prepared by dissolving 11mg BSO in 1ml dH_2O under sterile conditions. Unless otherwise stated, BSO was diluted in complete medium to a final concentration of 100μM. BSO was added 3 hours after passaging ES cells and incubated for 16 hours. At the end of the pre-treatment, the BSO-containing medium was discarded and the cells rinsed once with warm PBS. The cells were then exposed to the experimental treatment.

2.4.1.2 DEM

Using sterile technique, a 56mM DEM (Diethyl maleate, Sigma) stock was prepared by adding 1ml undiluted commercial DEM to 99ml dH_2O. Unless otherwise stated, DEM was diluted in complete medium to a final concentration of 20μM, incubated and administered identical to BSO.

2.4.1.3 GSH-MEE

Using sterile technique, GSH-MEE (Glutathione-monoethyl ester, Sigma) was dissolved in PBS to make a 100mM stock. Stocks were made fresh on the day of use and used immediately, or frozen. The administration and incubation of GSH-MEE was identical to BSO.

2.4.1.4 NAC

Using sterile technique, NAC (*N*-acetyl cysteine, Sigma) was dissolved in PBS to make a 100mM stock, and equilibrated to pH7.2 with NaOH. Stocks were stored at 4°C and used within 1 week of preparation. Unless specifically stated in the text, administration and incubation of NAC was identical to BSO.

2.4.2 Induction of oxidative stress

To identify a suitable oxidative stress-inducing agent that could be used to investigate the role of GSH and p53 in ES cell viability and death, five different oxidative stress-inducing agents were tested in ES cells. These were hydrogen peroxide, UVC-radiation, menadione and tBHQ.

At approximately 60% confluency, the medium was replaced with normal medium, or medium containing 100μM BSO (Sigma) and incubated for 16 hours. At the end of this pre-treatment the medium was discarded and the cells rinsed once with warm PBS. Aside from UV-C (section 2.4.2.4), all oxidative stress-inducing stimuli were applied as a solution in serum free (SF) culture media. All other medium components remained unaltered. Medium containing stress agents were prepared on the day of use and maintained at 37°C prior to application. Preceeding application, plates were rinsed twice with PBS to remove any traces of antioxidant-containing serum. Unless otherwise stated, all oxidative stress-inducing solutions were incubated with the cell culture for 1 hour. Following treatment, cells were rinsed twice with warm PBS and incubated with complete media until analysis.

2.4.2.1 Hydrogen peroxide

The concentration of undiluted hydrogen peroxide (H_2O_2) commercial solution (Sigma) was calculated from the molecular weight to be 8.8M. Each time this reagent was required, a 750mM stock was made by adding 0.6ml 8.8M H_20_2 to 4.4ml dH_2O. This was diluted, as a single bolus injection, to the required final concentration in SF medium.

2.4.2.2 Menadione (MQ)

A 100mM stock solution was prepared by adding 17mg MQ (2-Methyl-1,4-naptho-quinione, Sigma) to 1ml DMSO in an eppendorf, before incubation at 37°C with occasional vortexing. MQ stocks were prepared fresh at time of experimental use. Unless otherwise stated, the MQ stock was then diluted in SF media to a final concentration of 35μM. In high enough concentrations DMSO is itself toxic. Therefore, controls containing the same percentage of DMSO as that in the drug dilutions were included in each experiment.

2.4.2.3 tBHQ

A 100mM stock solution was prepared by adding 16mg tBHQ (*tert*-butyl hydroquinone, Sigma) to 1ml DMSO in an eppendorf, before incubation at 37°C with occasional vortexing. Stock tBHQ was diluted in SF media to working concentrations as required.

2.4.2.4 UV-irradiation

UVC-irradiation was performed at 254 nm using a Spectrolinker XL-1500 (Spectronics Corp.). The UVC-irradiation cabinet was previously tested for accuracy and recalibrated (S. Corbet, personal communication). At this time, the irradience was noted to be non-uniform across the floor of the delivery chamber. The highest irradience was in the centre of the chamber (5.58 m Wcm^{-2}), and this fell to almost half (2.92 m Wcm^{-2}) at the edges. By using only the central region (a square 20cm x 20cm) of the chamber this variation was shown to be restricted to less than 15%. Since the doses used were small, it was necessary to use an attenuator to achieve the appropriate irradience. Suitable attenuators were made from multiple layers of thin, semi-opaque plastic and were used in all subsequent experiments. These were suspended 4cm above the cell cultures and extended to the walls of the cabinet so as to prevent light leakage. The transmission, at 254nm, of an attenuator consisting of two layers of plastic was found to be $5.6x10^{-3}$ *(*+/- 5%) and a three layered attenuator $4.6x10^{-4}$ (+/- 5 %).

To ensure that the irradience was consistent from one dose to the next, the machine was pre-warmed for two minutes prior to irradiation. Immediately prior to irradiation the medium was aspirated, and the cells washed twice with PBS. Plates were then positioned in the center of the Spectrolinker, and the base plate exposed by removal of the cover plate before irradiation for the required time. Upon completion, the media and cover plate were replaced and whole plates replaced in the incubator.

2.4.3 Analysis of the effects of oxidative stress

2.4.3.1 Quantitation of sample protein concentration

This assay involves the formation of a colourimetric complex between bicinchonic acid and proteins whose absorbance can be read at 570nm (Bradford, 1976). This assay comes in the form of the "Bio-Rad Protein Assay" kit (Biorad). Note: samples used to measure GSH concentration were also used to determine protein concentration.

A sufficient volume of 5X assay reagent was diluted to 1X with dH_2O to provide 1ml reagent per protein standard/protein sample. Bovine serum albumin (NEB) was diluted to 5µg, 10µg, 15µg, 20µg, 25µg and 50µg in the same buffer as the sample, and used to generate a standard curve each time experimental samples were measured. 200µl 1X assay reagent was added to 10µl sample in a 96 well plate and left for 15 minutes at room temperature. The absorbence was recorded at 595nm on a multiwell plate reader. The protein concentration of each sample was calculated by comparing the absorbance with the recorded absorbencies of the known protein standards.

2.4.3.2 Intracellular total reduced glutathione (GSH) levels.

The main methods to measure the GSH concentrations of cells rely on HPLC (*h*igh *p*ressure *l*iquid *c*hromatography), flow cytometry or an enzymatic spectrophotometric shift. Here they are briefly discussed with reference to their benefits and limitations. Other techniques to measure GSH, such as a colourimetric

system (reviewed in (Floreani et al., 1997)), were not considered due to inconsistent results obtained.

One, HPLC. This technique relies upon passage and elution of cell extracts through a HPLC column. Detection is mediated by a GSH-specific dye such as *m*ono*c*hloro*b*imane (MCB), which fluoresces upon reaction with GSH. GSH is bound to a molecular tag, which ultimately permits either UV or electrochemical detection. The process is widely used and generally considered accurate. However, others have obtained non-physiological levels of glutathione (Sian et al., 1997) or found GSH depletion underestimated with MBC/HPLC (Ublacker et al., 1991). Furthermore, it is also slow (approximately 30 minutes/sample) and relatively expensive. Therefore HPLC was not selected for use in this investigation.

Two, flow cytometry. This process passes individual live cells through a laser beam, which detects fluoroescent GSH-MCB complexes. After extensive callibration, this technique is relatively rapid. Using this approach, it is possible to determine the GSH levels in multiple subpopulations of cells (Shrieve and Bump, 2001; Lee et al., 1989). For example, with suspensions of enzymatically digested solid tumours it can reveal the GSH content not only of transformed cells, but also stromal and immune cells that may be present. However, it can be difficult to obtain rigorous quantitative data with this approach (Cook et al., 1991). Since undifferentiated ES cells are the single cell type in this study and tissue culture (unlike the situation *in vivo*) ensures all cells receive homogenous treatment, there is no advantage in employing flow cytometry in this study.

Three, spectrophotometric enzyme assay. This assay was originally described by Tietze (Tietze, 1969). The assay involves the recycling of GSH by glutathione reductase (GR, Sigma) and β-nicotinamide adenine dinucleotide phosphate (NADPH, Sigma) as occurs *in vivo,* i.e. the glutathione redox cycle (see section 1.3.1.1). The procedure measures total intracellular glutathione (reduced and oxidised). In the presence of 5,5'dithio-bis-2-Nitrobenzoic acid (DTNB, Sigma), a compound which binds to thiol groups and forms a complex with an absorbance at

412nm, the amount of GSH which is produced during this cycle can be calculated by computer-driven analysis of 96 well plates. The Tietze mechanism is outlined below, where oxidised and reduced are indicated by Ox-DTNB and DTNB, respectively. Glutathione mixed disulphides are represented by DS-GSH.

$$\text{GSH} + \text{Ox-DTNB} \rightleftharpoons \text{DS-GSH} + \text{DTNB}$$

$$\text{GSH} + \text{DS-GSH} \rightleftharpoons \text{GSSG} + \text{DTNB}$$

$$\text{GSSG} + \text{NADPH} + \text{H}^+ \xrightleftharpoons{GR} 2\text{GSH} + \text{NADP}^+$$

DTNB is present in higher concentration than for the GSH assay so that the background is rapidly reached and any further absorbance is due only to GSH. The rate of formation of the DS-GSH complex is directly dependent on the concentration of GSH present in the sample. One limitation of the Tietze method is that it cannot be used to measure GSH in a heterogenous cell-type sample. However, this is not an issue with the homogeneity provided by the culture of ES cells. Despite the radically different approaches used to determine intracellular GSH levels, reports comparing GSH levels obtained by Tietze, flow cytometry and HPLC generally agree closely. For example, rates of GSH depletion in Chinese hamster ovary cells exposed to DEM were essentially the same using these three techniques (Rice et al., 1986). The Tietze approach is economical, rapid and sensitive. Moreover, since it is the most established of the techniques currently available - being used with numerous cell culture systems, the Tietze protocol was chosen to monitor GSH levels in ES cells.

Total glutathione was measured since this value represents both the oxidised and the reduced form of glutathione. The total figure gives an estimate of the available pool at any one time, which includes newly synthesised GSH, and potential GSH recovery via the GR-catalysed recycling of GSSG. Whilst this approach does not give GSSG detail, it provides an overall estimation of the effect MQ has on intracellular glutathione levels.

Cell culture treatment

Media was removed, cells rinsed thoroughly with PBS, trypsinised and neutralised. Resuspended cells were transferred to a 1.5ml eppendorf tube and spun at 3,000rpm for 5 minutes. Pellets were resuspended in PBS, spun at 3,000rpm for 5 minutes and all but approximately 100µl of the supernantent discarded, before storage of pellets at –20°C. Pellets were thawed slowly on ice before addition of 0.5ml of ice-cold 0.6% SSA/0.01% triton x-100 and cell lysed with freeze-thawing and repeated vortexing. Lysed samples were spun at 600 g for 5mins at 4°C, and stored at -20°C for up to 4 weeks.

GSH analysis

Samples were thawed on ice and keep on ice at all times to minimise auto-oxidation of GSH in air. To analyse 8 different samples, the following quantities of the two mixes were prepared:

GR/KPE mix		NADPH mix	
GR/KPE	2ml	NADPH/KPE	2ml
DTNB/KPE	2ml	KPE	4ml
KPE	8ml		
Total	12ml	Total	6ml

20µl each GSH standard (made up in 0.6% SSA and 0.01% triton) in the region of 0.167-2.5 nmoles were added on one side of a 96 well plate. Subsequently, 20µl of each sample was added in triplicate to separate wells. Lastly, 120µl DTNB/GR mix (8 units/ml GR: 0.4mg/ml DTNB) was added to all wells using a multi-pipettte and mixed. Plates were left at 25°C for 30 seconds so that any other low molecular weight thiol compounds could bind with the DTNB. 60ml NADPH mix (0.4mg/ml) was added to all wells and the change in absorbance at 412nm recorded using a Dynex-TC Multiplate reader. A standard curve was plotted for each plate using the GSH standards and linear regression used to estimate the GSH concentration of the samples. All results were expressed per mg of total protein present in the supematant.

2.4.3.3 Quantitation of apoptosis by acridine orange staining

A variety of techniques have developed to assess the level of apoptosis occurring in tissue cultured in the laboratory or removed from an organism. They fall into two broad categories: those that observe the defining attributes of apoptosis and those that measure associated, biochemical events. The positive and negative aspects of these approaches are briefly outlined.

The basis of detection via TUNEL (*T*dT-mediated X-d*U*TP *n*ick *e*nd *l*abelling) or ISEL (*in s*itu *e*nd *l*abelling) relies on identifying the 3' hydroxyl-termini of DNA strand breaks, characteristic of endonuclear cleavage (Drachenberg et al., 1997). TUNEL and ISEL have been used predominantly in histological samples, though reports of false positives or negative findings with these approaches are not uncommon. TUNEL in particular is sensitive to many parameters that require painstaking calibration, a process which does not always limit high degrees of variation (Saraste, 1999; Saraste and Pulkki, 2000). Despite recent advances, these techniques are yet to overcome these limitations.

An alternative protocol using strand breaks to identify apoptosis is DNA Laddering (Itoh et al., 1995). This approach works by running DNA extracted from cells on agarose gels – a characteristic laddering of the bands signifies nuclear degradation, a hallmark of apoptosis. Whilst this technique is usually a reliable indicator of apoptosis occurring, it is not sufficiently sensitive to produce quantitative data. Furthermore apoptosis can sometimes generate only high molecular weight DNA fragments (Susin et al., 1999) or, on occasion, not produce any obvious DNA laddering (Clarke, personal communication). For this reason DNA laddering was not used to detect ES cell rates in response to oxidative stress.

Other biochemical features associated with apoptosis include caspase activity, mitochondrial dysfunction, Ca^{2+} ions flux and phospholipid membrane alterations. For example, opening of the plasma membrane exposes phosphatidylserine (PI), which is localised in the inner leaflet of the membrane of many non-apoptotic cells (Fadok et al., 1992). Annexin V is a phospholipid binding protein with a high affinity

for PI. To measure the appearance of PI, vindelov flow analysis has been utilised in conjunction with labelled annexin V. This immunological approach offers detection of early apoptosis, prior to the external cellular features becoming apparent. Furthermore, vindelov flow analysis can enable the investigation of a large number of cultured cell types in a short time. However some cell types, including embryo myoblasts and embryonic megakaryoblasts, express PI on their cell surface when not undergoing apoptosis (Van den Eijinde et al., 1997) (Poelmann et al., 1998; Wang et al., 1999).

It is also possible to use EM (*e*lectron *m*icroscopy) to detect apoptosis by directly observing cellular morphology. This offers the advantage of accurately noting the subcellular features of apoptosis. Despite this attractive specificity, EM is cumbersome for large numbers of cells and is therefore very inefficient at producing quantitative information (Gorman et al., 1996).

A technique that can provide both morphological confirmation of apoptosis and quantitative data regarding apoptotic rates is the examination of fixed cells with light microscopy. Acridine orange is a metachromatic fluorochrome that differentially stains double stranded versus denatured DNA. The dye is an intercalating agent that, on excitation with UV light, emits green light when bound to double-stranded DNA and red light when bound to denatured DNA. The nucleus of a stained cell thus appears green under UV light whilst the cytoplasm stains red. Such staining permits for the detection of cells undergoing apoptosis by direct examination of nuclear morphology, outlined below. Endogenous phagocytosis reduces this techniques' sensitivity with tissue samples, however for use with cultured cells it remains a gold standard (Walsh et al., 1998; Saraste, 1999; van et al., 2000). For these reasons, morphological criteria were chosen as the method of choice in evaluating the response of ES cells to redox imbalance.

At six hours post treatment media was removed by pipette, and cells washed in warm PBS which was also removed by pipette. Both media and PBS washes were retained in a 15ml conical tube. Cells were trypsinised and centrifuged at 220g for 10 minutes

at 4°C, together with the retained medium and PBS from the pre-trypsinisation wash. The supematant was discarded, the pellet resuspended by flicking the tube gently and spun again. This wash was repeated once more before resuspension of the pellet in 0.5ml PBS, 1ml ice cold fix (90% ethanol, 10% formaline). Cell suspensions were stored in this form at 4°C for a maximum of 8 weeks. Prior to counting, cells were washed twice and resuspended in 1ml PBS. 10µl of the cell suspension was dropped onto a clean glass slide. An equal volume of acridine orange solution (10µg/ml, Sigma) was dropped onto a coverslip and carefully lowered onto the slide. Cell morphology was observed under fluorescence microscopy (Leitz).

Identification of apoptosis

Cells displaying the classical appearances of apoptosis, including condensed chromatin, fragmented nuclei and smaller size were counted (Corbet et al., 1999). Clusters of very small apoptotic bodies were considered to have undergone fragmentation and were assumed to have derived from one cell. Spherical retractile bodies that occurred in pairs were suspected to be mitotic and, unless they were perfectly spherical and failed to exhibit anchoring pseudopodia, were ignored. A total of 200 cells were counted in each field. The prevalence of apoptosis in the fields was expressed as the number of apoptotic (non-mitotic, retractile) bodies as a percentage of the number of live cells per field ("percentage apoptosis").

Due to the clear and consistent data provided by this approach (see section 5.8), a secondary confirmation of apoptotic cell death was not deemed a prerequisite. Additionally, it should be borne in mind that identification of apoptosis by a single biochemical attribute associated with it has inherent limitations. In contrast, the visual examination of cells made it possible to discriminate genuine apoptosis (as histologically defined) from such molecular alterations.

2.4.3.4 Estimation of immediate cell viability with the MTT assay

ES cell viability was determined by the *m*odified *t*etrazolium salt 3-(4-5-dimethylthiazoyl-2-yl) 2-5-diphenyl-*t*etrazolium bromide (MTT, Sigma) assay as

described (Hansen et al., 1989). The following protocol was used for 6 well tissue culture plates (Greiner). Media was removed, cells rinsed with warm PBS and 450µl media/150µl MTT (5 mg/ml in PBS) added to each well. Samples were incubated for 3 hours at 37°C, washed once with PBS and left to dry in a fume cupboard. When completely dried, 1.5ml dimethyl formamide (DMSO) was added and the plates gently swirled to dissolve the crystals. From each well 20µl - 80µl DMSO and 100µl neat sample was transferred to a 96-well plate and the plated agitated to mix. the optical densities at 590 nm were measured using a multiscanner autoreader (Dynatech MR 5000), with DMSO as a blank. Only mean values that fell in the optical density range of 0.1-0.8, where reading is accurate, were recorded.

2.4.3.5 Estimation of long-term viability with the clonogenic survival assay

Following incubation in SF-media or incubation with oxidative stress-inducing agents cells were trypsinised, and the trypsin neutralised with two volumes of cell culture medium. An aliquot of cell suspension was removed and loaded onto a haemocytometer to (a) determine the cell density, and (b) confirm the suspension only contains single cells and not clumps. Cells were plated out in triplicate at densities of $3.5x10^3$, $3.5x10^4$ and $3.5x10^5$ cells per 10cm plate. Plates were maintained for 10 days and cells fed as appropriate. After 10 days, the medium was removed and the cells fixed in 70% ethanol. Plates were stained with 5% Giemsa (Sigma), and colonies counted.

2.5 Statistical methods

All results were analysed using the statistical software package SigmaStat (SPSS), version 2.03. When comparing two groups Normality and Equal Variance are automatically tested. Where these criteria are met parametric (unpaired *t*) tests were applied, where these criteria were not met non-parametric (Mann Whitney rank sum) tests were applied. In instances where more than two simple comparisons were tested, a one way ANOVA analysis of variance was additionally employed with the Tukey Test, a conservative pairwise multiple comparison procedure.

Chapter 3

Cloning and characterisation of *γGCSh*

3.1 Introduction

A principal project aim was to characterise the role of γGCSh *in vitro* and *in vivo*. To this end, a targeted disruption of *γGCSh* was planned, an approach that relies upon the insertion of foreign sequences at specific loci to inactivate the gene of interest. To achieve efficient homologous recombination between exogenous DNA and endogenous loci, the sequences must be as similar and long as possible (see section 4.2.2). During the course of this project, mouse *γGCSh* genomic sequence was not in the public domain. Therefore the first requirement was to isolate a substantial section of the mouse *γGCSh* gene. This is routinely achieved via screening of genomic libraries with related DNA as a probe.

3.1.1 Recombinant DNA libraries

Recombinant libraries consist of a large number of DNA clones, each of which contains a different segment of foreign DNA. Since only a few of the thousands of clones in a library encode the desired nucleic acid sequence, the investigator must devise a procedure for identifying the desired clones. The optimal procedure involves a positive selection for a particular nucleic acid sequence. If the desired clone confers a phenotype that can be selected in bacteria, then it can be isolated under selective conditions. However, most eukaryotic genes do not encode proteins with a selectable function. Clones encoding nonselectable sequences are identified by screening libraries: the desired clone is identified either because it hybridises to a nucleic acid probe or because it expresses a segment of protein that can be recognised by an antibody (Schroder and Thorpe, 1987).

Screening libraries requires an assay to identify and purify clones containing the desired sequence (figure 3.1). This procedure is normally carried out on bacterial colonies containing plasmids, cosmids, bacteriophage plaques or by PCR on artificial

chromosomes. To test a large number of clones at one time, the library is spread out on agarose plates, then clones are transferred to nitrocellulose filters (see section 2.2.13). The clones can be simultaneously hybridised to a particular probe (see section 2.2.14) or bound to antibody.

3.1.2 Attempted isolation of the murine *γGCSh* gene using human cDNA

To screen a genomic DNA library, the selection procedure must first be chosen. Although mouse *γGCSh* cDNA was unavailable, full length human *γGCSh* cDNA had been previously cloned (Gipp et al., 1992). This was kindly provided (Dr C Smith) and used to probe the mouse genomic bacteriophage lambda (λ) 2000 library. Three attempts were made. Although initial screening of primary filters was successful (data not shown), each time, at the point of developing the secondary screen, no signal was recorded. The cause of this was not established.

3.2 Isolation of murine γGCSh cDNA

In consideration of the inability to progress beyond the primary screen of λ2000 using human *γGCSh* cDNA, this system was discarded and alternative systems investigated. Current gene isolation is predominantly accomplished in either recombinant bacteriophage libraries, such as λ2000, or BAC (*b*acterial *a*rtificial *c*hromosome) libraries. Typically, a BAC clone will contain up to 100kb whereas λ clones carry 15kb. To minimise the extent of characterisation required prior to construction of a suitable targeting vector, an alternative mouse bacteriophage library was screened. To identify clones, mouse *γGCSh* cDNA sequence was isolated for use as probe.

Figure 3.1 Flow chart for screening DNA libraries

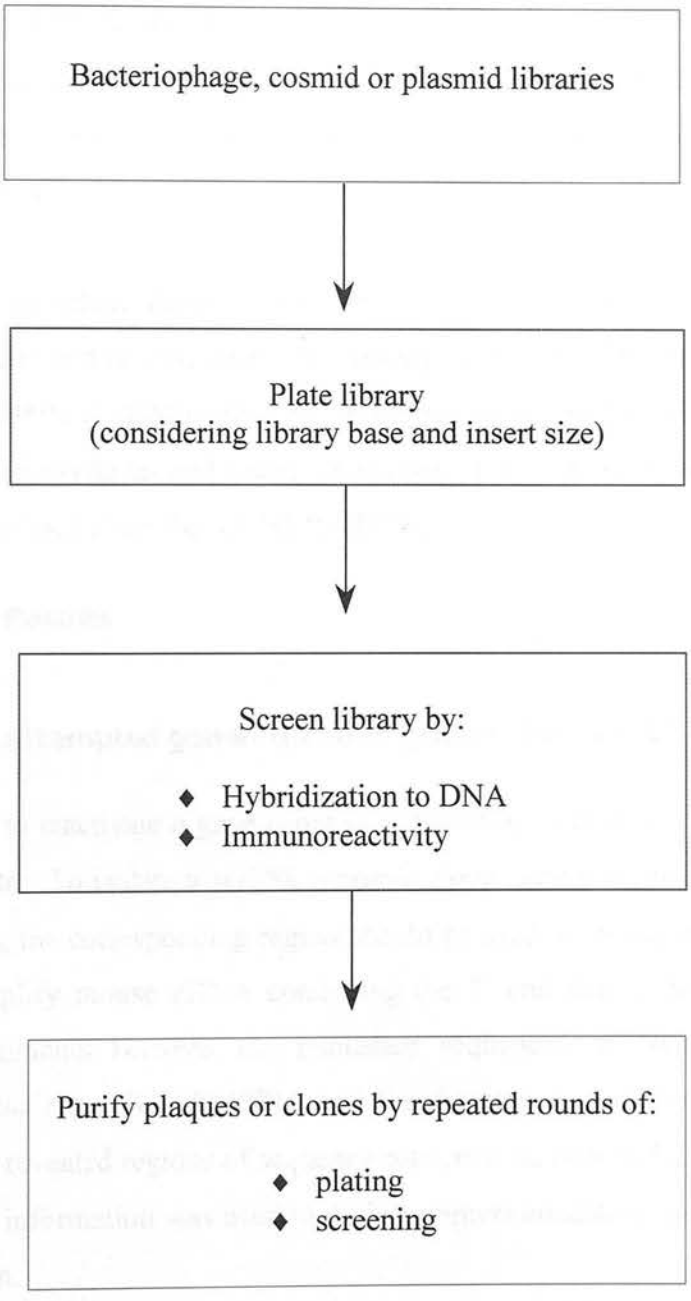

3.2.1 Strategy

There are two main approaches to clone a particular cDNA of interest. One is to screen a cDNA library with a sequence related to the target sequence. The second approach relies on reverse transcriptase (RT)-PCR to amplify mRNA from the target species, using primers designed on related sequences. Due to the problems encountered using human *γGCSh* cDNA as a probe with the λ2000-library, the RT-PCR strategy was selected. This approach first requires selection of the tissue from which to extract RNA.

Though all mammalian tissues contain GSH, the liver contains high levels of intracellular GSH and is considered the primary source of GSH for export (Deneke and Fanburg, 1989). Consequently, cells of hepatic origin are hypothesised to have a high rate of GSH synthesis and strong expression of *γGCSh*. Liver was therefore the site chosen to extract RNA for *γGCSh* RT-PCR.

3.2.2 Results

3.2.2.1 Attempted generation of 5' γGCSh cDNA by RT-PCR

One approach to inactivate a gene using gene targeting is to delete the transcription (ATG) start site. To isolate a *γGCSh* genomic clone containing this motif, a cDNA probe spanning the corresponding region should be used. In consideration of this, an attempt to amplify mouse cDNA containing the 5' end was undertaken. Multiple sequence alignments between the published sequences of *Homo sapiens* [GI: 3747102], *Ratus ratus* [GI: 204281] *and Saccharomyces cerevisiae* [GI: 218428] γGCSh cDNA revealed regions of sequence conservation (figure 3.2). To amplify the 5' region, this information was used to design primers annealing to the start site and a central region.

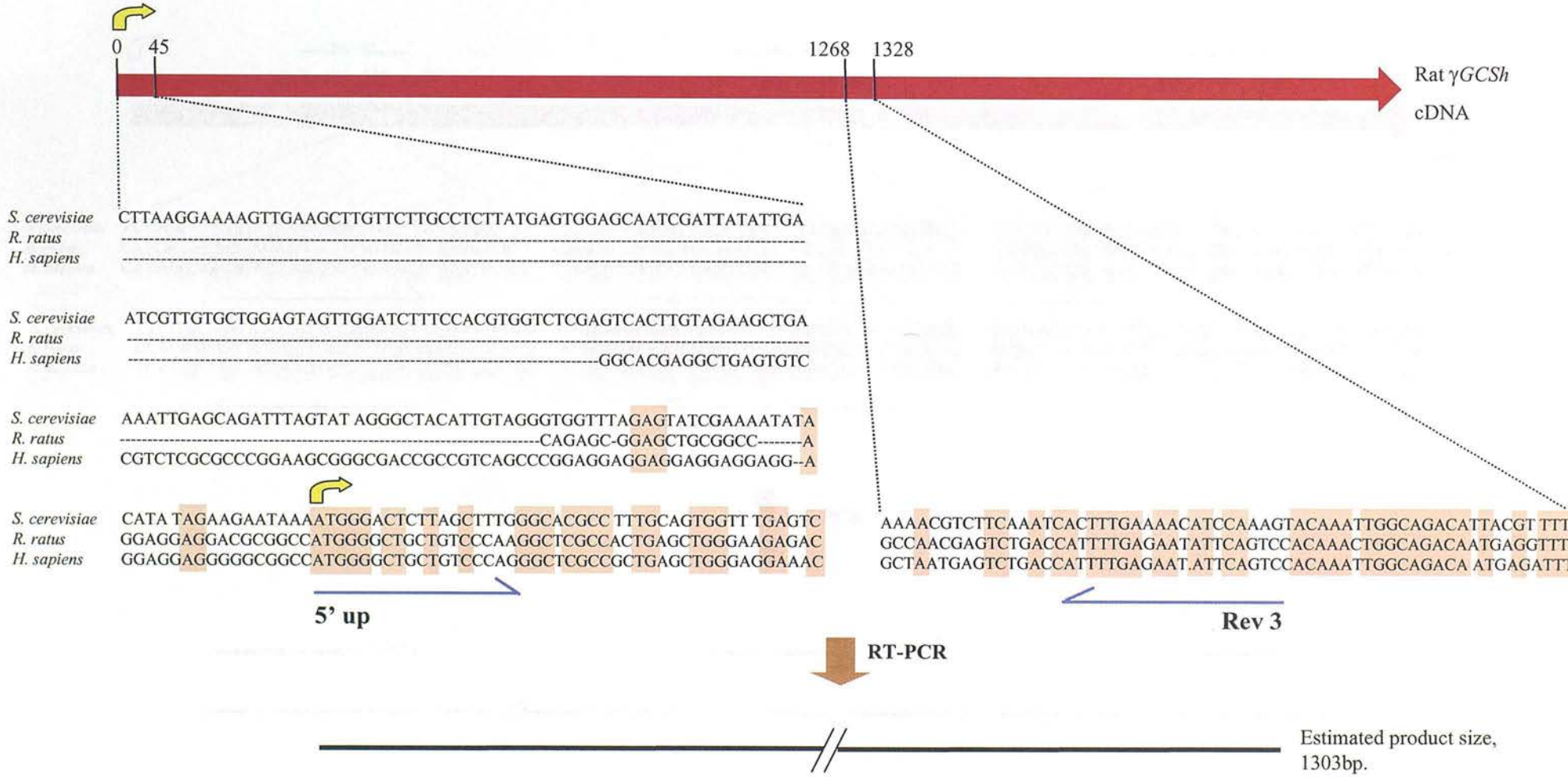

Figure 3.2 RT-PCR strategy to amplify 5' region of mouse *γGCSh* cDNA.

Top red arrow; representation of complete rat *γGCSh* cDNA (not to scale). Central text; multiple sequence alignment between *Saccharomyces cerevisiae, Homo sapiens*, and *Ratus ratus γGCSh* cDNA showing detail of nucleotide conservation, annealing location of PCR primers and, bottom, estimated size of corresponding 5' RT-PCR product. Yellow arrow defines transcription start site.

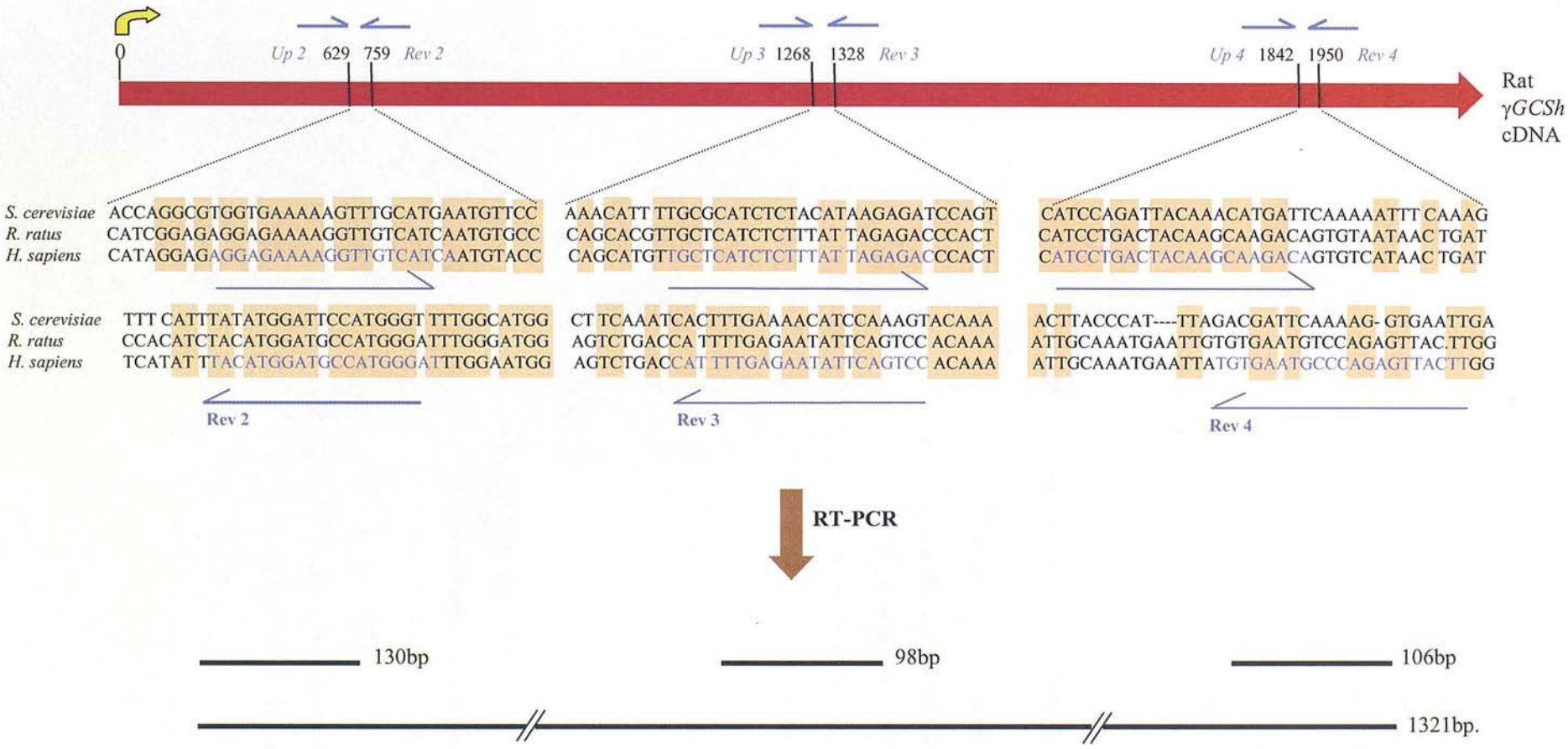

Figure 3.3. RT-PCR strategy to amplify the central region of mouse *γGCSh* cDNA.

Top, red arrow represents complete rat *γGCSh* cDNA (not to scale). Central, multiple sequence alignment between *Saccharomyces cerevisiae, Homo sapiens*, and *Ratus ratus γGCSh* cDNA showing detail of nucleotide conservation, annealing location of PCR primers and estimated sizes of corresponding RT-PCR products. Yellow arrow defines transcription start site.

Total RNA was extracted from C57/BL6 mouse liver, reverse transcribed (section 2.1.3) and PCR performed as described in section 2.2.1. No specific product was generated (data not shown). To maximise the probability of this PCR reaction working, a High Fidelity PCR kit (Boehringer) was used (section 2.2.1). This combines the simultaneous use of a primary and a 3'-5' proofreading polymerase in one reaction, resulting in an error rate significantly lower than that of conventional PCR with *Taq* alone (Barnes, 1994). Of particular note, the use of a two-polymerase system also elevates the efficiency and yield of PCR assays (Frey and Suppmann, 1995). However, despite varying magnesium ion and cycle optimisation parameters (see section 2.2.1), the use of standard or High Fidelity PCR yielded no cDNA product (data not shown).

3.2.2.2 Generation of the central region of γGCSh cDNA by RT-PCR

To amplify an alternative segment of *γGCSh* cDNA, a degenerate RT-PCR strategy was devised. PCR primers were designed along the length of the cDNA in areas of inter-species sequence homology. By attempting to amplify separate sections of the molecule, this tactic served to maximise the prospect of generating *γGCSh* cDNA sequence. Figure 3.3 illustrates the positions and predicted sizes of primer combinations. Mouse liver RNA was then used as a template for the degenerate RT-PCR reactions, outlined in 2.2.1. The PCR products generated by this approach correspond to the predicted sizes and are shown in figure 3.4.

3.2.2.3 Cloning PCR products

All four amplified PCR products were subsequently cloned directly into the pTAg vector (figure 3.5). This pre-linearised vector contains single deoxythymidine (T)-overhangs at the 3' ends of the DNA, to receive single 3' deoxyadenosine (A)-overhangs generated by β-polymerases (Clark, 1988). The resultant cDNA-containing plasmids are detailed in Figures 3.6a and 3.7a. Liberation of the fragments by restriction digestion with *Xho* I and *Xba* I, described in section 2.2.2, confirmed subcloning of PCR products (figure 3.6b and 3.7 b).

Figure 3.4 Degenerate RT-PCR products

Agarose gel electrophoresis of mouse RT-PCR from primers designed on conserved *γGCSh* cDNA sequence. Numbers next to actual product indicate predicted cDNA sizes. *A*, Short PCR products. Lane 1, failed ATG (5') end reaction; lane 2, primers 2+2; lane 3, primers 3+3; lane 4, primers 4+4 and lane 5, negative control showing primer-dimers. *B*, Long PCR products. Lanes 1-3, Primers 2+4; lane 4, positive control amplifying the house-keeping gene β-actin and lane 5, negative control.

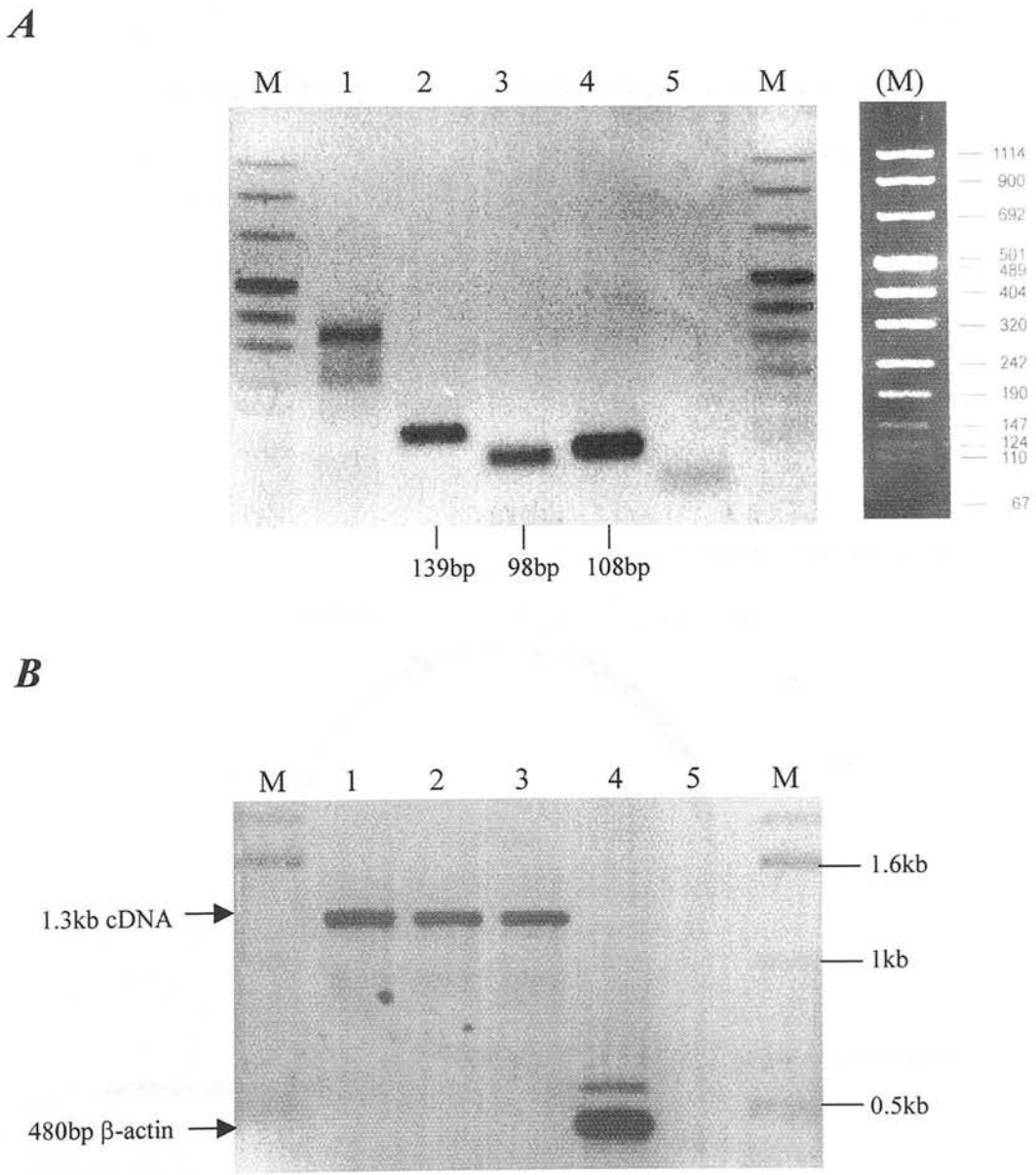

Figure 3.5 The pTAg plasmid

A, The linear, PCR-ready form with indicated A-overhangs and *B*, re-circularised.

A

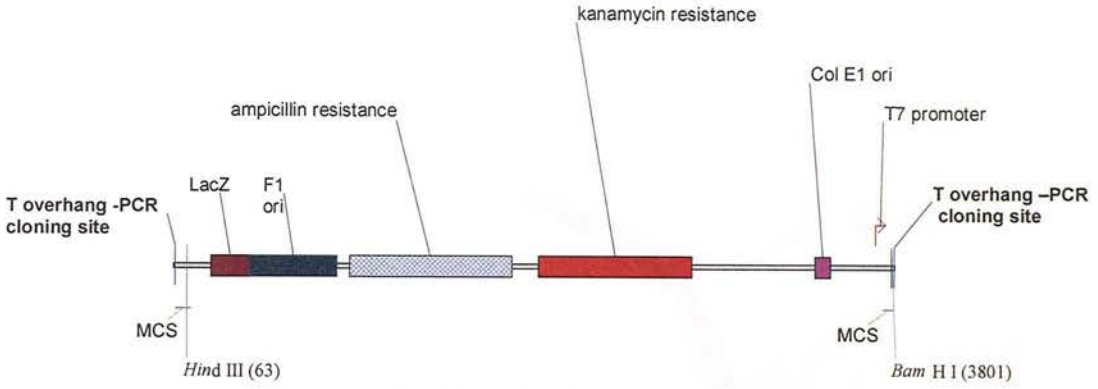

B

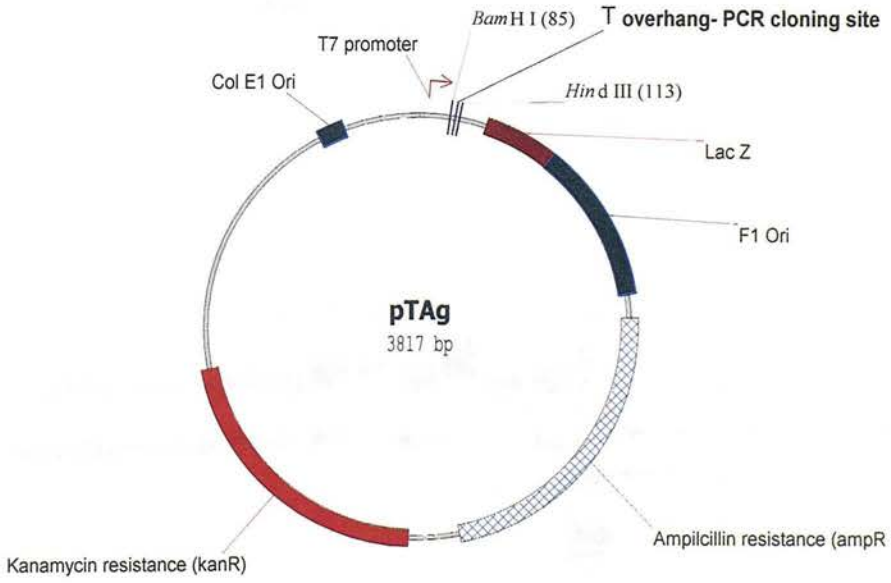

Figure 3.6 Cloning of 1.3kb RT-PCR product.

A, structure of cloned 1.3kb cDNA RT-PCR. *B*, Agarose gel electrophoresis of cloned RT-PCR products digested with *Eco* RI only. Lanes 1-3, 5 and 8 show 1.3kb cDNA liberated from pTAg; lanes 3, 6, and 7, no 1.3kb cDNA; lane 9, marker.

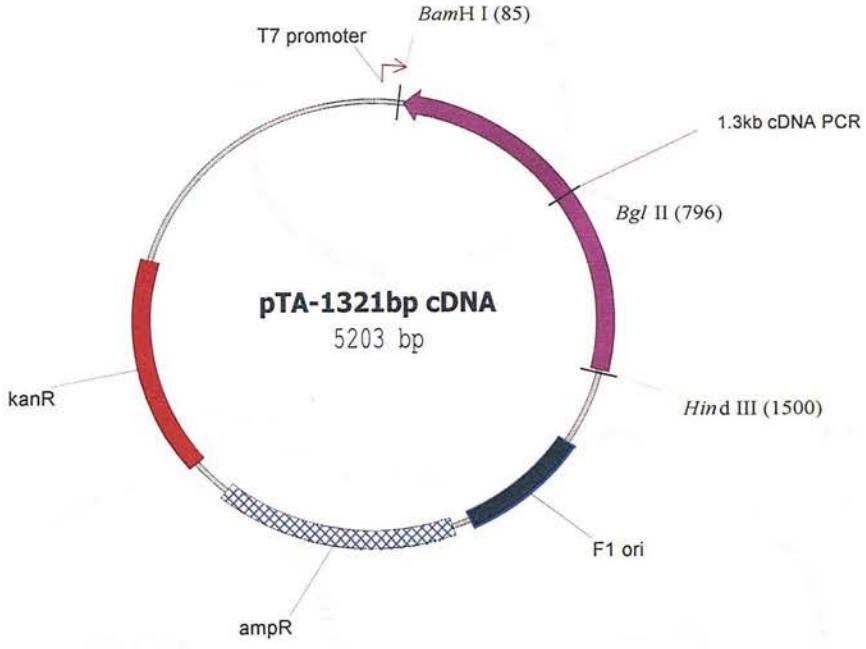

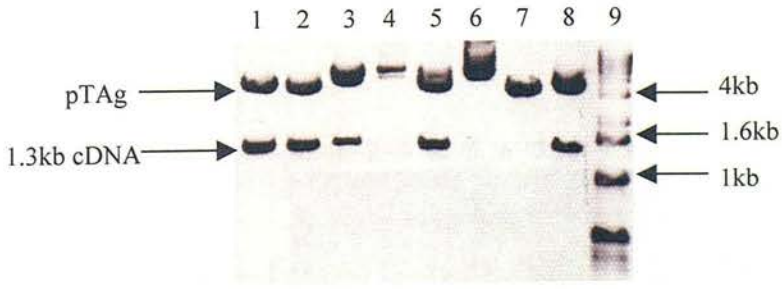

Figure 3.7 Cloning of small RT-PCR products.

A, structures of cloned small RT-PCR products. *B*, Agarose gel electrophoresis of cloned RT-PCR products. Lanes 1,3, 4 and 8 show the liberated cDNA fragments 108bp, 98bp and 139bp, respectively.

A

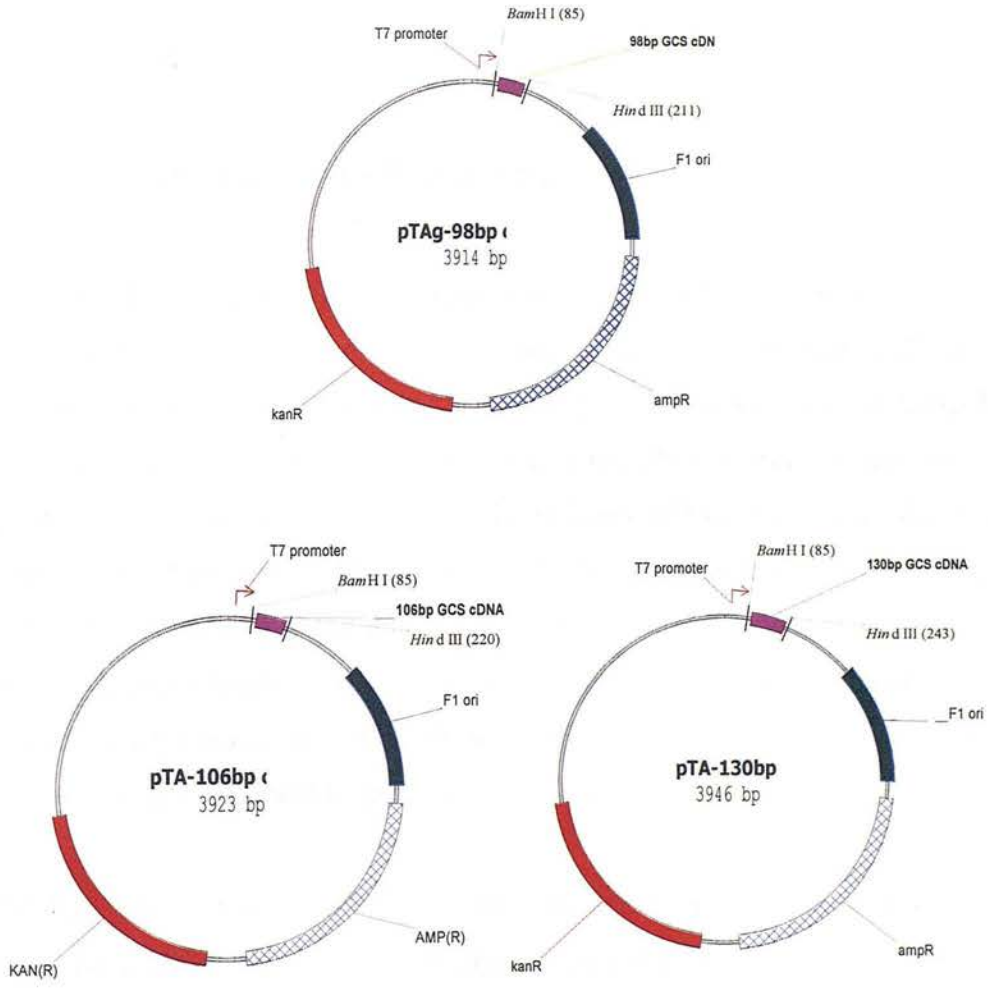

B

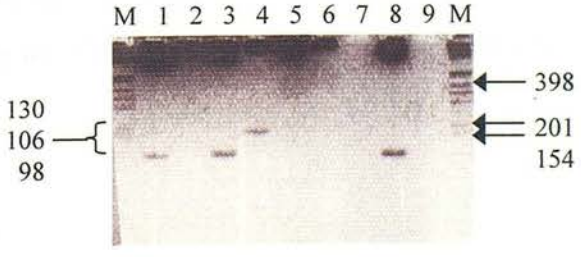

3.3 Characterisation of *γGCSh* cDNA

Section 3.4.1-3.4.3 describes the amplification and cloning of cDNA products of the size predicted by comparison with the *γGCSh* sequence of other species. Prior to screening a genomic library using this sequence as a probe, it was necessary to conclusively demonstrate that the DNA encoded *γGCSh* sequence.

3.3.1 Results

3.3.1.1 Confirmation of *γGCSh* sequence

(1) By restriction analysis. Human, rat and yeast *γGCSh* cDNA sequences all contain a single *Bgl* II and two *Pvu* II restriction endonuclease sites (not shown). These sites are in useful positions for examining the identity of the cloned mouse 1.3kb PCR product. Subsequently, published full-length mouse cDNA shows the exact sites and predicted sizes after restriction digestion (figure 3.8a). pBS-1.3kb was incubated with *Xho* and *Not* I to liberated the PCR product, which was excised from the gel, purified and checked. Incubation of the pure 1.3kb PCR product with *Bgl* II generated two fragments, approximately 640bp and 690bp, while incubation with *Pvu* II produced fragments of approximately 750, 390 and 200bp (figure 3.8b). These correspond closely to the sizes predicted from the mouse cDNA restriction map.

(2) By PCR. The cloned 1.3kb PCR product was used as a template for *γGCSh* PCR. Figure 3.8a outlines the position of primers and predicted size of the product. Conditions for amplification were identical to the original degenerative strategy and yielded products of the length predicted (figure 3.8c).

(3) By sequencing. (Described in section 2.2.9). Figure 3.9 shows the DNA encoded sequence that closely matched the sequence of rat *γGCSh* cDNA.

Figure 3.8 Characterisation of 1.3kb RT-PCR product

Confirmation of *γGCSh* sequence in cloned 1.3kb cDNA PCR product prior to use as a probe. *A*, Schematic representation of full length and cDNA fragments to illustrate diagnostic restriction digestion and PCR products. Predicted *Bgl* II fragments (light green), *Pvu* II fragments (dark green) and PCR product (blue) are indicated. *B*, Gel of purified 1.3kb DNA after digestion with *Bgl* II (lane 1) or *Pvu* II (lane 2). Numbers refer to sizes of DNA bands in bp. *C*, Gel of PCR on 1.3kb cDNA using primers Up2+RevB with 1.3kb cDNA as a template (lane 1), or no template (lane 2).

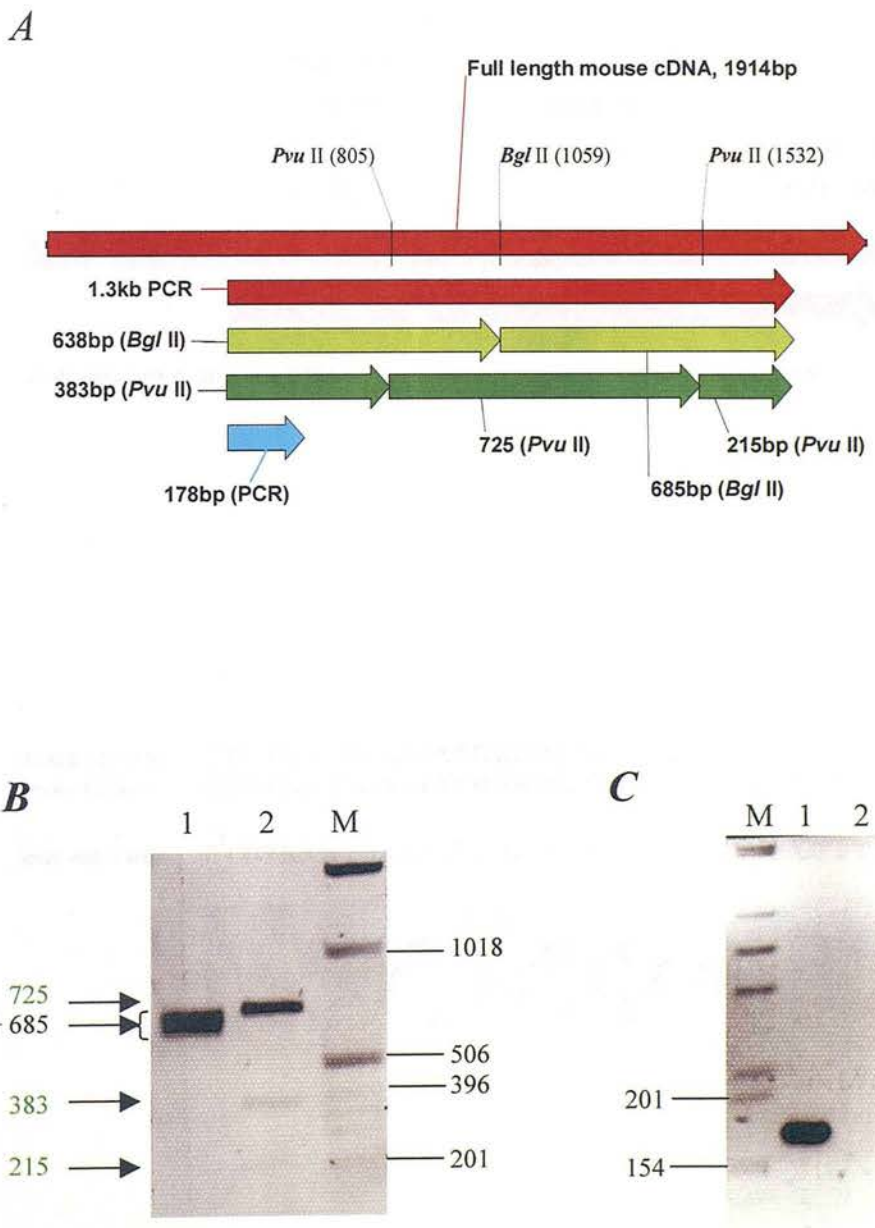

Figure 3.9 Sequence analysis of 1.3kb RT-PCR product

Confirmation of γGCSh sequence in cloned 1.3kb cDNA RT-PCR product prior to use as a probe *II*. *A*, Comparison of cloned 1.3kb mouse γGCSh cDNA with full-length cDNA, showing relative position of 1.3kb cDNA. *B*, Gel electrophoresis of sequence from mouse 1.3kb RT-PCR compared with published γGCSh cDNA sequences. * indicates non-identical sequence matches.

A

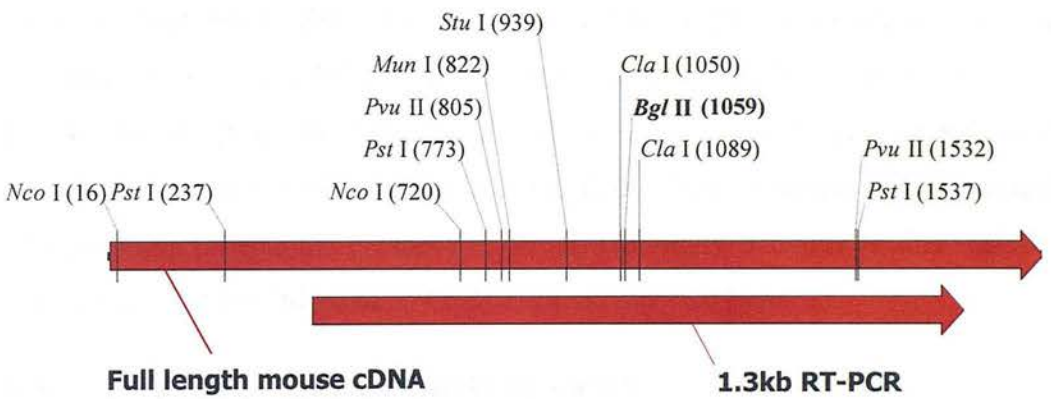

B

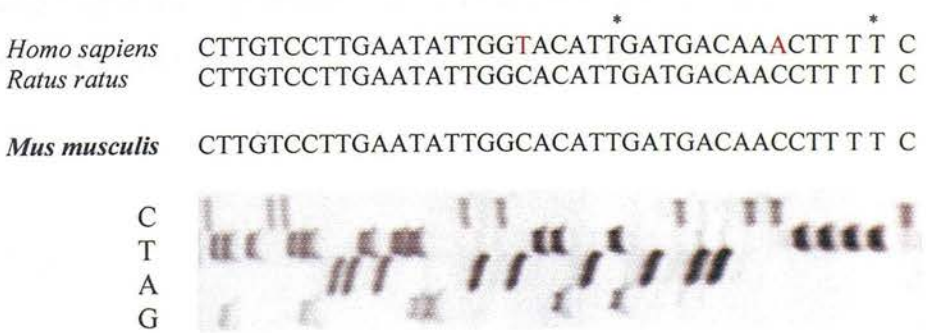

3.3.3 Summary and discussion

These sections have introduced the different approaches to clone complimentary and genomic DNA sequences, and covered an attempt to clone *γGCSh* genomic sequence from λ2000 using human cDNA as a probe. After an unsuccessful endeavour to generate the 5' region of mouse cDNA for use as a substitute probe, amplification of the central area of mouse cDNA was successful by RT-PCR. The cloning and comparative analysis of these novel sequences confirmed approximately 70% of the mouse *γGCSh* cDNA sequence had been isolated: sufficient to probe λ-libraries.

Later, in September 1997, the sequence of full-length mouse cDNA was made available (Reid et al., 1997). This information [GI:1815761] was entered in the primer design program "Primer3", located at http://www-genome.wi.mit.edu/. However, no primer could be placed in the first 103bp of mouse γGCSh sequence. This probably reflects the presence of strong secondary structure in this region and may account for the failure of 5' PCR reactions reported here.

3.4 Isolation of genomic γGCSh sequence

The techniques routinely used to isolate clones containing a significant length of the gene of interest are discussed elsewhere (section 3.2). However, due to the successful generation of a mouse cDNA probe with RT-PCR using "conserved oligonucleotides", this approach was employed to explore a potential shortcut to generating fragments of genomic DNA. At the same time, the mouse *γGCSh* cDNA was used as a probe to screen a newly acquired λ library.

3.4.1 Results

3.4.1.1 PCR was not a viable technique to generate large sections of *γGCSh* gene sequence

After successful amplification of regions of *γGCS* cDNA, the same primers were used in an attempt to amplify corresponding *γGCSh* gene sequences. As no gene structure was available, the genomic distances between cDNA primers were unknown. Therefore lengthened *Taq* extension times were attempted (detailed in table 2.1). Using the primer combination up2 and rev2 (figure 3.3), a genomic PCR product of approximately 230bp was generated (figure 3.10a), as opposed to the 139bp cDNA product. This was subcloned into pTAg and sequenced (figure 3.10b). This revealed the presence of 139bp coding sequence and an 87bp intron, the latter of which accounted for the size difference compared to the cDNA. Unfortunately, other primer combinations generated no larger fragments (data not shown). It is likely the primers were too far apart, or the fragile nature of long-distance genomic PCR may have prevented consistent rounds of amplification. Due to these considerations, the PCR approach to cloning large fragments of genomic *γGCSh* was abandoned.

3.4.1.2 Isolation of independent clones by screening λ-PS library

A second bacteriophage genomic library, λ–PS, was obtained (Molecular Biologische Technologie). The λ–PS system is a novel library that has a facility to enhance subcloning, described in the following section. λ–PS is a replacement vector of λ phage origin, which accommodates mouse 129/Sv male embryonic stem cell DNA inserts of approximately 14kb (Nehls et al., 1994). The library was plated and replica filters made as described in section 2.2.13. Purified 1.3kb *γGCSh* cDNA was randomly labelled with dCTP-P^{32} (see section 2.2.11) and used to probe for genomic homologs. Three rounds of screening were carried out, as outlined in section 2.2.14. 10 clones were picked at primary screen, but only 3 remained

Figure 3.10 Direct *γGCSh* genomic PCR

A, Agarose gel analysis of *γGCSh* genomic DNA PCR. Numbered arrows refer to sizes of DNA bands in bp. Lanes 1-6, PCR with primers 2+2; lanes 7-12, PCR with primers 3+3 (for primer information, see figure 3.3) and blank lanes, negative controls. Increasing product between lanes 1-6 and 7-12 is reflective of increased template concentration only. *B*, Extract of 230bp PCR product sequence detail, showing novel intron-exon boundary.

A

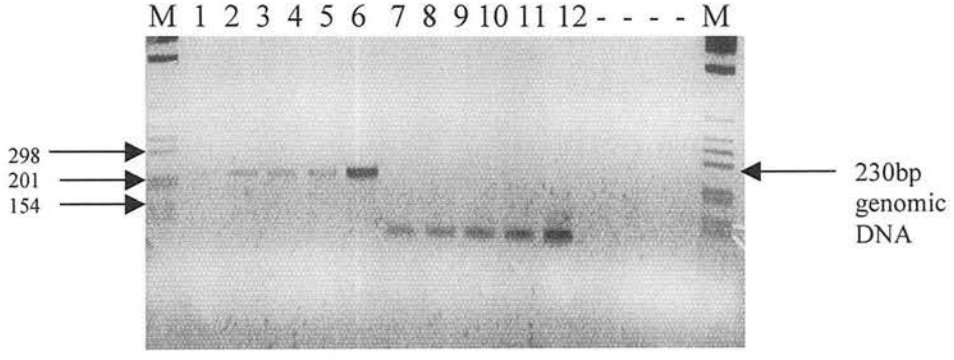

B

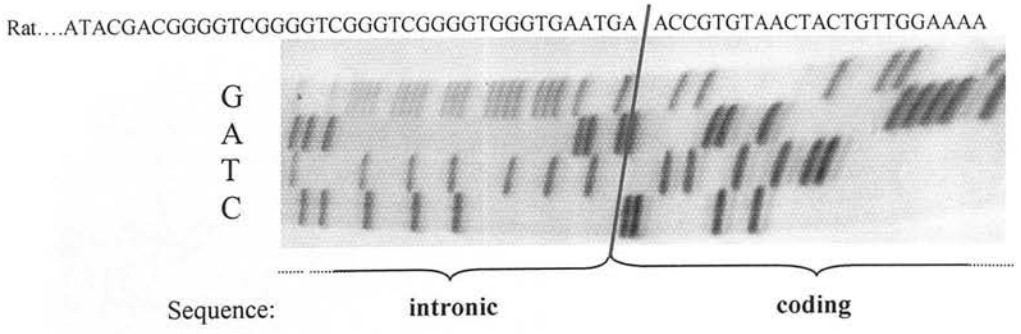

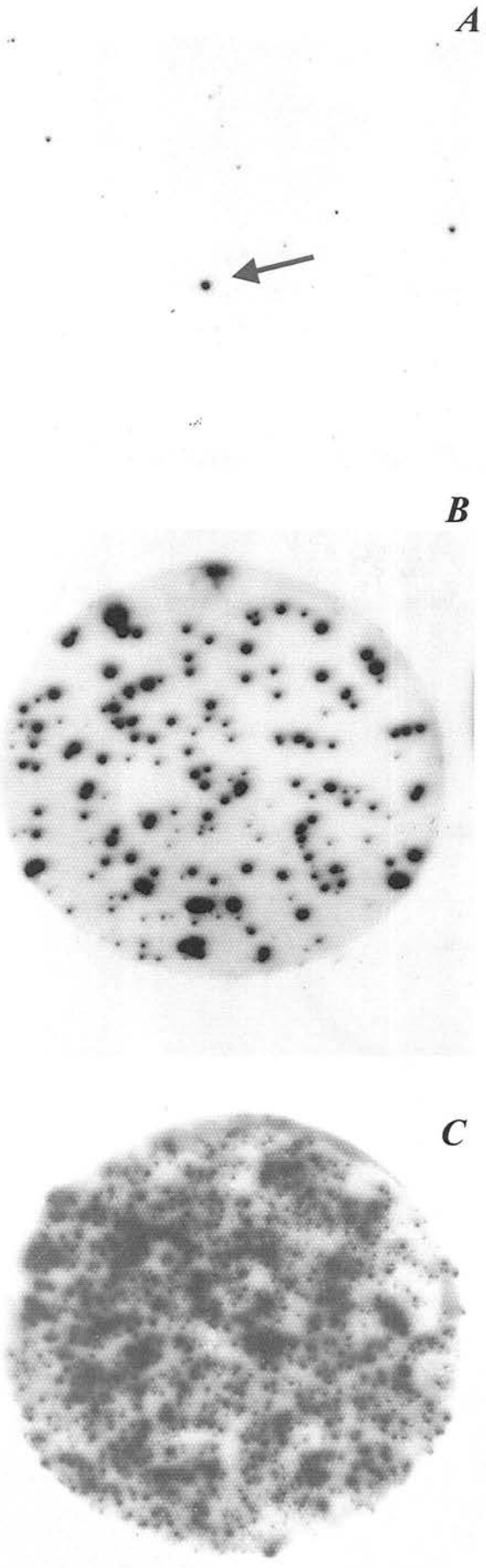

Figure 3.11 Screening the λ-PS library

Representative autoradiographs showing screening rounds of the λ-PS library using mouse 1.3kb *γGCSh* cDNA as a probe. Increased purification of *γGCSh*-containing phage is shown from initial picking of a positive clone (indicated by the arrow) in the primary screen (*A*), through the secondary (*B*) and tertiary screen (*C*).

Figure 3.12 Subcloning the insert λ-PS clones 1-3

A, Strategy to subclone phage insert from λ-PS into pBluescript (pBS). Top, Simplified λ-PS structure. Black boxes represent phage arms (Cos R and L). Also shown are polylinkers, position of loxP sites (yellow arrows), foreign genomic insert (purple line) and pBS (grey line). Middle, Cre-catalysed recombination at loxP sites excises the insert and pBS from the λ genome. Phage recombination products not shown. *B*, Agarose gel showing resultant bands representing whole λ1, 2 and 3 clones linearised with *Sac* II.

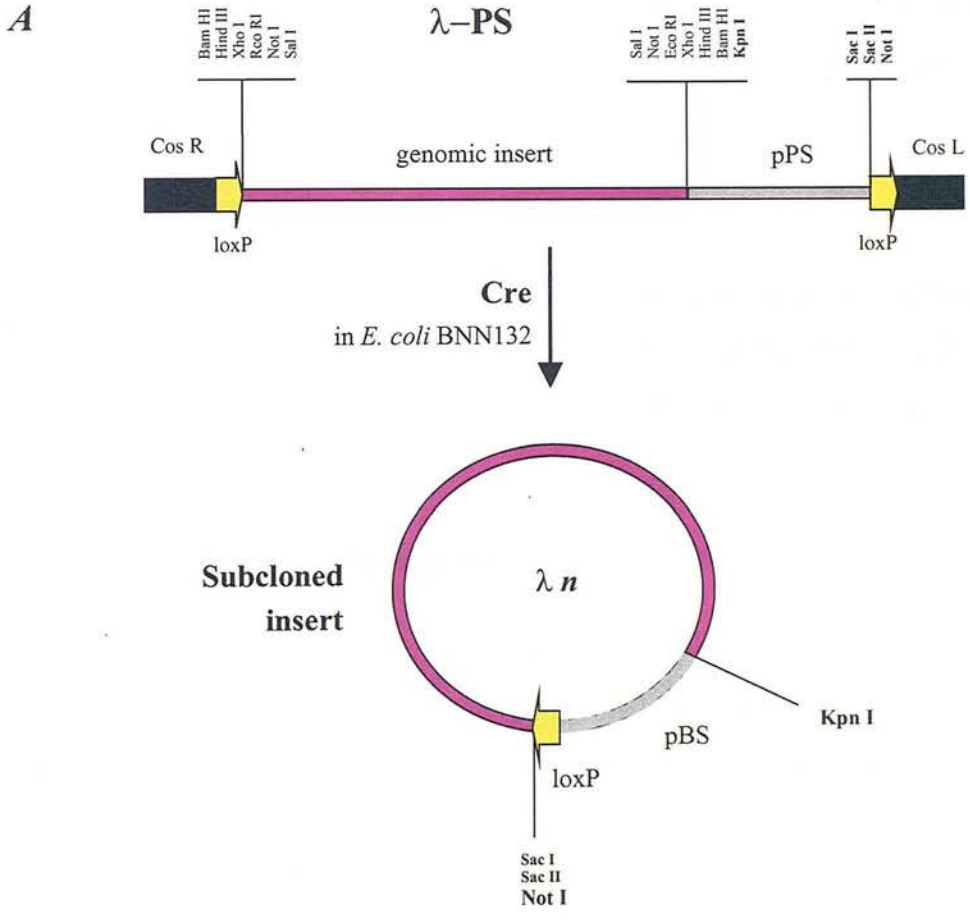

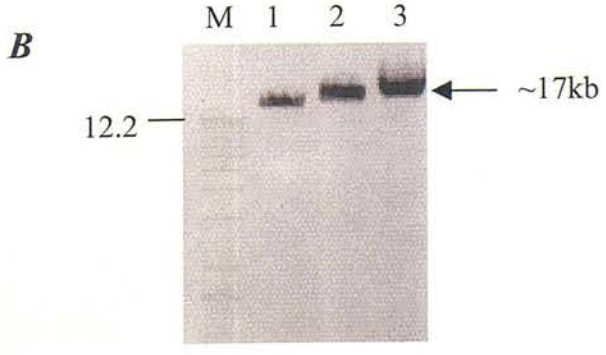

positive at the second screen, designated λ–phage 1, 2 and 3 (figure 3.11a-b). One additional screening step was made to purify the positive phage (figure 3.11c).

3.4.1.3 Subcloning the phage insert

The structure of the λ-PS vector is shown in figure 3.12a. The genomic insert is ultimately flanked by two phage arms that permit viral replication. To construct a restriction map of the insert, this phage arm DNA must be removed. The λ-phage contain two loxP sites in direct orientation flanking pBluescript (pBS). Recombination between these two sites is mediated by Cre recombinase, leading to excision of the insert-pBS fragment from the phage genome (see section 4.3.2). This was achieved by transforming *E. coli* strain BNN132, which constitutively expresses Cre, with λ–phage 1-3 (figure 3.12b). The subcloned inserts of λ-phage 1-3 are subsequently referred to as λ1, 2 and 3.

3.4.2 Discussion

With the system utilised, PCR could not generate genomic fragments of sufficient size to use as regions of homology in a targeting vector. However, at the end of this section, three independent λ clones that potentially contain *γGCSh* gene sequence had been purified, expanded and the inserts subcloned.

3.5 Characterisation of partial *γGCSh* locus

For any of the three clones to be of use in targeting vector construction, it was necessary to first identify the DNA that they carried. On confirmation that the insert contained *γGCSh* DNA the generation of a restriction map of the phage insert would be carried out.

3.5.1 Results

3.5.1.1 Restriction analysis of λ1-3 to seclude a single clone for further investigation

A preliminary examination was undertaken to (1) confirm the size of the insert, and (2) identify suitable restriction patterns that would facilitate subsequent analysis. In particular, the fragments must be easily separable and be of amenable size to clone, restriction map and sequence. Therefore, the following relatively rare cutting enzymes were chosen to restrict λ1-3: *Sac* I, *Cla* I, *Nco* I, *Bgl* II, *Pvu* II and *Sty* I.

Figure 3.13 shows *Pvu* II restricted all clones in excess (cutting >x12), whilst *Cla* I and *Nco* I cut all clones insufficiently (x2-3). *Sac* I, *Bgl* II and *Sty* I digest particular clones into an array of fragments of useful sizes.

The *Bgl* II enzyme has extra analytical potential, however, as there is a unique *Bgl* II site in the centre of the 1.3kb cDNA probe used to isolate λ1-3. Knowledge of this site could assist in the downstream analysis of the genomic DNA (outlined in section 3.7.1.2). Digestion of λ1 with *Bgl* II generates 5 fragments of approximately 6, 5.5, 2.3, 1.8 and 1 kb: all useable sizes. It was therefore decided to dedicate all further analysis upon the *Bgl* II-restriction products of on λ1.

3.5.1.2 Southern analysis of λ1 restricted with *Bgl* II

Identification of DNA fragments containing coding sequence can be achieved by southern analysis using related cDNA sequence as a probe. Identical southern blots of λ1 digested with *Bgl* II were made in parallel. Linearised 1.3kb γGCSh cDNA and pBluescript were purified (figure 3.14), labelled and used to probe discrete filters. Bands annealing to cDNA and bands annealing to pBluescript will harbour respective sequences. This approach identified the 1, 2.3 and 6kb *Bgl* II fragments as containing exonic sequence (figure 3.15b). Comparison of the two blots shows the 5.5kb band contains the pBS backbone (figure 3.15c).

Figure 3.13 Restriction analysis of λ1-3

A, Agarose gel showing restriction digestion of λ1-3 with multiple single enzymes. Horizontal numbers identify the clone analysed, vertical numbers indicate size of DNA fragments in kb. *Bgl* II restricts λ1 into sizes amenable to further characterisation (6, 5.5, 2.3, 1.8 and 1kb) and the λ1insert size is correct (~17kb).

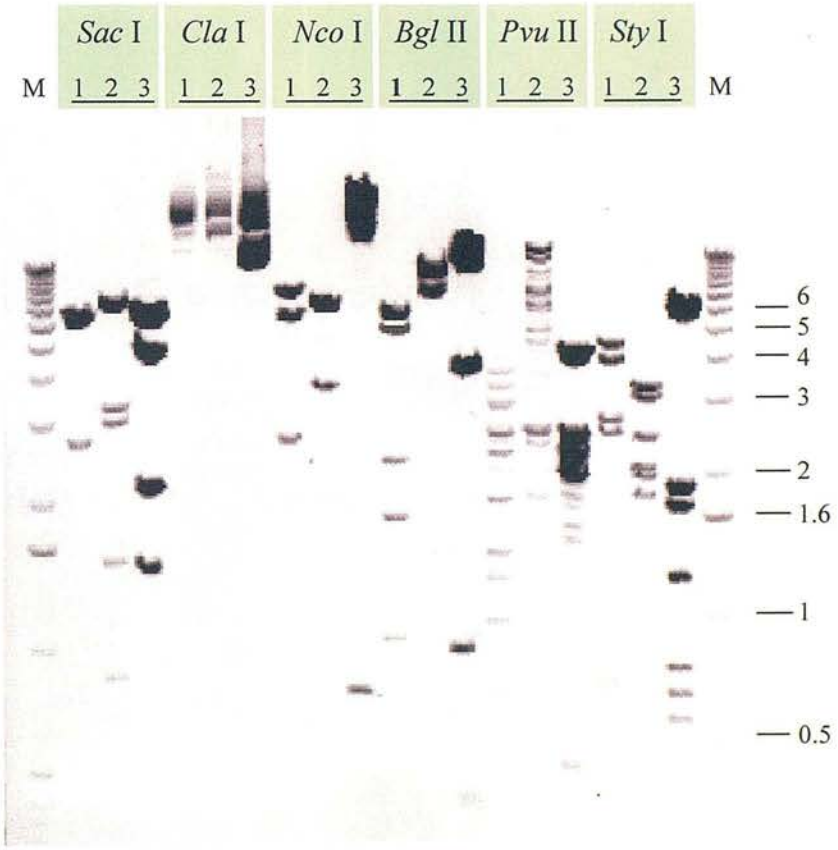

Figure 3.14 Purified *γGCSh* cDNA and pBluescript probes

Agarose gel showing gel excised and purified 1.3kb *γGCSh* cDNA (lane 1) and 2.9kb linearised pBS (lane 2), prior to random P^{32}-labelling.

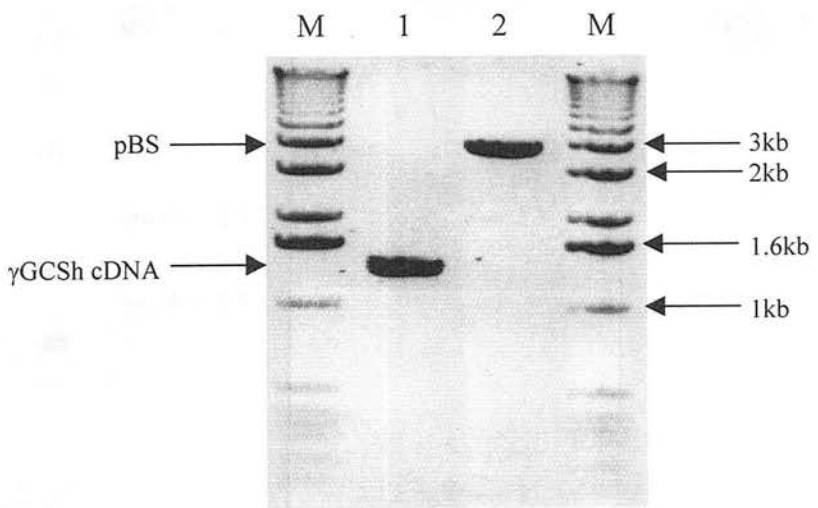

Figure 3.15 Southern analysis of λ1 with *γGCSh* cDNA and pBuescript

Determination of λ1 *Bgl* II bands that hybridise *γGCSh* coding sequence and plasmid sequence. *A*, Gel electrophoresis of *Bgl* II–digested λ1. *B* and *C*, Autoradiographs of identical southern blots of *A* probed with 1.3kb *γGCSh* cDNA and pBluescript, respectively. Numbers indicate sizes of DNA bands in kb.

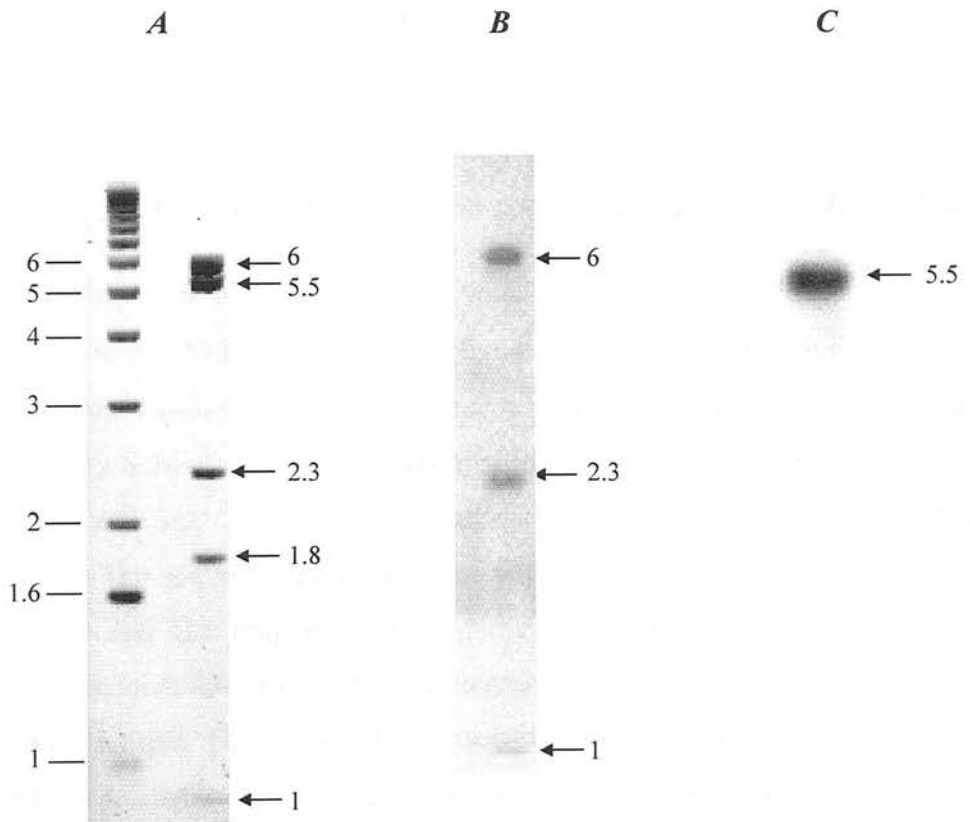

3.5.1.3 Subcloning λ1 fragments.

If, as the southern analysis data suggest, λ1 contained *γGCSh* gene sequence then the unique cDNA *Bgl* II site would permit confirmation of it. The genomic *Bgl* II site corresponding to the unique cDNA site, carried in the 1.3kb probe, will have neighbouring exonic sequence. Thus, two of the five *Bgl* II fragments were expected to contain coding sequence at one termini.

Therefore, all five *Bgl* II fragments were cloned separately, into *Bgl* II-complimentary *Bam* HI-linearised pBS. Liberation of each fragment by restriction digestion with *Xho* I and *Not* I confirmed all fragments were subcloned (figures 3.16a and 3.18a).

3.5.1.4 Confirmation of *γGCSh* coding sequence in λ1 fragments.

Subsequently, all cloned fragments were partially sequenced to detect for the presence of *γGCSh* coding sequence (figure 3.19-3.22). Sequencing was carried out within our laboratory manually and externally using automated sequencers (Veterinary School, Summerhall, Edinburgh). This approach identified the 1.8kb 5' terminus and 1kb 3' terminus as harbouring a *Bgl* II site and adjacent coding sequence. The sequence data correlated with the southern analysis data in showing the 6, 2.3 and 1kb fragments to contain exonic sequence. In total, five complete exons were identified: two in the 6kb fragment, two in the 2.3kb fragment and one in the 1kb fragment. The exons were consecutive and permitted alignment of all *Bgl* II fragments relative to one another. Figures 3.19-3.22 also show partial restriction site maps of the sequence represented in λ1, generated from the sequence information.

3.5.1.5 Generation of restriction maps

Since the complete sequencing of fragments greater than 1kb was not undertaken, a partial restriction map was made. Only the 6kb fragment, owing to the large quantity of unknown sequence contained within it, was subject to a concerted mapping

Figure 3.16 Cloning genomic *Bgl* II fragments

A, 1% agarose gels showing subcloned λ1 *Bgl* II fragments in pBS (2.9kb). All plasmids digested with *Xho* I and *Not* I to liberate cloned fragments: Lane 1, 6kb; lane 2, 1.8kb; lane 3, 1kb and lane 4, pBS only. *B*, Structure of the 6kb-pBS plasmid, showing insert orientation.

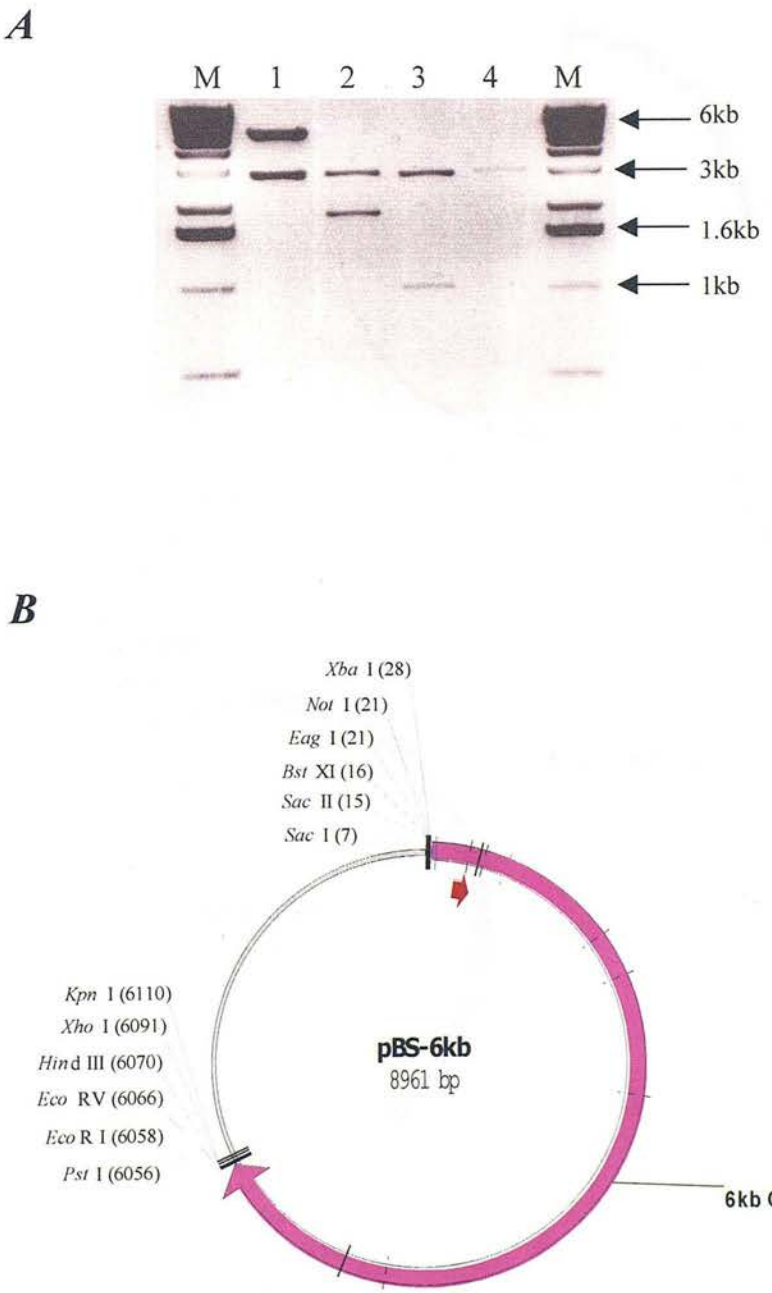

Figure 3.17 Structure of cloned 1 and 1.8kb λ1 *Bgl* II gene fragments

Schematic diagrams showing orientation of cloned fragments in pBS. *A*, 1kb genomic fragment and *B*, 1.8kb genomic fragment.

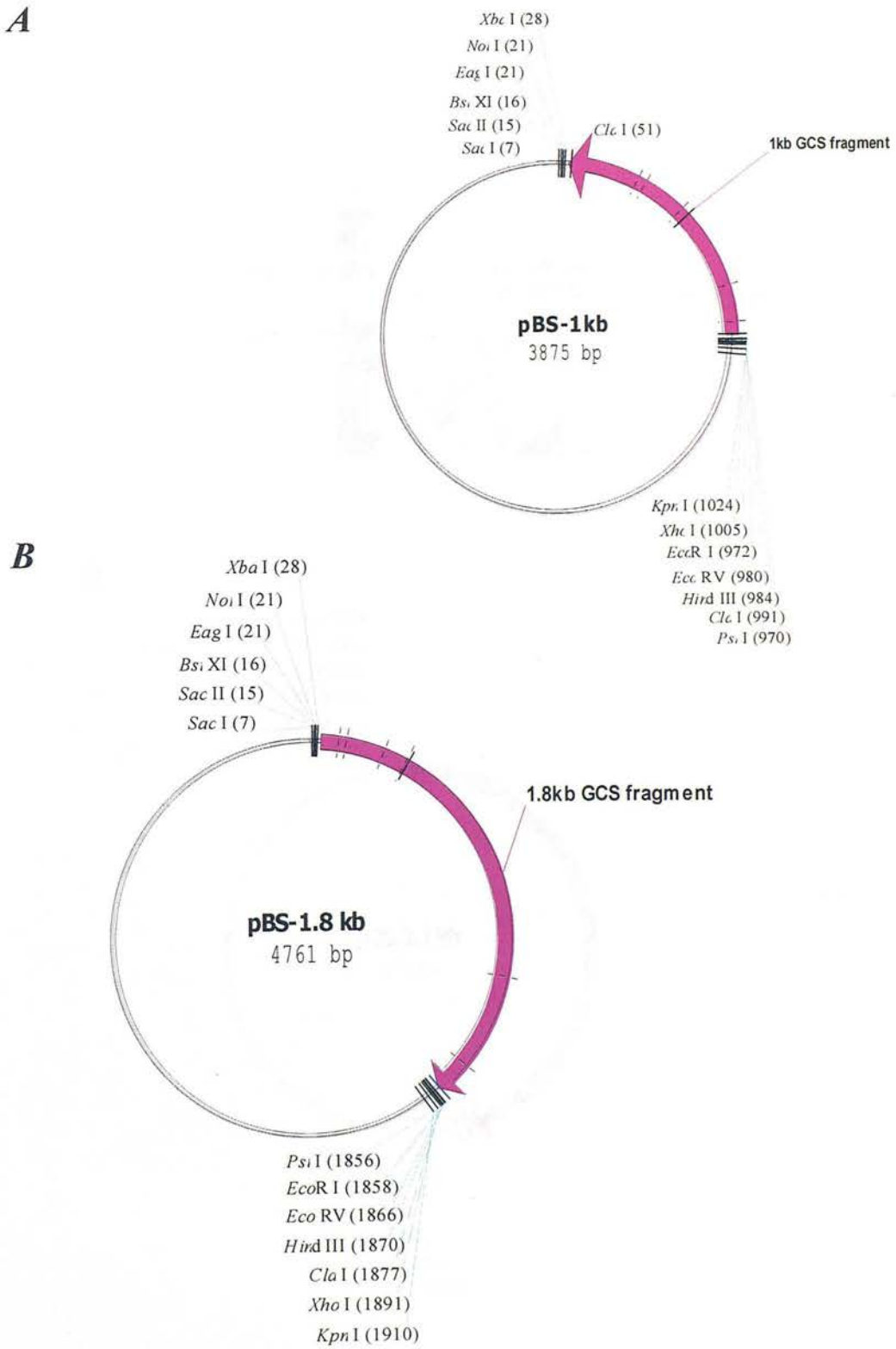

Figure 3.18 Cloning genomic *Bgl* II 2.3kb fragment.

A, Agarose gel showing liberation of subcloned 2.3kb fragment from pBS by digestion with *Xho* I and *Not* I (lanes 5 and 6). *B*, Structure of the 2.3kb-pBS plasmid.

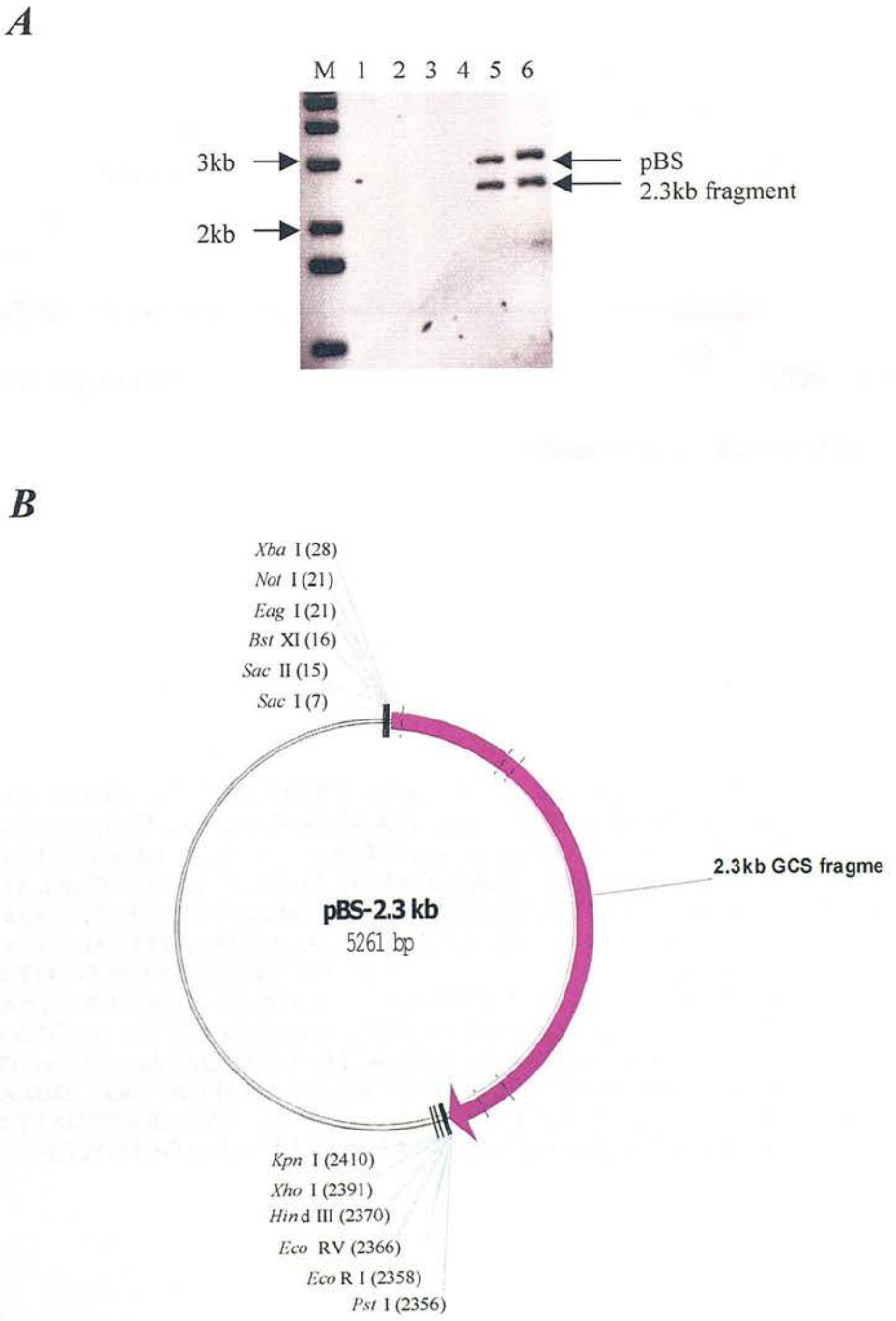

Figure 3.19 Confirmation of gene sequence in λ1 6kb *Bgl* II band

A, linear representation showing partial restriction site and functional map. *B*, 3' sequence data (completed externally). Green letters, pBluescript; black letters, intronic sequence; red letters, coding sequence (as compared to human and rat cDNA, data not shown).

A

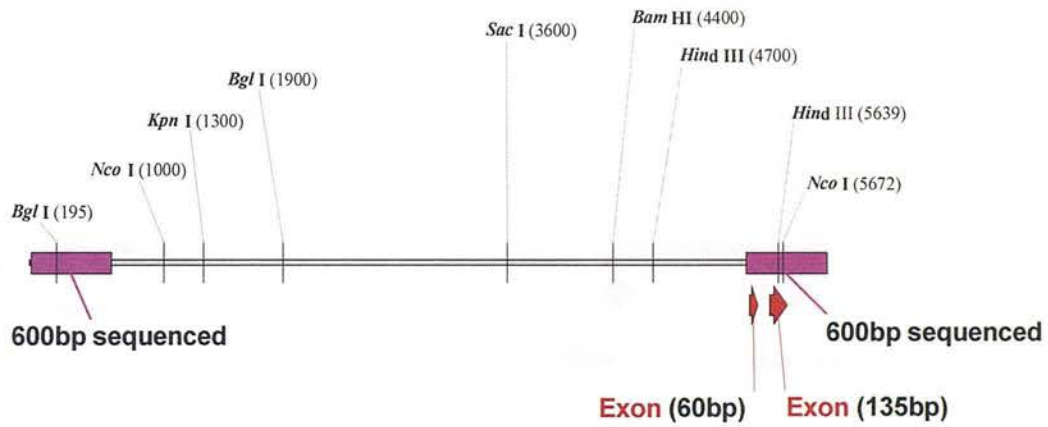

B

3'

TGCAGCCCGGGGGATCTGAGCCTTGTATAATATCCTCAAAGGCTGTCA
CTAGATGGCGGTAAAAAATCAGGCATCTAAAAAGGGCATTCACCAAC
ATCTGTTTACCAATAGATACCAAGTTTAGTAACAACCACACACCTCTG
TGGTAAACTGTGAATTTTCAGTCAAAAGACAGCTACAAAAGACTTTAC
TAAAGCAACATCATTTTTCAGAAGGTAAGCTATCTTTCGAATCAGATT
AGAAGGTGACTTTAAACCAGACACATGCATAGTGAAGAGGACATTTA
AGTCTCCATACAACACAGGCAATACCTGGAGACAGCAGTTGCCCATC
CCGAATCCCATGGCATCCATGTAGATATGGTCTGGCTGAGAAGCTTTG
ATGCCTCCGCATCTTCTGGAAATGTTTCTACAAATGGAGATGGTGTAT
TCTTGTCCTTGAATACTGCATTATTAATGAAAAGAAGAGGAGCTGAGA
ATCAAGGCTGCCGGTTGGACTATGCTGCCCAGCCCAGCCCAGCCCCAC
CCACTTACTTGGCACATTGATGACAACCTTTTCTCCTCTCCGATGCCGG
ATGTTTCTTGTTAGAGTACTACAGCAAGCAAACAAAAGGACAGGTCA
C

294bp intronic

Exon: 135bp

Intron: 87bp

Exon: 60bp

5'

Figure 3.20 Confirmation of gene sequence in λ1 2.3kb Bgl II band

A, Linear representation showing partial restriction map, including a unique *Mun* I restriction site used in section 4.6.3 for screening recombinant ES cell clones. The positions of exons 6 and 7 are indicated. *B*, Extract of corresponding sequence data of 2.3kb, compared to published rat cDNA sequence.

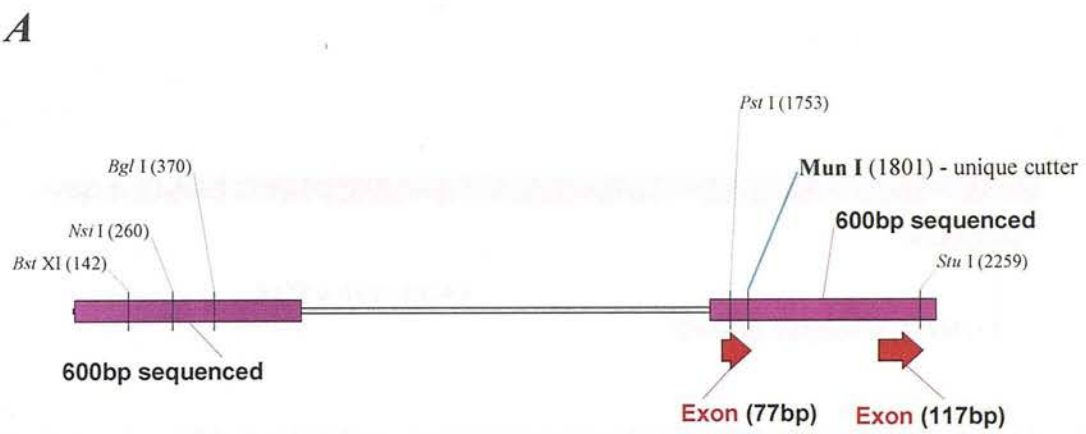

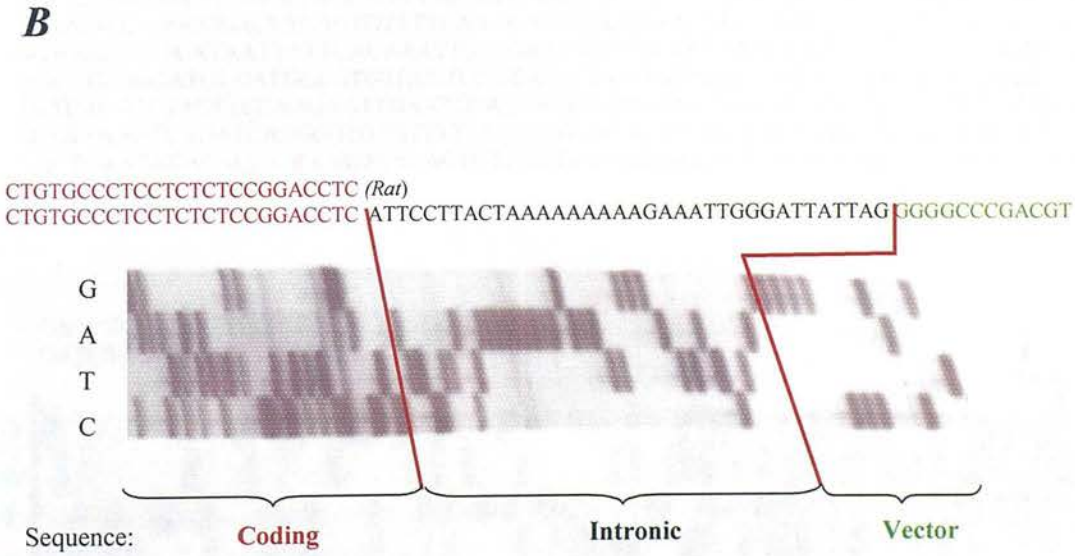

Figure 3.21 Confirmation of genomic sequence in 1kb *Bgl* II band.

A, partial RE map of the whole 1kb molecule showing position of exon 8, the remaining sequence of which is located in the 1.8kb fragment. *B*, complete sequence data, and *C*, representative sequence autoradiograph corresponding to the 3' end, compared to published rat sequence (green font).

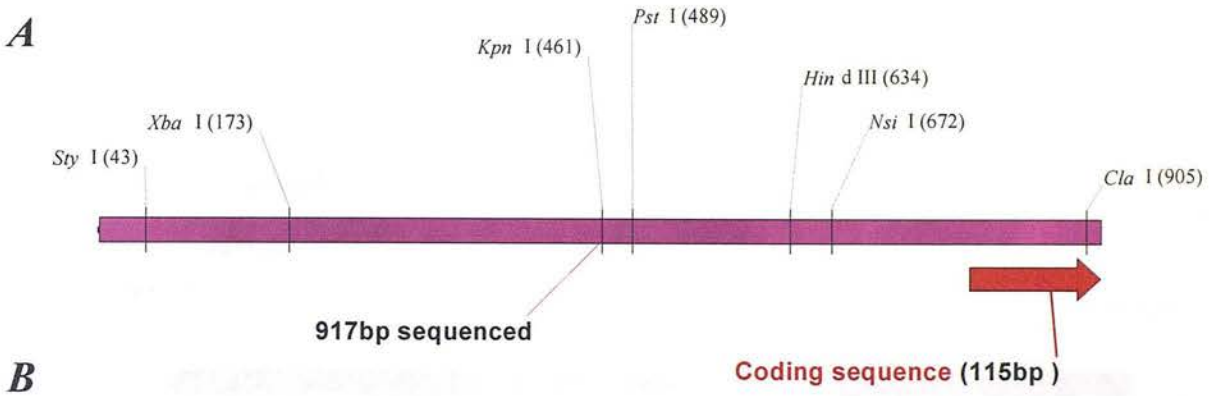

B

5'
GATCTTTTGCATCACACCGGGGACCTGTGTATATTGTAACCCCTTGGCATTTTGAAGTCTCCTTAGATGTT
TACCCTCTGGGTGTCCACATCAGGGAAGAGAATACAGGTAGTGAGCCGGCTTTGTTTTAAGTGGGTACAC
AGGAGGAAGGTACTTGGTTTGGGTGGGAAGTCTAGAAATCTGCATTAGATATAGCTTCCTTTAAAAATAC
TGGCCATTTTGTGCTGTAGCAGTCACACCGGCAGCTGTTTTACCAAAAGGCTCTGGCCACTGCCTTCTGTC
CAGTAGTTTCTGCTAGGAAGCTGGGTGATGTTCTCATTTGAAGGCTTTAGGCTTTACCCTGTAAGTCAGG
TTAGCCGTATTAGCATTTCTTGTCCATGCTGAACTGTAGTAGTGTGTCCTTTTAACTCCTTTTAGCACCAG
GAGCATGTATCACCACCCACCTCAAAGAGCCAGGTACCCATGTTCATGCTAGGTTAGACTCTGCAGGAC
AAGGACCTGGCCGACCTCAGTGTTTTCAAAGACTTGCACAAGGGACATCTTGCACTATGGGCATTTCTGC
TCTGGCCTTTCATAATTATTCACAAATTGTTGAACATATTCTATAATTTTGTGGCTGTGTATGAAAGAGAA
AGCTTGGGGATGGCATGGCGTGTGCCTGAGCACATGCATGGAGGTCAGAGCAACACTGTAAGTCTGTCC
TGTCACTCTGAGTTCCAAGAATTGAATGTAGGTCCCAGGGAAGGGTGCTCTGTGACAATTAATTACCTGG
GTGTTAAGTCAGATCATGCGTGTGTTTTAGCCTGTGACAACAATCGTTTAGGATCAGTAAGTCTCGGTAT
GACTCAATAGATAGCTACCTGTCTAAGTGTGGGGAGAAGTACAATGACATCGACCTGACCATCGATAAG
GAGATC
3'

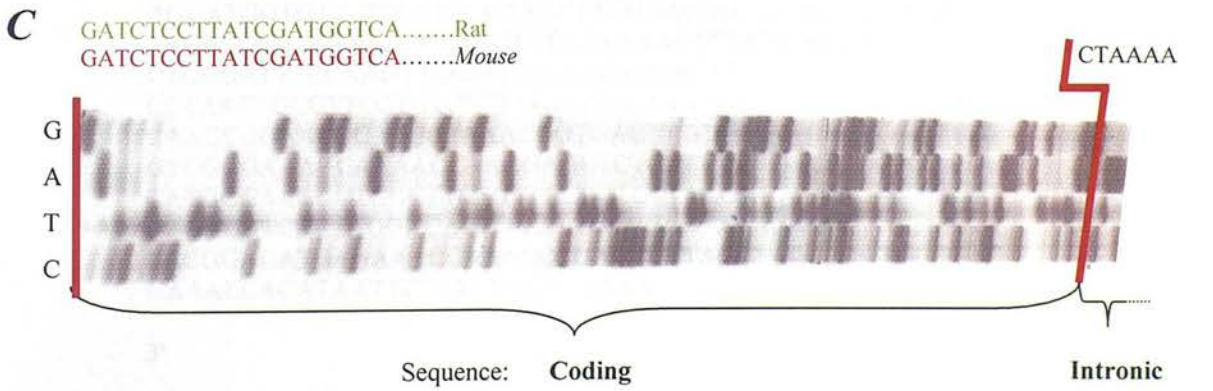

Figure 3.22 Confirmation of genomic sequence in λ1 1.8kb *Bgl* II band

A, linear representation showing partial restriction site and functional map. *B*, 5' sequence data (completed externally). Green letters, pBluescript; black letters, intronic sequence; red letters, coding sequence (as compared to human and rat cDNA, data not shown).

A

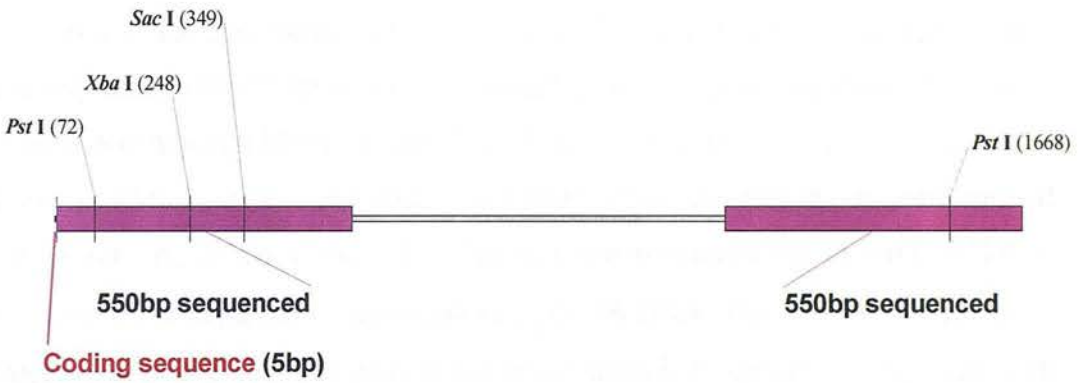

B

5'

TCTAGAACTAGTGGATCTATGTCTGTCCTGTGACTGTTAGGCATGTTCC
TGTGCATTACTCTTTAGTTTTGCAAAGATACTGCAGTGACAACTTTTCT
AGGATGGTGTCTTTCCTTGGTAGCTTGGGACAGAGTAGGATTCGTAGG
TACATCCTGAAAAACCCAGCTTTAGAAAACTCTATGAAGAGGAGGGA
CTGGGATTTCCAAGTTGCAGTGTAACAACAGTTATCGTAAGTAGATTT
CCTAACTGCCTTCCTGTCTCTAGAGCCGAAACACTCTGCGCATCAAGT
CAAGCGGAACGCACGCTAAACGGTGACTTTCATAAACAGTGACTTTG
GTGGGGAAAGCAAAACCAAGGAGCTCTGACCCCTGACAAAGGCATAG
CACGGGAAGGCTGGCTTCTGTTGCCCTCCTAAGAGATCCCACGGGAG
GAGACGTCACTAGGACACTGACAGGAGGGAAGGAGGACCTGTGAAA
CACGGAGATGAGAAACCAAACCCGACACTTACCTAGAATCTGGTTTT
GAAACCACATAATTCTCTTAAGTAGAAA

coding seq.

intronic

3'

exercise. Figure 3.23 details the frequency of restriction enzymes cutting the 6kb fragment. Those enzymes cutting once were subsequently incubated in double digests to position the restriction sites relative to one another (data not shown). This approach produced a limited overall map of the 6kb fragment that is incorporated with the sequence-derived restriction site data (figure 3.19a). In addition, limited restriction analysis was carried out in other λ1 *Bgl* II fragments to both confirm the presence of sites predicted by sequence analysis, and to identify the presence of restriction sites in areas not sequenced. This data is summarised in figure 3.24.

3.5.1.6 Determining and cloning the terminal ends of λ1

The 5' and 3' termini represent the final area of λ1 that remained uncharacterised. Extra sequence at the 5' terminus was desired to act as a potential external probe in screening recombinant ES cell clones. The 5.5kb *Bgl* II band contains, because it was the only band to hybridise pBS, the whole vector backbone and the extreme ends of the λ1 insert. As 2.9kb of the 5.5kb fragment are accounted for by pBS, 2.7kb of remaining insert sequence is represented by *γGCSh* DNA. This 2.7kb of sequence is divided between the 3' and 5' ends of the insert, though the quantity comprising each end was unknown. The size of the 5' sequence was established by a restriction mapping strategy of the whole λ1 outlined in figure 3.25. This showed that of the 2.7kb, 1.4kb was located at the 5' and 1.3kb located at the 3' end, respectively.

Thus the extreme 5' end, at 1.4kb, was of sufficient size to potentially use as a probe in downstream targeting experiments. Due to the similar size of the 5' and 3' termini, both fragments were subcloned to prevent accidental isolation of the incorrect (3') DNA. The 5.5kb band was cloned by gel excision, purification and simply re-circularising in an otherwise unmodified ligation reaction, confirmed by linearisation with *Not* I (data not shown). The 5' and 3' ends were subsequently cloned as described in figure 3.26. This represents the final characterisation of λ1.

Figure 3.23 Frequency of restriction endonucleases cleaving the λ1 6kb *Bgl* II fragment.

A, The presence or absence of restriction endonuclease sites (RES) in the purified 6kb *Bgl* II fragment was determined by systematic single digestion tests with the listed enzymes. *B*, Representative agarose gel. Lane 1-9, *Kpn* I, *Hind* III, *Bam* HI, *Eco* RI, *Nco* I, *Sac* I, *Sty* I, *Not* I and uncut 6kb, respectively. Numbers on left-hand margin indicate sizes of bands in kb, numbers in blue panel show amount of bands produced by each enzyme and the number of corresponding sites present.

A

RES not in 6kb	RES present @ x1 in 6kb	RES present @ >x1 in 6kb
Apa I	*Bam* HI	*Apo* I
Bgl II	*Bgl* I	*Bst* XI
Dra III	*Bss* HII	*Eco* RI
Eco RV	*Kpn* I	*Fsp* I
Mlu I	*Mun* I	*Hind* III
Nde I	*Sac* I	*Nco* I
Not I	*Sph* I	*Nhe* I
Pml I		*Nsi* I
Pst I		*Pvu* II
Sma I		*Sty* I
Stu I		
Sac II		
Xba I		
Xho I		

B

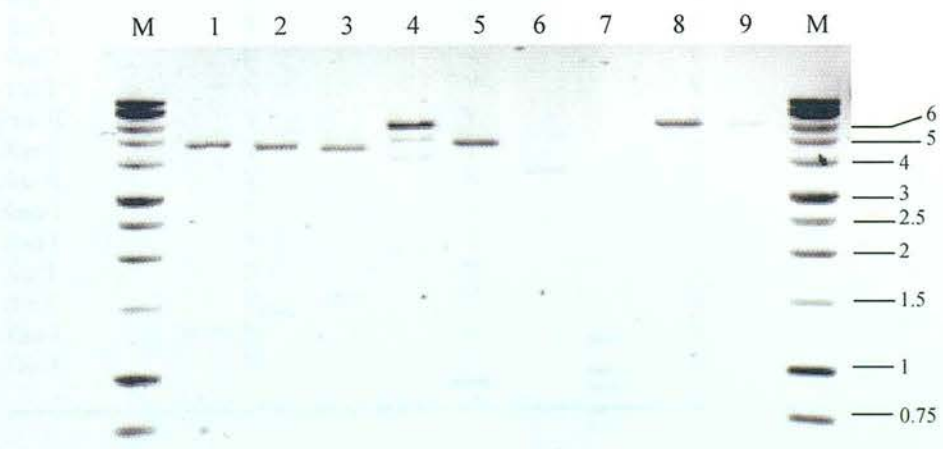

Number of fragments:	2	2	2	4+	2	2	5+	1	1
Number of RES:	1	1	1	>1	1	1	>1	0	-

Figure 3.24 Presence of RES in all *Bgl* II fragments.

Presence of restriction enonuclease sites (RES) in different λ1 *Bgl* II fragments. N= not present, Y= present and - = unknown. All information was determined by single restriction digests of respective plamsids and, in areas of doubt, purified fragments (data not shown).

	RES presence in:			
RES	**6** kb	**2.3** kb	**1** kb	**1.8** kb
Apa I	N	N	-	-
Apo I	Y	Y	N	Y
Bam HI	Y	N	N	-
Bgl I	N	Y	N	-
Bgl II	N	N	N	N
Bss HII	Y	-	N	-
Bst XI	Y	Y	N	N
Cla I	-	N	Y	-
Dra III	N	N	-	-
Eco RI	Y	Y	-	-
Eco RV	N	N	N	N
Fsp I	Y	-	N	-
Hind III	Y	-	Y	-
Kpn I	Y	-	Y	-
Mlu I	Y	N	-	-
Mun I	Y	Y	N	N
Nde I	N	N	N	Y
Not I	N	N	N	N
Nco I	Y	Y	Y	Y
Nhe I	Y	-	-	-
Nsi I	Y	Y	Y	-
Pml I	N	-	-	-
Pst I	N	Y	Y	-
Pvu II	Y	Y	Y	-
Sac I	Y	Y	N	Y
Sac II	Y	N	N	N
Sma I	N	-	-	-
Sph I	Y	-	-	-
Stu I	N	N	N	N
Sty I	Y	Y	Y	Y
Xba I	N	N	Y	N
Xho I	N	N	N	N

Figure 3.25 Determination of the 5′ and 3′ ends of λ1.

The termini of λ1 were examined by restriction analysis. The 5' (*Kpn* I) and 3' (*Not* I) restriction sites are common to all subcloned λ-PS-derived clones (*Mo Bi Tec*, 1996). The *Kpn* I sites in the 6 and 1.8kb *Bgl* II fragments were mapped manually (data not shown). Knowledge of these four RE sites allows identification of the 5' and 3' ends by comparative mapping. Numbers on gels refer to sizes of fragments in kb.

A, Agarose gel (1%) of initial determination using whole λ1. Lane 1, λ1 digested with *Kpn* I; lane 2, λ1 digested with *Kpn* I and *Not* I.

B, Final determination on 2% agarose gel. Lane 1, 5.5kb *Bgl* II fragment cut with *Kpn* I and *Not* I; lane 2, 2kb 3' fragment from λ1 restricted with *Bgl* II only.

C, Resulting structure of whole λ1. Green numbers show position and sizes of all *Bgl* II restriction fragments, brown and pink numbers correspond to DNA fragments in A and B, respectively.

Figure 3.25 Determination of the 5′ and 3′ ends of λ1

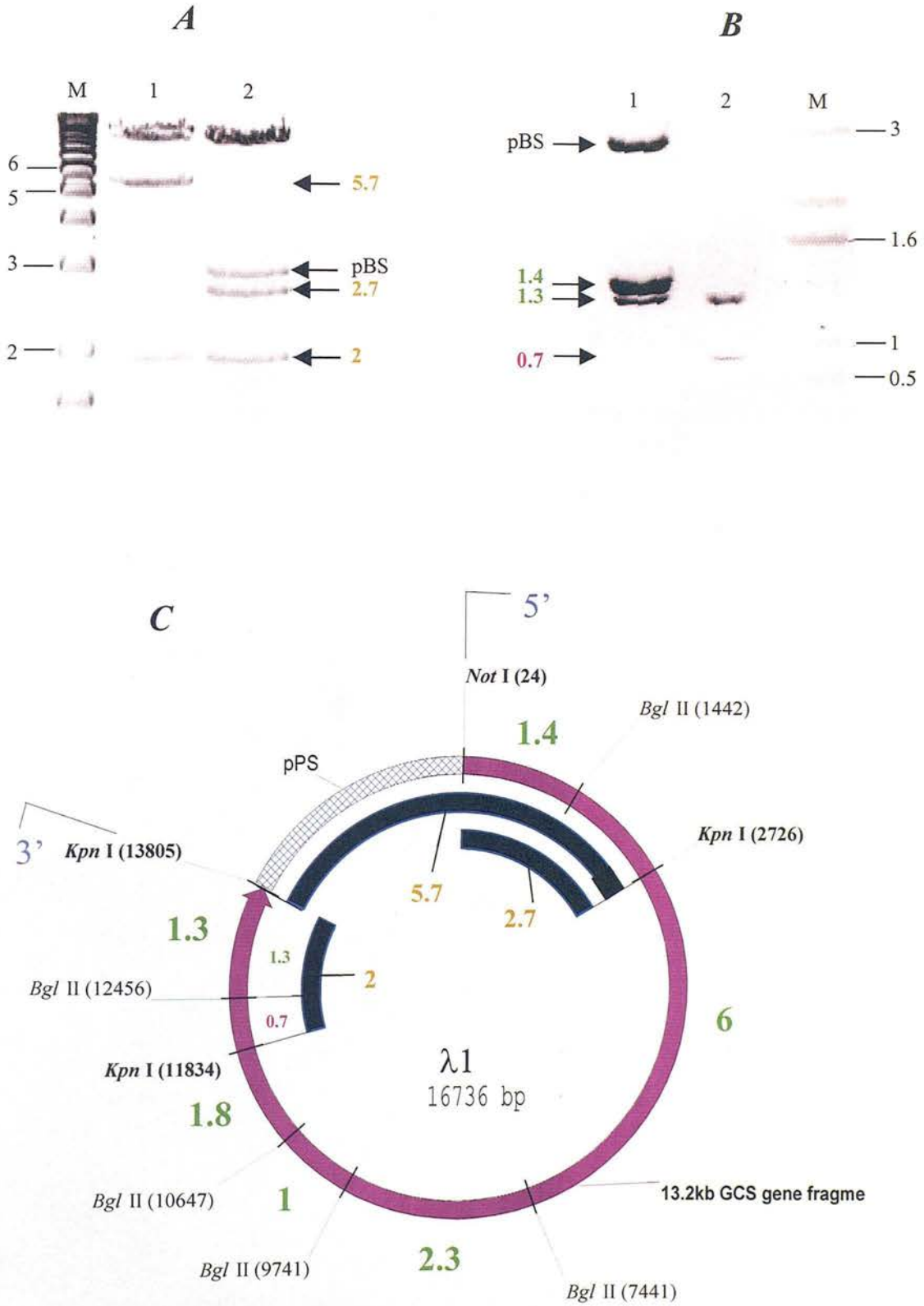

Figure 3.26 **Subcloning the 5′ and 3′ termini of the λ1 insert**

Recircularisation

The linear 5.5.kb Bgl II fragment was separated from the 6kb by agarose gel electrophoresis, gel excised and purified. Incubation of this DNA in a ligase reaction re-circularises the the molecule at the exposed *Bgl* II termini. The reaction was used to transform *E.coli* and generate large quantites of the circular plasmid. Pure 5.5kb DNA preparations were treated separately as follows.

Restriction digestion

The circular 5.5kb was digested with either *Bgl* II and *Not* I to liberate the 5' terminus, or with *Bgl* II and *Kpn* I to liberate the 3' terminus. Each fragment was gel excised and purified. and Restriction with of the resulting plasmid with *Kpn* I and *Not* I excises the 5' 1.4kb terminus (lower panel, lane 2).

Subcloning

The 5' fragment was subcloned into pBluescript linearised with *Bam* HI and *Kpn*, the 3' fragment ligated to pBluescript linearised with *Bam* HI and *Not* I. 3' and 5' termini were liberated for pBS with *Kpn* I and *Not* I (lower panel, lane 1 and 2, respectively).

Figure 3.26 Subcloning the λ1 5′ and 3′ termini.

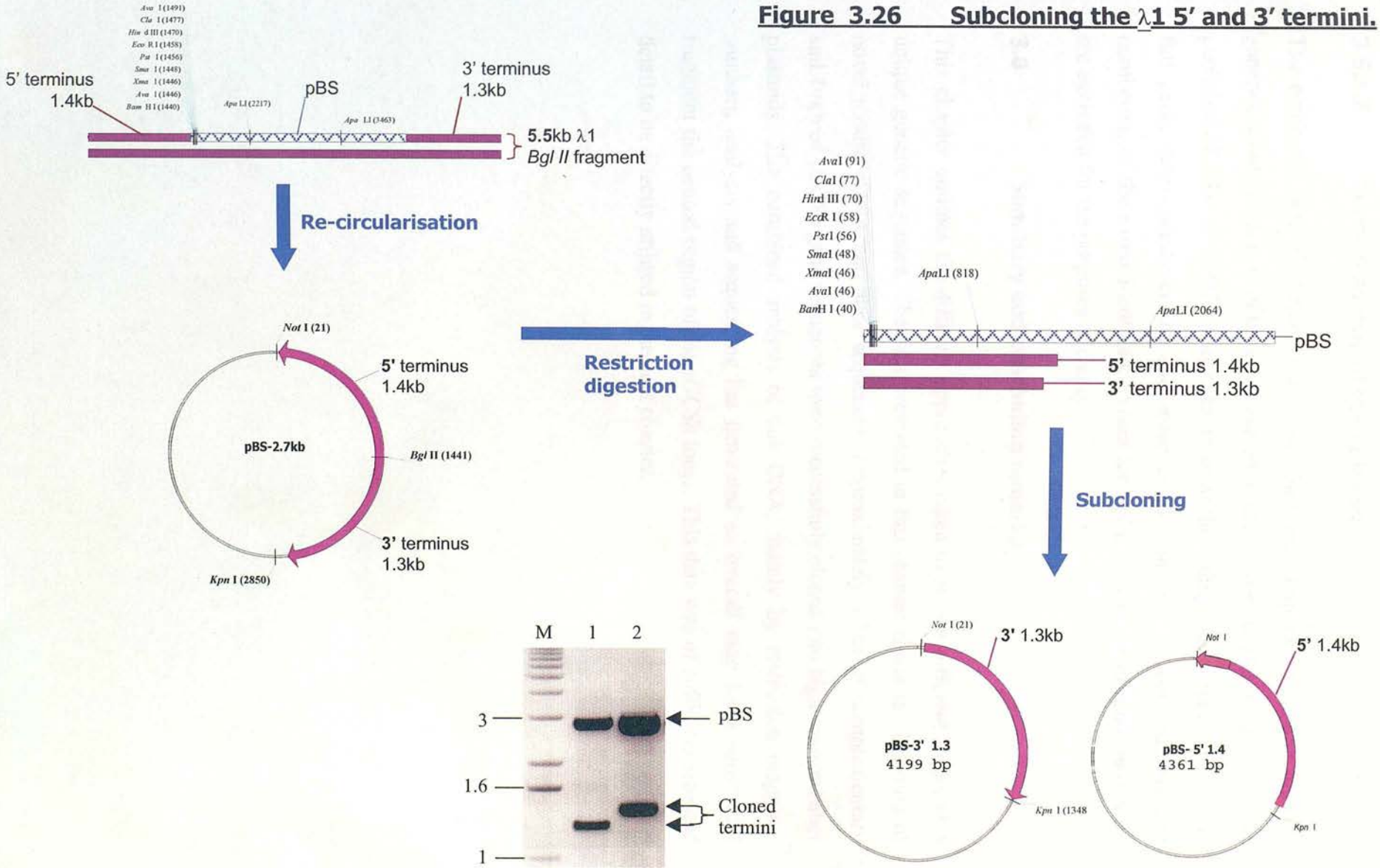

3.5.1.7 Concluding map of the λ1 insert

The combined data of chapter 3 are assembled and simplified in figure 3.27 to generate a functional map of the area covered in λ1. Full-length cDNA, subsequently published (Reid et al., 1997), is included to show the coding area spanned in λ1. The full gene, subsequently cloned and sequenced by *Shi et al.,* 2000, has allowed numbering of the exons identified. Except for *Bgl* II, restriction endonuclease sites are excluded for the purposes of clarity.

3.6 Summary and concluding remarks

This chapter outlines the different approaches taken to isolate different forms of a unique genetic sequence. The data presented in this chapter charts the isolation of novel mouse cDNA and gene sequences. Approximately 1.3kb of complementary and 14kb of *γGCSh* gene sequences were successfully cloned into high-copy number plasmids. The combined analysis of this DNA, mainly by restriction mapping, southern analysis and sequencing has generated an overall map for a substantial fragment the central region of the *γGCSh* locus. This data was of sufficient size and detail to be directly utilised in the next chapter.

Figure 3.27 Combined sequence data of λ1 showing central region of mouse γGCSh gene

Simplified figure of total region characterised (approximately 13,700bp). All features are representative of actual sizes except exons (numbered yellow boxes) and full length mouse γGCSh cDNA (yellow line). Purple numbers show length of gene areas sequenced; bold black numbers show orientation respective *Bgl* II fragments to one another. Grey line represents partially characterised sequence; narrow green lines, diagnostic *Bgl* II restriction sites.

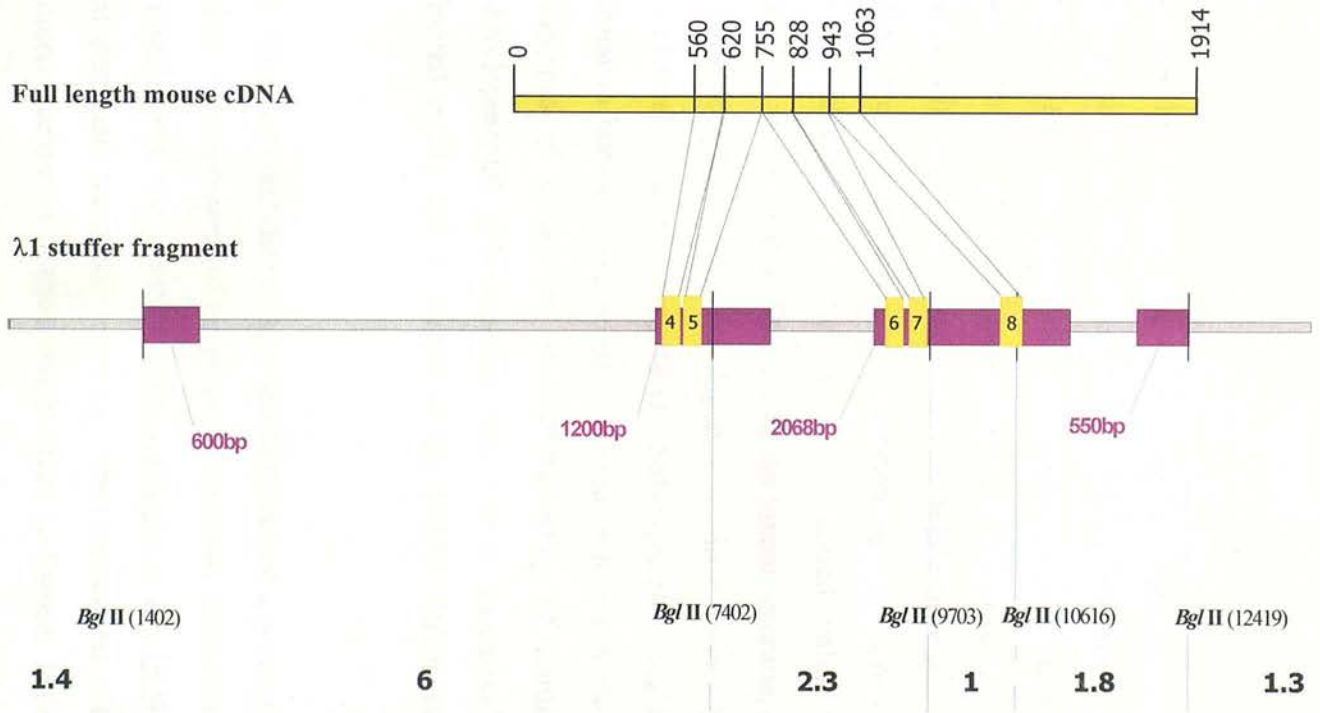

Chapter 4

Gene Targeting of *γGCSh*

4.1 Introduction

A multitude of human pathologies have origins that reside in the genetic sequence. The bulk of early research investigating the role of hereditary factors in disease were carried out on organisms such as yeast, the nematode, *Caenorhabditis elegans* and the fruit fly, *Drosphila melanogaster*. These species have short replicative cycles and relatively small genomes that permit rapid analysis of mutations. While information gleaned from this work laid the foundations for understanding mechanisms mediating gene expression and development, they were of limited value in understanding the genetic disorders of vertebrates. The size of the human genome, at approximately $3x10^9$ bp, and the complex interaction of genes within it cannot be accurately reproduced in relatively simple organisms. Subsequently, higher mammals physiologically similar to humans have become utilised as research tools to model disease. The advantages of mouse models for the study of human physiology, disease and developmental abnormalities have been extensively reviewed (Jaenisch, 1988; Bedell et al., 1997a; Bedell et al., 1997b; Rubin and Smith, 1997).

Processes that can artificially introduce candidate disease genes represent a powerful aid to elucidate gene function. Development of pronuclear injection techniques allowed foreign DNA to be inserted into the germline of mice (Hogan et al., 1994). Subsequently, the creation of transgenic mammals carrying genes associated with human dysfunction has facilitated elucidation of their involvement in disease. There are constraints, however, in the use of transgenic animals to develop disease models. Transgenes integrate at random genomic sites, where local regulatory sequences often exert their control. This leads to unpredictable elevations (al-Shawi et al., 1991) or depressions (Jaenisch, 1988) in transgene expression, which can be further compounded by integration of variable copy numbers. In addition, analysis of the

phenotype may be complicated by indiscriminate recombination with endogenous genes. Indeed, significant phenotypic differences in lines of transgenic mice expressing the same transgene have been reported (Bedell et al., 1997a). While some of the above shortcomings have been resolved by the use of YACs (*y*east *a*rtificial *c*hromosomes), the limiting factor of transgenic models remains that genetic material can only be inserted, not deducted, from the genome.

A deficiency in a single gene yields a more intimate insight into gene function. Gene targeting is a technique that permits introduction of site-specific mutations into endogenous genes *in vitro* and *in vivo*. The original protocol relies upon generating a vector containing two sequences of DNA homologous with the cellular locus, separated by a selectable marker. The endogenous process of homologous recombination is harnessed to insert the marker at loci isogenic to the vector DNA sequences, inactivating the target gene.

4.2 Homologous recombination (HR)

The first reports of homologous recombination were from yeast (Orr-Weaver et al., 1981), though the phenomenon was soon proven to occur in somatic mammalian cells (Folger et al., 1982). The process involves the exchange of genetic material between associated DNA sequences and can occur during DNA replication and repair. During the repair of strand breaks in both models, a dynamic search for a homologous partner takes place by a mechanism that encompasses a large chromosomal domain (Inbar and Kupiec, 1999). Upon identification, genetic information is transferred between the interacting DNA sequences (gene conversion). Despite an explosion of new applications dependent on homologous recombination, the underlying mechanism remains obscure. However, two main models have been proposed to account for it (reviewed in (Hooper et al., 1987b).

4.2.1 Models of HR

In the first model, developed by Meselson and Radding (1975), recombination is initiated by a single chromosomal strand break (figure 4.1). An alternative theory

Figure 4.1 Single-strand break model of homologous recombination

The exposed 3' end of a single strand nick acts as a primer for DNA synthesis (a). With extension, the new strand displaces its proximal homologue which invades the exogenous homologue, displacing a D-loop (b). Degradation of the D-loop precedes ligation of the invading strand, forming an intermediate asymmetric heteroduplex. Concurrent synthesis of the donor strand and degradation of the recipient chromatid expands the region of heteroduplex (c). Ligation of the 5' and 3' single strand ends produces a Holliday junction (d), which can migrate along the molecules as a symmetric duplex. Resolution of the Holliday junction can be achieved by one of two methods, branch migration (e) or isomerisation (f). Restriction of the crossed strands yields a parental strand and a strand that has undergone gene conversion without crossover (e). Alternatively, by isomersiation, the original crossed strands uncross and vice versa. Subsequent restriction of the crossed strands yields a region of gene conversion (f).

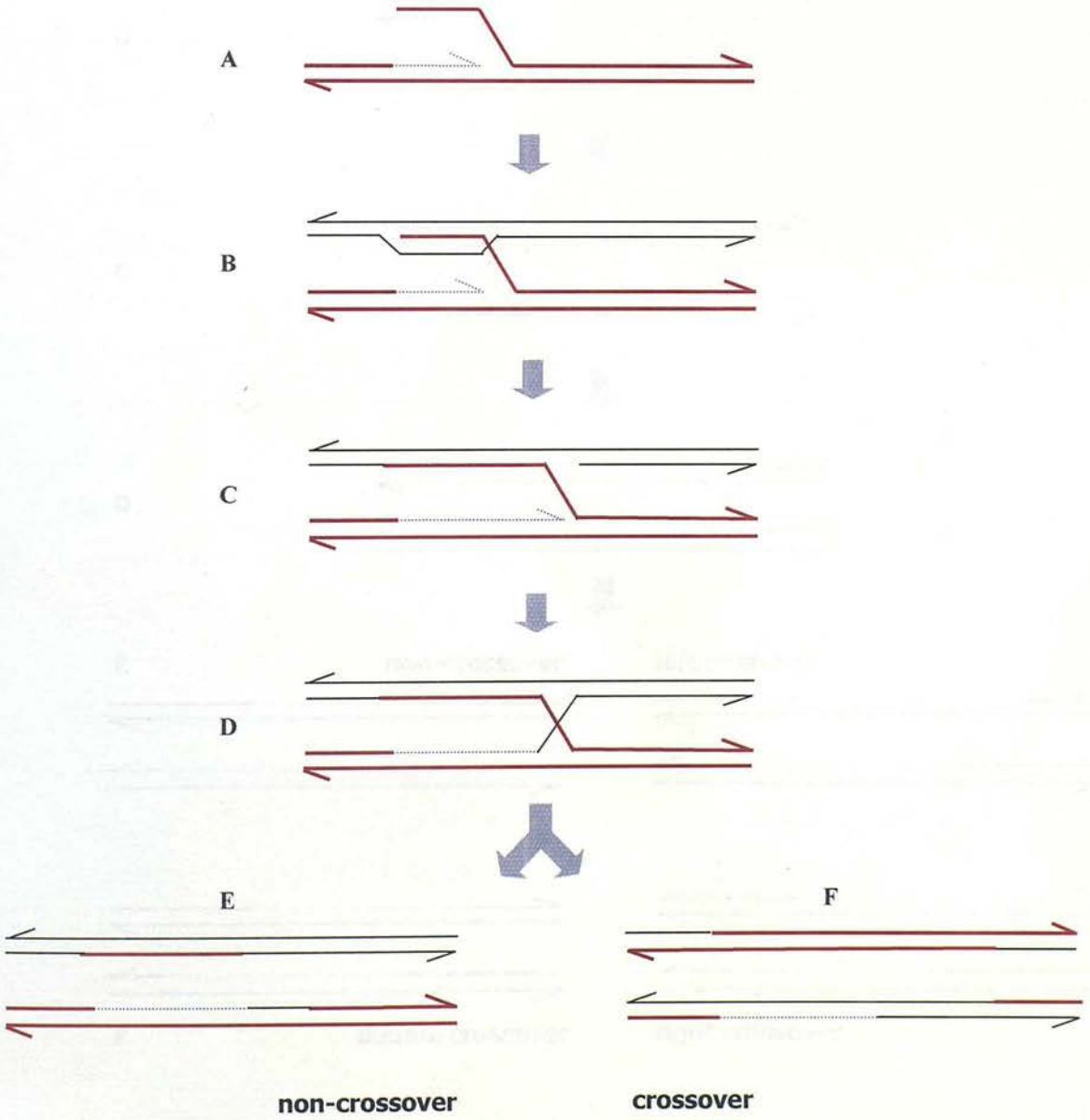

Figure 4.2 Double-strand break model of homologous recombination

Recombination is initiated by a break in both strands. 3' exonuclease activity generates a gap flanked by 3' single strands (a). One 3' end invades a homologous duplex, displacing a D-loop (b). Extension of the invading strand expands the D-loop until the other 3' end can anneal a complimentary single stranded sequence (c). Synthesis from the second 3' end concludes the gap repair (d). Ligation of remaining ends produces two Holliday junctions. Junction isomerisation determines the final configuration, occurring at either the left-hand (G), the right-hand (H), neither (E), or both junctions (F). Isomerisation at (G) or (H) resolve in crossover, (E) and (F) do not.

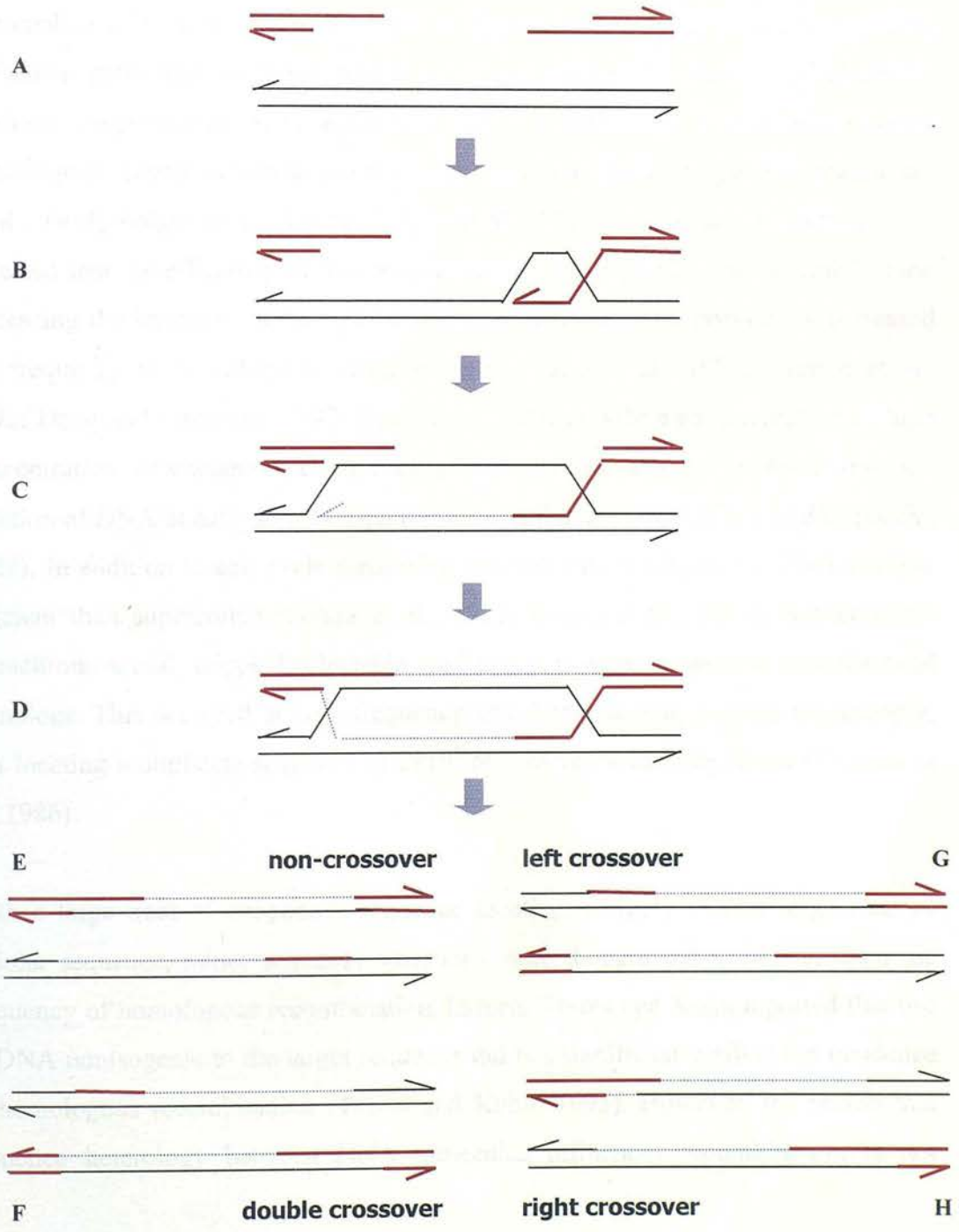

invokes a double strand break to inaugurate the process of strand exchange (figure 4.2) (Orr-Weaver et al., 1981; Stahl, 1996; Szostak et al., 1983).

4.2.2 Factors affecting the frequency of HR

While the mechanism of homologous recombination has yet to be fully resolved, progress has been made in determining the factors that control the frequency of its occurrence. Early work using two species of crippled selectable marker genes showed homologous recombination occurred between non-integrated plasmids in mammalian cells. Each plasmid carried a distinct, deactivating mutation in a drug resistance gene that conferred tolerance to an antibiotic. Survival of clones in medium supplemented with antibiotic was dependent upon extrachromosomal homologous recombination to reconstruct a functional resistance gene (Kucherlapati et al., 1984; Folger et al., 1985a; Folger et al., 1985b). Importantly, related work revealed that the efficiency of this recombination was dependent on several factors: increasing the length of homology between two sequences proportionally increased the frequency of homologous recombination (Ayares et al., 1986; Thomas et al., 1992; Deng and Capecchi, 1992; Hasty et al., 1991a). While administration of high concentrations of exogenous DNA does not enhance homologous recombination, the addition of DNA at early to mid S-phase of the cell cycle does (Wong and Capecchi, 1987). In addition to cell cycle sensitivity, recombination with linear DNA is more efficient than supercoiled (Folger et al., 1982; Bollag et al., 1989). Subsequently extrachromosomal, crippled selectable marker genes were targeted to chromosomal homologs. This occurred at high frequency and demonstrated, perhaps surprisingly, that locating a duplicate sequence in $3x19^9$ bp was not a limiting factor (Thomas et al., 1986).

With a large tract of exogenous sequence locating a highly similar large tract of cellular sequence, minor sequence variations were thought not to impact upon the frequency of homologous recombination. Indeed, Torres and Kuhn reported that use of DNA nonisogenic to the target sequence did not significantly affect the incidence of homologous recombination (Torres and Kuhn, 1995). However, the notion that sequence heterology between DNA molecules influences recombination is not

generally contested. Targeting of murine strain BALB/c DNA to 129/Sv ES cells was found to be 20% less efficient than targeting 129/Sv to 129/Sv (te Riele et al., 2000; Deng and Capecchi, 1992). Thus, interstrain sequence polymorphisms, such as small deletions, insertions and base pair substitutions may influence the fidelity of targeted recombination.

While the above factors relate mainly to exogenous and recipient DNA, protein factors are known to influence the frequency of recombination. RecA is an *E. coli* protein with homologous DNA pairing and strand exchange activities. Overexpression of nuclear-tagged RecA increased the frequency of homologous recombination 10-fold in mouse teratocarcinoma cells (Shcherbakova et al., 2000). Structural homologs of RecA are widely distributed in higher eucaryotes, including mouse and man. An excess of the human RecA homolog, hRAD51, led to a similar increase in gene targeting frequencies in human cells (Yanez and Porter, 1999). These studies suggest cell type differences in chaperones dedicated to mediating reciprocal DNA exchange will lead to cell-type differences in DNA recombination rates and may, with further characterisation, be open to enhancement.

Combined knowledge of these factors can be used to attenuate the frequency of non-homologous integrations. Nevertheless, homologous recombination between exogenous DNA and chromosomal loci usually occurs at much lower efficiency than random recombination (Thomas et al., 1986). In the absence of a selectable phenotype, isolation of cells harbouring infrequent homologous recombination events would be difficult to detect. Use of intact marker genes, within and out with the targeting vector region of homology, enables enrichment of clones bearing a targeted gene.

4.3 Approaches to disrupt endogenous loci

Selectable marker cassettes have become the predominant enrichment vehicle for homologous recombination events. A typical cassette comprises a complimentary DNA sequence of a marker gene flanked by a robust promoter and poly adenosine signal: a construction formula that maximises expression of the marker protein

regardless of the integration site. The gene for *hprt* (*h*ypoxanthine *p*hospho*r*ibosyl *t*ransferase) was originally utilised to select for recombinants, since it was possible to select for its presence in HAT medium or absence in 6-thioguanine. With time alternative genes have been utilised to enhance selection. The bacterial *neo* gene (*neo*mycin phosphotransferase) confers resistance to the antibiotic G418, while the gene for *tk* (*t*hymidine *k*inase), derived from the herpes simplex virus, imparts susceptibility to the nucleoside analogue gancyclovir. Genes encoding potent toxins, such as DT-A (*D*iptheria *t*oxin *A*) and Ricin A have also been used to deplete cell populations (Arase et al., 1999). Positioning of cassettes internal (positive selection) and external (negative selection) to the recombination region provides a mechanism to select for targeted recombination. For example, as a consequence of embedding a *neo* cassette within the targeting vector region of homology and a *tk* cassette adjacent to the region of homology, proliferation in G418-containing medium intimates plasmid integration, and resistance to gancyclovir implies loss of *tk* by recombination (figure 4.3). Such negative, or counterselection, enriches for recombination specifically between *neo* and *tk*, where there is sequence similarity between vector and the genome. This dual "positive-negative" selection procedure is a powerful tool for isolating rare recombination events.

Implanting a vector-borne selectable marker into an endogenous coding sequence identifies that event, but also acts as a mutagen. When the goal is to constitutively deactivate a gene, there are a variety of approaches to ablate gene function using this key premise.

4.3.1 Null alleles

One method involves implanting a selectable marker, along with the complete targeting construct, in the genomic locus. This type of "insertion" targeting vector relies on the large quantity of foreign DNA in the coding sequence of a gene to deactivate it through gross sequence disruption (figure 4.4a). However, insertion vectors can cause the formation of tandem duplications. Such duplications are unstable and may undergo intrachromososmal recombination, resulting in elimination of the vector sequence and reversion of the locus to its wild-type state

Figure 4.3 Positive-negative selection.

A, Homologous recombination between replacement vector and endogenous locus leads to targeted replacement of a gene segment with *neo*, and loss of *tk*. Clonal cells are G418 and gancyclovir resistant. B, non-homologous recombination between vector and genome leads to insertion of *neo* and *tk*. Clonal cells are resistant to G418 but sensitive to gancyclovir.

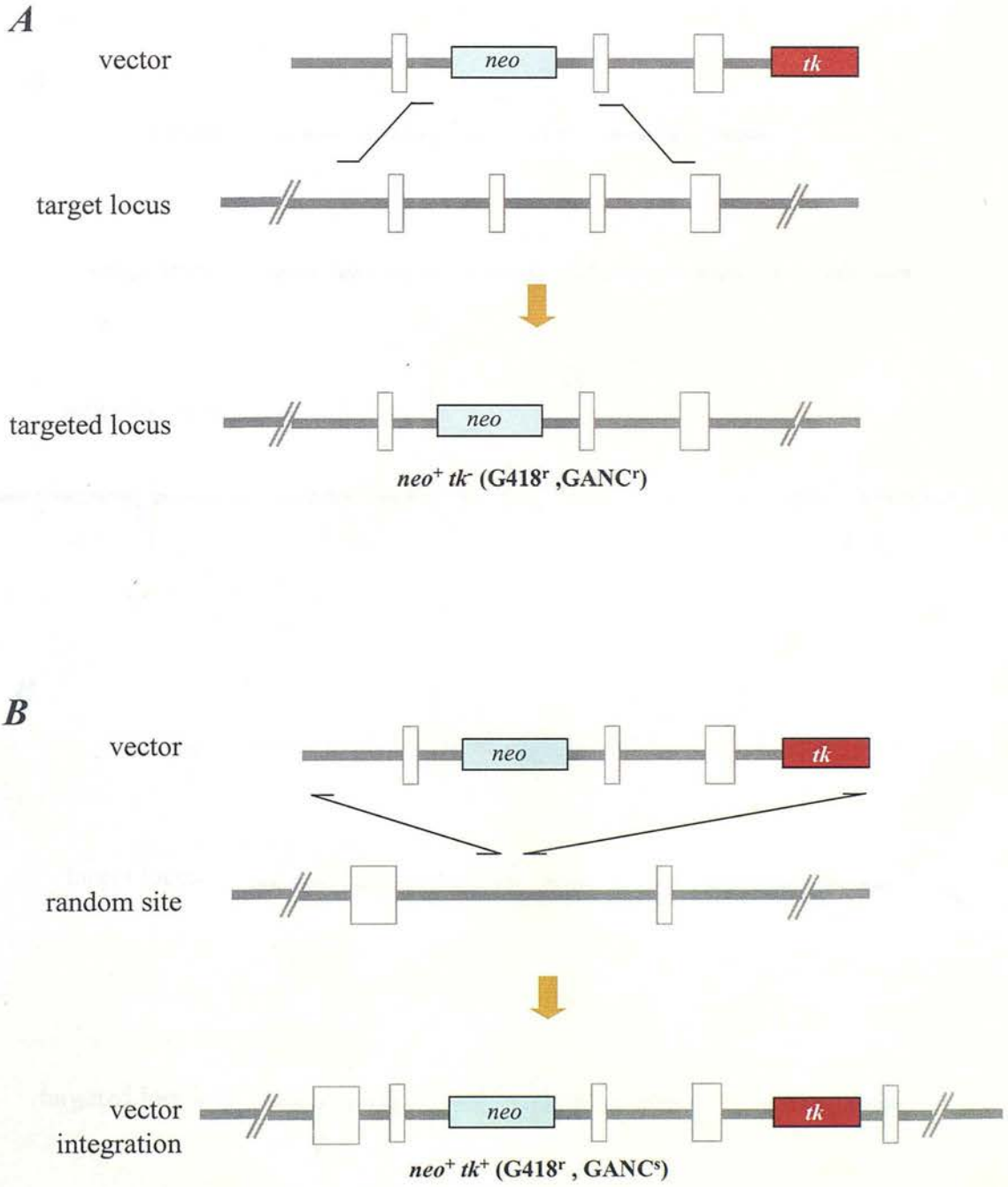

Figure 4.4 Gene inactivation by replacement or insertion

A, Insertion of vector sequence disrupts endogenous loci. Vector is linearised within the region of homology. Exchange between the exposed ends of the vector with homologous endogenous sequences is followed by recombination at the double strand break. Vector insertion generates a partial locus duplication. *B*, Replacement of endogenous sequence with exogenous *neo* sequence. Vector is linearised in plasmid backbone and homologous recombination with locus deletes gene segment. Open boxes represent coding sequence; grey lines, intronic sequence and narrow green lines, vector backbone.

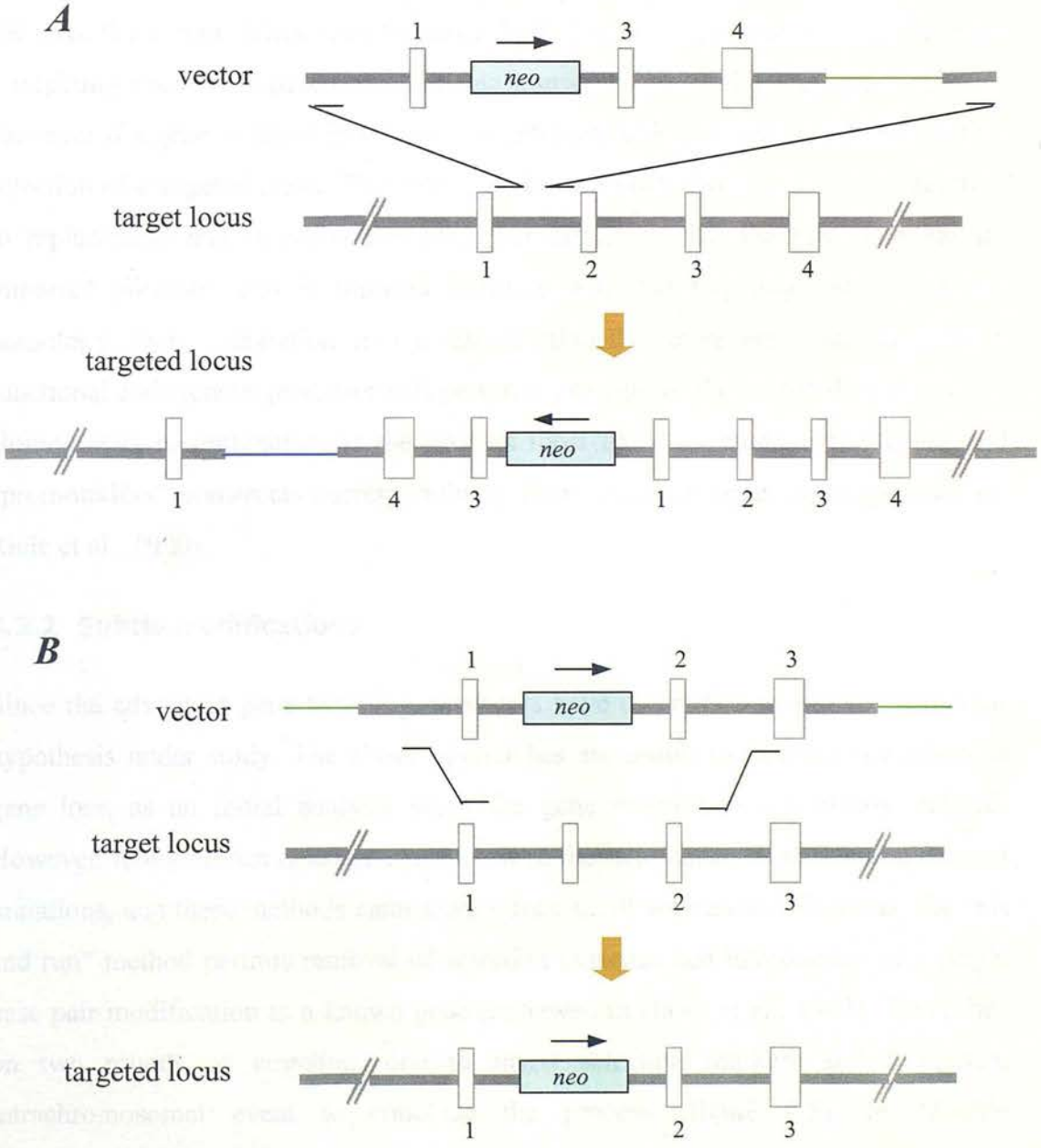

(Thomas et al., 1992). A different technique is to replace a designated segment of coding sequence of an endogenous gene with the selectable marker, thereby causing a deletion of that segment (figure 4.4b). This "replacement" type of targeting vector leaves the modified genomic locus free of other sequences present in the vector. According to different sources, the replacement approach yields a higher (Thomas et al., 1992), lower (Hasty et al., 1991b), or no (Thomas and Capecchi, 1987; Thomas et al., 1986) discernable difference in the targeting fidelity.

Insertion and replacement approaches utilise a strong promoter imported with the plasmid to drive expression of the selectable markers. If a gene is not expressed in ES cells, these approaches have the advantage of permitting selection of clones with a targeting vector integrated at otherwise transcriptionally silent genomic regions. However if a gene is active in ES cells, an alternative design may be taken to enrich selection of a targeted clone. This strategy utilises a vector with similar configuration to replacement and insertion plasmids, but differs in that the *neo* gene has no imported promoter and is inserted in-frame with the targeting vector genomic homology. Only integration into a transcriptionally active area, and distal to a functional endogenous promoter will permit expression of the marker-fusion protein. Homologous recombination is the process most likely to mediate this event and "promoterless" constructs correspondingly show elevated targeting frequencies (te Riele et al., 1990).

4.3.2 Subtle modifications

Since the advent of gene targeting, protocols have diversified to suit the particular hypothesis under study. The above approaches are useful to examine the effect of gene loss, as an initial analysis when the gene function is not clearly defined. However, many human diseases correlate with the inheritance or acquisition defined mutations, and these methods cannot reproduce small aberrations. However, the "hit and run" method permits removal of selection cassettes and introduction of a single base pair modification in a known gene (reviewed in Hasty et el., 1993). This relies on two rounds of targeting, one to insert selection markers and a second, intrachromosomal event to conclude the process (figure 4.5). In "double

Figure 4.5 "Hit and run" gene targeting

The vector carries the mutation of choice and has *neo* and *tk* cassettes out with the area of homology. "Hit": linearisation within the area of homolgy precedes insertion via homologous recombination (HR) between the exposed vector ends and the locus. This renders cells resistant to G418 and sensitive to gancyclovir. Clones with the desired intermediate structure are isolated by screening and expanded. "Run": resolution of the duplication is by intrachromosomal homologous recombination (IR), a process occurring spontaneously at low frequency in targeted ES cells. Resistance to G418 and gancyclovir selects for this event. Bold blue numbers indicate exons derived from the targeting vector; *, a specific mutation and solid arrows, the direction of selection cassette orientation.

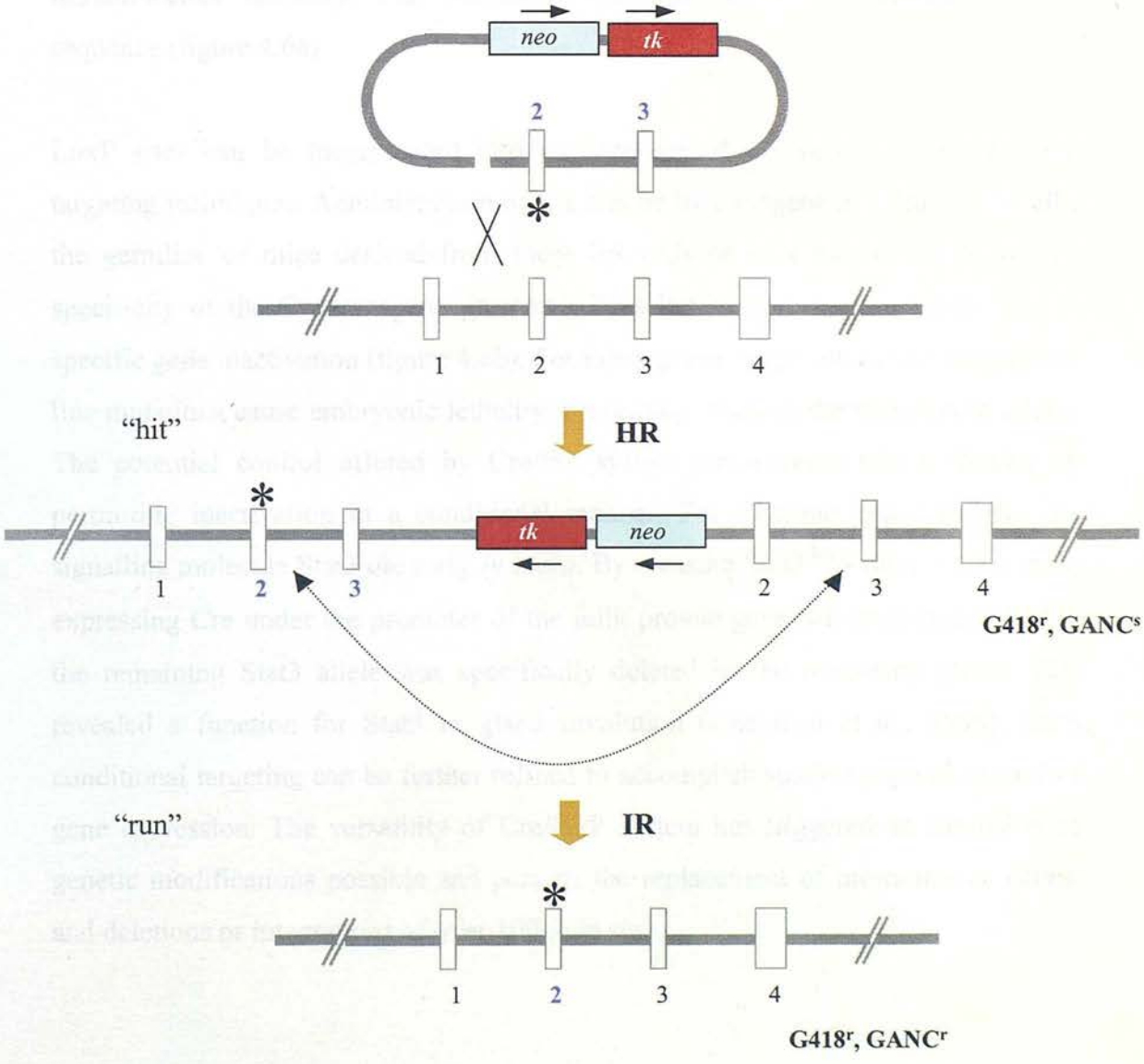

replacement", a variation of hit and run, the latter step is substituted with a second targeting vector (Stacey et al., 1994; Wu et al., 1994).

More recently, gene targeting technologies not reliant on homologous recombination have emerged and been harnessed. In "site-specific recombination" exchange occurs at specific positions that are the targets of specific recombinases, rather than between DNA molecules sharing regions of extensive sequence homology. The "Cre/loxP" recombination system relies upon exchange between 34bp "loxP" sites, mediated by the bacteriophage P1-derived protein Cre (*c*atalysed *re*combinase). The unmodified system is functional in mammalian cells and opens new avenues in the mode of mutation delivery. When loxP sites (*lo*cus of crossover (*x*) in *P*1) are placed in the same orientation on a linear DNA molecule, Cre catalyses a loxP-loxP intramolecular exchange that concludes with excision of intervening "floxed" sequence (figure 4.6a).

LoxP sites can be incorporated into the genome of ES cells via conventional targeting techniques. Administration of Cre can be by transgene in cultured ES cells, the germline of mice derived from these ES cells or in a manner based on the specificity of the Cre-transgene promoter. This latter approach can permit tissue-specific gene inactivation (figure 4.6b). For many genes, large and inactivating germ-line mutations cause embryonic lethality, preventing study of the mutation in adults. The potential control offered by Cre/lox system circumvents this limitation by permitting inactivation in a conditional manner. For example, mice null for the signalling molecule Stat3 die early *in utero*. By crossing $Stat3^{flox}/-$ mice with a strain expressing Cre under the promoter of the milk protein gene β-lactoglobulin (BLG), the remaining Stat3 allele was specifically deleted in the mammary gland. This revealed a function for Stat3 in gland involution (Chapman et al., 1999). Such conditional targeting can be further refined to accomplish spatio-temporal control of gene expression. The versatility of Cre/loxP system has triggered an explosion of genetic modifications possible and permits the replacement of promoters or genes, and deletions or integrations of over 100kb in size.

Figure 4.6 Cre/loxP system and conditional gene inactivation

A, Excision products of Cre-catalysed recombination between two directly repeated loxP sites (green triangles) on linear DNA. One loxP site persists on each product. *B*, Strategy for conditional gene targeting *in vivo*. Upper left, a mouse strain carrying a functional loxP flanked allele, generated in ES cells. Upper right, a transgenic mouse strain expressing Cre constitutively or in an conditional fashion (purple area). Lower centre, result of crossing the two strains. In the cells expressing Cre, catalysed recombination between loxP sites excises the intervening sequence. The animals must be homozygous for the loxP-flanked allele to achieve complete gene ablation.

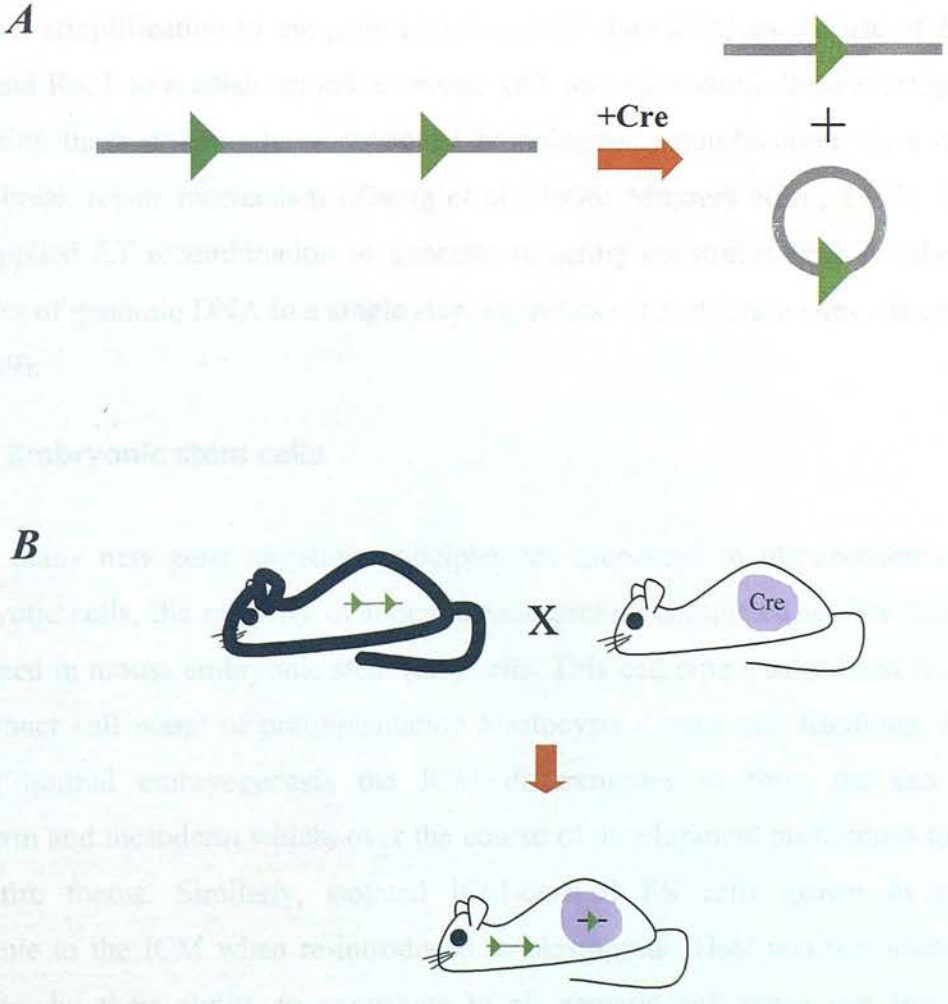

4.3.3 Recent advances

Strategies to modify gene structure continue to flourish. One-step sequence deletions have been achieved at high frequency using PCR in the fungus *Ashbya gossypii*. PCR-generated 45bp target homologies at the termini of a selectable marker gene are sufficient to mediate homologous recombination with the endogenous gene. PCR-targeting does not demand prior cloning and characterisation of target genes, or the construction of standard insertion cassettes. Conventional PCR screening strategies can confirm locus modification (Wendland et al., 2000). This relatively simple technology has been successfully applied in *E. coli* (Murphy et al., 2000). Both of these species have high levels homologous recombination, and whether it will operate in mammalian cells remains to be reported.

A further simplification to the gene targeting procedure involves the use of *E. coli* RecE and RecT to mediate strand exchange (ET recombination). Strains ectopically expressing these proteins have enhanced homologous recombination via a double strand break repair mechanism (Zhang et al., 1998; Muyrers et al., 1999). Others have applied ET recombination to generate targeting constructs from a subcloned fragment of genomic DNA in a single step, regardless of restriction sites (Angrand et al., 1999).

4.4 Embryonic stem cells

Whilst many new gene targeting principles are pioneered in ultra-recombingenic prokaryotic cells, the majority of targeted mutagenesis completed to date has been performed in mouse embryonic stem (ES) cells. This cell type was isolated from the ICM (*i*nner *c*ell *m*ass) of preimplantation blastocysts (Evans and Kaufman, 1981). During normal embryogenesis the ICM differentiates to form the ectoderm, endoderm and mesoderm which, over the course of development proliferates to form the entire foetus. Similarly, isolated ICM-derived ES cells grown in culture contribute to the ICM when re-introduced to blastocysts. Thus undifferentiated ES cells are, by their ability to contribute to all somatic cell types and functional

gametes, both pluripotent and totipotent. This trait permits transmission of targeted mutations generated *in vitro* to the germline and analysis *in vivo*.

Without specific blockers of differentiation however, explanted ES cells can differentiate into multiple cell phenotypes (Matsui et al., 1992). To prevent *in vitro* differentiation, ES cells were initially cultured on feeder layers of mitotically inactivated mouse fibroblasts (Evans and Martin, 1975). Experimentation with media supplements preceded the purification of efficient anti-differentiation factors, in particular a molecule eventually shown to be identical to LIF (*l*eukaemia *i*nhibitory *f*actor). Use of LIF, now cloned and routinely extracted, has made the requirement for feeder layers redundant (Williams et al., 1988; Smith et al., 1988; Moreau et al., 1988). Careful maintenance of ES inhibits differentiation, in turn permitting continuous proliferation and ensures retention, even with protracted passage, of pluripotency.

The property of continuous proliferation facilitates genetic manipulation of ES cells. The introduction of site-specific modifications to the ES cell genome, using gene targeting techniques, does not greatly alter their culture potential. Moreover, the extensive culture process to generate ES cells bearing specific deactivated genes does not reduce, once microinjected into a blastocyst, their ability to repopulate in the ICM. Implantation of recombinant ES cell-containing blastocysts in a pseudo pregnant mouse can initiate normal development, generating chimearic progeny that harbour recombinant ES cell-derived somatic and germline tissues. (Stewart et al., 1994; Matsui et al., 1992).

Most of the ES cell lines currently in use are derived from a congenic 129/SvJ strain of mice carrying wild-type alleles at the *albino* (*c*) and *pink* eyed dilution (*p*) coat colour loci. The mice derived from these cells are thus agouti in coat colour. Most host blastocysts used for ES cell microinjection are derived from C57BL/6J mice that are non-agouti. Thus mice that are produced by injection of blastocysts with ES cells are chimaeric for the desired mutation and pigmentation, and must be further bred to

test for germ-line transmission of the mutant allele and to generate mice hetrozygous and homozygous for the modification (Livy and Wahlsten, 1991; Gerlai, 1996).

The unique properties of ES cells permits the creation, by homologous recombination, of cells that can ultimately transmit defined mutations at defined loci to cell lineages comprising the mature organism.

4.5 Aims and experimental strategy

The normal physiological function of *γGCSh* in somatic tissue and during embryogenesis were unknown when work for this thesis was in progress. Generation of a *γGCSh*-/- phenotype should therefore provide valuable information regarding these roles. Consequently, advanced targeting strategies to introduce specific mutations were rejected and a "replacement" type approach, described in section 4.3.1, chosen to disrupt the *γGCSh* gene.

Using the genomic sequence characterised in chapter 3, a replacement targeting vector was designed and constructed. The plasmid, pGCSh-TV2, shown in figure 4.7, incorporates a neomycin resistance cassette (*neo*) as a positive selectable marker and replacement agent, and a herpes simplex virus thymidine kinase (*tk*) cassette as a counter-selectable marker. Homologous recombination between pGCSh-TV2 and *γGCSh* locus would replace a 2.3kb genomic fragment with *neo* (figure 4.7). This event would also introduce an alteration in the downstream open reading frame (ORF) (figure 4.8). The extent of sequence disruption introduced by targeted recombination is over 60%, and is detailed in table 4.1. At the time of writing, the relative positions of active sites, inter disulphide bridge(s) and other regions crucial to performing catalysis remain unidentified. In consideration of this, it is not possible to assert that a partial polypeptide sequence may retain residual enzymatic activity. However, a mutation altering >60% of the protein would be very likely, by radical transformation of the tertiary structure, to completely ablate catalytic activity.

Figure 4.7 Relationship between γGCSh cDNA, λ1 clone, targeting vector and gene.

Sizes do not accurately represent sequence length. Yellow boxes indicate coding sequence; dashed line shows the area covered in λ1 in comparison to full length complimentary DNA; cross-hatched area, position of the 1.3kb probe used to screen the λ-PS library; B, diagnostic *Bgl* II restriction sites, and bold numbers refer to sizes of λ1 *Bgl* II fragments in kb.

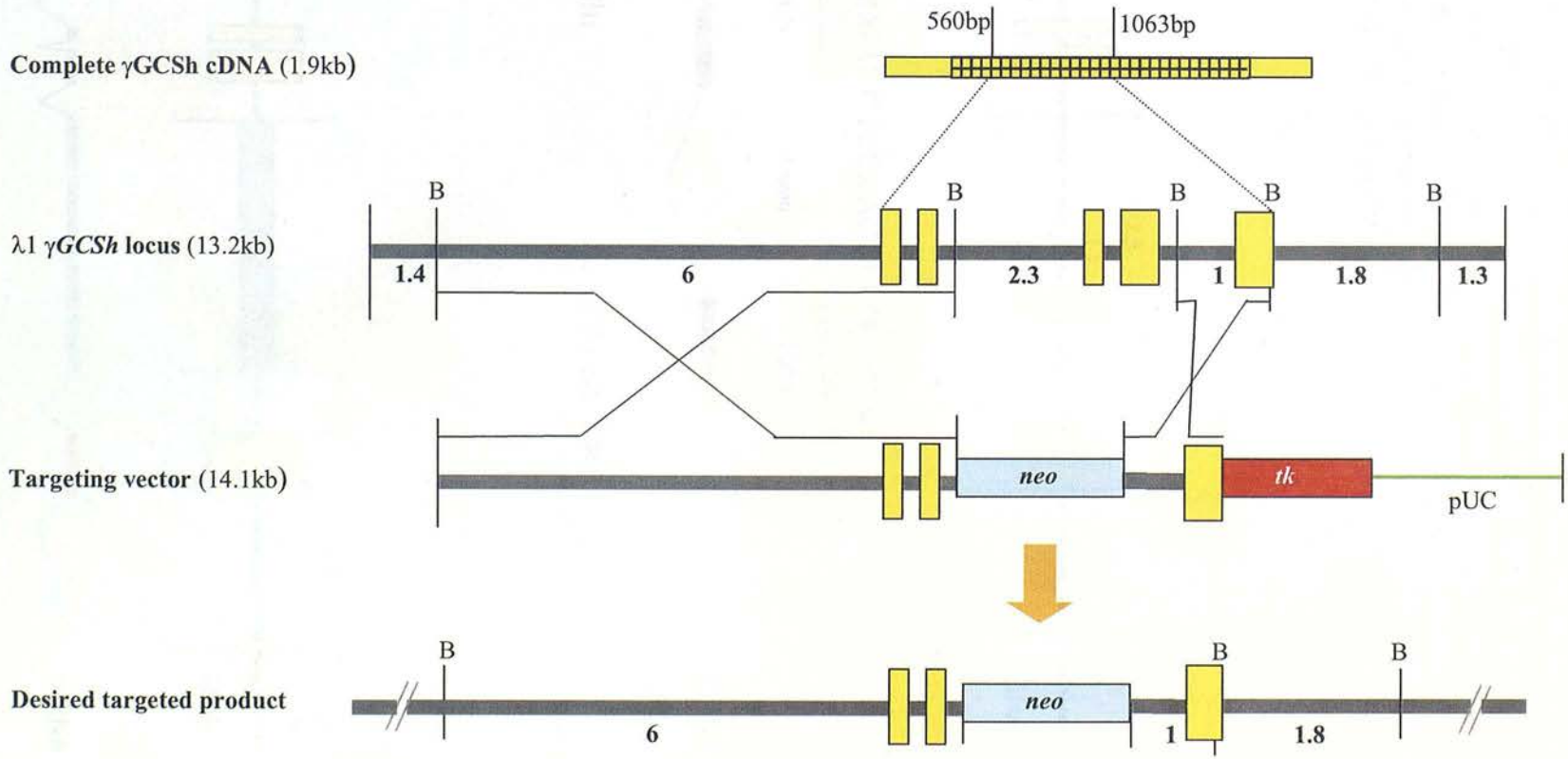

Figure 4.8 Introduction of frameshift mutation

Schematic representation of the predicted missense mutation in the *γGCSh* locus by gene targeting. *A*, local splicing in a wild-type *γGCSh* locus and, *B*, predicted splicing after homologous recombination between the targeting vector and endogenous gene causes a shift on ORF. Thick grey lines signify unknown or intronic sequence, blue lines neomycin phosphotransferase sequence, red lines sequence with a change in ORF and yellow boxes, coding sequence.

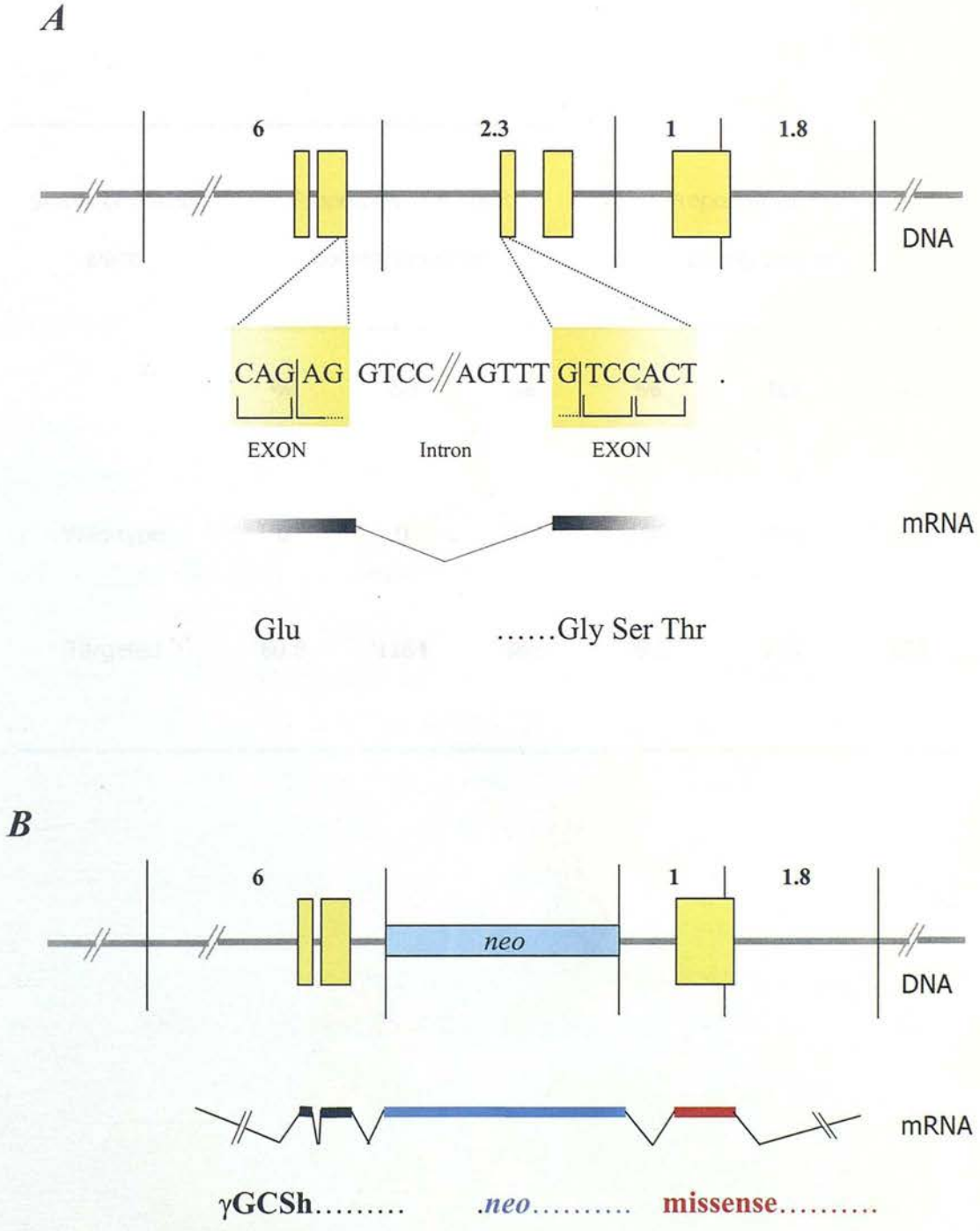

Table 4.1 Predicted *γGCSh* sequence disruption

Comparison of the total normal sequence in a wild-type *γGCSh* allele with a potential pGCS-TV2-targeted allele. 1164/1914 bp or 388/638 amino acids (60.8%) would be constitutively altered.

Status of *γGCSh* allele	Proportion of mutant coding sequence			Proportion of normal coding sequence		
	%	**bp**	**aa**	**%**	**bp**	**aa**
Wild-type	0	0	0	100	1914	638
Targeted	60.8	1164	388	39.2	750	250

4.6 Results

4.6.1 Construction of γGCSh Targeting Vector

At the time of experimentation, detail of the *γGCSh* gene structure available was confined to that elucidated in this thesis. The area, spanned by the insert carried in λ1, covered the central domain of the gene (figure 4.7). The sequence information derived from λ1 characterisation was used to design a targeting vector with a total homology of approximately 7kb. This required a two-step cloning strategy utilising the base vector pPNT (kindly provided by Dr S Selbert), outlined in figure 4.9.

The first step in the targeting vector construction was the non-directional insertion of a λ1 917bp *γGCSh Bgl* II fragment into pPNT. This represents the 3' arm of homology. Whole λ1 was digested with *Bgl* II, and the 917bp fragment purified from other fragments prior to subcloning into *Bgl* II-compatible *Bam* HI-lineraised pPNT. This cloning step generates two products, one plasmid containing the 917bp 3' arm of homology in the 5'-3' (correct) orientation: pGCSh-TV1, and one in the 3'-5' (incorrect) orientation: pGCSh-TV1*. Analysis of plasmids by restriction digestion with *Nsi* I and *Eco* RI permits resolution of these products (Figure 4.10).

The final step of the targeting vector construction was the directional insertion of a λ1 6kb *γGCSh* fragment into pGCSh-TV1. The pBS-6kb and pGCSh-TV1 plasmids were digested with *Not* I and *Xho* I. This liberates the original 6kb *γGCSh Bgl* II fragment with an additional 77bp of polylinker sequence and linearises pGCSh-TV1 at the 5' polylinker. Ligation of these sequences subclones the 6kb *γGCSh* fragment, in the correct orientation, into pGCSh-TV1. The resulting plasmid, pGCSh-TV2, is the completed vector. Liberation of the 6kb fragment from pGCSh-TV2 by digestion with *Not* I and *Xho* I confirmed the final construction step (Figure 4.11).

Figure 4.9 pPNT

Base plasmid for construction of *γGCSh* targeting vector. Schematic representation of pPNT functional features and restriction endonuclease map of enzymes used in targeting vector construction.

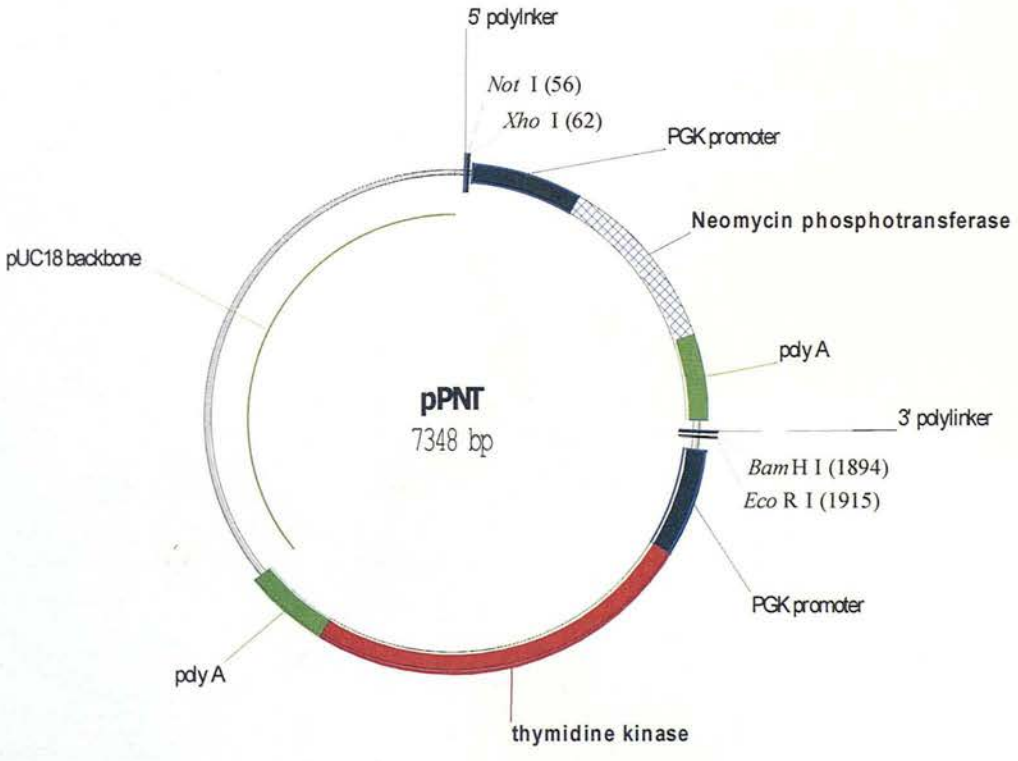

Figure 4.10 **Targeting vector construction: cloning step 1 of 2, and orientation of 3' *γGCSh* homology**

Top: Gels of the diagnostic restriction analysis of the two species of intermediate plasmid, pGCSh-TV1 and pGCSh-TV1*, with *Nsi* I and *Eco* RI. Plasmids carrying the 3' homology in the 3'-5' orientation, pGCSh-TV1*, generate a 694 and 7571bp fragment (A, lane 1). Plasmids bearing the homology in the 5'-3' orientation release a 264bp and 8001bp fragment (A, lane 2; and confirmed in high resolution (4% agarose) electrophoresis B, lanes 1-3,). Identification of the 264 and 694bp DNA fragments by size were used to resolve the 3' homology status of parental vectors. Vertical numbers represent size of DNA in bp. Bottom: Schematic organisation of intermediate plasmids, showing insertion of the 917bp 3' homology in the 5'-3' and the 3'-5' direction (C and D, respectively).

Figure 4.10 pGCS-TV1 construction

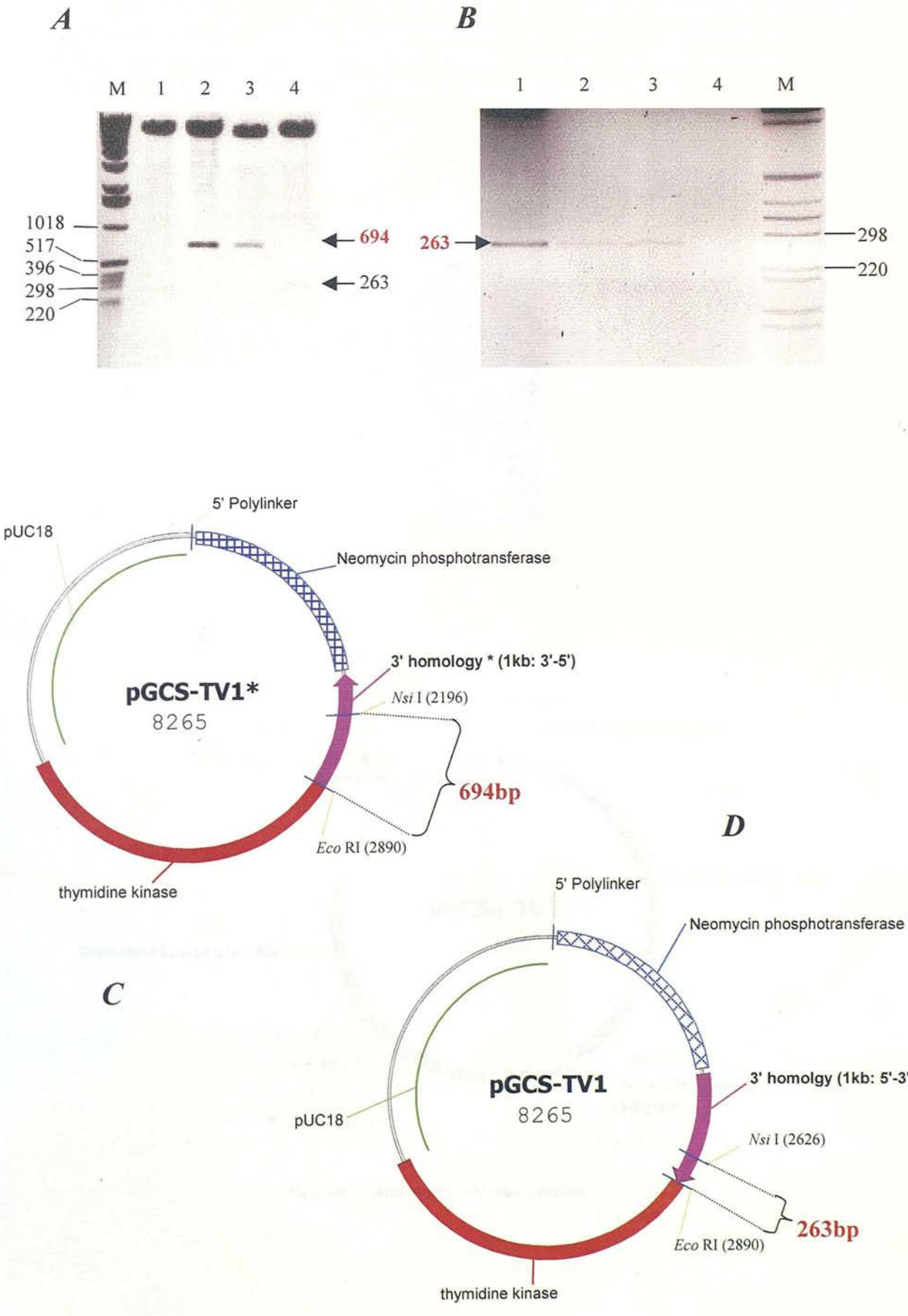

Figure 4.11 Targeting vector construction, cloning step 2 of 2

Directional insertion of 5' *γGCSh* homology into *Not* I and *Xho* I-linearised pGCSh-TV1 produces the final plasmid, pGCSh-TV2. *A*, gel of diagnostic restriction analysis: lane 1, pGCSh-TV2 digested with *Not* I and *Xho* I. This liberates the 5' arm (6kb), leaving linearised pGCSh-TV1 (8.2kb). Vertical numbers represent size of DNA in kb. *B*, schematic representation of final plasmid structure.

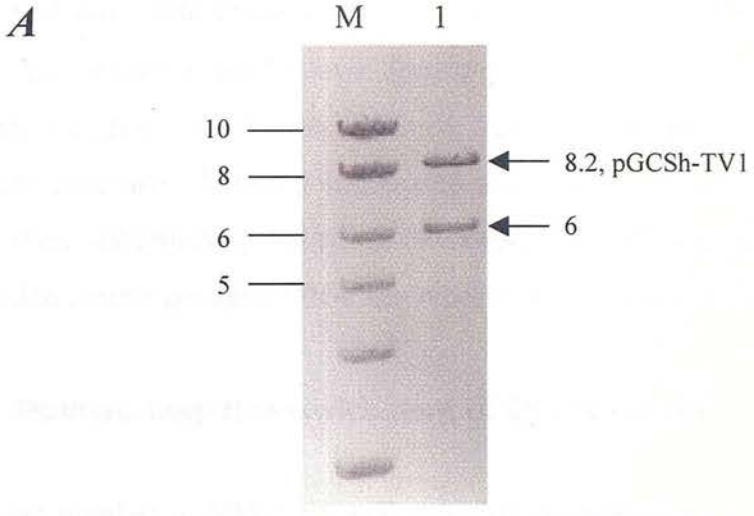

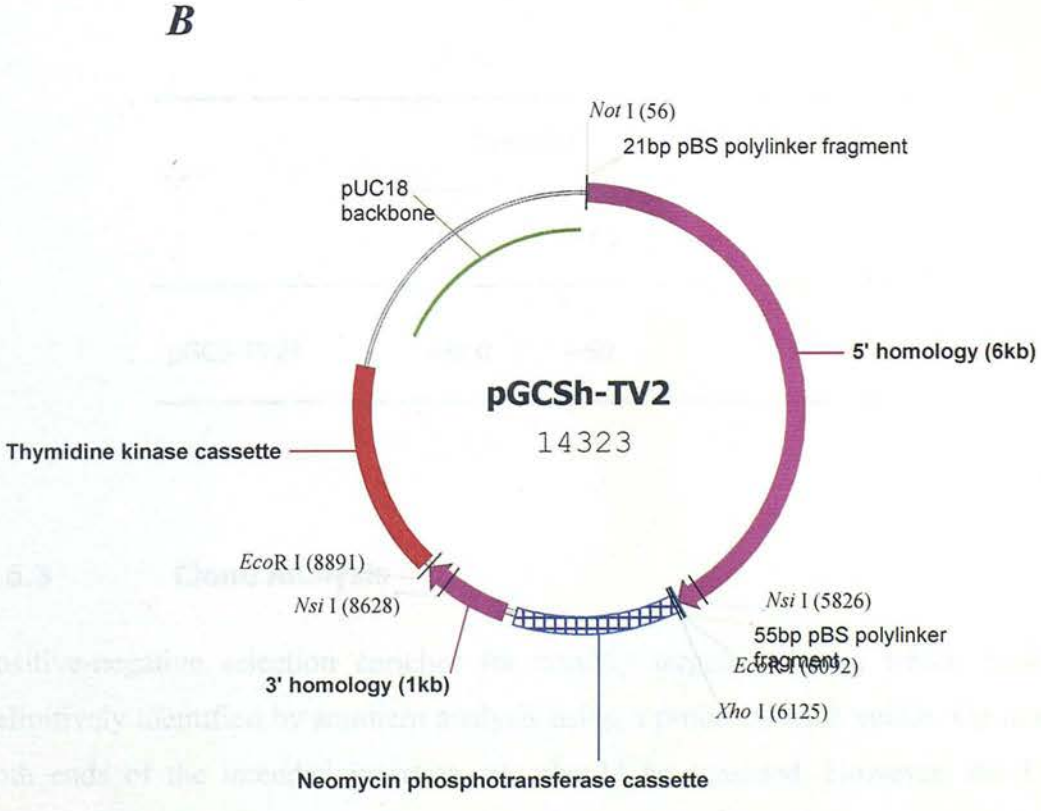

4.6.2 Obtaining antibiotic-resistant clones

Prior to electroporation into ES cells, pGCSh-TV2 was linearised by digestion with *Not* I and prepared as described in section 2.3.2. *Not* I has a unique recognition site 6bp upstream from the terminus of the 5' homology (figure 4.12). After introduction of the linear DNA in to 129Sv HM-1 ES cells by electroporation, clones were selected for 10-12 days with either 200μg/ml G418 alone (positive selection) or in combination with 50μg/ml gancyclovir (positive-negative selection). Table 4.2 details the number of resistant colonies obtained, showing a 18-fold enrichment with positive-negative selection. At this point, clones were picked and grown in isolated wells. Clones were subsequently split into two duplicate wells (outlined in section 2.3.3), one used to isolate genomic DNA, the other stored at –80°C for future use.

Table 4.2 Positive-negative enrichment of ES cell clones

Details the mean number of HM-1 ES cell colonies obtained per plate with single, positive selection (G418) or double selection (G418 and gancyclovir).

	Selection		Fold enrichment
	(+)	(+/-)	
pGCS-TV2*	~900	~50	18

4.6.3 Clone Analysis

Positive-negative selection enriches for corrctly targeted clones, which must be definitively identified by southern analysis using a probe external vector. Optimally, both ends of the intended insertion site should be screened. However, the DNA

Figure 4.12 Linearised pGCS-TV2

Analysis of pGCSh-TV1 prior to electroporation into ES cells. *A*, Gel showing: Lane 1: 5µg *Not* I-linearised pGCSh-TV2; Lane 2, 15µg *Not* I-linearised pGCSh-TV2. *B*, Schematic represenation of pGCSh-TV2 linearised with the unique cutter, *Not* I.

A

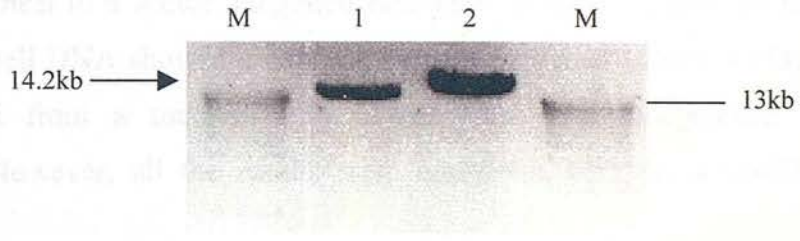

B

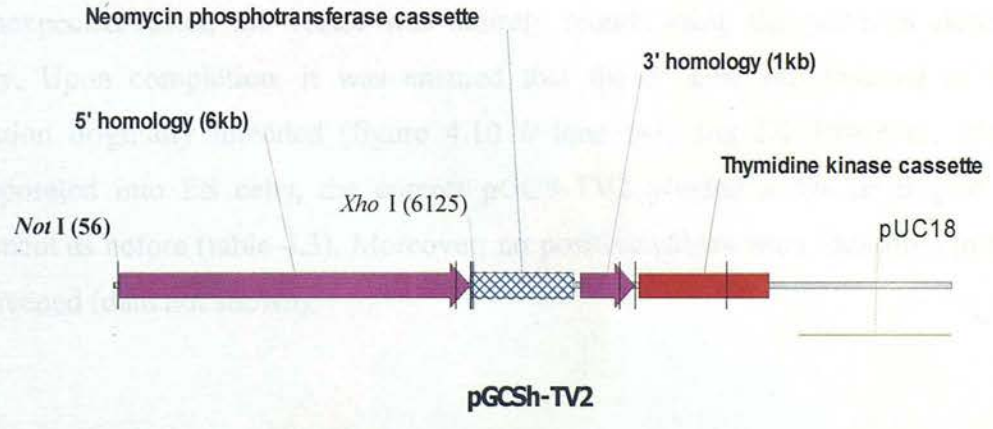

intended to act as a 5' probe incorporated radiolabelled nucleotides at low levels and hybridised non-specific sequences on southern blots (data not shown). An alternative 5' probe was not isolated, due to the small size (1.4kb) and incomplete restriction site information of the extreme 5' region of λ1.

However, an external 3' probe, "P" (figure 4.13), originating from the λ1 1.8kb *Bgl* II fragment labelled normally. The southern strategy adopted in this experiment to differentiate between clones containing a wild-type and a modified locus is outlined in figure 4.14. P can only show a band shift pattern if the endogenous gene is altered as it cannot anneal to a vector integrated randomly. A test 3' screen performed on wild-type ES cell DNA showed a band of the size predicted (figure 4.15a). Results were obtained from a total of 556 clones from two independent targeting experiments. However, all the results were consistent with an unmodified locus (figure 4.15b).

4.6.4 pGCSh-TV2 modification and re-targeting

Due to negative results obtained in section 4.6.3, the pGCS-TV2 vector was re-analysed. It was found that the 3' arm of homology was inserted in the 3'-5' orientation during construction, an error not detected by the initial mapping analysis and only found on subsequent examination (figure 4.10 *A* lane 2-3, and *C*). In light of this unexpected result, the vector was entirely rebuilt using the previous cloning strategy. Upon completion, it was ensured that the 3' arm was inserted in the orientation originally intended (figure 4.10 *B* lane 1-3, and *D*). However, when electroporated into ES cells, the correct pGCS-TV2 yielded a similar degree of enrichment as before (table 4.3). Moreover, no positive clones were identified in the 285 screened (data not shown).

Figure 4.13 Preparation of 3′ probe for southern analysis

A, schematic representation showing the origin of probe "P" relative to the cloned λ1 1.8kb *Bgl* II fragment. Purple arrow indicates position and orientation of the 1.8kb fragment. *B*, gel showing purified 570bp genomic probe P (lane 1) liberated from pBS-1.8kb by restriction with *Nco* I and *Not* I.

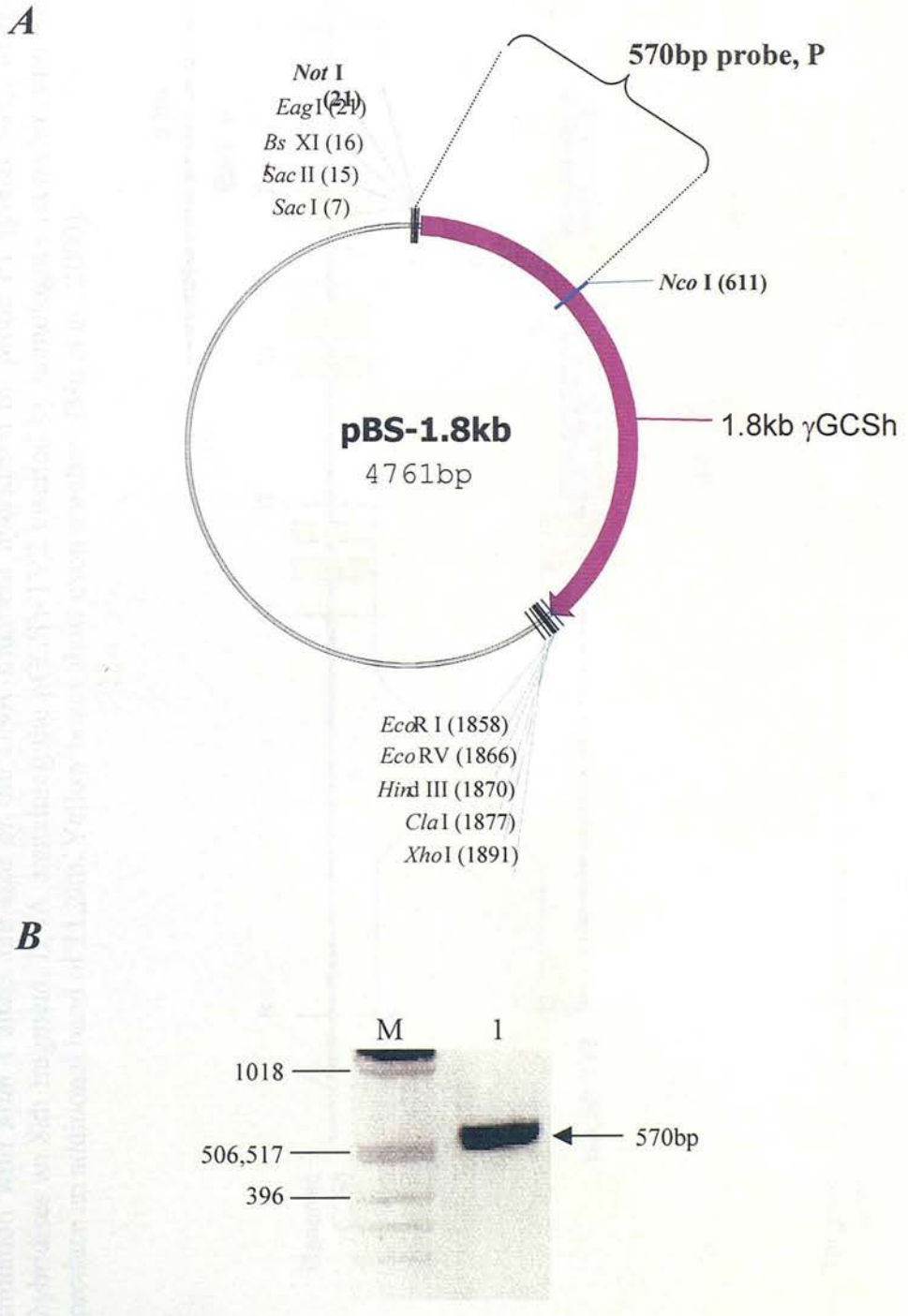

Figure 4.14 Southern screen strategy to identify a targeting event

Figure represents the wild-type gene (top), pGCS-TV2 (centre) and homologous recombination between pGCSh-TV2 and the *γGCSh* gene (bottom). Replacement of 2.3kb *γGCSh* genomic DNA with *neo* deletes a *Mun* I restriction site. Digestion of DNA bearing this mutation with *Mun* I alters the size of the DNA fragment hybridised by probe P1 (green box). In the wild-type *γGCSh* loci, P hybridises an 8kb fragment. DNA containing the pGCSh-TV2 inserted by homologous recombination will, when treated identically, produce an additional band of 11.2kb. Yellow boxes show exon numbers (Shi et al., 2000).

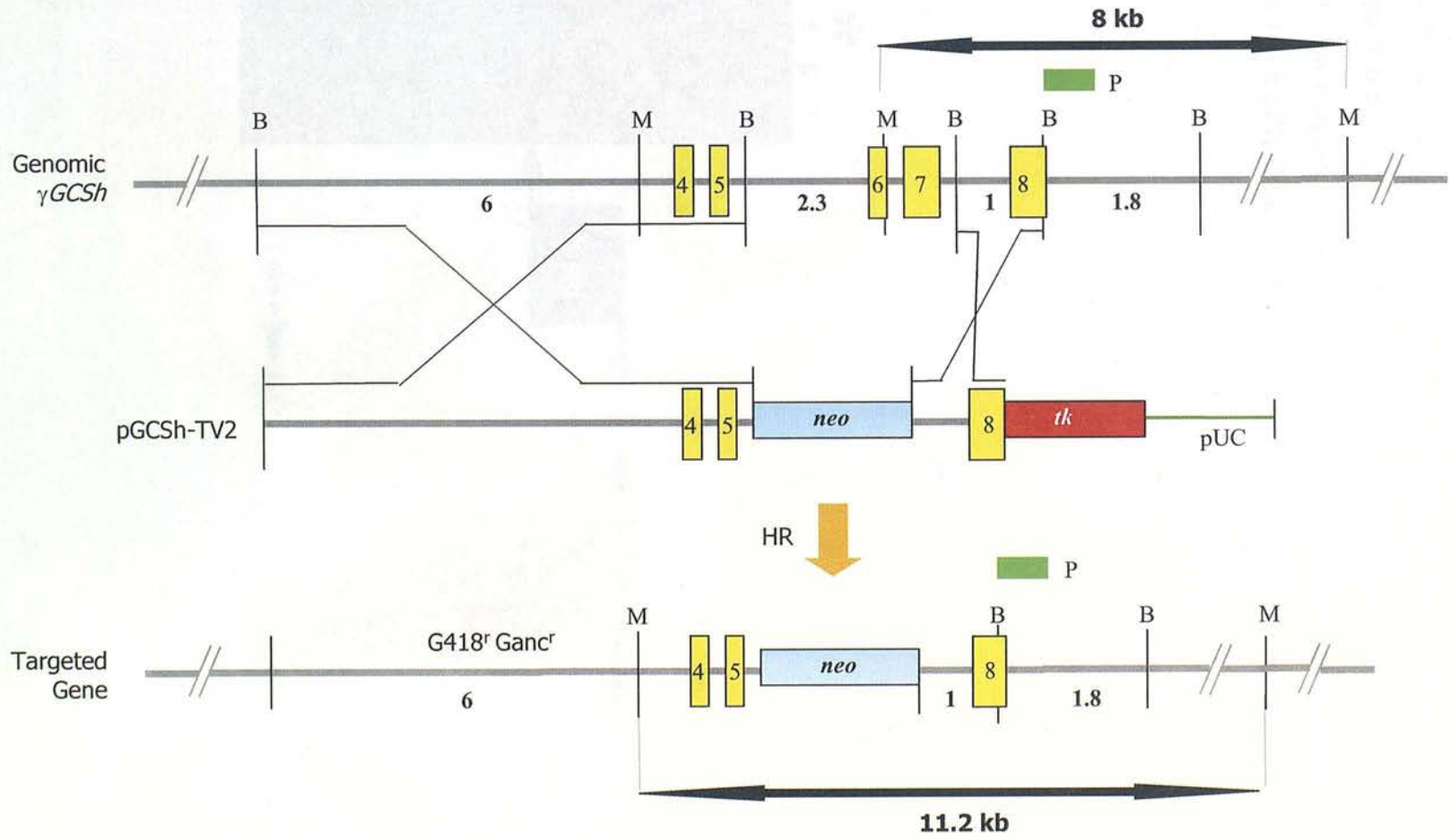

Figure 4.15 Wild-type and clone DNA analysis

Autoradiographs of the Southern screen, probed with 570bp *γGCSh* DNA external to the 3' region of homology in pGCSh-TV2. ***A***, wild-type ES cell DNA digested with: lane 1; *Sph 1*, lane 2; *Sac II*, lane 3; *Xba I*, lane 4; *BamHI*, lane 5; *Mun I* (highlighted with * to show the 8kb band), lane 6; *Bst XI* and lane 7; *Cla I*. ***B***, representative autoradiograph of *Mun I*-digested clone DNA, from a total of 285 clones screened. Lane A shows the 1.6kb pBR322-derived marker band, lanes B-G show single 8 Kb bands only.

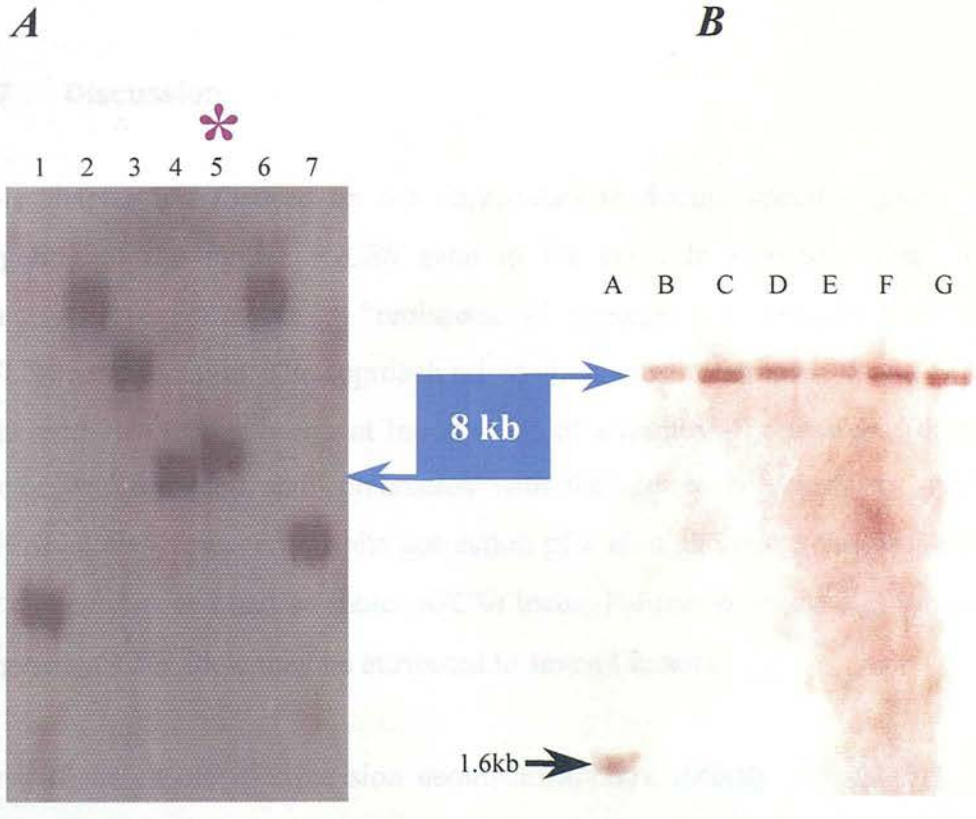

Table 4.3 Positive-negative enrichment of ES cell clones

Details the mean number of HM-1 ES cell colonies obtained per plate with single, positive selection (G418) or double selection (G418 and gancyclovir).

	Selection		Fold enrichment
	(+)	(+/-)	
Incorrect targeting vector, pGCS-TV2*	900	50	18
Correct targeting vector, pGCS-TV2	375	25	15

4.7 Discussion

This chapter has focused on the approaches to disrupt specific genes and gene targeting of the mouse *γGCSh* gene in ES cells. In common with most gene inactivation experiments, a "replacement" strategy was employed to inactivate *γGCSh* gene function. The approach relied upon substitution of 2.3kb of endogenous gene with *neo,* and subsequent introduction of a frameshift mutation. To this end, a vector was designed and constructed with the aim to constitutively deactivate a *γGCSh* allele. However, despite correction of a cloning error in the original vector, all clones screened had an intact *γGCSh* locus. Failure to isolate a clone carrying a targeted *γGCSh* allele may be attributed to several factors.

First, if the enforced expression neomycin applies, directly or indirectly, an ROS burden to ES cells, it is conceivable that the proliferative capacity of *γGCSh*-targeted ES cells would be reduced. As such, slow clone growth would reduce the apparent targeting frequency. However, insufficient data is available to support this argument, and as such it remains unsubstantiated.

Similarly, it was also thought conceivable, though unlikely, that *γGCSh* heterozygosity could impact upon ES viability. A situation could be envisaged where a *γGCSh*-targeted ES cell, with a compromised reducing capacity, could be selected against non-targeted cells with a complete reducing capacity. However, experiments performed later in this thesis show that transient reduction of the intracellular GSH level of ES cells with a specific inhibitor of γGCS, BSO, had no detectable effect on long- or short-term indicators of cellular viability. These experiments were conducted in a culture environment similar to that imposed by the process of gene targeting. Further work indicated that only when a degree of additional oxidative stress is applied, does the GSH level of ES cells become critical to maintain viability. Moreover, the proposition is likely to be incorrect since the generation of *γGCSh-/-* mice using HPRT as a positive selection marker (Shi et al., 2000). Shi *et al* showed that while complete GSH deficiency led to embryonic lethality at day 8.5, the proliferation of *γGCSh-/-* ES cells in media supplemented with NAC was comparable to wild-type ES cells (Shi et al., 2000). These cells had undetectable levels of GSH and confirms that *γGCSh* hetrozygosity would not affect the ability of ES cells to survive the process of gene targeting.

In consideration of the above points, other factors must have prevented a high frequency of homologous recombination. These factors may relate to the structure of the plasmid. First, the length and division of homology flanking the selectable marker are thought to directly affect the identification, strand pairing, branch migration and resolution of recombination junctions. Although the overall homology of pGCS-TV2 to the target locus is sufficient at approximately 7kb, the 3' homology, at 917bp, is relatively short. However, whilst this region is usually longer it remains within the periphery of the size recommended by others (Torres and Kuhn, 1995). Indeed, homologous recombinants have occurred successfully with constructs with a short arm of less than 0.5kb, as long as the "long" arm is generally greater than 4 – 5kb (Hasty et al., 1991a; Torres and Kuhn, 1995), though aberrant recombination products are found at higher frequency using shorter arms. This trend could be reversed when the homology was distributed equally (Thomas et al., 1992). This adds weight to a prediction of Thomas et al., (1987), that the use of a short arm may

preferentially depress the frequency of homologous recombination when using replacement targeting vectors. While it was acknowledged at the time of construction that the sequence balance of pGCS-TV2 was unequal, the position and frequency of restriction endonuclease sites in the λ1 insert were not fully known. A complete genomic map would have permitted optimal use of the sequence, perhaps allowing a configuration of the targeting vector with approximately equal lengths of homology. In addition, the requirement of probes external to the region of homology was a further consideration. In this respect, the total length of the λ1 insert presented an additional construction constraint, and it should be noted the targeting vector was designed with these delimiters in place.

Second, an important variable determining the frequency of homologous recombination is the extent of sequence similarity. Until recently, the significance of this factor was thought restricted to that of between strains, for example, 129 DNA is twenty times more efficient at targeting the retinoblastoma locus in 129-derived ES cells than in BALB/c-derived ES (te Riele et al., 2000). The ES cell line used in this thesis for electroporation was 129Sv HM-1, while the genomic λ-clone obtained in section 3 and used to construct the targeting vector was derived from a 129Sv strain "most commonly used in gene targeting" (Mo Bi Tec, 1996). Later, analysis showed some 129/Sv substrains had diverged enough to cause graft rejections. Historical tracing of substrains revealed λ1 DNA: 129/Sv D3 (substrain "steel") was discrete from the ES cell DNA: 129/Sv HM-1 (substrain "parental"). Although analysis of 25 protein markers from 129/Sv HM-1 and 129/Sv D3 strains showed little variation, some allelic differences were detected using simple sequence length polymorphisms (SSLP) (Simpson EM et al., 1997). Therefore λ-PS 129/Sv D3 library DNA is subtly distinct from the 129/Sv HM-1 ES cells used for electroporation. While the exact impact of this factor is difficult to predict, substrain genetic disparity may have aversely affected the frequency of homologous recombination between pGCSh-TV2 and the *γGCSh* locus.

Third, although 295 individual colonies were successfully examined by southern blot analysis this may have actually been insufficient. It is conceivable that if many more

clones were studied a positive targeting event may have been detected. Last, it should be noted that different targeting experiments, undertaken in similar conditions often produce substantially different targeting frequencies (Torres and Kuhn, 1995; Deng and Capecchi, 1992). Clearly, the process of homologous recombination between exogenous and cellular sequences remains to be fully elucidated in mammalian cells. Subsequently there are likely to be parameters left unoptimised in the system used in this investigation. In conclusion, aside from the sometimes unpredictable nature of gene targeting, the low frequency of predicted recombination here is most likely attributable to the combined effects of a relatively unequal distribution of homology, marginal sequence variation and, due to time constraints, the restricted quantity of ES cell clones screened.

Chapter 5

Responses of ES cells to oxidative stress

5.1 Introduction

ROS produced during normal metabolism or following exposure to exogenous pro-oxidants may adversely affect embryogenesis by causing DNA lesions, lipid peroxidation and protein degradation (section 1.1.2). Cellular mechanisms to maintain redox homeostasis and curb oxidative injury includes a complex array of chemical and enzymatic reducing agents, damage sensors and response effectors (outlined in section 1.2.1).

A key determinant in the maintenance of the redox equilibrium is the tripeptide GSH. GSH is the most abundant intracellular thiol, which affords protection against oxidative stress directly, or indirectly as a co-factor in repair reactions catalysed by GSTs and GPx (section 1.3.1.3). Cells under oxidative stress can respond by expanding the GSH pool. The mechanism mediating this GSH-response, though complex and poorly understood, frequently incorporates transactivation of *γGCSh* (section 1.3.2.2).

Another central factor involved in the maintaining cellular integrity is the stress-surveillance transcription protein, p53 (Lotem et al., 1996; Renzing et al., 1996). In response to a variety of stress signals, p53 co-ordinates the cellular processes of cell cycle arrest, DNA repair and apoptosis (section 1.5.4) (Lane, 1992; Clarke et al., 1993; Smith et al., 1995; Levine, 1997). In addition to its role as a tumour suppressor gene, section 1.5.5 details strong evidence that p53 also plays a significant role during embryogenesis. For example, many p53 deficient animals fail to develop normally and show a variety of defects, particularly related to neural tube malformations (Armstrong et al., 1995; Sah et al., 1995). How p53 performs such a function is unknown, but I hypothesise that it mediates removal of cells bearing oxidative injury.

ROS can activate p53 (section 1.5.2.3) and induce p53-dependent apoptosis (Symonds et al., 1994; Lowe et al., 1994; Kroemer et al., 1997). Accordant with this, cells can be rescued from apoptosis in some instances by addition of GSH (Jiang et al., 2000) or *γGCSh* overexpression (Manna et al., 1999) (and section 1.4.5). ROS are also implicated as downstream effectors in the execution phase of p53-dependent cell death (O'Connor et al., 1990; Lennon et al., 1991; Johnson et al., 1996; Lee, 1998), via transactivation of redox-related genes (Polyak et al., 1997) (see also section 1.5.3). Moreover, the discovery that p53 transactivates the GPx gene (Tan et al., 1999) opens a potential link between the p53 pathway and GSH regulation: a hypothesis developed in section 5.7.1. The function of GSH was therefore investigated in wild-type and p53-/- ES cells.

Data regarding ES cell GSH status was unavailable at the time of writing. Therefore this chapter (section 5.2 to 5.5) covers the preliminary work, utilising inducers of oxidative stress and GSH-depletion agents, required to create an *in vitro* experimental model. The model is then used to explore the role of GSH and p53 in the response of ES cells to oxidative injury (sections 5.6 to 5.9). Specifically, this chapter tests whether p53 and GSH affect both the immediate and long-term tolerance of ES cells to oxidative stress, and if p53 mediates tolerance through regulation of GSH levels. Furthermore, possible mechanisms by which p53 and GSH act as 'guardians' during early embryogenesis are addressed.

5.2 Synthesis of *γGCSh* and GSH in ES cells

5.2.1 Introduction

Though GSH is thought to be present in all mammalian cells, the levels of GSH deviate considerably between cell types. Embryonic cells, proliferating in a low (5%) oxygen environment, may be expected to metabolise oxygen at a lower rate than mature tissue at atmospheric oxygen tensions. Due to these considerations, we analysed whether *γGCSh* is expressed and GSH is present in ES cells.

5.2.2 Results

5.2.2.1 ES cells express *γGCSh*

Using primers designed for isolation of mouse liver *γGCSh* cDNA (section 3.2.2.2), RT-PCR was performed on total RNA extracted from subconfluent wild-type mouse ES cells. This generated two separate fragments that correspond to the sizes predicted from published human and rat sequences (figure 5.1). The larger of the two fragments contained the unique *Bgl* II site present in *γGCSh* cDNA (data not shown), and identifies the DNA as *γGCSh* sequence.

5.2.2.2 ES cells contain GSH

The total GSH levels, measured by the Tietze method (as described in section 2.4.3.2), showed the basal intracellular GSH level of wild-type ES cell extracts was 16.1 nmoles mg total protein-1 ±1.5. Untreated p53-/- ES cell extracts contained 16.01 nmoles mg total protein-1 ±1.9. Table 5.1 compares the GSH content of ES cells with that of other cell types.

5.2.3 Discussion

The RT-PCR data confirms that ES cells constitutively express *γGCSh*. However, it should be noted that this procedure is non-quantitative and does not indicate the level of expression. The GSH assay data shows ES cells also contain GSH, in levels comparable to other embryonic tissue but substantially lower than the majority of cell lines analysed, which are predominantly transformed (table 5.1). It was expected ES cells would produce GSH. This is predicted from a wealth of data, summarised in section 1.3.5, which suggests GSH is required for modulating ROS throughout early developmental processes.

Figure 5.1 ES cells express γ*GCSh* transcripts

RT-PCR strategy to detect the presence of γ*GCSh* mRNA in ES cells. (*A*) Dashed blue lines represent PCR products, solid black line cDNA template. γ*GCSh* exonic primers up2 + rev2 generate a 139bp product, up2+ rev4 a 1321bp product. (*B*) Agarose gel electrophoresis of RT-PCR performed on total RNA isolated from subconfluent wild-type HM-1 ES cells. M: 1kb ladder, lane 1: PCR with up2 + rev2, lane 2: up2 + rev4, lane 3: positive control amplifying the housekeeping gene encoding β-actin (480 bp product), lane 4: negative control.

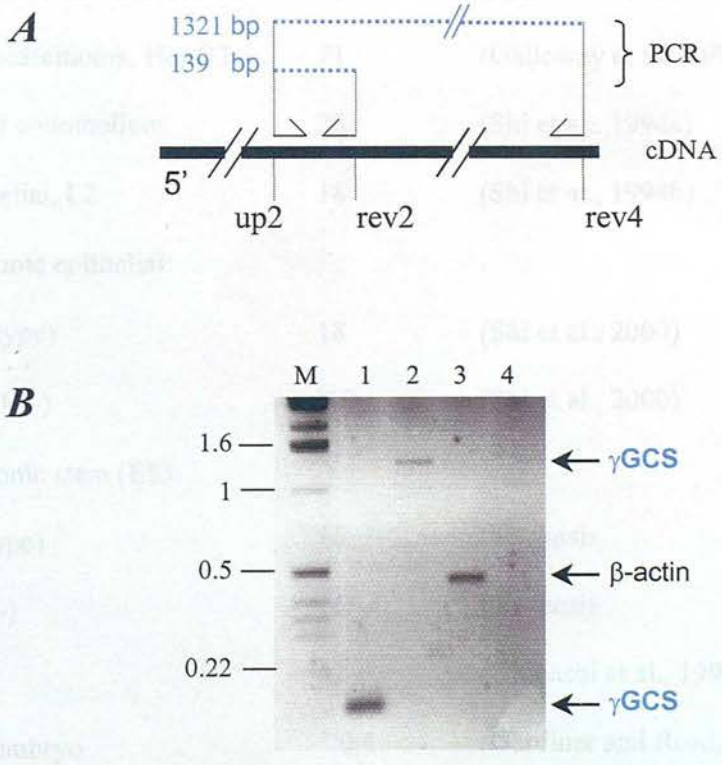

Table 5.1 Levels of GSH in different cell types

Illustrates the GSH level of ES cells in comparison to levels of intracellular GSH detected in other tissues. All GSH values are expressed as nmol/mg protein except values marked *, expressed as pmol/embryo. ND = no detectable level of GSH.

Cell type	Basal [GSH]	References
Human alveolar carcinoma, A549	150	(Rahman et al., 1996)
Human hepatocarcinoma, HepG2	71	(Galloway et al., 1999)
Bovine arterial endothelium	20	(Shi et al., 1994a)
Rat lung epithelial, L2	18	(Shi et al., 1994b)
Mouse embryonic epithelial:		
BDC-1 (wild type)	18	(Shi et al., 2000)
GCS-1 (*γGCSh*-/-)	ND	(Shi et al., 2000)
Mouse embryonic stem (ES):		
HM-1 (wild-type)	16	this thesis
HG287 (p53-/-)	16	this thesis
Rat embryo	12	(Ishibashi et al., 1996)
Mouse 2 cell embryo	* 0.4	(Gardiner and Reed, 1995)
Mouse blastocyst	* 0.2	(Gardiner and Reed, 1995)

5.3 Optimising depletion of ES cell GSH

5.3.1 Introduction

Considering the complexity of GSH synthesis, there are a number of approaches to depleting cellular GSH *in vitro*. BSO (*b*uthionine *s*ulph*o*ximine, figure 5.2a), a specific and irreversible inhibitor of γGCS (Griffith and Meister, 1979), is the most widespread reagent utilised for this purpose and is used clinically to deplete tumour GSH levels (reviewed in (Bailey, 1998). BSO competes with glutamate for the γGCS glutamate-binding site, where it binds as a transition state analogue. Inhibition occurs via a stable interaction between the *S*-alkyl moiety of BSO and γGCS (Griffith and Mulcahy, 1999).

Other workers have used the anti-inflammatory glucocorticoid steroid DEM (*di*ethyl *m*aleate, figure 5.3a) to deplete cellular GSH. Whereas BSO inhibits new synthesis, DEM acts on pre-existing GSH via a GST-catalysed reaction which produces a GSH-thioester conjugate (Gardiner and Reed, 1995b; Garcia-Ruiz et al., 1995; Watson et al., 1996).

The degree of GSH depletion depends on the species and cell-specific kinetics of GSH turnover (Deneke and Fanburg, 1989). Thus, the conditions necessary for these inhibitors to exert their effect varies between cell types. To estimate the optimum concentration of BSO and DEM to use on ES cells, cellular GSH levels and viability were measured following administration of a series of dosages. Cell viability was determined using the MTT assay (section 2.4.3.4), which measures dehydrogenase activity, and plotted as a percentage of untreated controls.

5.3.2 Results

5.3.2.1 BSO depletes ES cell GSH

Cells were pre-incubated for 16 hours in full GMEM medium supplemented with BSO (section 2.4.1.1). This treatment confirmed the ability of BSO to reduce GSH levels, although the reduction was similar for all BSO concentrations within the 25-250 μM

range employed (figure 5.2b). 100μM BSO reduced wild-type ES cell GSH levels by 69.8% ±2.10 (*t*-test P=0.001), though no impact on the MTT index registered until used at 250μM (figure 5.2c). This concentration has not been frequently used in previous studies, and was included as an indicator of ES cell tolerance to BSO. P53-/- ES cells showed a 70.4% ±2.81 (*t*-test P=0.001) depletion in GSH levels when incubated with 100μM BSO. To see any effect of a shorter incubation period, BSO at 100μM was also applied for 6 hours. This variation did not effect the level of GSH reduction observed (data not shown).

5.3.2.2 DEM depletes ES cell GSH and is dose sensitive

Figure 5.3b shows the degree of GSH depletion by DEM is dependent upon the dosage. At concentrations between 5-50μM, DEM reduces cellular GSH levels by approximately 70% and does not alter the MTT index (figure 5.3c). Higher DEM doses depletes GSH levels further, though treatment with DEM at 100μM and 300μM reduced MTT values by 41.22% ±3.87 and 45.42% ±2.51 (Mann-Whitney Rank Sum test P=0.035, for both values), respectively. Though DEM acts upon on pre-existent GSH and may thus act rapidly, a shorter incubation was not included in this experiment in case a protracted incubation period provided maximal GSH depletion.

5.3.2.3 BSO and DEM fully deplete ES cell GSH

In an attempt to lower ES cell GSH levels below that afforded by incubation with BSO or DEM alone, whilst not affecting viability, wild-type ES cells were co-incubated with both 100μM BSO and 20μM DEM. This treatment was found to reduce GSH levels 99.8% ±1.07, *t*-test P=0.001), approximately that of non-cellular controls. However, the combined treatment also reduced the MTT index by 41.1% ±3.27 (*t*-test P=0.001).

Figure 5.2 Depletion of GSH with BSO

Chemical structure of BSO (*A*). Total GSH content (*B*) and viability (*C*) of wild-type ES cells after incubation with a gradient of BSO concentrations, or without BSO. Error bars represent SEM values from 3 or more independent experiments.

A

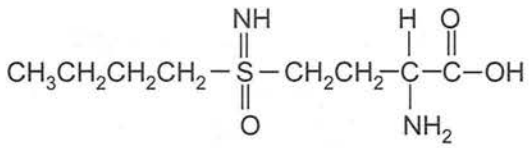

B

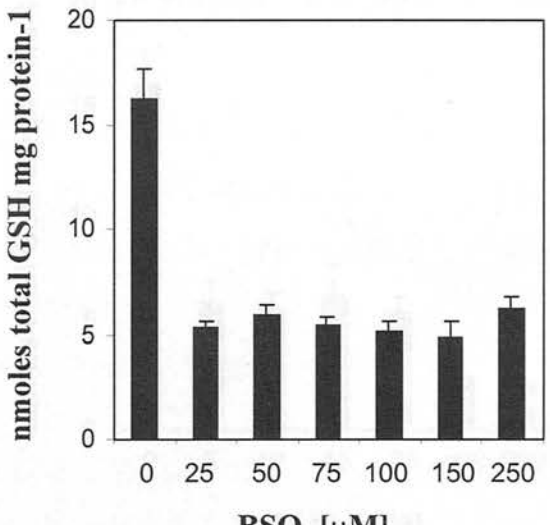

C

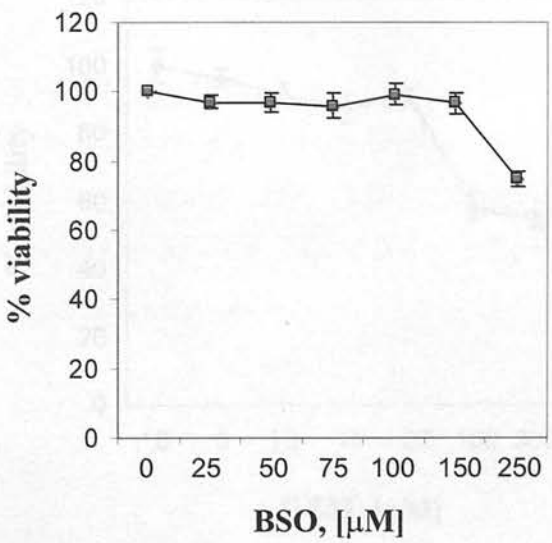

Figure 5.3 Depletion of GSH with DEM

Chemical structure of DEM (*A*). Total GSH content (*B*) and viability (*C*) of wild-type ES cells after incubation with a gradient of DEM concentrations, or without DEM. Error bars represent SEM values from 3 or more independent experiments.

A

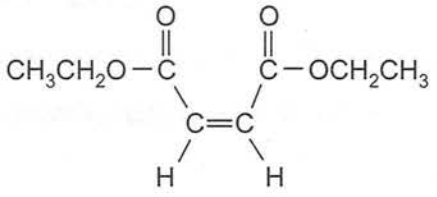

B

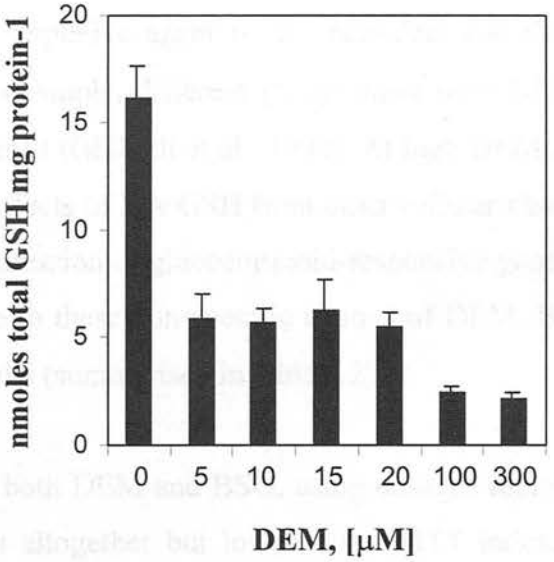

C

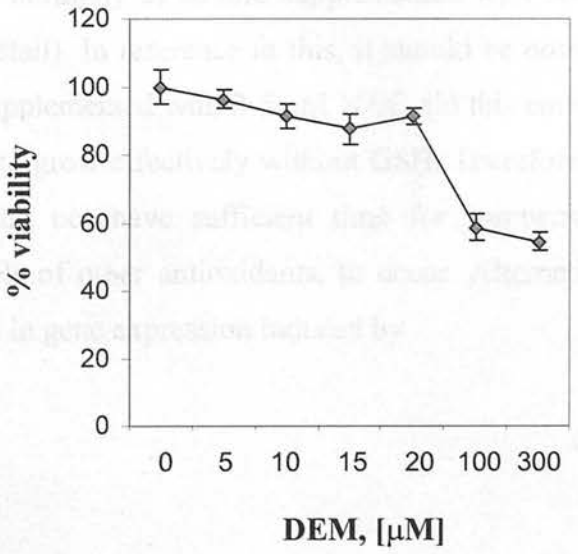

5.3.3 Discussion

Many studies performed on diverse cell types use BSO in the 50-100μM range. At these concentrations BSO is non-toxic and effectively depletes ES cell GSH levels, suggesting *de novo* GSH synthesis occurs in this cell type. The extent of GSH depletion in ES cells is broadly consistent with that obtained for the culture of other mammalian tissues with BSO, which ranges from <75% (Lu et al., 1999) to >90% (Aliosman et al., 1996). Although dose-sensitivity was not recorded with this concentration range, treatment with BSO at less than 25μM may have revealed dose-dependent reduction of GSH.

20μM DEM significantly reduced ES cell GSH levels without loss of viability. The use of DEM as a GSH depletive agent is less prevalent and the concentration used more heterogeneous. For example, different groups have used DEM at 10μM (Gardiner and Reed, 1995b) and 2mM (Ghibelli et al., 1998). At high DEM levels it may be impossible to differentiate the effects of low GSH from other cellular changes induced, most notably alterations in the expression of glucocorticoid-responsive genes (reviewed in (Barnes and Adcock, 1993). Due to these non-specific actions of DEM, BSO was selected to reduce GSH levels in ES cells (summarised in table 5.2).

Co-incubation with both DEM and BSO, using dosages individually non-toxic, depleted ES cell GSH levels altogether but lowered the MTT index, signifying a reduction in viability. However a *γGCSh-/-* embryonal cell line, subsequently generated by others, proliferates almost normally in culture supplemented with NAC (Shi et al., 2000) (see section 5.7.3 for detail). In reference to this, it should be noted that only with extended culture in media supplemented with 2-5mM NAC did this embryonic cell line eventually acquire the ability to grow effectively without GSH. Therefore, one possible explanation is that ES cells did not have sufficient time for compensatory responses, such as increasing the levels of other antioxidants, to occur. Alternatively or additionally, it is possible alterations in gene expression induced by

Table 5.2 Effects of BSO on wild-type and p53-/- ES cells

ES cells were treated for 16 h with 100μM BSO in full media. Immediately after treatment, cytosolic extracts were prepared and stored as described (section 2.4.3.2), prior to determination of GSH levels via the Tietze method. Cell viability twenty-four hours post BSO exposure was evaluated using the MTT assay. Data are mean ± SEM values from at least 9 independent experiments performed in triplicate. GSH reduction: * and ‡, *t*-test $P = 0.001$ vs untreated value.

Genotype	Treatment	*n*	GSH (nmoles/ mg protein)	GSH reduction (%)	Cell viability (%)
Wild-type	Untreated	18	16.1 ±1.5	0	100
	BSO 100μM	9	4.93 ±0.45	69.82 ±2.10 *	102.5 ±1.26
p53-/-	Untreated	9	16.01 ±1.9	0	100
	BSO 100μM	9	4.54 ±0.7	70.4 ±2.81 ‡	98.8 ±2.35

DEM may be incompatible with blocked GSH resynthesis. Since the mechanism underlying the observed fall in viability was not clear, BSO and DEM were not used in conjunction in subsequent experiments.

5.4 Pro-oxidant cytotoxicity in wild-type ES cells

5.4.1 Introduction

To assess the role of GSH and p53 in oxidative stress, a model oxidising agent was required. Oxidative stress can be induced by a plethora of naturally occurring and synthetic chemicals, ionising and ultraviolet radiation and biological signalling factors. Many of these compounds produce ROS in different ways (discussed in section 1.1.1) and as such require particular methods of detoxification. A series of compounds were chosen on the basis of their diverse mechanisms to generate oxidative stress, and tested on ES cells to define the range in which moderate cytotoxicity was induced.

5.4.2 Results

5.4.2.1 Hydrogen peroxide

Hydrogen peroxide (H_2O_2, figure 5.4 A1) is membrane permeable and produced naturally within cells, at low levels, though it can be released in large quantities by activated leukocytes during inflammation. H_2O_2 is catabolised to water by GPx, using GSH as a co-factor, or by catalase. The toxicity of H_2O_2 is thought to mainly rest on its local conversion, in the presence of neighbouring metal ions such as Fe^{2+}, to the highly reactive OH• radical. Possibly owing to the presence of cell-specific metabolic pathways, different groups predominantly attribute the toxicity of H_2O_2 to DNA damage (Wu et al., 1998), protein disulphide production (Rahman et al., 1995) or lipid peroxidation (Kyle et al., 1989). Figure 5.4 A2 shows, unexpectedly, that ES cells are resistant to relatively H_2O_2 high concentrations: at 500μM H_2O_2 does not significantly impact on viability (*t*-test P=0.411). However, 1mM H_2O_2 reduces the MTT index by 55.07% (*t*-test P=<0.001).

Figure 5.4 Kill curves for pro-oxidant compounds

Chemical structure of H_2O_2 (*A1*) and MQ (*B1*) are shown. Viability of wild-type ES cells twenty-four hours post incubation with a dosage gradient of H_2O_2 (*A2*) and MQ (*B2*), in comparison to untreated controls. Error bars represent SEM values from 3 independent experiments. * and † show significant reductions compared to untreated controls: ANOVA P=<0.001 and P=0.029, respectively.

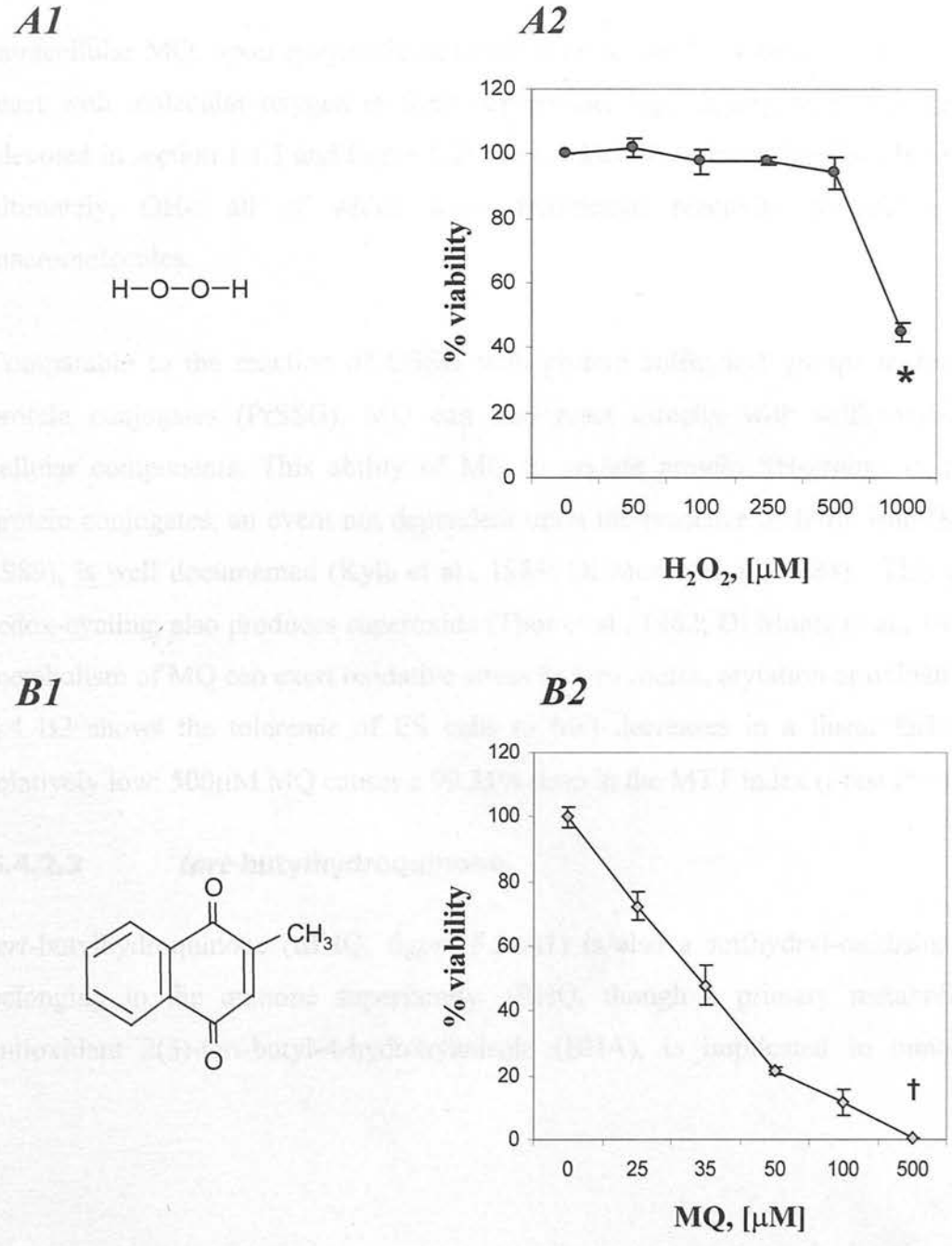

5.4.2.2 2-Methyl-1,4-naphthoquinone

2-Methyl-1,4-naphthoquinone or menadione (MQ, figure 5.4 B1), is a synthetic member of the quinone family that occurs widely in nature, and due to a relative absence of side effects is increasingly used as a chemotherapy agent (Wu et al., 1993; Nishikawa et al., 1995; Taper et al., 1996; Yaguchi et al., 1997). Quinones can exist in various redox states and diffuse across the lipid bilayer of plasma membranes.

Intracellular MQ, upon enzymatic semireduction to the MQ• radical can spontaneously react with molecular oxygen to form superoxide, regenerating MQ. This redox cycle (detailed in section 1.1.1 and figure 1.2) can produce ROS including $O_2^{\bullet -}$, H_2O_2, $^1O_2$ and, ultimately, OH•: all of which have detrimental reactivity towards endogenous macromolecules.

Comparable to the reaction of GSSG with protein sulfhydryl groups to form GSSG-protein conjugates (PrSSG), MQ can also react directly with sulfhydryl-containing cellular components. This ability of MQ to arylate protein SH-groups to form MQ-protein conjugates, an event not dependent upon the presence of ferric iron (Kyle et al., 1989), is well documented (Kyle et al., 1989; Di Monte et al., 1984). This event, like redox-cycling, also produces superoxide (Thor et al., 1982; Di Monte et al., 1984). Thus, metabolism of MQ can exert oxidative stress by two routes, arylation or oxidation. Figure 5.4 B2 shows the tolerance of ES cells to MQ decreases in a linear fashion and is relatively low: 500μM MQ causes a 99.31% drop in the MTT index (*t*-test P=<0.001).

5.4.2.3 *tert*-butylhydroquinone

tert-butylhydroquinone (tBHQ, figure 5.5 A1) is also a sulfhydryl-oxidising chemical belonging to the quinone superfamily. tBHQ, though a primary metabolite of the antioxidant 2(3)-tert-butyl-4-hydroxyanisole (BHA), is implicated in tumourigenesis

Figure 5.5 Kill curves for pro-oxidant compounds (continued)

Chemical structure of tBHQ (*A1*). Viability of wild-type ES cells twenty-four hours post incubation with a dosage gradient of tBHQ (*A2*) or UV (*B*), calculated relative to untreated controls. Error bars represent SEM values from 3 independent experiments. * and † show significant reductions compared to untreated controls (in both instances ANOVA $P=<0.001$).

A1

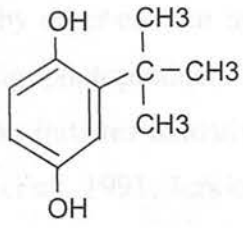

A2

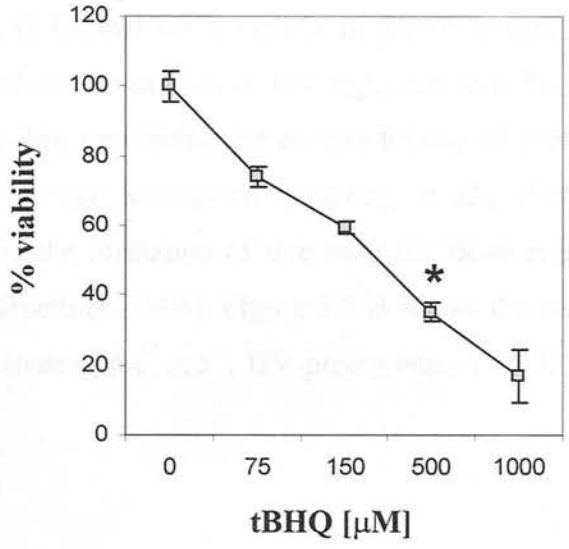

B

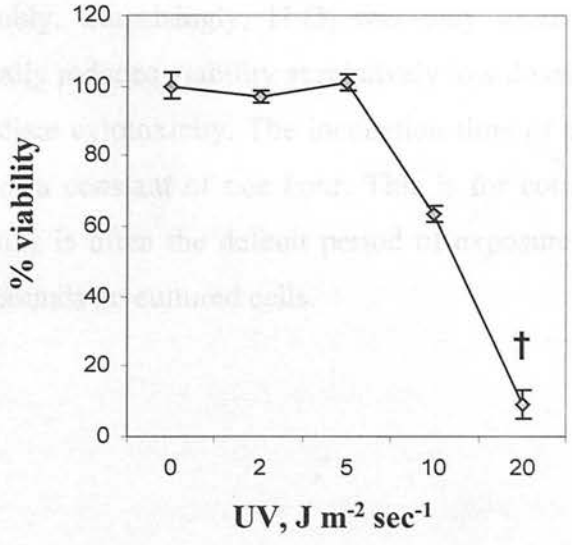

(Prochaska and Talalay, 1988; Rushmore et al., 1991). Figure 5.5 A2 shows the resistance of ES cells to tBHQ at a variety of concentrations. At 500μM tBHQ the MTT index falls by 64.94% compared to untreated controls (*t*-test $P=<0.001$).

5.4.2.4 Ultraviolet light

UV was used as an alternative vehicle to induce oxidative stress from that initiated by incubation with chemical agents. At high doses, ultraviolet light (UV) produces mutagenic dimers in DNA thought capable of initiating (Hall et al., 1988) and promoting (Romerdahl et al., 1989) malignancy. Exposure of mammalian cells to UV light triggers a global stress response (Devary et al., 1992) that can conclude in growth arrest, repair of DNA by NER or apoptosis (discussed in section 1.5.4). UV light can also be absorbed directly by other cellular macromolecules, preventing the correct folding of proteins and generating photoproducts following energy absorption (Renzing et al., 1996). UV irradiation initiates oxidative stress via the formation of free radicals (Bose et al., 1990; Konishi et al., 1991; Jurkiewicz and Buettner, 1994). Figure 5.5 B shows the survival of ES cells after UV irradiation. At 20 Joules min^{-1} sec^{-1}, UV precipitates a 36.32% fall in MTT index (*t*-test $P=<0.001$).

5.4.3 Summary

All the selected agents have genotoxic potential and demonstrate cytotoxicity to ES cells. The purpose of these experiments was define appropriate doses with which to challenge wild-type and p53-/- ES cells. In this regard, the toxicity of these compounds towards wild-type ES cells varied considerably. Surprisingly, H_2O_2 was only toxic at high concentrations, whereas UV dramatically reduced viability at relatively low doses and the quinone moieties exerted an intermediate cytotoxicity. The incubation time of chemical agents were pre-set and maintained at a constant of one hour. This is for comparative purposes since, in previous studies, this is often the default period of exposure used to examine the effects of cytotoxic compounds on cultured cells.

5.5 Effect of BSO and GSH on pro-oxidant cytotoxicity

5.5.1 Introduction

The objective of this experiment was to identify compounds selectively detoxified by GSH, for use in subsequent experiments.. Therefore, concentrations of pro-oxidants tested in section 5.4 that caused a ~50% loss of viability were tested for toxicity on wild-type ES cells with low GSH levels. Increasing the quantity of cellular antioxidants in cells prior to oxidative insult generally provides protection against the effects of ROS. Therefore, the selected agent was also tested with GSH homologues to discern the effect of excess thiols.

5.5.2 Results

5.5.2.1 BSO preferentially potentiates the cytotoxicity of MQ

Figure 5.6 shows the toxicity of H_2O_2 remained largely unchanged when cellular GSH levels were pre-lowered: viability altered from 43.02% ±2.56 to 36.12 ±1.55 (*t*-test P=0.06), an insignificant shift. BSO enhanced the toxicity of tBHQ and UV in ES cells by 33.51% (*t*-test P=0.018) and 41.50% (*t*-test P=<0.001), respectively. In comparison, the viability of ES cells exposed to MQ after BSO pre-treatment fell from 46.04 ±6.15 to 17.21 ±1.29, a reduction of 62.62% (*t*-test P=0.003). Thus, BSO enhances the cytoxicity of MQ by the greatest margin.

5.5.2.2 Excess GSH homologues are partially toxic to ES cells

GSH, unable to enter the majority of cells intact, is broken down extracellularly and the components imported prior to intracellular resynthesis (see section 1.3.1.3). To analyse the cellular effect of GSH repletion *in vitro*, many investigators utilise the lipid soluble GSH-monoethyl-ester, GSH-MEE (figure 5.7). The effect of GSH-MEE on normal and ES cells undergoing MQ-induced oxidative stress is shown in figure 5.7. As expected in a non-stressed environment treatment with 2mM GSH-MEE, a standard working concentration, does not impact upon ES cell viability. Unexpectedly, incubation of ES

Figure 5.6 Effect on GSH depletion on pro-oxidant cytotoxicity

Viability of wild-type ES cells 24 hrs post incubation with pro-oxidants +/- prior GSH depletion by BSO. Control cultures were incubated with serum free (SF) media, whilst experimental cultures were exposed to 1mM H_2O_2, 35μM MQ, 150μM tBHQ or 10J m^{-1} sec^{-1}. Error bars represent SEM values from 4 independent experiments. Symbols indicate significantly reduced values in comparison to (adjacent) controls: * ANOVA P=0.003, † t-test P=0.018 ‡ t-test P=<0.001. See text for details.

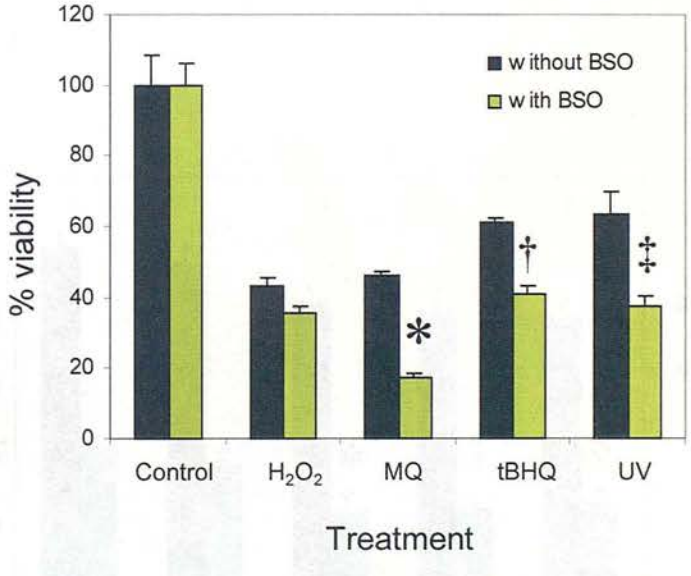

Figure 5.7 Effect of GSH-MEE on MQ cytotoxicity

Viability of wild-type ES cells 24 hrs post incubation +/- 35μm MQ +/- prior treatment with GSH-MEE (structure summarised, top). Cultures were incubated with either GSH-MEE only (black bars), or GSH-MEE prior to MQ exposure (blue bars). CM indicates complete media; PBS, phosphate buffered saline. Error bars represent SEM values from 3 independent experiments. *, ‡ and § indicate lower values compared to MQ-only control (ANOVA P=0.03, P=0.007 and P=0.029, respectively).

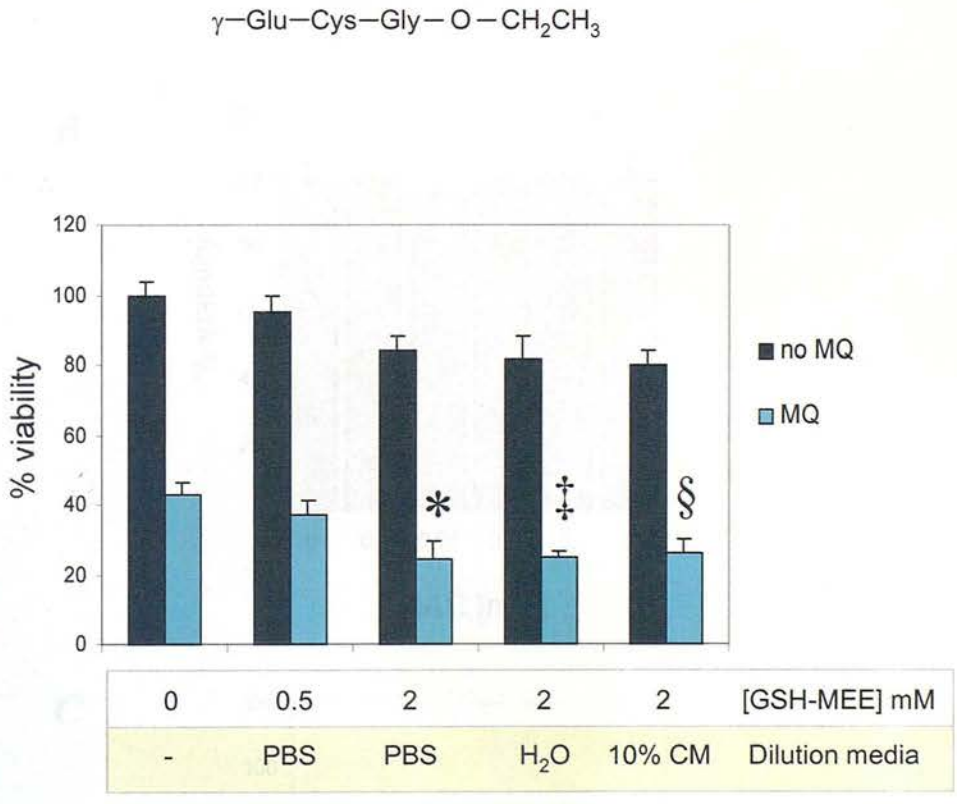

Figure 5.8 Effect of NAC addition on MQ cytotoxicity

Chemical structure of DEM (*A*). Viability of wild-type ES cells twenty-fours hours post incubation with or without NAC only (*B*), or MQ with or without prior incubation with NAC (*C*). Error bars represent SEM values from 4 independent experiments. * significant vs MQ only control (*t*-test P=<0.001), see text for details.

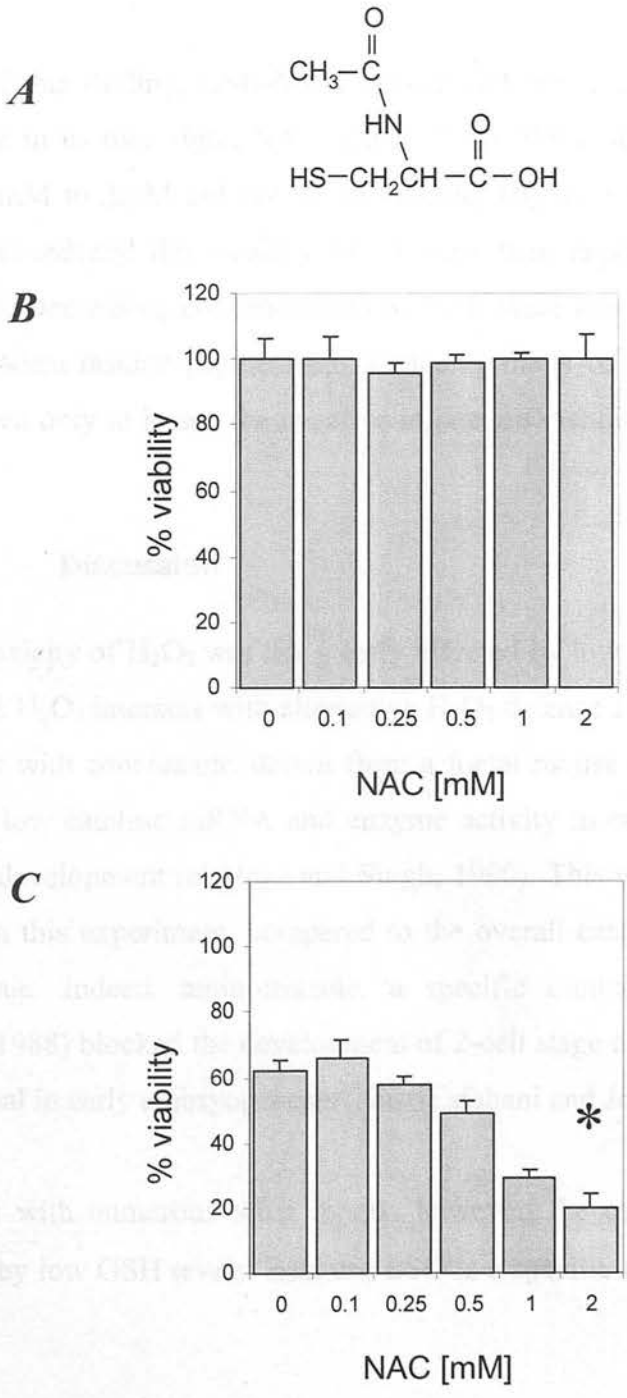

cells with 2mM GSH-MEE prior to 35μM MQ served to sensitise ES cells to oxidative challenge: viability fell by 43.52% (*t*-test P=0.03) from 43.08% ±4.36 to 24.33% ± 5.03. Figure 5.7 also demonstrates dilution of GSH negated this effect, whereas the medium of dilution had no effect. This impact of 2mM GSH-MEE was also observed with MQ at different concentrations, tBHQ and H_2O_2 (data not shown). GSH-MEE was incubated for 16 hours, in line with the majority of previous studies demonstrating a protective function against a wide variety of oxidant-induced injuries. Therefore a time-course of incubation periods was not pursued.

In light of this finding, GSH-MEE was instead replaced with the GSH derivative and antioxidant in its own right, NAC (figure 5.8a). Without stress, NAC at concentrations from 0.25mM to 2mM did not affect viability (figure 5.8b). However, incubation with 2mM NAC reduced the viability of ES cells then exposed to MQ by 80.14% (*t*-test P=<0.001). Decreasing concentrations of NAC were less toxic after MQ treatment, in a dose-dependent fashion (figure 5.8c). Reducing the NAC incubation period from 16 to 4 hours served only to lessen the negative impact on viability after MQ treatment (data not shown).

5.5.3 Discussion

The cytotoxicity of H_2O_2 was not greatly affected by low GSH levels. This suggests that in ES cells H_2O_2 interacts with alternative H_2O_2 defence factors, such as catalase. This is in contrast with conclusions drawn from a foetal mouse study by El-Hage et al, which showed a low catalase mRNA and enzyme activity in early embryogenesis, but which rose with development (el-Hage and Singh, 1990). This may be explained by the use of ES cells in this experiment, compared to the overall catalase levels obtained from total foetal tissue. Indeed, aminotriazole, a specific inhibtor of catalase (Michiels and Remacle, 1988) blocked the development of 2-cell stage embryos, indicating this enzyme is functional in early embryogenesis (Nasr-Esfahani and Johnson, 1992).

Consistent with numerous other reports however, the cytotoxicity of MQ was greatly enhanced by low GSH levels. Because BSO is a specific inhibitor of γGCS, non-toxic in

ES cells and other types examined (Martensson et al., 1991; Rahman et al., 1998; Sagara et al., 1998), this is indicative of a dependence on GSH. Although the cytotoxicity of UV and tBHQ were also increased by GSH depletion, the extent of this was less marked. It should be noted that UV has multiple and ill-understood effects at the cellular level (Devary et al., 1992). The objective of this study was to elucidate the ES cell GSH- and p53-dependent response mechanisms specifically to oxidative stress. Therefore, MQ was selected as a paradigm reagent to deliver oxidative stress in following experiments.

Prior addition of GSH-MEE or GSH precursors to culture systems can be associated with increased cell GSH levels and resistance to oxidative stress (Trocino et al., 1995; Ishibashi et al., 1996; Deneke, 2000). In other systems no protective benefit of GSH-MEE is reported (Gardiner and Reed, 1994; Mulier et al., 1998). The data presented here show that, in ES cells, high concentrations of GSH-MEE and NAC have a deleterious effect under oxidative stress.

The GSH-MEE and NAC experiments were included to reveal any protective effect addition of these agents might confer upon ES cells to counter oxidative stress. If such an effect was found, then the intracellular concentration of GSH would have been ascertained. Since this was not found to be the case, the value in pursuing this line of investigation was naturally diminished. Therefore, GSH levels were not monitored in this particular instance.

However, that ES cells were sensitised suggests that a critical GSH concentration is required for ES cells to deal with the effects of MQ. Mulier and co-workers also proposed that a specific thiol level was required to protect pulmonary epithelia against the effects of H_2O_2. ES cells usually grow in conditions of low oxygen and are uniquely sensitive to DNA damage: they undergo apoptosis more readily than growth arrest (Aladjem et al., 1998; Choi and Donehower, 1999). It is possible that perturbation of their redox equilibrium, such as that imposed by a GSH or NAC surplus, is detrimental to their capacity to recover from MQ.

Low GSH levels, via altering the redox state, are reported to upregulate compensatory antioxidants including catalase, SOD and quinone oxidoreductase (NQO1) in bacteria (Storz et al., 1990) and a variety of mammalian cell types (Loven, 1988). Excess GSH may equally downregulate ES cell antioxidants and sensitise the culture to subsequent oxidative challenge. Certainly, the antioxidant potency of NQO1 (for mechanism, see figure 1.2) has been verified by the increased toxicity of MQ in *NQO1*-/- mice (Radjendirane et al., 1998) and increased mutagenicity of MQ during NQO1 inhibition (Chesis et al., 1984). Thus it is tempting to speculate that dowregulation of NQO1 alone, or in combination with other factors, reduces the overall antioxidant capacity in this case.

An alternative explanation relates to thiol-mediated radical engendering. Under some conditions, GSH in surplus is known to be a source of thionyl radicals (see table 1.1) and lipid peroxidation (Tien et al., 1982; Ross et al., 1985). However, since both low GSH levels and excess GSH enhance the cytotoxicity of MQ, I argue that disturbance of a critical ES cell GSH level accounts for the effect of GSH-MEE and NAC.

5.6 Dependency of MQ cytotoxicity on p53 and GSH levels

5.6.1 Introduction

After demonstrating physiological levels of GSH are required for full neutralisation of MQ in wild-type ES cells, the joint effect of p53 and GSH deficiency on the ability of ES cells to cope with oxidative stress was examined. To discern any function in the response to oxidative stress, time courses of the immediate viability (defined as zero to forty-eight hours post treatment) of wild-type and p53-/- ES cells were compared, using the MTT assay.

5.6.2 Results

5.6.2.1 p53 deficiency confers immediate survival advantage post MQ

Figure 5.9 shows that wild-type ES cells displayed a sustained decline in viability in the period post treatment, dropping to 17.03% ±1.02 of control values at forty-eight hours post stress. Pre-treatment of wild-type ES cells with BSO augmented MQ cytotoxicity at all time points, reducing viability to <5% of control levels at forty-eight hours.

Following exposure to MQ, p53-/- ES cells displayed a considerably higher viability than their wild-type counterparts throughout the experimental period. The magnitude of this difference expanded with time, from 20.82% (*t*-test P=0.01) at six hours to 31.69% (*t*-test P=0.002) at twenty-four hours, and 51.51% (*t*-test P=<0.001) at forty-eight hours. Pre-treatment of p53-/- ES cells with BSO also exacerbated MQ cytotoxicity at all time points. However, p53-/- cells receiving this treatment displayed a higher viability than

Figure 5.9 Immediate tolerance of ES cells to MQ and BSO

Short-term viability of wild-type (WT, black lines) and p53-/- (red lines) ES cells twenty-four hours post incubation +/- MQ +/- previous treatment with BSO (see figure for key). Error bars represent SEM values from 3 independent experiments. * and ‡ indicate the difference in comparison to wild-type ES cells treated with MQ only (P=<0.001 t-test) and with MQ+BSO (P=<0.001 t-test), respectively.

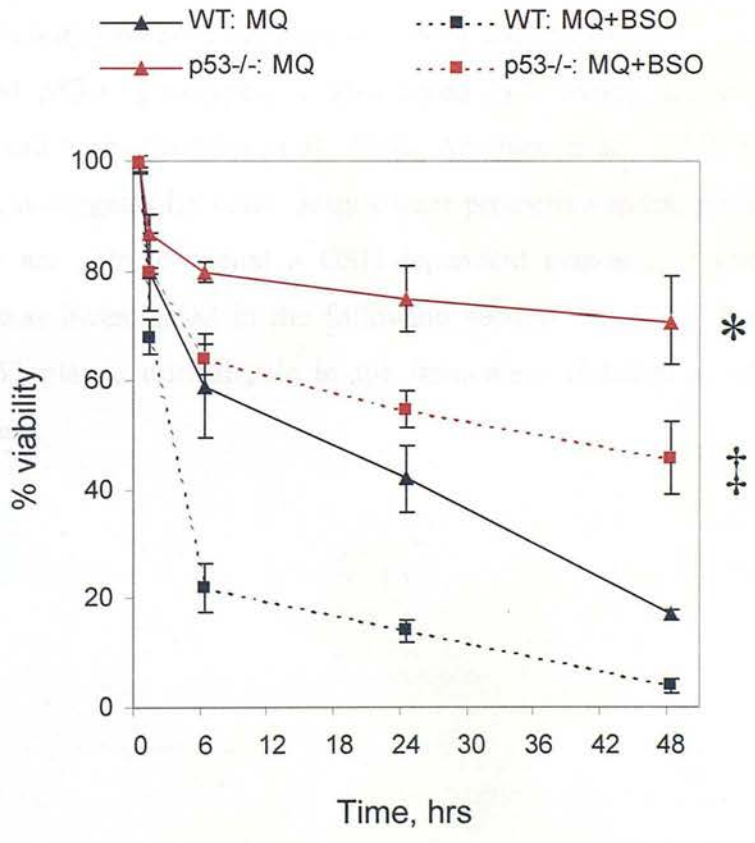

their wild-type counterparts at six (41.48%, *t*-test $P=<0.001$), twenty-four (40.97%, *t*-test $P=<0.001$) and forty-eight hours (42.30%, *t*-test $P=<0.001$).

5.6.3 Discussion

Cells with non-functional p53 display a striking survival advantage post-oxidative stress. Similar results have been obtained using cell lineages ranging from normal fibroblasts (Yin et al., 1998) to breast carcinomas (Shatrov et al., 2000). That this effect became more pronounced over time in ES cells suggests it is mediated by loss of damage checkpoints that normally halt cell division, or trigger programmed cell death. This conjecture is investigated in section 5.8.

A role for GSH in the response of ES cells to oxidative stress is supported by the increase in MQ cytotoxicity observed after pre-treatment with BSO. This effect, apparent in both wild-type and p53-/- genotypes, is also noted in a variety of transformed and non-transformed cell types (Mehlen et al., 1996; Arsalane et al., 1997; Sagara et al., 1998). Furthermore, it suggests ES cells, despite their protective environment *in vivo* (Gardiner et al., 1998) are able to mount a GSH-dependent response to oxidative stress. This proposition was investigated in the following section. Together, the data indicate that GSH and p53 play a critical role in the immediate viability of ES cells exposed to oxidative stress.

5.7 Role of p53 in the GSH response to oxidative stress

5.7.1 Introduction

Oxidative stress is known to activate p53 (Renzing et al., 1996; Yin et al., 1999), causing nuclear translocation (Uberti et al., 1999) prior to up or downregulation of p53 target genes. Depending upon the nature and level of the damage, p53 can transactivate redox-regulation genes that concur with the onset of apoptosis, or inhibition of apoptosis (described in sections 1.5.3-1.5.4). One member of the latter category is the GSH-dependent enzyme, GPx (Tan et al., 1999).

The p53-dependent transactivation of GPx directly links the p53 response with the antioxidant response. Consequently, p53 may play a role in the GSH-response to oxidative injury. Such a link could manifest on multiple levels. For example, via a p53-dependent transactivation of GSH synthetic enzymes, such as *γGCSh*. Indeed, GPx can be co-upregulated with *γGCSh* (see table 1.5) via an unknown mechanism (Thanislass et al., 1995; Kojima et al., 1998a; Kojima et al., 1998b). Furthermore, GSH levels are implicated in the activation of the stress JNK kinase pathway (Liu et al., 1996; Wilhelm et al., 1997; Kurata, 2000), which controls cellular responses to stress signals. JNK activation can lead to both p53:mdm2 dissociation (Fuchs et al., 1998b) and elevated GSH levels (Erdos et al., 1995; Guyton et al., 1996; Liu et al., 1996; Fuchs et al., 1998a). Therefore GSH levels may also be involved in p53 activation.

Alternatively, p53 may downregulate basal *γGCSh* or *γGCSl* expression. Constitutive upregulation of GSH is associated with acquired drug resistance in many tumour-derived cell lines. Transiently transfected p53 downregulates steady state SOD levels and activity in mouse fibroblaststs (Pani et al., 2000). If p53 performed a similar function on γGCS, loss of p53 would accord with the observation of elevated drug resistance of many p53-/- human tumours.

5.7.2 Results

5.7.2.1 p53-independent elevation of GSH in response to MQ

In order to assess any alteration in the level of GSH subsequent to MQ exposure, intracellular levels were monitored at different time points post exposure to MQ. Following incubation with 35μM MQ, wild-type ES cells showed a rapid elevation of free GSH levels at six hours (ANOVA P=0.005). GSH levels peaked at 34.39 ±2.56 nmol mg protein^{-1} twenty-four hours post exposure, before subsiding to basal levels forty-eight hours (figure 5.10). The fluctuation of GSH levels seen in untreated controls is consistent with the degree of confluency, as reported with other cell types (Shi et al., 1994b; Kojima et al., 1998a; Reiners et al., 2000).

Next the response to BSO removal, which reduces ES cell cellular GSH levels by approximately 70% (for details, see table 5.2), was examined. When incubated with fresh media, ES cells depleted of GSH recovered basal levels by twenty-four hours. Importantly, ES cells pre-incubated with BSO failed to induce an elevation in GSH when treated with 35μM MQ. Furthermore, GSH levels remained suppressed, with recovery to control levels only achieved at forty-eight hours. P53-/- cells also showed a clear GSH response post MQ treatment. Indeed, the GSH levels did not significantly differ between wild-type and p53-/- cells at six hours (ANOVA P=0.57) or twenty-four hours (ANOVA P=0.59).

Figure 5.10 GSH response of wild-type and p53-/- ES cells to MQ

Total free GSH levels in wild-type (top panel) and p53-/- ES cells (bottom panel) +/- 35μM MQ and +/- 100μM BSO treatment: see figure legend for key. Time at 0h = end of the MQ treatment. Error bars represent SEM of 3 independent experiments. * indicates the difference in comparison to MQ-treated p53-/- ES cells (P=0.57 ANOVA), and ‡ signifies the difference compared to untreated wild-type cells (P=0.59 ANOVA).

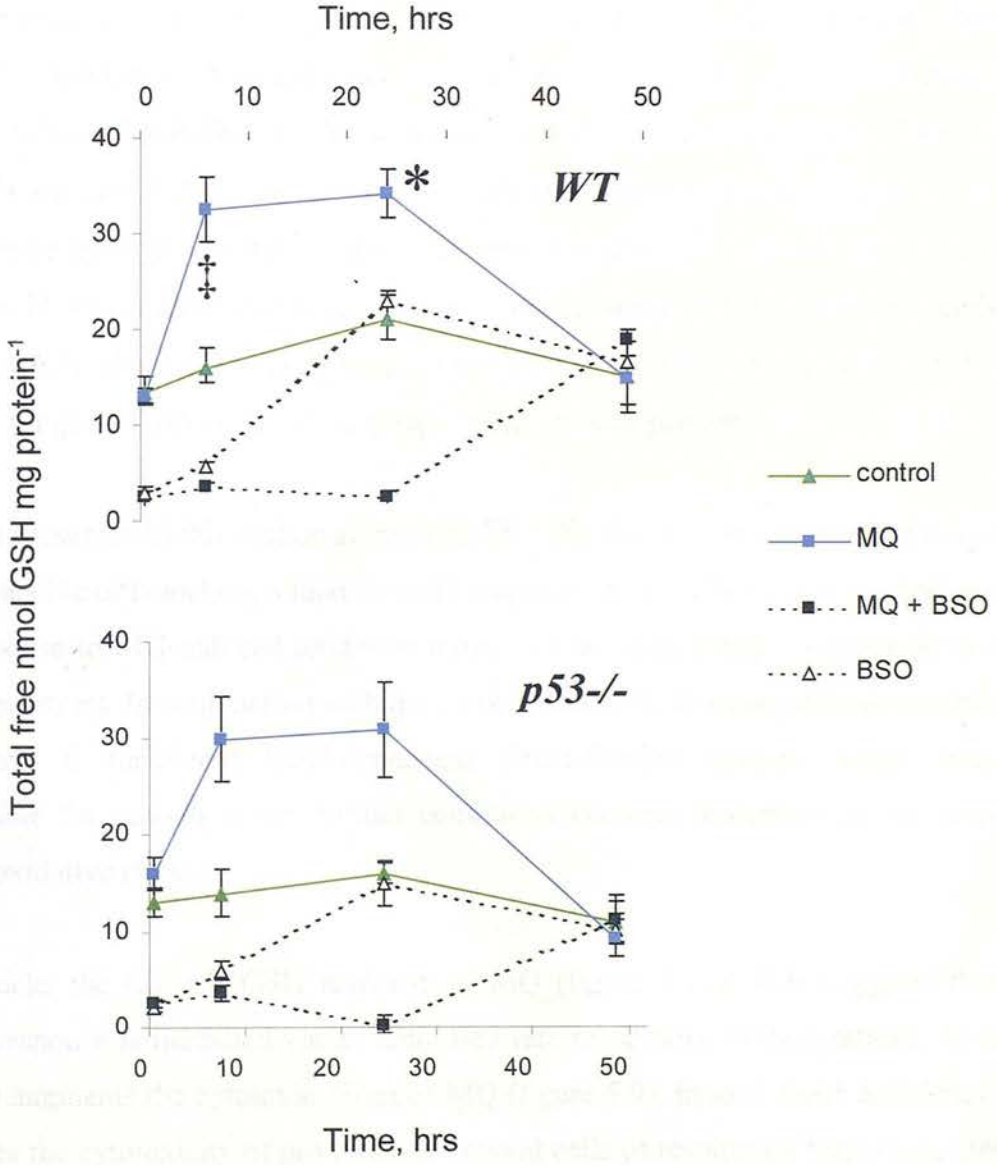

5.7.3 Discussion

The aim of this work was threefold. First, to reveal the presence and characteristics of any ES cell GSH response to oxidative stress. Second, to investigate whether a correlation exists between cellular GSH levels and viability under oxidative stress. Third, to establish whether the GSH and p53 pathways are functionally associated. Though published evidence supports the concept of a functional interplay between the GSH- and p53-response, no work to date has proposed or tested this conjecture.

Different groups report GSH is of critical (Trocino et al., 1995; Ishibashi et al., 1996) or marginal importance (Nasr-Esfahani and Johnson, 1992) in early development. A blastocyst-derived *γGCSh*-/- epithelial cell line (GCS-1), since created by others (Shi et al., 2000), has clarified this issue. *γGCSh*-/- cells die in culture unless supplemented with GSH, where upon they uptake a minimal amount (~2% of wild-type cells) and grow normally. However after continued passage in the presence of NAC, *γGCSh*-/- cells can grow normally, albeit at a slightly reduced rate (Shi et al., 2000). Thus, while GSH is not required for growth *per se*, a reducing equivalent must be present.

The data presented in this section shows that ES cells, the earliest embryonic lineage, are indeed capable of launching a modest GSH response. As for other cell types and stresses this response to MQ-induced oxidative injury is transitory, being complete forty-eight hours post stress. In conjunction with the work of Shi et al, this data indicates embryonic cells have a functional GSH-dependent detoxification system, which although dispensable for growth under normal conditions becomes necessary in the response against oxidative stress.

BSO blocks the ES cell GSH response to MQ (figure 5.10). This suggests that the normal response is mediated via an amplified rate of *de novo* GSH synthesis. In doing so, BSO augments the cytotoxic effect of MQ (figure 5.9). Indeed, GSH deficiency also magnifies the cytotoxicity of pro-oxidants toward cells of respiratory (Shi et al., 1994b), hepatic (Morales et al., 1997b), nervous (Iwata-Ichikawa et al., 1999), endocrine (Urata et al., 1996), vascular (Moellering et al., 1998) cardiac and renal origin (Park et al.,

1998). As such, many authors consider the elevation in GSH to perform an important protective function against oxidative injury. The results presented here support this premise.

One apparent anomaly is the observed initial fall in GSH levels, evident in other cell types exposed to MQ, was not seen in ES cells. A pilot study testing the effects of 70μM MQ at a range of incubation periods also showed no early GSH depletion (data not shown).

Two principle mechanisms are thought to mediate the toxicity of MQ. Damage can occur via oxidation from redox cycling (Rossi et al., 1986) (van Ommen et al., 1988; Schnellmann et al., 1989)or covalent arylation of macromolecules (Powis et al., 1981; Thor et al., 1982; d'Arcy et al., 1987) (see also section 1.1.1-1.1.2). Utilising quinones closely related to MQ, but which have either enhanced propensity to arylate or negligible arylation potential, the relative contribution of oxidative versus conjugative processes has been studied. In liver cells, the toxicity of MQ is predominantly mediated via arylation reactions (Gant et al., 1988; Stone et al., 1996; Qiu et al., 1998), whereas in variety of other tissue types it is attributed to redox cycling (Nicotera et al., 1990a; Brown et al., 1991). It is now apparent that the mode of cytotoxicity which predominates is heavily dependent on the exact model used.

The Tietze method used in this study measures total glutathione levels: reduced and oxidised. However GSH-conjugates such as PrSSG, formed by arylation reactions, are not detected and their formation would register as a loss of glutathione. It is therefore probable that GSH scavenges MQ-generated ROS, and that arylation reactions are not predominant in ES cells. Thus oxidation of GSH to GSSG, coupled with rapid GSH synthesis, could account for the lack of a preliminary fall in total GSH levels.

The two ES cell strains utilised contrasted solely by their capacity to produce functional p53. The results show the steady state GSH level in ES cells was unaffected by p53 status. This makes a role for p53 in basal transcription of *γGCSh* or related enzymes

unlikely, and is consistent with the notion that p53 transcribes target genes only when activated by cellular injury. Moreover, the GSH response profile of wild-type and p53-/- ES cells under oxidative stress were virtually superimposable and statistically indistinguishable. This is strong evidence that oxidative stress induces GSH via a mechanism independent of p53.

It is possible that the increase in GSH is instead mediated via transcriptional alteration by other redox-sensitive transcription factors, such as NF-kβ and AP-1. These have been shown to elevate GSH in a variety of cell types, coincident with an upregulation of *γGCSh* (Sekhar et al., 1997b; Morales et al., 1998; Rahman et al., 1999; Kitteringham et al., 2000). However, at the time of writing no evidence regarding their activity in ES cells was available.

5.8 Effect of p53 deficiency on MQ-induced cell death

5.8.1 Introduction

Exposure of wild-type ES cells to MQ leads to a rapid reduction in viability, a decline potentiated by GSH deficiency. With normal or depleted GSH levels, the decline observed in p53-/- ES cell viability was markedly less. ES cells are highly sensitive to forms of genotoxic stress, and can react by arresting growth or initiating death in a controlled (apoptotic) or uncontrolled (necrotic) fashion. However, the MTT assay does not differentiate between these cellular fates. Given the prominent role of p53 in these processes, the mechanism underlying this reduction in ES cell viability was examined. This was accomplished directly, by analysing cellular morphology (as described in section 2.4.3.3).

5.8.2 Results

5.8.2.1 MQ induces apoptosis in wild-type and p53-/- ES cells

No difference in the rate of apoptosis between untreated and BSO-treated wild-type or p53-/- ES cells was detected (figure 5.11). This correlates with unchanged MTT indicies

Figure 5.11 Effect of BSO or MQ on the induction of apoptosis

Wild-type and p53-/- ES cells were treated with 100μM BSO or 35μM MQ. Cell death was examined 6 hours post MQ removal and the percentage apoptosis occurring in each experiment was assessed directly, using morphological criteria. Blue bars represent percentage of intact cells, black bars percentage of apoptotic cells. Error bars represent SEM values from 3 independent experiments. ANOVA statistical indicators are shown as: §, (P=<0.001) vs. untreated wild-type ES cells; ‡, (P=0.019) vs. untreated p53-/- ES cells, and *, (P=<0.001) vs. wild-type ES cells exposed to MQ.

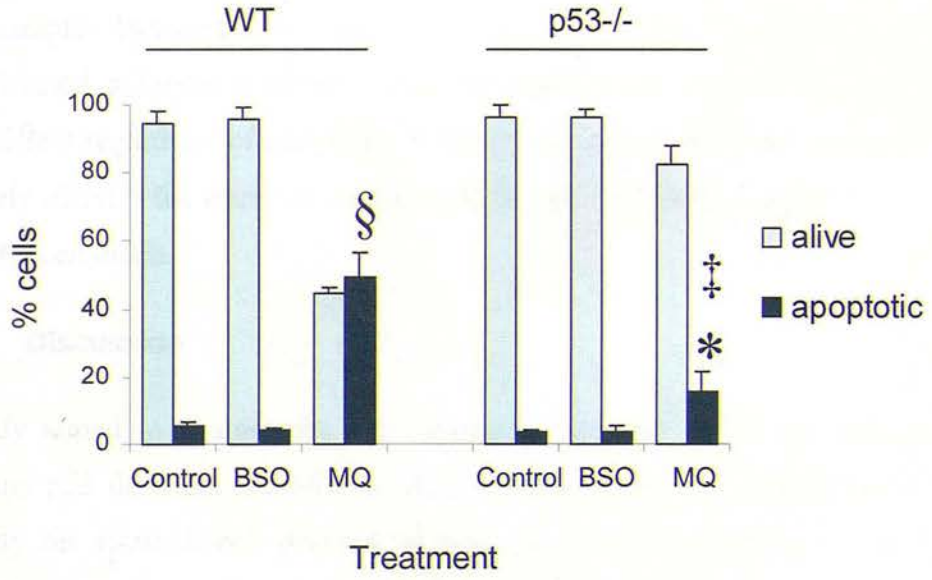

for these samples (data not shown). Compared to untreated controls, wild-type ES cells initiate a strong apoptotic response (52.5% ±3.6, ANOVA P=<0.001) six hours following MQ exposure. This correlates with a fall in the MTT index at the same time point (figure 5.9). In response to MQ treatment, p53-/- ES cells also displayed a significant apoptotic response in comparason to control cultures (15.8% ±3.48, ANOVA P=0.019). However, the incidence was considerably reduced in comparison to that observed for wild-type cells (ANOVA P=<0.001), concordant with high MTT indices for p53-/- cells at this time (figure 5.9).

5.8.2.2 BSO appears to convert MQ-induced apoptosis to necrosis

In comparison to samples treated with MQ, the proportion of ES cells remaining intact post BSO and MQ exposure was reduced. However, there was no evidence of apoptosis in these samples. Instead the cells appeared lysed: the cellular contents were liberated and locally diffused, adjacent to membraneous fragments (data not shown). This observation was consistent regardless of genotype. Whilst no further experiments were performed to definitively identify the cause of these cellular fragments, the morphology was indicative of necrotic cell death.

5.8.3 Discussion

This study aimed to characterise the cellular events associated with the exposure of normal and p53 deficient ES cells to MQ. ES cells, being the progenitors of all tissue types, rely on accurate cell division to pass on an intact genome to daughter cells. Sustained damage is thought to be eradicated by apoptosis rather than risking improper or incomplete repair. The results show the oxidative injury inflicted by MQ to wild-type ES cells is sufficient to cause a strong apoptotic response. Thus the results are consistent with the "primed to die" property thought to ensure proliferation of only gentically healthy cell populations.

Oxidative damage activates p53 (Renzing et al., 1996; Ngo et al., 1998; Meplan et al., 2000), and p53 is required to induce apoptosis in mouse embryo fibroblasts in response to it (Yin et al., 1998; Yin et al., 1999). However the data presented here indicate that, in the

absence of p53, oxidative stress can commence an alternative apoptotic programme in ES cells. These findings serve to underline the complex role played by p53 in the response of ES cells to damage. Aladjem *et al* observed only p53-independent apoptosis in response to ribonucleotide depletion and DNA damage, whilst Corbet *et al* showed both p53-dependent and p53-independent apoptosis in response to UV (Aladjem et al., 1998; Corbet et al., 1999). It is becoming apparent that ES cells, perhaps due to their pluripotent role, excite a very precise response to counter the nature of particular stress agents.

While MQ initiates apoptosis in both p53-/- and wild-type ES cell lines, the immediate apoptotic response was weaker in p53-/- ES cells. It is likely that the higher viability of p53-/- ES cells post MQ treatment is accounted for by an attenuated rate of early apoptosis, and the low viability of wild-type cells by the higher rate of early apoptosis.

The lower incidence of apoptosis observed in p53-/- ES cells at six hours does not necessarily imply an attenuated p53-/- apoptotic response. Others have revealed, with extended time courses, the presence of a delayed wave of p53-independent apoptosis (Clarke et al., 1994; Merritt et al., 1997; Frenkel et al., 1999). Thus the lower apoptotic index observed at six hours post MQ treatment is interpreted as a kinetic shift, rather than a reduced response *per se*. This is also in agreement with the primed to die function where, even in the absence of p53, ES cells recognise injury and activate a death pathway. Because ROS act as downstream mediators in some apoptotic pathways, it is possible that MQ, via ROS generation, may directly activate apoptotic factors in the absence of the p53 protein (Qiu et al., 1998).

It should be noted that, as well as DNA damage inflicted by MQ and the subsequent induction of apoptosis, the embryonic toxicity of MQ may manifest via a subtle re-programming of gene expression. Such alterations are difficult to monitor *in vitro* and could effect cellular changes not detected within this study.

MQ is known to initiate apoptosis in a variety of cell systems (McConkey et al., 1988; Hockenbery et al., 1993; Schulze-Osthoff et al., 1994; Caricchio et al., 1999). However, MQ and other inducers of oxidative stress can also initiate necrosis. In these instances,

the type of cell death is determined by the concentration of pro-oxidant: with lower concentrations initiating apoptosis and higher dosages causing necrosis (Dypbukt et al., 1994; Sata et al., 1997; Vayssier et al., 1998). Similarly BSO can convert oxidant-induced, but not etoposide-induced apoptosis into necrotic cell death (Fernandes and Cotter, 1994). This parallels the observed shift in ES cell morphology from apoptotic to necrotic death.

The active site of caspases are known to contain redox-sensitive cysteines (Alnemri et al., 1996; Nobel et al., 1997). This led Lemaire *et al* and others to propose the switch from apoptosis to necrosis is mediated via caspase inactivation (Lemaire et al., 1998; Samali et al., 1999). It is possible that such a mechanism accounts for the effect MQ has on BSO-treated ES cells, though this evidently requires additional experimentation to verify.

5.9 Effect of p53 and GSH deficiency on long-term ES cell viability

5.9.1 Introduction

The ability of cells to maintain genomic integrity is vital for survival and proliferation. Previously, approaches to analysing the impact of oxidative stress concentrated on monitoring the viability of primary or transformed cell lines. However, there are clear limitations when extrapolating viability data from immortalised cell lines to the normal situation *in vivo*. One restriction irrecoverably associated with an alternative system, primary culture, is the duration of the period under scrutiny. Many studies estimate the cytotoxicity of a particular oxidative agent by analysing viability several hours post exposure. However, oxidative stress can cause DNA damage, an injury that may not impact on the immediate health of the cell. Indeed, DNA lesions inflicted by MQ have been dissociated from short-term cell death in hepatocytes (Coleman et al., 1989) and fibroblasts (Renzing et al., 1996).

Genotoxic injury may have long-term effects on the cell and, when propagated by mitosis, may become detrimental to the development of the organism. The ability of ES cells to proliferate in culture allows assessment of the long-term effects of oxidative

stress on a physiologically normal cell population. In comparison to wild-type ES cells, p53-/- ES cells are refractory to apoptosis at six hours post MQ exposure (section 5.8) and display an immediate survival advantage over wild-type cells, manifested up to 48 hours post exposure (section 5.6). To ascertain whether loss of p53 conferred a continued growth advantage over an extended period, we compared the clonogenic survival of wild-type and p53-/- ES cells after exposure to MQ. This assay tests the ability of cells to tolerate a given stress: cells that survive and that sufficiently recover from injury to proliferate form, in time period of approximately 10-12 days, a clonal population.

5.9.2 Results

5.9.2.1 p53 attenuates MQ-reduced clonogenicity

A small difference in plating efficiency was detected between genotypes, with wild-type cells showing a plating efficiency of 85.4% compared to p53-/- cells. To control for this difference, all data was calculated relative to untreated controls of the respective genotype. Unexpectedly, following treatment with 35μM MQ, the long-term ability of p53-/- ES cells to form clones was lower than wild-type ES cells (figure 5.12). This clonogenic survival difference between wild-type and p53-/- ES cells was significant (17.34%, ANOVA P=0.004). Reduction of GSH with BSO prior to MQ exposure served to exacerbate the disparity between genotypes (21.8%, ANOVA P=0.002).

5.9.3 Discussion

This result implies that, following exposure to MQ, the strong and early apoptotic response of wild-type ES cells leads to a greater long-term survival than p53-/- ES cells. Considering the widely acknowledged role for p53 as an anti-proliferation factor, this may at first seem paradoxical. However, in addition to causing death p53 also has an increasingly recognised function in facilitating repair (Abramova et al., 1997), especially via BER (Offer et al., 1999; Nakano et al., 2000; Zhou, 2001). This pathway acts to ensure surviving cells are genetically normal. Thus, in the presence of p53-dependent repair, surviving ES cells are likely to carry a lower level of DNA damage – which could

Figure 5.12 Clonogenic survival of ES cells following exposure to MQ

The long-term (>10 day) viability of ES cells after exposure to 35μM MQ with or without prior 100μM BSO treatment. Wild-type ES cells are represented as solid bars and p53-/- cells as shaded bars. Error bars represent SEM values of 3 independent experiments. * indicates the statistical significance in comparison to wild-type ES cells treated with MQ only (P=0.004 ANOVA), and ‡ represents the significance in comparison to wild-type ES cells treated with MQ+BSO (P=0.002 ANOVA).

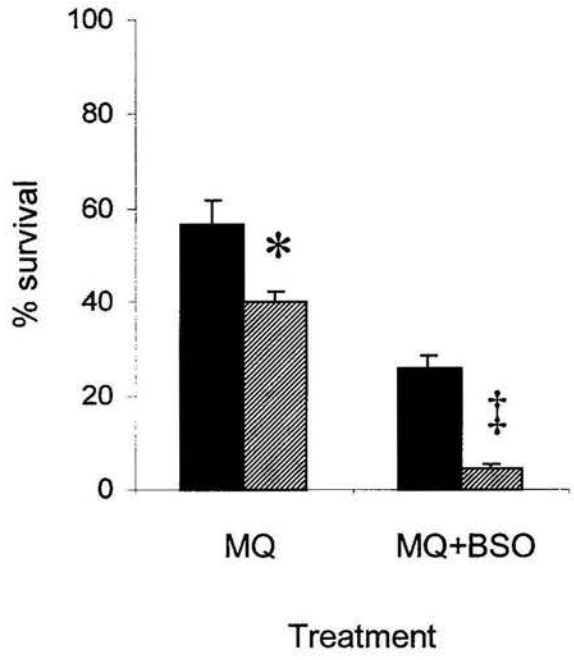

permit effective replication. Equally, in a p53-free environment accumulation of DNA damage may reduce repair, lower clonogenicity and ultimately disrupt development.

Alternatively, in the absence of p53 genotoxic stress could trigger delayed p53-independent pathways that halt cell proliferation. Such a reserve pathway may terminate either in permanent G1 arrest or in apoptotic cell deletion. Delayed p53-independent apoptosis has been previously reported in ES cells subjected to ribonucleotide depletion (Aladjem et al., 1998) and UV irradiation (Corbet et al., 1999). It is clear this could provide an explanation for the lower long term survival of p53-/- ES cells exposed to MQ, with or without prior depletion of GSH. This is in agreement with the conclusions reached by Frenkel *et al.*, 1999 who showed p53-/- embryos, upon irradiation, display not only altered patterns of apoptosis but accentuated levels of delayed death compared to their wild type counterparts (Frenkel et al., 1999). This is also consistent with the broader view that in development loss of cells is less detrimental to the organism than retention of damaged cells. Thus the data presented here, with that of section 5.8, point toward a strong, delayed p53-independent response. It should be remembered that these results reflect early organogenesis (<10 days post fertilization) and may not be the case for later development, where p53 levels decrease with differentiation.

GSH deficiency potentiated the long-term effects of MQ in both genotypes. To date, most studies investigating the effects of GSH depletion on drug cytotoxicity extend into the short term only. These studies have shown that lowered GSH levels in diseased tissue and cell cultures exposed to oxidant challenge are associated with increased lipid peroxidation (Thanislass et al., 1995), DNA damage (Park et al., 1998), protein oxidation (Tapper et al., 2000), and stunted foetal growth (Ishibashi et al., 1996). Here it is demonstrated that inhibition of the GSH response, which appears complete at forty-eight hours post stress, nevertheless effects the ability to survive up to 8 days later. This further underscores the protective function of the GSH response. This result is also supporting evidence for a requirement of a critical GSH concentration in ES cells to prevent oxidative damage.

Chapter 6

Concluding summary and discussion

Disruptions in GSH homeostasis and the p53 gene are implicated in many human disorders, including malignancy and developmental dysfunctions such as teratogenesis. A number of other groups have used gene targeting technology to investigate the function of p53 and various antioxidants in mice. Aside from the previously discussed γGCS*h* knockout of Shi et al (section 1.3.5 and 5.7.3), and Dalton et al (section 1.3.5), the most relevant to this study are the knockout strains of GST-P, the selenoenzyme GPx1 and the transmembrane GSH salvage protein, γGT. To date, GR, GS and alternative GPx/GST isoenzymes have not been specifically inactivated *in vivo*.

GPx1 was originally deleted via homologous recombination in 1997 (see table 6.1 for targeting vector detail of this and other genes discussed herein). Despite an important role predicted for this widely expressed isoform, homozygous *GPx1-/-* progeny grew to term at a normal rate. Furthermore, they were fertile and other than an 18% rise in the activity of liver GR, were initially indistinguishable from their wild-type littermates (Ho et al., 1997). This was attributed to redundancy between GPx family members or other cellular antioxidants, and strongly points toward a limited role of GPx1 under physiological conditions. More surprising was a lack of a statistical difference between *GPx1-/-* and wild type mice in either viability or lipid and protein oxidation levels post exposure to >99% oxygen (Ho et al., 1997).

An alternative GPx1 knockout similarly confirmed that *GPx1-/-* offspring were healthy (Cheng et al., 1997). Furthermore, this study also found that under conditions of vitamin E or selenium deficiency, *GPx1* loss did not affect growth rates or GPx isoenzyme mRNA levels. However, de Haan and colleagues have revealed a notable effect of *GPx1* deletion. Intraperitoneal treatment with the pro-oxidant paraquat at a dose 1/7 of the normal LD_{50} was 100% lethal to *GPx1-/-* mice within five hours,

Table 6.1 Approaches to deactivate GSH-system/antioxidant enzymes

The approach employed in this study to delete γGCS*h* is compared with that utilised to deactivate genes involved in the GSH-cycle and other antioxidants. For selection cassettes, lower case italics designate a reporter gene, while upper cases refer to the following promoters driving it; PGK, phosphoglycerate kinase-1; HSV, herpes simplex virus and POLII, DNA polymerase II. Dashes signifies information not published.

Gene -/-	Total homology size, kb	Distribution of homology, kb	Targeting strategy	Positive selector	Negative selector	References
γGCS*h*	7	6 / 1	Replacement	PGK-*neo*	PGK-*tk*	(This thesis)
γGCS*h*	7.7	3.5 / 4.2	Replacement	PGK-*hprt*	MC1-*tk*	(Shi et al., 2000)
γGCS*h*	4.4	1.8 / 2.6	Replacement	PGK-*hprt*	HSV-*tk*	(Dalton et al., 2000)
GPx1	-	-	Replacement	PGK-*neo*	PGK-*tk*	(Cheng et al., 1997)
GPx1	5.2	-	Replacement	MC1-*neo*	HSV-*tk*	(de et al., 1998)
GPx1	5.3	-	Replacement	PGK-*neo*	PGK-*tk*	(Ho et al., 1997)
γGT	7	2.2 / 4.8	Replacement	PGK-*neo*	MC1-*tk*	(Lieberman et al., 1996)
GST-P	9	6 / 3	Promoterless	*Neo*	-	(Henderson et al., 1998)
SOD1	11	6 / 5	Replacement	PGK-*neo*	PGK-*tk*	(Reaume et al., 1996)
SOD1	6.3	3.5 / 2.8	Replacement	PGK-*hprt*	-	(Matzuk et al., 1998)
SOD2	-	-	Replacement	POLII-*neo*	PGK-*tk*	(Li et al., 1995)

whilst wild-type mice remained alive at ten days (de Haan et al., 1998). Wild-type mice were found to upregulate GPx activity 2-fold in the lung, whereas *GPx1-/-* mice displayed no GPx activity. Furthermore neuronal viability, as assayed by the MTT technique in culture, showed that normal cells was unaffected by 65μM H_2O_2: a concentration that caused a 30% decline in viability of cells derived from *GPx1-/-* mice (de Haan et al., 1998).

This study therefore showed an effect of GPx1 absence *in vivo* and in culture, not under developmental or physiological conditions, but under particular forms of oxidative stress. Subsequent work showed exposure to paraquat increased lipid and protein oxidation, whilst lowering NADPH/NADP and NADH/NAD ratios in *GPx1-/-* mice liver (Cheng et al., 1999). This latter observation is purported to signify an altered redox status, an assertion yet to be confirmed or confounded.

Whilst a function for GPx1 became evident only after extensive experimentation, targeted deletion of *γGT* generated a clear phenotype under non-stressed conditions. Mice carrying a *γGT-/-* genotype grow slower than wild-type mice, with 6 week old males and females weighing approximately 45% and 57% of their littermates, respectively (Lieberman et al., 1996). This was found to be largely reversible by dietary addition of NAC. Furthermore, 100% of *γGT-/-* mice developed cataracts, displayed reproductive abnormalities and by week 25 over 80% had died (Lieberman et al., 1996). Such mice had a dramatically higher plasma and urine GSH content, while GSH levels were lowered in most tissue (except the kidney and small intestine, cell types thought able to uptake intact GSH (Deneke and Fanburg, 1989)).

In a separate analysis, Kumar and co-workers revealed detailed morphological, histological and functional abnormalities in the reproductive tract of *γGT-/-* mice. For example, males had lower testosterone levels, smaller testes, a fraction of the normal sperm count (which were immotile) and a severely hypoplastic epididymis (Kumar et al., 2000). Liver cultured from *γGT-/-* mice was found to have, in comparison to wild-type liver, over 50% mitochondrial GSH depletion and impaired respiration.

NAC is reported to restore mitochondrial GSH levels, respiration (Will et al., 2000) and partially prevent both male and female abnormalities (Kumar et al., 2000).

The GST-P enzyme has also been deleted in mice by gene targeting. Both *GST-P* heterozygote and homozygote null mice are normal throughout life and do not show compensatory increases in hepatic GSH content, γGCS or GS activity (Henderson et al., 1998). However, *GST-P-/-* mice develop significantly more skin papillomas than wild-type mice after treatment with either carcinogen 7,12-dimethylbenz anthracene or 12-*0*-tetradecanoylphorbol-13-acetate (Henderson et al., 1998). This suggests a direct role for GST-P in detoxification of these compounds, and is a good example of the insight that can be gained into gene function by gene targeting.

Further to knockout models of GSH-enzymes, the SOD family have been subject to gene targeting. *SOD2* codes for the mitochondrial form of the enzyme, Mn-SOD. *SOD2-/-* disruption causes neonatal lethality at approximately 10 days. However, both *SOD2-/-* mitochondrial structure and DNA mutation rates were indistinguishable from unaltered mice (Li et al., 1995). What appears to be accumulated lipid droplets were visible by electron microscopy in muscle and liver. Furthermore animals had an abnormal heart structure, whilst activities of the respiratory enzymes succinate dehydrogenase and aconitase are reportedly lower than found in wild-type mice (Li et al., 1995). Thus Mn-SOD appears necessary to maintain normal mitochondrial function.

In contrast, deletion of *SOD1*, the gene encoding Cu,Zn-SOD (the cytosolic enzyme which accounts for 80% of cellular SOD) surprisingly had no measurable impact upon development, growth or lipid peroxidation (Reaume et al., 1996). In comparison to wild-type mice, *SOD1-/-* mice did however display neuromuscular pathologies (Flood et al., 1999) and retarded motor neuron survival post transection (Reaume et al., 1996). *SOD1-/-* mice also have reduced numbers of corpora lutea and reduced fertility, in terms of offspring/litter and litters/month, compared to heterozygote mice (Matzuk et al., 1998). A possible reason for lack of more prominent effect of *SOD1* deactivation is the increased expression of the antioxidant

metallotheionein proteins I and II, detected in livers of *SOD1-/-* mice (Ghoshal et al., 1999). However it is possible, as argued by Reaume et al, that MnSOD performs an essential neutralisation function of constantly produced mitochondrial radicals, whereas CuSOD, dispensable for normal physiological conditions, becomes important only in protecting against injury. Such contentions remain to be proved correct. The phenotypes of other antioxidant-related genes knocked out in mice are briefly detailed in table 6.2.

In deciding which gene to target to model GSH dysfunction, there are six main options to consider. These include those enzymes directly involved in the GSH-cycle, namely the GST and GPx families, γGT, γGCS, GS and GR. The positive and negative aspects of these candidates are addressed individually.

Removal of enzymes that use GSH as a co-factor in detoxification reactions is one possibility. However, the GST family comprises many members with overlapping substrate specificities (Hayes and McLellan, 1999) and deletion of one is unlikely to provide explicit information regarding the importance of GSH alone. Similarly the main value of excising a GPx isoenzyme is limited to understanding the function of that enzyme. Besides, loss of these enzymes would not reveal important functions of GSH that are not dependent upon catalysis.

In contrast to enzymes that utilise GSH, enzymes that maintain intracellular levels of GSH are more appropriate targets for use in a gene targeting strategy. However, although deletion of *GR* would effectively block recycling of GSSG, production of GSH could continue unabated, and even become increased. Thus residual GSH is likely to be present in a *GR-/-* model, so GR is not an ideal choice to examine GSH function. γGT is a better candidate since this protein is usually required to import the constituent amino acids for GSH synthesis. There are known exceptions however, such as cells of the small intestine and kidney, that can import GSH from the extracellular melieu intact (Deneke and Fanburg, 1989). Therefore γGT is also not an ideal candidate to achieve total GSH depletion.

Table 6.2 Summary of other antioxidant and related genes deleted via gene targeting

Square brackets detail whether allele removal is compatible with normal growth. Reported phenotype of mice (or cells derived from embryos) is briefly outlined – in response to exposure to stress agents.

Gene	Genotype	Summarised phenotype	Reference
Multidrug resistance protein, MRP	-/-	[Healthy]. Elevated γGCS activity and tissue GSH	(Lorico et al., 1997)
		Hypersensitive to anti-cancer agent etoposide and impaired inflammation	(Wijnholds et al., 1997)
Heme Oxygenase-1	+/-	[Healthy]. Increased ischemia/repurfusion injury	(Yoshida et al., 2001)
Heme Oxygenase-2	-/-	[Healthy]. Sensitised to hyperoxia, despite elevated basal lung GSH and HO-1	(Dennery et al., 1998)
Nrf1 transcription factor	-/-	[Die *in utero*]. Reduced fibroblast GSH and enhanced susceptibility to oxidants	(Chan et al., 1998) (Kwong et al., 1999)
ApoE	-/-	Imbalance in hippocampal oxidant/antioxidant ratio	(Ramassamy et al., 2001)
CYP1A2 and CYP2E1	-/- and -/-	[Healthy]. Reduced quinone toxicity	(Zaher et al., 1998)
Metal-responsive promoter MTF-1	-/-	[Die *in utero*]. Embryos fail to transcribe metallothionein I and II, show decreased γGCSh expression. Null fibroblasts showed increased sensitivity to H_2O_2.	(Gunes et al., 1998)
Metallothionein I and II	-/- and -/-	[Healthy]. No basal increase in GSH, SOD, GPx or catalase. γ-irradiation toxicity identical in wild-type and MT-/- mice	(Conrad et al., 2000)
		Increased cisplatin sensitivity, further enhanced by BSO treatment	(Satoh et al., 2000)
		More susceptible to arsenic toxicity	(LIU et al., 2000)

This leaves the genes coding for GSH-synthetic enzymes, γGCS and GS. Deletion of either of these genes would permanently and completely halt GSH synthesis, and should therefore expose the normal role of GSH. Of the two enzymes γGCS is rate limiting in GSH production and the γGCS product, γ-glutamyl-cysteine, is thought to have partial antioxidant activity itself (Deneke and Fanburg, 1989). Thus, of these two enzymes γGCS is the more attractive option to create a GSH- and GSH-precursor free model. To deactivate it completely, removal of the subunit containing the catalytic sites is the obvious choice. Thus, the *γGCSh* gene was selected for targeted deletion in this study.

In an attempt to create an ES cell line with a deactivating mutation in *γGCSh*, >16kb novel mouse *γGCSh* cDNA and gene sequences were successfully isolated, cloned and characterised. This process yielded sufficient detail to permit construction a replacement-style targeting vector, pGCS-TV2. Electroporation of the final vector into ES cells, followed by selection in antibiotic-containing medium yielded resistant clones as expected. However, screening ES cell DNA by southern analysis failed to isolate a clone bearing the desired genetic modification.

The approach successfully taken by Shi et al to delete *γGCSh* was subtly different. The total region of homology was slightly longer (approximately 0.7kb), but of possibly more note was the distribution of the homology. Shi and colleagues utilised a vector with roughly equal distribution (3.5/4.2 kb), whereas in this study the majority of homology resided the in the 5' arm (6/1 kb). Although this arrangement is thought less optimal by some (Thomas and Capecchi, 1987; Thomas et al., 1992), others report that as long as one arm is at least 0.8kb, it makes little difference how the homology is distributed (Hasty et al., 1991b; Torres and Kuhn, 1995). This discrepancy remains to be fully resolved and, as such, the distribution of homology in pGCS-TV2 could have potentially reduced recombination with the *γGCSh* gene.

Shi and co-workers also employed southern analysis to screen antibiotic resistant clones. The band shift size expected and observed for a mutant allele was 2.95kb

(10.3 to 7.35), comparable to the 3.2kb (8 to 11.2) shift sought in this work. Both these strategies provide clear means to discern mutant and undisturbed alleles.

Another difference was the use of neomycin transferase as a positive reporter. Shi incorporated a HPRT cassette into their vector, although again *neo* cassettes identical to that used in this work has been used extensively in previous targeting experiments (for examples, see table 6.1). Both the strategy presented here and that of Shi used gancyclovir to enrich for integration events that excluded *tk* incorporation. Therefore, selection cassette choice is an area not anticipated to impact negatively on the targeting frequency recorded in this work.

The last difference between the published approach to deactivate *γGCSh* and that presented here is the strain of donor DNA and recipient cell line. The available information regarding this states '129/Sv' DNA was used for vector construction, electroporated into 'AB2.1' ES cells. These ES cells belong to the 'Steel' 129/Sv substrain, as does the λ-library DNA used in this study to construct the targeting vector pGCSh-TV2. However, 129/Sv is now recognised as a large family incorporating three parent strains and many distinct sub-strains (Simpson et al., 1997). Consequently, it may be possible that the differences in targeting succes may have arisen as a consequence of subtle differences in the level of homology between targeting vector and targeting sequence, however the degree of any such difference is impossible to ascertain from the published data.

Thus, from the information available, the only definite differences that can be asserted between the strategy of Shi *et al* and that pursued here relates to the cumulative effects of non-optimal distribution of homology. Refer to section 4.7 for a dedicated discussion of this topic. With the power of hindsight, recommendations for others embarking on a gene targeting project can be offered. These are (*i*) produce a targeting vector with a balanced homology size; (*ii*) ensure the similarity between DNA sequences of vector and target gene are as close as possible, and (*iii*) plan for laboratory assistance to isolate, expand and screen large quantities of clones.

Should a *γGCSh* heterozygote have been isolated as anticipated, the downstream experiments that would have been initiated fall into two categories. First, culture of *γGCSh+/-* ES cells in high concentration antibiotic (such as G418) to generate a *γGCSh-/-* line, a standard technique used to generate many null lines. Upon confirmation of a correct and stable karyotype (normal mice cells contain 40 chromosomes), *γGCSh-/-* cells would be transferred to a dedicated departmental unit to generate *γGCSh-/-* chimeric mice via C57BL/6 blastocyst injection. By crossing these mice to Ola 129 mice we would identify those chimaeras with a germline contribution and so would generate heterozygous and subsequently homozygous null mice for *γGCSh.*

Second, a series of ES cell culture assays would have been pursued in parallel as follows. To ascertain whether *γGCSh+/-* cells had diminished GSH levels and confirm *γGCSh-/-* ES cells contained negligible GSH, the GSH levels would be determined. Oxidants produced during normal metabolism or following exposure to xenobiotics may adversely affect maturation by causing DNA strand breaks, lipid peroxidation and protein degradation. Indeed, GSH appears critical in protecting early embryos from oxidative stress (Trocino et al., 1995; Ishibashi et al., 1996) - though no work to date has used a mammalian system devoid of GSH to conclusively examine this assertion. Thus, the ability of *γGCSh+/-* and *γGCSh-/-* ES cells to withstand oxidative insult would be tested and compared to genetically normal cells. Immediate and long term viability tests would reveal the extent of protection afforded by GSH to oxidative stress induced by MQ. Additionally, a lipid peroxidation assay would serve as a marker for the extent of oxidative damage sustained, which is expected to (a) be greater than in ES cells with GSH depletion induced by BSO, and (b) corroborate with viability data.

The presence of GSH is thought, along with other factors, to influence gene expression by modulating the activity and binding of transcription factors to DNA (Schultz, 1993; Wasserman and Fahl, 1997; Rahman et al., 2001). This can adversely affect subsequent organogenesis (Beckman and Ames, 1997; Lopes et al., 1998). The RNase protection assay can probe for transcription of GSH-system enzymes and

other stress-response factors, such as p53 target genes - transactivation of which lead to apoptosis, or cell cycle arrest and DNA repair. Contrasting the band patterns obtained from *γGCSh-/-* and normal ES cells to MQ should reveal the spectrum of embryonic genes activated by oxidative stress, in comparison to a panel of house-keeping genes. Moreover, it would indicate whether the redox environment of a GSH-free cell alters the genetic responses to oxidative stress.

Disruption of the intracellular redox equilibrium also affects the balance between cell death, proliferation and senescence (Powis et al., 1995; Wang et al., 1998b). For example, exposure of a neuronal cell line to H_2O_2 results in migration of cytoplsamic p53 to the nucleus, prior to caspase activation and apoptosis (Uberti et al., 1999). Dorsal apoptotic cell death is also purported to mediate neonatal lethality of *γGCSh-/-* mice (Shi et al., 2000). P53 cytospin tests in *γGCSh-/-* and wild-type ES cells would reveal if loss of GSH influences translocation of p53 to the nucleus, prior to MQ or H_2O_2-induced cell death. Others have shown the existence of a delayed apoptosis in ES cells, after exposure to UV light (Corbet et al., 1999). Therefore, the long-term apoptotic response would be examined with a time-course extending to cover 72 hours post stress, to estimate whether presence of GSH directly effects the existence and strength of a delayed p53-independent apoptosis. This should provide a fuller appreciation of the impact of GSH loss on the ability to engage apoptosis, a critical event in development.

It is estimated that, due to damage, over 50% of human fertilisations are aborted early (Hall and Lane, 1997). Indeed, it would make good evolutionary sense to efficiently abort foetuses with DNA lesions, if failure to repair injuries resulted in progeny with compromised reproductive fitness (Janus et al., 1999). Quantifying the levels of oxidative damage, cell viability and cell death, along with gene expression in *γGCSh-/-* ES cells would together gauge the breadth of functions GSH plays in the early embryo.

To prepare for the eventuality of analysing a *γGCSh-/-* ES cell line, the roles of GSH in the response of wild-type ES cells to oxidative injury were investigated. Since no

previous work examining this had been done, an *in vitro* wild-type model was successfully designed and optimised. This work first involved demonstrating that ES cells express *γGCSh* and contain GSH. Second, the base line tolerances of wild-type ES cells under diverse pro-oxidative stresses, including hydrogen peroxide, UV irradiation and aromatic quinones were established. Last, characterisation of the response to BSO, pre-incubation with which was shown to deplete GSH levels and further, that of the agents tested, the quinone menadione (MQ) was preferentially neutralised by GSH.

MQ-generated ROS can cause single strand breaks in DNA and induce wild-type p53 (Messmer et al., 1994; Upadhyay et al., 1995; Uberti et al., 1999). The GSH-dependent GPx enzyme is a transcriptional target of activated p53 (Tan et al., 1999). Therefore, subsequent assays measuring GSH levels, cellular viability and apoptosis performed on this model were replicated on a karyotypically normal p53-/- ES cell line.

This thesis presents data that shows wild-type ES cells are acutely sensitive to MQ-induced oxidative injury and respond by initiating a rapid, transient elevation of GSH. Pre-incubation with BSO blocked the GSH response and greatly enhanced MQ-cytotoxicity. Thus, the GSH response is interpreted as (a) performing a protective function at the cellular level and, (b) being mediated, at least in part, via an increase in *de novo* GSH synthesis. These conclusions are in agreement with data derived from a variety of cell systems in previous studies. Combination of this data with that derived from a *γGCSh*-/- embryonic cell line, subsequently generated by others (Shi et al., 2000), indicates that embryonic GSH is unnecessary for normal growth *in vitro* but is necessary for the response against oxidative stress.

A cluster of redox-regulation genes, including the GSH-dependent enzymes GPx and a GST have been identified as downstream effectors of p53 signalling (Tan et al., 1999; Polyak et al., 1997). I therefore reasoned that p53 may have a role in the GSH response to oxidative stress, possibly via modulation of γGCS expression. However, the magnitude and duration of the MQ-induced GSH response was unaffected by p53

status. Consequently, it is highly probable that embryonic GSH levels are regulated through mechanisms distinct from p53. Candidate pathways include those that terminate in Nrf2, NF-κβ or AP-1 activation.

However, a role for p53 in the global response was established as, in comparison to wild-type cells, p53-/- ES cells had a decreased rate of apoptosis and increased viability immediately following oxidative stress. This implies the existence of distinct p53-dependent and independent death factors that mediate the deletion of damaged ES cells. Within the embryonic field, this result contributes to the view that p53 orchestrates complex dosage- and agent-specific responses to stress, and that broad simplifications of function do not hold.

Prior depletion of GSH converted the MQ-induced apoptotic response of both genotypes to a non-apoptotic form of cell death. This finding is in line with results sourced from diverse cell types and pro-oxidants. BSO and GSH homologues (at high concentration) were also found to become cytotoxic under oxidative stress. These effects are likely to reflect a requirement for a critical GSH concentration band in ES cells to deal with oxidative injury: a proposition advanced for some types of differentiated cells (Mulier et al., 1998). It is tempting to speculate that on a low GSH background, oxidative damage inflicted is severe and overwhelms the ES cell response machinery, leading to catastrophic cell death. Further work out with the time limitations of this project are required to confirm this conjecture.

Inhibition of the ephemeral GSH response was found to reduce the long-term replicative potential of both genotypes exposed to oxidative stress. Apoptosis is known to delete cells carrying a high degree of genetic damage. I propose that, in instances where the normal GSH response failed to protect against MQ-induced oxidative damage, ES cell apoptosis is triggered via multiple pathways (figure 6.1).

In summary, these findings are consistent with the accepted broader role of (a) GSH as an inducible protective agent and, (b) p53 as an inducible transcription factor responding to damage and triggering a complex cascade of responses. However, the

Figure 6.1 Proposed response of p53 and GSH in ES cells exposed to MQ

MQ enters the cell and redox cycles, producing a constant stream of ROS. This oxidises GSH to GSSG, altering the redox equilibrium and causing cellular injury. These two events trigger mechanisms to rapidly increase the level of GSH. This response is part mediated via (i) an increased rate of *de novo* GSH synthesis (in turn mediated by *a*, release of γGCS negative inhibition, and conceivably *b*, *γGCSh* transactivation) and (ii) recycling GSSG to GSH by the actions of GR, *c*. If the GSH response fails to prevent a threshold of cellular damage occurring, then p53 becomes activated which results in either ES cell apoptosis or cell cycle arrest and repair. In the absence of p53, DNA damage activates alternative, p53 independent pathways, which increase apoptosis or reduce repair, leading to reduced long-term survival.

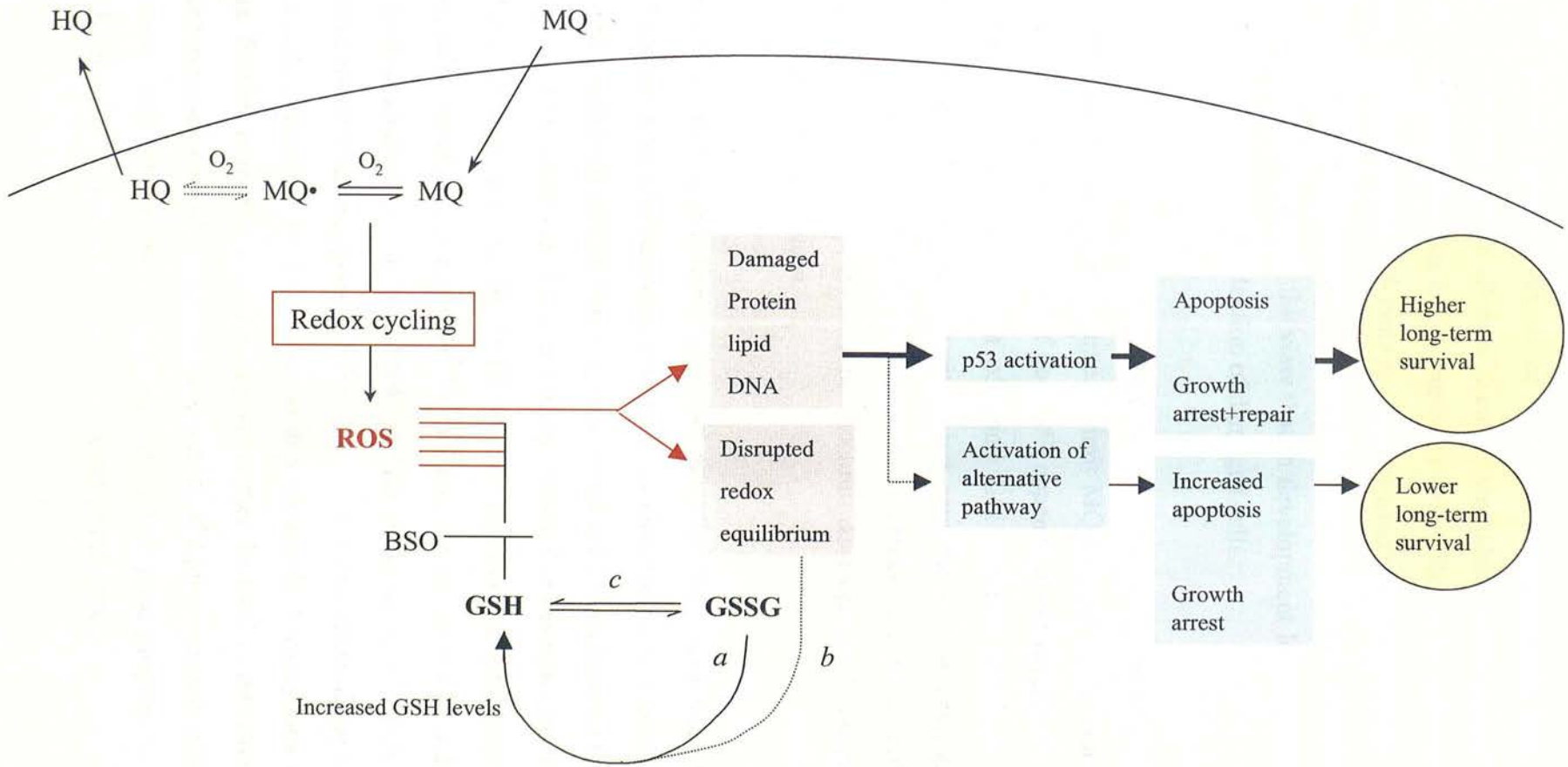
HQ
MQ
HQ
O_2
MQ•
O_2
MQ
Redox cycling
ROS
BSO
GSH
c
GSSG
a
b
Increased GSH levels
Damaged
Protein
lipid
DNA
Disrupted
redox
equilibrium
p53 activation
Activation of
alternative
pathway
Apoptosis
Growth
arrest+repair
Increased
apoptosis
Growth
arrest
Higher
long-term
survival
Lower
long-term
survival

impact of p53 on clonogenic survival serves to underline the complex role played by p53 in embryogenesis. I propose that, in the absence of functional p53, MQ-induced DNA breaks accrue and activate alternative embryonic death pathways that prevent the persistence of genetic lesions in differentiated cells. This is in agreement with previous work which showed p53-/- embryos, upon γ-irradiation, display accentuated levels of delayed apoptosis compared to their wild type counterparts (Frenkel et al., 1999). This is also consistent with the view that in development loss of cells is less detrimental to the organism than retention of damaged cells.

These mechanisms are perhaps reliant upon other p53 family members, such as the homologues p63 and p73. GSH may serve to limit MQ-induced DNA damage and therefore indirectly prevent induction of both p53 dependent and independent death pathways. Thus the data indicate that p53 and GSH operate, through discrete mechanisms, to ensure that cellular integrity is not compromised by environmental oxidative stress during development. Investigation of pathways independent of p53 is clearly an area that may yield potential routes to limit developmental abnormalities induced by oxidative stress *in utero*.

Since the *γGCSh-/-* phenotype is lethal, questions regarding the precise role of γGCS in the GSH response remain pertinent. One route to characterise this could be the generation of a conditional *γGCSh* mouse system, using cre-lox technology (outlined in section 4.3.2, and reviewed in (Lobe and Nagy, 1998). For example, introduction of a floxed *γGCSh* allele into *γGCSh*+/+ ES cells by replacement gene targeting of the wild type allele would make a $\gamma GCSh^{flox}$/+ cell line. To test excision, addition of cre would lead to inactivation of the floxed *γGCSh* allele *in vitro*, which in this instance would create a heterozygous cell line. Chimeras derived from these ES cells could be used to generate mice heterozygous and ultimately homozygous for the floxed allele. Further rounds of intercrossing would then be used to introduce a cre transgene, the expression of which is under the control of a promoter only active in a particular tissue. This strategy would therefore ultimately yield progeny to permit analysis of the effect of GSH loss in a particular organ or cell type.

GSH is potentially critical in limiting redox imbalances caused by inhalation of environmental pollutants and the inflammatory response of lung pathologies, including idiopathic pulmonary fibrosis (IPF) and emphysema (reviewed in Rahman and MacNee, 2000). These conditions are also allied with an imbalance between proteases, such as elastase (sourced from neutrophils and other inflammatory cells), and ambient protease inhibitors (reviewed in (Sethi and Rochester, 2000). Both processes are thought to damage to the lung structure. It is generally anticipated that, due to interactions such as that of GSH with antiproteases and inflammatory cytokines, complex relationships between oxidative and proteolytic mechanisms of lung disorder exist (Morris and Bernard, 1994).

Thus examination of the effect of local GSH deficiency in the lung under oxidative stress would be desirable. To delete *γGCSh* specifically in the lung requires the presence of cre limited to respiratory tissue. This could be achieved using a cre transgene driven by a lung-specific promoter, such as the surfactant gene SPC (*s*urfactant *p*rotein *C*). Pulmonary surfactant is a compound of phospholipids and four unique proteins, SPA, SPB, SPC and SPD (Rooney et al., 1994), which prevents alveolar collapse via lowering of surface tension (Bernhard et al., 2001) and its anti-adhesive properties (Daniels and Orgeig, 2001). Whilst the lung is composed of over forty different cell types (Royce et al., 1996) murine SPC synthesis, as determined by a variety of techniques, is predominantly localised in distal bronchiolar and type II alveolar cells (Glasser et al., 1991; Glasser et al., 2000). This makes the 5' regulatory sequences of the SPC gene a plausible promoter to generate GSH-compromised respiratory epithelia. Indeed SPC has been used successfully to drive lung-specific expression of p53 (Morris et al., 1998), α1-antitrypsin (Dhami et al., 1999), platelet-derived growth factor (Hoyle et al., 1999) and the adenovirus protein E3-14.7K (Harrod et al., 1998) in mice. Cloned mouse SPC promoter was available within our laboratory, and SPC transgenic mice are under preparation (A. R. Clarke, personal communication).

Crossing *γGCSh*^{flox}/- mice with transgenic SPC-Cre mice should result in deactivation of the remaining *γGCSh* allele specifically within the bronchiolar-

alveolar duct regions. If these mice survived to adulthood, it would be necessary to confirm that excision of *γGCSh* occurred in such animals, and was confined to the respiratory epithelia. This would be achieved by Southern blotting techniques on DNA extracted from alveolar and bronchial cells. Upon confirmation, this model would represent a powerful tool to investigate the role of GSH in respiratory disorders. Since there is evidence that GSH is connected with many aspects of lung function, including maintenance of a normal surfactant system (Martensson et al., 1991; Li et al., 1998; Khalak et al., 1999), early lethality, or at least respiratory distress may be predicted. If so, an inducible model that allows for deletion of *γGCSh* in adult tissue represents an alternative avenue for exploration.

To generate a conditional *γGCSh* model, I would propose a version of the promoter strategy of Zhang and co-workers, under development in this department. This approach requires fusion of cre with the ligand binding domain of a mutant oestrogen receptor (▲), connected to the SPC promoter. This mutant receptor cannot bind oestradiols, but specifically recognises the anti-oestrogen drug, tamoxifen. Addition of tamoxifen to the culture medium of ES cells (Zhang et al., 1996) or neonatally to mature animals leads to efficient activation of the cre fusion protein, as measured by reporter genes (Fiel et al., 1996; Schwenk et al., 1998). Crossing $\gamma GCSh^{flox}$/- females with males that bear a SPC-cre▲ transgene can yield progeny with the potential for temporal control of gene excision. Injection of tamoxifan into the lung cavity would be predicted to initiate excision of the floxed *γGCSh* allele within the lower respiratory tract.

Thus, this technique can permit analysis of the effect of complete *γGCSh* deficiency on respiratory tissue in mature animals. To study the function of GSH in the response to oxidative stress in this model, examination of GSH levels in different tissues must first be carried out to identify tissues with effectively deactivated *γGCSh*. Upon demonstration of success with either constitutive lung or inducible lung strategies an experimental program would be initiated. First, comparison of the LD_{50} values of wild-type and lung *γGCSh*-/- mice exposed to cigarette smoke would indicate the crude extent of reliance on the GSH system of the lower respiratory tract to limit

smoking-induced lung injury. This may be expected to be high, since GSH is normally a highly abundant antioxidant and is thought necessary to ameliorate oxidative damage to endogenous biomolecules (Cantin et al., 1987; Brown, 1994; Deneke, 2000).

Second, to investigate the pathology of mice with *γGCSh-/-* lung to oxidative stress, tissues would be prepared for histological analysis. Morphologic evaluation of lung sections from wild-type and lung *γGCSh-/-* mice under light microscopy would assess any remodelling of lung architecture. In particular, fibrotic lesions and increased airspace permeability – phenomena associated with idiopathic pulmonary fibrosis and emphysema in man (MacNee and Rahman, 1995; Rahman and MacNee, 2000). Airspace area would be measured by first capturing digital images under light microscopy, technology available in the imaging suite of the Pathology department. Following this, analysis with publically available NIH image software (http:rsb.info.nih.gov/nih-image/downloads.html), would be done as described (Hoyle et al., 1999).

Third, lung sections would also be used to estimate apoptotic rates between genetically normal and lung-*γGCSh-/-* tissue, with and without oxidative stress. Apoptosis is potentially implicated in lung disorders (Morris and Bernard, 1994). If apoptotic rates significantly alter between lung genotypes, and correlate with the acquisition of histological features of respiratory disease, this result would flag apoptosis as an area worthy of further investigation. If not, it would suggest that dysregulated cell death is not a critical factor in development of inflammatory lung pathologies.

Forth, to probe for mechanisms underlying pathologies recorded, lungs from both genotypes with and without smoking-induced oxidative stress would be perfused, the distal portions isolated, homogenated then divided into GSH, cytosolic and RNA samples. Others have shown GSH decreased 45% in lungs of rats exposed to cigarette smoke (Park et al., 1998). Therefore GSH levels, as well as the activities of SOD and other antioxidant enzymes from cytosolic fractions would be analysed.

This would indicate whether loss of *γGCSh-/-* results in complete ablation of pulmonary GSH, or whether secondary sources of GSH can re-supply lungs. Comparing the enzyme activities with northern blotting data for the same factors would suggest whether GSH deficiency leads to compensatory antioxidant responses, and whether alterations in activity concur with changes in gene expression. The former is likely since rats exposed to 90% oxygen for seven days demonstrated substantial increases in MnSOD (245%), GPx (317%), and GR (175%) over controls (Kimball, 1976).

Fifth, the ensuing inflammatory response is thought to exacerbate the initial injuries sustained, and represent an important phase in many types of lung disease. To examine the role of GSH in this response, it would be possible to investigate whether *γGCS* loss in the respiratory epithelium modified the number of accumulated lumenal macrophages, eosinophils or neutrophils. This could be achieved by immunohistochemistry on lung sections with murine monoclonal antibodies against such inflammatory cells, as used previously (Luna, 1968; Liu et al., 1996).

Sixth, it would be interesting to determine the GSH content of the respiratory lining fluid (RLF) from *γGCSh-/-* and genetically normal mouse lung. This would indicate sources of lumenal GSH other than from the pulmonary tract, including net GSH exporters such as liver. RLF GSH pools are reduced in the respiratory disorders IPF (Cantin et al., 1989; Rahman et al., 1999) and acute respiratory distress syndrome (Bunnell and Pacht, 1993). However, in response to chronic smoking, GSH levels in RLF rise (Eiserich et al., 1995; Morrison et al., 1999). Examination of GSH levels found in RLF from *γGCSh-/-* lung exposed regularly to cigarette smoke would indicate whether this elevation was mediated predominantly, or not, by synthesis from within the respiratory epithelia. If so, strategies to modulate antioxidant gene expression in the pulmonary tract may represent a potential therapeutic target to augment RLF GSH levels.

Seventh, to assess whether GSH loss in RLF affects antiprotease function. α_1-proteinase inhibitor (α_1PI) previously isolated from the lungs of cigarette smokers

was found to have oxidised methionine residues and lower capacity to inhibit elastase (Carp et al., 1982; Hubbard et al., 1987). It would be instructive to know whether α_1PI, recovered from smoking-damaged *γGCSh-/-* lung, has lower activity and greater methionine oxidation than that of wild-type lung. If confirmed, this add weight to the theory that GSH plays a direct role in maintaining antiprotease function.

Overall, the effect of lung *γGCSh* loss on mice would be analysed by correlating induced oxidant/antioxidant or protease/antiprotease imbalances with anatomical and biochemical features of lung disease. This would clarify the roles of GSH in these paradigms and may open new areas for subsequent exploration, or refine experimental regimens to correct the low GSH levels associated with lung pathologies. Using the materials generated and the information presented in this thesis, it is hoped murine models to provide insights to these pertinent areas will be developed by others.

Appendix I: References

Abarzua, P., LoSardo, J.E., Gubler, M.L., et al. Restoration of the transcription activation function to mutant p53 in human cancer cells. *Oncogene* 13:2477-2482, 1996.

Abate, C., Patel, L., Rauscher, F.J. and Curran, T. Redox regulation of Fos and Jun DNA-binding activity in vitro. *Science* 249:1157-1161, 1990.

Abbott, J., Pei, J.F., Qi, Y., et al. Structure prediction and active site analysis of the metal binding determinants in γ–glutamylcysteine synthetase. *J Biol Chem* 276:42099-42107, 2001.

Abramova, N.A., Russell, J., Botchan, M. and Li, R. Interaction between replication protein A and p53 is disrupted after UV damage in a DNA repair-dependent manner. *Proc Natl Acad Sci U S A* 94:7186-7191, 1997.

Afford, S. and Randhawa, S. Apoptosis. *Mol Pathol* 53:55-63, 2000.

Agarwal, M.L., Agarwal, A., Taylor, W.R. and Stark, G.R. p53 controls both the G2/M and the G1 cell cycle checkpoints and mediates reversible growth arrest in human fibroblasts. *Proc Natl Acad Sci U S A* 92:8493-8497, 1995.

Akazawa, S., Unterman, T. and Metzger, B.E. Glucose metabolism in separated embryos and investing membranes during organogenesis in the rat. *Metabolism* 43:830-835, 1994.

Akman, S.A., O'Connor, T.R. and Rodriguez, H. Mapping oxidative DNA damage and mechanisms of repair. *Ann N Y Acad Sci* 899:88-102, 2000.

al-Shawi, R., Burke, J., Wallace, H., et al. The herpes simplex virus type 1 thymidine kinase is expressed in the testes of transgenic mice under the control of a cryptic promoter. *Mol Cell Biol* 11:4207-4216, 1991.

Aladjem, M.I., Spike, B.T., Rodewald, L.W., et al. ES cells do not activate p53-dependent stress responses and undergo p53-independent apoptosis in response to DNA damage. *Curr Biol* 8:145-155, 1998.

Aliosman, F., Antoun, G., Wang, H., Ranjagopal, S. and Gagucas, E. Buthionine sulphoximine induction of gamma-glutamyl-L-cysteine synthetase gene-expression, kinetics of glutathione depletion and resynthesis, and modulation of carmustine-induced DNA-DNA cross-linking and cytotoxicity in human glioma-cells. *Mol Pharmacol* 49:1012-1020, 1996.

Allen, T. Ultrastructural aspects of cell death. In: *Perspectives on Mammalian Cell Death*, edited by Potten, C. Oxford: Oxford University Press, 1987, p. 36-65.

Alnemri, E.S., Livingston, D.J., Nicholson, D.W., et al. Human ICE/CED-3 protease nomenclature [letter]. *Cell* 87:171-171, 1996.

Ames, B.N., Shigenaga, M.K. and Hagen, T.M. Oxidants, antioxidants, and the degenerative diseases of aging. *Proc Natl Acad Sci U S A* 90:7915-7922, 1993.

Amstad, P., Moret, R. and Cerutti, P. Glutathione peroxidase compensates for the hypersensitivity of Cu,Zn-superoxide dismutase overproducers to oxidant stress. *J Biol Chem* 269:1606-1609, 1994.

Anderson, M.E., Underwood, M., Bridges, R.J. and Meister, A. Glutathione metabolism at the blood-cerebrospinal fluid barrier. *FASEB J* 3:2527-2531, 1989.

Anderson, M.E., Woelker, B., Reed, M., Wang, P. and Tegtmeyer, P. Reciprocal interference between the sequence-specific core and nonspecific C-terminal DNA

binding domains of p53: implications for regulation. *Mol Cell Biol* 17:6255-6264, 1997.

Angrand, P.O., Daigle, N., van der Hoeven, F., Scholer, H.R. and Stewart, A.F. Simplified generation of targeting constructs using ET recombination. *Nucleic Acids Res* 27:e16-e161999.

Arase, K., Saijo, K., Watanabe, H., Konno, A., Arase, H. and Saito, T. Ablation of a specific cell population by the replacement of a uniquely expressed gene with a toxin gene. *Proc Natl Acad Sci U S A* 96:9264-9268, 1999.

Armstrong, J.F., Kaufman, M.H., Harrison, D.J. and Clarke, A.R. High-frequency developmental abnormalities in p53-deficient mice. *Curr Biol* 5:931-936, 1995.

Arriola, E.L., Lopez, A.R. and Chresta, C.M. Differential regulation of p21waf-1/cip-1 and Mdm2 by etoposide: etoposide inhibits the p53-Mdm2 autoregulatory feedback loop. *Oncogene* 18:1081-1091, 1999.

Arsalane, K., Dubois, C.M., Muanza, T., et al. Transforming growth factor-beta(1) is a potent inhibitor of glutathione synthesis in the lung epithelial cell line A549: Transcriptional effect on the GSH rate-limiting enzyme gamma- glutamylcysteine synthetase. *Am J Resp Cell Mol Biol* 17:599-607, 1997.

Ashcroft, M., Kubbutat, M.H. and Vousden, K.H. Regulation of p53 function and stability by phosphorylation. *Mol Cell Biol* 19:1751-1758, 1999a.

Ashcroft, M. and Vousden, K.H. Regulation of p53 stability. *Oncogene* 18:7637-7643, 1999b.

Atadja, P., Wong, H., Garkavtsev, I., Veillette, C. and Riabowol, K. Increased activity of p53 in senescing fibroblasts. *Proc Natl Acad Sci U S A* 92:8348-8352, 1995.

Awad, J.A., Morrow, J.D., Takahashi, K. and Roberts, L.J. Identification of non-cyclooxygenase-derived prostanoid (F2-isoprostane) metabolites in human urine and plasma. *J Biol Chem* 268:4161-4169, 1993.

Ayares, D., Chekuri, L., Song, K.Y. and Kucherlapati, R. Sequence homology requirements for intermolecular recombination in mammalian cells. *Proc Natl Acad Sci U S A* 83:5199-5203, 1986.

Baek, S.H., Min, J.N., Park, E.M., et al. Role of small heat shock protein HSP25 in radioresistance and glutathione-redox cycle. *J Cell Physiol* 183:100-107, 2000.

Bailey, H.H. L-S,R-buthionine sulfoximine: historical development and clinical issues. *Chemico-Biological Interactions* 112:239-254, 1998.

Bakalkin, G., Selivanova, G., Yakovleva, T., et al. p53 binds single-stranded DNA ends through the C-terminal domain and internal DNA segments via the middle domain. *Nucleic Acids Res* 23:362-369, 1995.

Bandyopadhyay, S., Starke, D.W., Mieyal, J.J. and Gronostajski, R.M. Thioltransferase (glutaredoxin) reactivates the DNA-binding activity of oxidation-inactivated nuclear factor I. *J Biol Chem* 273:392-397, 1998.

Bannai, S. Transport of cystine and cysteine in mammalian cells. *Biochim Biophys Acta* 779:289-306, 1984.

Barak, Y. and Oren, M. Enhanced binding of a 95 kDa protein to p53 in cells undergoing p53-mediated growth arrest. *EMBO J* 11:2115-2121, 1992.

Barford, D., Jia, Z. and Tonks, N.K. Protein tyrosine phosphatases take off. *Nat Struct Biol* 2:1043-1053, 1995.

Bargonetti, J., Manfredi, J.J., Chen, X., Marshak, D.R. and Prives, C. A proteolytic fragment from the central region of p53 has marked sequence-specific DNA-binding

activity when generated from wild-type but not from oncogenic mutant p53 protein. *Genes Dev* 7:2565-2574, 1993.

Barnes, P.J. and Adcock, I. Anti-inflammatory actions of steroids: molecular mechanisms. *Trends Pharmacol Sci* 14:436-441, 1993.

Barnes, W.M. PCR amplification of up to 35-kb DNA with high fidelity and high yield from lambda bacteriophage templates. *Proc Natl Acad Sci U S A* 91:2216-2220, 1994.

Basu, A.K. and Marnett, L.J. Unequivocal demonstration that malondialdehyde is a mutagen. *Carcinogenesis* 4:331-333, 1983.

Bauskin, A.R., Alkalay, I. and Ben-Neriah, Y. Redox regulation of a protein tyrosine kinase in the endoplasmic reticulum. *Cell* 66:685-696, 1991.

Beckman, K.B. and Ames, B.N. Oxidative decay of DNA. *J Biol Chem* 272:19633-19636, 1997.

Bedell, M.A., Jenkins, N.A. and Copeland, N.G. Mouse models of human disease. Part I: techniques and resources for genetic analysis in mice. *Genes Dev* 11:1-10, 1997a.

Bedell, M.A., Largaespada, D.A., Jenkins, N.A. and Copeland, N.G. Mouse models of human disease. Part II: recent progress and future directions. *Genes Dev* 11:11-43, 1997b.

Bellomo, G., Vairetti, M., Stivala, L., Mirabelli, F., Richelmi, P. and Orrenius, S. Demonstration of nuclear compartmentalization of glutathione in hepatocytes. *Proc Natl Acad Sci U S A* 89:4412-4416, 1992.

Benton, W.D. and Davis, R.W. Screening lambdagt recombinant clones by hybridization to single plaques in situ. *Science* 196:180-182, 1977.

Bergendi, L., Benes, L., Durackova, Z. and Ferencik, M. Chemistry, physiology and pathology of free radicals. *Life Sci* 65:1865-1874, 1999.

Berlett, B.S. and Stadtman, E.R. Protein oxidation in aging, disease, and oxidative stress. *J Biol Chem* 272:20313-20316, 1997.

Bernhard, W., Gebert, A., Vieten, G., et al. Pulmonary surfactant in birds: coping with surface tension in a tubular lung. *Am J Physiol Regul Integr Comp Physiol* 281:R327-R3372001.

Bessette, P.H., Aslund, F., Beckwith, J. and Georgiou, G. Efficient folding of proteins with multiple disulfide bonds in the Escherichia coli cytoplasm. *Proc Natl Acad Sci U S A* 96:13703-13708, 1999.

Bhagwat, M. and Gerlt, J. 3' and 5'-strand cleavage reactions catalysed by the Fpg protein from E. coli occur via successive d- and d- elimination- mechanisms, respectively. *Biochemistry* 35:659-665, 1995.

Biemond, P., van Eijk, H.G., Swaak, A.J. and Koster, J.F. Iron mobilization from ferritin by superoxide derived from stimulated polymorphonuclear leukocytes. Possible mechanism in inflammation diseases. *J Clin Invest* 73:1576-1579, 1984.

Bladier, C., Wolvetang, E.J., Hutchinson, P., de Haan, J.B. and Kola, I. Response of a primary human fibroblast cell line to H2O2: senescence-like growth arrest or apoptosis? *Cell Growth Differ* 8:589-598, 1997.

Blattner, C., Sparks, A. and Lane, D. Transcription factor E2F-1 is upregulated in response to DNA damage in a manner analogous to that of p53. *Mol Cell Biol* 19:3704-3713, 1999.

Bodmer, W., Bishop, T. and Karran, P. Genetic steps in colorectal cancer. *Nat Genet* 6:217-219, 1994.

Bohr, V.A. and Dianov, G.L. Oxidative DNA damage processing in nuclear and mitochondrial DNA. *Biochimie* 81:155-160, 1999.

Boise, L.H., Gonzalez-Garcia, M., Postema, C.E., et al. bcl-x, a bcl-2-related gene that functions as a dominant regulator of apoptotic cell death. *Cell* 74:597-608, 1993.

Bollag, R.J., Waldman, A.S. and Liskay, R.M. Homologous recombination in mammalian cells. *Annu Rev Genet* 23:199-225, 1989.

Borellini, F. and Glazer, R.I. Induction of Sp1-p53 DNA-binding heterocomplexes during granulocyte/macrophage colony-stimulating factor-dependent proliferation in human erythroleukemia cell line TF-1. *J Biol Chem* 268:7923-7928, 1993.

Borroz, K.I., Buetler, T.M. and Eaton, D.L. Modulation of gamma-glutamylcysteine synthetase large subunit messenger-rna expression by butylated hydroxyanisole. *Toxicol Appl Pharmacol* 126:150-155, 1994.

Bose, B., Agarwal, S. and Chatterjee, S.N. Membrane lipid peroxidation by UV-A: mechanism and implications. *Biotechnol Appl Biochem* 12:557-561, 1990.

Boue, A., Boue, J. and Gropp, A. Cytogenetics of pregnancy wastage. *Adv Hum Genet* 14:1-57, 1985.

Bouvard, V., Zaitchouk, T., Vacher, M., et al. Tissue and cell-specific expression of the p53-target genes: bax, fas, mdm2 and waf1/p21, before and following ionising irradiation in mice. *Oncogene* 19:649-660, 2000.

Bradford, M.M. A rapid and sensitive method for the quantitation of microgram quantities of protein utilizing the principle of protein-dye binding. *Anal Biochem* 72:248-252, 1976.

Brain, R. and Jenkins, J.R. Human p53 directs DNA strand reassociation and is photolabelled by 8-azido ATP. *Oncogene* 9:1775-1780, 1994.

Brison, D.R. and Schultz, R.M. Apoptosis during mouse blastocyst formation: evidence for a role for survival factors including transforming growth factor alpha. *Biol Reprod* 56:1088-1096, 1997.

Brown, L.A. Glutathione protects signal transduction in type II cells under oxidant stress. *Am J Physiol* 266:L172-L1771994.

Brown, P.C., Dulik, D.M. and Jones, T.W. The toxicity of menadione (2-methyl-1,4-naphthoquinone) and two thioether conjugates studied with isolated renal epithelial cells. *Arch Biochem Biophys* 285:187-196, 1991.

Brugarolas, J., Chandrasekaran, C., Gordon, J.I., Beach, D., Jacks, T. and Hannon, G.J. Radiation-induced cell cycle arrest compromised by p21 deficiency. *Nature* 377:552-557, 1995.

Buchhop, S., Gibson, M.K., Wang, X.W., Wagner, P., Sturzbecher, H.W. and Harris, C.C. Interaction of p53 with the human Rad51 protein. *Nucleic Acids Res* 25:3868-3874, 1997.

Buckbinder, L., Talbott, R., Velasco-Migule, S., et al. Induction of the growth inhibitor IGF-binding protein 3 by p53. *Nature* 377:646-649, 1996.

Buckley, C.D., Pilling, D., Henriquez, N.V., et al. RGD peptides induce apoptosis by direct caspase-3 activation. *Nature* 397:534-539, 1999.

Bunnell, E. and Pacht, E.R. Oxidized glutathione is increased in the alveolar fluid of patients with the adult respiratory distress syndrome. *Am Rev Respir Dis* 148:1174-1178, 1993.

Bustamante, J., Tovar, B., Montero, G. and Boveris, A. Early redox changes during rat thymocyte apoptosis. *Arch Biochem Biophys* 337:121-128, 1997.

Buttke, T.M. and Sandstrom, P.A. Oxidative stress as a mediator of apoptosis. *Immunol Today* 15:7-10, 1994.

Caelles, C., Helmberg, A. and Karin, M. p53-dependent apoptosis in the absence of transcriptional activation of p53-target genes. *Nature* 370:220-223, 1994.

Cai, J.X., Huang, Z.Z. and Lu, S.C. Differential regulation of gamma-glutamylcysteine synthetase heavy and light subunit gene expression. *Biochem J* 326:167-172, 1997.

Cai, J.X., Sun, W.M. and Lu, S.C. Hormonal and cell-density regulation of hepatic gamma- glutamylcysteine synthetase gene-expression. *Gastroenterology* 108:A1043-A10431995.

Cairns, C.A. and White, R.J. p53 is a general repressor of RNA polymerase III transcription. *EMBO J* 17:3112-3123, 1998.

Campisi, J. Gene expression in quiescent and senescent fibroblasts. *Ann N Y Acad Sci* 663:195-201, 1992.

Campisi, J. Replicative senescence: an old lives' tale? *Cell* 84:497-500, 1996.

Canman, C., Gilmer, T., Coutts, S. and Kastan, M. Growth factor modulation of p53-mediated growth arrest versus apoptosis. *Genes Devel* 9:600-611, 1995.

Cantin, A.M., Hubbard, R.C. and Crystal, R.G. Glutathione deficiency in the epithelial lining fluid of the lower respiratory tract in idiopathic pulmonary fibrosis. *Am Rev Respir Dis* 139:370-372, 1989.

Cantin, A.M., North, S.L., Hubbard, R.C. and Crystal, R.G. Normal alveolar epithelial lining fluid contains high levels of glutathione. *J Appl Physiol* 63:152-157, 1987.

Cappelli, E., Taylor, R., Cevasco, M., Abbondandolo, A., Caldecott, K. and Frosina, G. Involvement of XRCC1 and DNA ligase III gene products in DNA base excision repair. *J Biol Chem* 272:23970-23975, 1997.

Caricchio, R., Kovalenko, D., Kaufmann, WK. and Cohen, PL. Apoptosis provoked by the oxidative stress inducer menadione (vitamin K3) is mediated by the Fas/Fas ligand system. *Clinical immunology* 93:65-74, 1999.

Caron, d.F. and Soussi, T. TP53 tumor suppressor gene: a model for investigating human mutagenesis. *Genes Chromosomes Cancer* 4:1-15, 1992.

Carp, H., Miller, F., Hoidal, J.R. and Janoff, A. Potential mechanism of emphysema - alpha-1-proteinase inhibitor recovered from lungs of cigarette smokers contains oxidized methionine and has decreased elastase inhibitory capacity. *Proceedings Of The National Academy Of Sciences Of The United States Of America-Biological Sciences* 79:2041-2045, 1982.

Chandel, N.S., Vander, H., Thompson, C.B. and Schumacker, P.T. Redox regulation of p53 during hypoxia. *Oncogene* 19:3840-3848, 2000.

Chapman, R.S., Lourenco, P.C., Tonner, E., et al. Suppression of epithelial apoptosis and delayed mammary gland involution in mice with a conditional knockout of Stat3. *Genes Dev* 13:2604-2616, 1999.

Chen, Q., Fischer, A., Reagan, J.D., Yan, L.J. and Ames, B.N. Oxidative DNA damage and senescence of human diploid fibroblast cells. *Proc Natl Acad Sci U S A* 92:4337-4341, 1995.

Chen, X., Ko, L.J., Jayaraman, L. and Prives, C. p53 levels, functional domains, and DNA damage determine the extent of the apoptotic response of tumor cells. *Genes Dev* 10:2438-2451, 1996.

Chen, Y., Saari, J.T. and Kang, Y.J. Expression of gamma-glutamylcysteine synthetase in the liver of copper-deficient rats. *Proc Soc Exp Biol Med* 210:102-106, 1995.

Chen, Y.W. and Frank, L. Differential gene-expression of antioxidant enzymes in the perinatal rat lung. *Pediatric Research* 34:27-31, 1993.

Cheng, W., Fu, Y.X., Porres, J.M., Ross, D.A. and Lei, X.G. Selenium-dependent cellular glutathione peroxidase protects mice against a pro-oxidant-induced oxidation of NADPH, NADH, lipids, and protein. *FASEB J* 13:1467-1475, 1999.

Cheng, W.H., Ho, Y.S., Ross, D.A., Valentine, B.A., Combs, G.F. and Lei, X.G. Cellular glutathione peroxidase knockout mice express normal levels of selenium-dependent plasma and phospholipid hydroperoxide glutathione peroxidases in various tissues. *J Nutr* 127:1445-1450, 1997.

Chernov, M.V., Ramana, C.V., Adler, V.V. and Stark, G.R. Stabilization and activation of p53 are regulated independently by different phosphorylation events. *Proc Natl Acad Sci U S A* 95:2284-2289, 1998.

Chernyak, B.V. and Bernardi, P. The mitochondrial permeability transition pore is modulated by oxidative agents through both pyridine nucleotides and glutathione at two separate sites. *Eur J Biochem* 238:623-630, 1996.

Chesis, P.L., Levin, D.E., Smith, M.T., Ernster, L. and Ames, B.N. Mutagenicity of quinones: pathways of metabolic activation and detoxification. *Proc Natl Acad Sci U S A* 81:1696-1700, 1984.

Chesnokov, I., Chu, W.M., Botchan, M.R. and Schmid, C.W. p53 inhibits RNA polymerase III-directed transcription in a promoter-dependent manner. *Mol Cell Biol* 16:7084-7088, 1996.

Chiou, S.K., Rao, L. and White, E. Bcl-2 blocks p53-dependent apoptosis. *Mol Cell Biol* 14:2556-2563, 1994.

Chittenden, T., Harrington, E.A., O'Connor, R., et al. Induction of apoptosis by the Bcl-2 homologue Bak. *Nature* 374:733-736, 1995.

Cho, S., Hazama, M., Urata, Y., et al. Protective role of glutathione synthesis in response to oxidized low density lipoprotein in human vascular endothelial cells. *Free Radic Biol Med* 26:589-602, 1999.

Cho, Y., Gorina, S., Jeffrey, P.D. and Pavletich, N.P. Crystal structure of a p53 tumor suppressor-DNA complex: understanding tumorigenic mutations. *Science* 265:346-355, 1994.

Choi, H.S.M.D.D. Induction of c-fos and c-jun Gene Expression by Phenolic Antioxidants. *Molecular Endocrinology* 7:1596-1602, 1993.

Choi, J. and Donehower, L.A. p53 in embryonic development: maintaining a fine balance. *Cell Mol Life Sci* 55:38-47, 1999.

Clark, J.M. Novel non-templated nucleotide addition reactions catalyzed by procaryotic and eucaryotic DNA polymerases. *Nucleic Acids Res* 16:9677-9686, 1988.

Clarke, A.R., Gledhill, S., Hooper, M.L., Bird, C.C. and Wyllie, A.H. p53 dependence of early apoptotic and proliferative responses within the mouse intestinal epithelium following gamma-irradiation. *Oncogene* 9:1767-1773, 1994.

Clarke, A.R., Purdie, C.A., Harrison, D.J., et al. Thymocyte apoptosis induced by p53-dependent and independent pathways. *Nature* 362:849-852, 1993.

Coleman, J.B., Gilfor, D. and Farber, J.L. Dissociation of the accumulation of single-strand breaks in DNA from the killing of cultured hepatocytes by an oxidative stress. *Mol Pharmacol* 36:193-200, 1989.

Cook, J.A., Pass, H.I., Iype, S.N., et al. Cellular glutathione and thiol measurements from surgically resected human lung tumor and normal lung tissue. *Cancer Res* 51:4287-4294, 1991.

Corbet, S.W., Clarke, A.R., Gledhill, S. and Wyllie, A.H. P53-dependent and -independent links between DNA-damage, apoptosis and mutation frequency in ES cells. *Oncogene* 18:1537-1544, 1999.

Cornillon, S., Olie, R.A. and Golstein, P. An insertional mutagenesis approach to Dictyostelium cell death. *Cell Death Differ* 5:416-425, 1998.

Corroyer, S., Maitre, B., Cazals, V. and Clement, A. Altered regulation of G1 cyclins in oxidant-induced growth arrest of lung alveolar epithelial cells. Accumulation of inactive cyclin E-DCK2 complexes. *J Biol Chem* 271:25117-25125, 1996.

Cranston, A., Bocker, T., Reitmair, A., et al. Female embryonic lethality in mice nullizygous for both Msh2 and p53. *Nat Genet* 17:114-118, 1997.

Cristofalo, V.J., Pignolo, R.J. and Rotenberg, M.O. Molecular changes with in vitro cellular senescence. *Ann N Y Acad Sci* 663:187-194, 1992.

Czene, S., Tiback, M. and Harms-Ringdahl, M. pH-dependent DNA cleavage in permeabilized human fibroblasts. *Biochem J* 323 (Pt 2):337-341, 1997.

d'Arcy, D., Rodgers, A. and Cohen, G.M. Mechanisms of toxicity of 2- and 5-hydroxy-1,4-naphthoquinone; absence of a role for redox cycling in the toxicity of 2-

hydroxy-1,4-naphthoquinone to isolated hepatocytes. *J Appl Toxicol* 7:123-129, 1987.

Dalton, T.P., Dieter, M.Z., Yang, Y., Shertzer, H.G. and Nebert, D.W. Knockout of the mouse glutamate cysteine ligase catalytic subunit (Gclc) gene: embryonic lethal when homozygous, and proposed model for moderate glutathione deficiency when heterozygous. *Biochem Biophys Res Commun* 279:324-329, 2000.

Dameron, K.M., Volpert, O.V., Tainsky, M.A. and Bouck, N. Control of angiogenesis in fibroblasts by p53 regulation of thrombospondin-1. *Science* 265:1582-1584, 1994.

Dang, C.V. and Lee, W.M. Nuclear and nucleolar targeting sequences of c-erb-A, c-myb, N-myc, p53, HSP70, and HIV tat proteins. *J Biol Chem* 264:18019-18023, 1989.

Daniels, C.B. and Orgeig, S. The comparative biology of pulmonary surfactant: past, present and future. *Comp Biochem Physiol A Mol Integr Physiol* 129:9-36, 2001.

Darmon, A., Nicholson, D. and Bleackley, R. Activation of the apoptotic protease Cpp32 by cytotoxic T-cell derived granzyme-B. *Nature* 377:4481995.

Davis, J.B. and Maher, P. Protein-kinase-c activation inhibits glutamate-induced cytotoxicity in a neuronal cell-line. *Brain Research* 652:169-173, 1994.

de Groot, H. and Littauer, A. Hypoxia, reactive oxygen, and cell injury. *Free Radic Biol Med* 6:541-551, 1989.

de Haan, J.B., Bladier, C., Griffiths, P., et al. Mice with a homozygous null mutation for the most abundant glutathione peroxidase, Gpx1, show increased susceptibility to the oxidative stress-inducing agents paraquat and hydrogen peroxide. *J Biol Chem* 273:22528-22536, 1998.

Debbas, M. and White, E. Wild-type p53 mediates apoptosis by E1A, which is inhibited by E1B. *Genes Dev* 7:546-554, 1993.

Deffie, A., Wu, H., Reinke, V. and Lozano, G. The tumor suppressor p53 regulates its own transcription. *Mol Cell Biol* 13:3415-3423, 1993.

Del Sal, G., Ruaro, E.M., Utrera, R., Cole, C.N., Levine, A.J. and Schneider, C. Gas1-induced growth suppression requires a transactivation-independent p53 function. *Mol Cell Biol* 15:7152-7160, 1995.

Deneke, S.M. Thiol-based antioxidants. *Curr Top Cell Regul* 36:151-180, 2000.

Deneke, S.M. and Fanburg, B.L. Regulation of cellular glutathione. *Am J Physiol* 257:L-L1989.

Deng, C. and Capecchi, M.R. Reexamination of gene targeting frequency as a function of the extent of homology between the targeting vector and the target locus. *Mol Cell Biol* 12:3365-3371, 1992.

Deng, C., Zhang, P., Harper, J.W., Elledge, S.J. and Leder, P. Mice lacking p21CIP1/WAF1 undergo normal development, but are defective in G1 checkpoint control. *Cell* 82:675-684, 1995.

Denu, J.M. and Tanner, K.G. Specific and reversible inactivation of protein tyrosine phosphatases by hydrogen peroxide: evidence for a sulfenic acid intermediate and implications for redox regulation. *Biochemistry* 37:5633-5642, 1998.

Desagher, S., Osen-Sand, A., Nichols, A., et al. Bid-induced conformational change of Bax is responsible for mitochondrial cytochrome c release during apoptosis. *J Cell Biol* 144:891-901, 1999.

Devary, Y., Gottlieb, R.A., Smeal, T. and Karin, M. The mammalian ultraviolet response is triggered by activation of src tyrosine kinases. *Cell* 71:1081-1091, 1992.

Devary, Y., Rosette, C., Didonato, J.A. and Karin, M. Nf-kappa-b activation by ultraviolet-light not dependent on a nuclear signal. *Science* 261:1442-1445, 1993.

Dhami, R., Zay, K., Gilks, B., Porter, S., Wright, J.L. and Churg, A. Pulmonary epithelial expression of human alpha1-antitrypsin in transgenic mice results in delivery of alpha1-antitrypsin protein to the interstitium. *J Mol Med* 77:377-385, 1999.

Di Monte, D., Ross, D., Bellomo, G., Eklow, L. and Orrenius, S. Alterations in intracellular thiol homeostasis during the metabolism of menadione by isolated rat hepatocytes. *Arch Biochem Biophys* 235:334-342, 1984.

Dimmeler, S., Haendeler, J., Sause, A. and Zeiher, A.M. Nitric oxide inhibits APO-1/Fas-mediated cell death. *Cell Growth Differ* 9:415-422, 1998.

Dimri, G.P., Lee, X., Basile, G., et al. A biomarker that identifies senescent human cells in culture and in aging skin in vivo. *Proc Natl Acad Sci U S A* 92:9363-9367, 1995.

Donehower, L.A. The p53-deficient mouse: a model for basic and applied cancer studies. *Semin Cancer Biol* 7:269-278, 1996.

Dong, Z., Saikumar, P., Weinberg, J.M. and Venkatachalam, M.A. Internucleosomal DNA cleavage triggered by plasma membrane damage during necrotic cell death. Involvement of serine but not cysteine proteases. *Am J Pathol* 151:1205-1213, 1997.

Drachenberg, C.B., Ioffe, O.B. and Papadimitriou, J.C. Progressive increase of apoptosis in prostatic intraepithelial neoplasia and carcinoma: comparison between in situ end-labeling of fragmented DNA and detection by routine hematoxylin-eosin staining. *Arch Pathol Lab Med* 121:54-58, 1997.

Duhe, R.J., Evans, G.A., Erwin, R.A., Kirken, R.A., Cox, G.W. and Farrar, W.L. Nitric oxide and thiol redox regulation of Janus kinase activity. *Proc Natl Acad Sci U S A* 95:126-131, 1998.

Dulic, V., Kaufmann, W.K., Wilson, S.J., et al. p53-dependent inhibition of cyclin-dependent kinase activities in human fibroblasts during radiation-induced G1 arrest. *Cell* 76:1013-1023, 1994.

Dutta, A., Ruppert, J.M., Aster, J.C. and Winchester, E. Inhibition of DNA replication factor RPA by p53. *Nature* 365:79-82, 1993.

Dypbukt, J.M., Ankarcrona, M., Burkitt, M., et al. Different prooxidant levels stimulate growth, trigger apoptosis, or produce necrosis of insulin-secreting RINm5F cells. The role of intracellular polyamines. *J Biol Chem* 269:30553-30560, 1994.

editorial. Odds and SODs. *Nat Genet* 3:275-276, 1993.

Eiserich, J.P., Vandervliet, A., Handelman, G.J., Halliwell, B. and Cross, C.E. Dietary antioxidants and cigarette smoke-induced biomolecular damage - a complex interaction. *American Journal Of Clinical Nutrition* 62:S1490-S15001995.

el-Deiry, W.S., Kern, S.E., Pietenpol, J.A., Kinzler, K.W. and Vogelstein, B. Definition of a consensus binding site for p53. *Nat Genet* 1:45-49, 1992.

el-Hage, S. and Singh, S.M. Temporal expression of genes encoding free radical-metabolizing enzymes is associated with higher mRNA levels during in utero development in mice. *Dev Genet* 11:149-159, 1990.

Erdos, G., Lee, Y.J., Cho, J.M. and Corry, P.M. Heat-induced bfgf gene-expression in the absence of heat-shock element correlates with enhanced ap-1 binding-activity. *Journal Of Cellular Physiology* 164:404-413, 1995.

Evans, M.J. and Kaufman, M.H. Establishment in culture of pluripotential cells from mouse embryos. *Nature* 292:154-156, 1981.

Evans, M.J. and Martin, G.R. *The differentiation of clonal teratocarcinoma cell cultures in vitro.*, 1975. pp. 237-250.

Ewen, M.E., Oliver, C.J., Sluss, H.K., Miller, S.J. and Peeper, D.S. p53-dependent repression of CDK4 translation in TGF-beta-induced G1 cell-cycle arrest. *Genes Dev* 9:204-217, 1995.

Fadok, V.A., Voelker, D.R., Campbell, P.A., Cohen, J.J., Bratton, D.L. and Henson, P.M. Exposure of phosphatidylserine on the surface of apoptotic lymphocytes triggers specific recognition and removal by macrophages. *J Immunol* 148:2207-2216, 1992.

Fernandes, R.S. and Cotter, T.G. Apoptosis or necrosis: intracellular levels of glutathione influence mode of cell death. *Biochem Pharmacol* 48:675-681, 1994.

Fernandez-Checa, J., Kaplowitz, N. and Garcia-Ruiz, C. Transport in mitochondria: defence against TNF-induced oxidative stress and alcohol-induced defect. *Am J Physiol* 273:G7-G171997.

Fiel, R., Brocard, J., mascrez, B., Lemeur, M., metzger, D. and Chambon, P. Ligand-activated site-specific recombination in mice. *Proc Natl Acad Sci U S A* 93:10887-10890, 1996.

Fields, S. and Jang, S.K. Presence of a potent transcription activating sequence in the p53 protein. *Science* 249:1046-1049, 1990.

Flood, D.G., Reaume, A.G., Gruner, J.A., et al. Hindlimb motor neurons require Cu/Zn superoxide dismutase for maintenance of neuromuscular junctions. *Am J Pathol* 155:663-672, 1999.

Floreani, M., Petrone, M., Debetto, P. and Palatini, P. A comparison between different methods for the determination of reduced and oxidized glutathione in mammalian tissues. *Free Radic Res* 26:449-455, 1997.

Folger, K.R., Thomas, K. and Capecchi, M.R. Efficient correction of mismatched bases in plasmid heteroduplexes injected into cultured mammalian cell nuclei. *Mol Cell Biol* 5:70-74, 1985a.

Folger, K.R., Thomas, K. and Capecchi, M.R. Nonreciprocal exchanges of information between DNA duplexes coinjected into mammalian cell nuclei. *Mol Cell Biol* 5:59-69, 1985b.

Folger, K.R., Wong, E.A., Wahl, G. and Capecchi, M.R. Patterns of integration of DNA microinjected into cultured mammalian cells: evidence for homologous recombination between injected plasmid DNA molecules. *Mol Cell Biol* 2:1372-1387, 1982.

Ford, J.M. and Hanawalt, P.C. Li-Fraumeni syndrome fibroblasts homozygous for p53 mutations are deficient in global DNA repair but exhibit normal transcription-coupled repair and enhanced UV resistance. *Proc Natl Acad Sci U S A* 92:8876-8880, 1995.

Ford, J.M. and Hanawalt, P.C. Expression of wild-type p53 is required for efficient global genomic nucleotide excision repair in UV-irradiated human fibroblasts. *J Biol Chem* 272:28073-28080, 1997.

Frade, J.M. and Michaelidis, T.M. Origin of eukaryotic programmed cell death: a consequence of aerobic metabolism? *Bioessays* 19:827-832, 1997.

Frenkel, J., Sherman, D., Fein, A., et al. Accentuated apoptosis in normally developing p53 knockout mouse embryos following genotoxic stress. *Oncogene* 18:2901-2907, 1999.

Frey, B. and Suppmann, B. Demonstration of the Expand TM PCR system's greater fidelity ang higher yields with a lacl-based fidelity assay. *Biochemica* 2:8-9, 1995.

Friedlander, P., Haupt, Y., Prives, C. and Oren, M. A mutant p53 that discriminates between p53-responsive genes cannot induce apoptosis. *Mol Cell Biol* 16:4961-4971, 1996.

Fucci, L., Oliver, C.N., Coon, M.J. and Stadtman, E.R. Inactivation of key metabolic enzymes by mixed-function oxidation reactions: possible implication in protein turnover and ageing. *Proc Natl Acad Sci U S A* 80:1521-1525, 1983.

Fuchs, S.Y., Adler, V., Buschmann, T., et al. JNK targets p53 ubiquitination and degradation in nonstressed cells. *Genes Dev* 12:2658-2663, 1998a.

Fuchs, S.Y., Adler, V., Pincus, M.R. and Ronai, Z. MEKK1/JNK signaling stabilizes and activates p53. *Proc Natl Acad Sci U S A* 95:10541-10546, 1998b.

Fukasawa, K., Choi, T., Kuriyama, R., Rulong, S. and Vande Woude, G. Abnormal centrosome proliferation in the absence of p53. *Science* 271:1744-1747, 1996.

Gaiddon, C., Moorthy, N.C. and Prives, C. Ref-1 regulates the transactivation and pro-apoptotic functions of p53 in vivo. *EMBO J* 18:5609-5621, 1999.

Galloway, D.C., Blake, D.G. and McLellan, L.I. Regulation of gamma-glutamylcysteine synthetase regulatory subunit (GLCLR) gene expression: identification of the major transcriptional start site in HT29 cells. *Biochim Biophys Acta* 1446:47-56, 1999.

Galloway, D.C., Blake, D.G., Shepherd, A.G. and McLellan, L.I. Regulation of human gamma-glutamylcysteine synthetase: co-ordinate induction of the catalytic and regulatory subunits in HepG2 cells. *Biochem J* 328:99-104, 1997.

Galloway, D.C. and McLellan, L.I. Inducible expression of the gamma-glutamylcysteine synthetase light subunit by t-butylhydroquinone in HepG2 cells is not dependent on an antioxidant-responsive element. *Biochem J* 336 (Pt 3):535-539, 1998.

Galter, D., Mihm, S. and Droge, W. Distinct effects of glutathione disulphide on the nuclear transcription factor kappa B and the activator protein-1. *Eur J Biochem* 221:639-648, 1994.

Gant, T.W., Rao, D.N., Mason, R.P. and Cohen, G.M. Redox cycling and sulphydryl arylation; their relative importance in the mechanism of quinone cytotoxicity to isolated hepatocytes. *Chem Biol Interact* 65:157-173, 1988.

Garcia-Martinez, V., Macias, D., Ganan, Y., et al. Internucleosomal DNA fragmentation and programmed cell death (apoptosis) in the interdigital tissue of the embryonic chick leg bud. *J Cell Sci* 106 (Pt 1):201-208, 1993.

Garcia-Ruiz, C., Colell, A., Morales, A., Kaplowitz, N. and Fernandez-Checa, J.C. Role of oxidative stress generated from the mitochondrial electron transport chain and mitochondrial glutathione status in loss of mitochondrial function and activation of transcription factor nuclear factor-kappa B: studies with isolated mitochondria and rat hepatocytes. *Mol Pharmacol* 48:825-834, 1995.

Gardiner, C.S. and Reed, D.J. Status of glutathione during oxidant-induced oxidative stress in the preimplantation mouse embryo. *Biol Reprod* 51:1307-1314, 1994.

Gardiner, C.S. and Reed, D.J. Glutathione redox cycle-driven recovery of reduced glutathione after oxidation by tertiary-butyl hydroperoxide in preimplantation mouse embryos. *Arch Biochem Biophys* 321:6-12, 1995a.

Gardiner, C.S. and Reed, D.J. Synthesis of glutathione in the preimplantation mouse embryo. *Arch Biochem Biophys* 318:30-36, 1995b.

Gardiner, C.S., Salmen, J.J., Brandt, C.J. and Stover, S.K. Glutathione is present in reproductive tract secretions and improves development of mouse embryos after chemically induced glutathione depletion. *Biol Reprod* 59:431-436, 1998.

Gerlai, R. Gene-targeting studies of mammalian behavior: is it the mutation or the background genotype? *Trends Neurosci* 19:177-181, 1996.

Ghibelli, L., Fanelli, C., Rotilio, G., et al. Rescue of cells from apoptosis by inhibition of active GSH extrusion. *FASEB J* 12:479-486, 1998.

Ghoshal, K., Majumder, S., Li, Z., Bray, T.M. and Jacob, S.T. Transcriptional induction of metallothionein-I and -II genes in the livers of Cu,Zn-superoxide dismutase knockout mice. *Biochem Biophys Res Commun* 264:735-742, 1999.

Gilbert, S. *Development Biology*, Massachusetts:Sinauer Association, Sunderland, 1991. Ed.3rd pp. 193-197.

Ginsberg, D., Mechta, F., Yaniv, M. and Oren, M. Wild-type p53 can down-modulate the activity of various promoters. *Proc Natl Acad Sci U S A* 88:9979-9983, 1991.

Gipp, J.J., Bailey, H.H. and Mulcahy, R.T. Cloning and sequencing of the cdna for the light subunit of human liver gamma-glutamylcysteine synthetase and relative messenger-rna levels for heavy and light subunits in human normal-tissues. *Biochem Biophys Res Comm* 206:584-589, 1995.

Gipp, J.J., Chang, C. and Mulcahy, R.T. Cloning and nucleotide sequence of a full-length cDNA for human liver gamma-glutamylcysteine synthetase. *Biochem Biophys Res Commun* 185:29-35, 1992.

Glasser, S.W., Burhans, M.S., Eszterhas, S.K., Bruno, M.D. and Korfhagen, T.R. Human SP-C gene sequences that confer lung epithelium-specific expression in transgenic mice. *Am J Physiol Lung Cell Mol Physiol* 278:L933-L9452000.

Glasser, S.W., Korfhagen, T.R., Wert, S.E., et al. Genetic element from human surfactant protein SP-C gene confers bronchiolar-alveolar cell specificity in transgenic mice. *Am J Physiol* 261:L349-L3561991.

Godley, L.A., Kopp, J.B., Eckhaus, M., Paglino, J.J., Owens, J. and Varmus, H.E. Wild-type p53 transgenic mice exhibit altered differentiation of the ureteric bud and possess small kidneys. *Genes Dev* 10:836-850, 1996.

Goldstein, S. Replicative senescence: the human fibroblast comes of age. *Science* 249:1129-1133, 1990.

Gomi, A., Masuzawa, T., Ishikawa, T. and Kuo, M.T. Posttranscriptional regulation of MRP/GS-X pump and gamma- glutamylcysteine synthetase expression by 1-(4-amino-2-methyl-5- pyrimidinyl) methyl-3-(2-chloroethyl)-3-nitrosourea and by cycloheximide in human glioma cells. *Biochem Biophys Res Comm* 239:51-56, 1997a.

Gomi, A., Shinoda, S., Masuzawa, T., Ishikawa, T. and Kuo, M.T. Transient induction of the MRP/GS-X pump and gamma-glutamylcysteine synthetase by 1-(4-amino-2-methyl-5-pyrimidinyl) methyl-3-(2- chloroethyl)-3-nitrosourea in human glioma cells. *Cancer Research* 57:5292-5299, 1997b.

Gonin, S., Diaz-Latoud, C., Richard, M.J., et al. p53/T-antigen complex disruption in T-antigen transformed NIH3T3 fibroblasts exposed to oxidative stress: correlation with the appearance of a Fas/APO-1/CD95 dependent, caspase independent, necrotic pathway. *Oncogene* 18:8011-8023, 1999.

Gonzalez-Flecha, B. and Demple, B. Genetic responses to free radicals. Homeostasis and gene control. *Ann N Y Acad Sci* 899:69-87, 2000.

Gopalakrishna, R., Chen, Z.H. and Gundimeda, U. Selenocompounds induce a redox modulation of protein kinase C in the cell, compartmentally independent from cytosolic glutathione: its role in inhibition of tumor promotion. *Arch Biochem Biophys* 348:37-48, 1997a.

Gopalakrishna, R., Gundimeda, U. and Chen, Z.H. Cancer-preventive selenocompounds induce a specific redox modification of cysteine-rich regions in Ca(2+)-dependent isoenzymes of protein kinase C. *Arch Biochem Biophys* 348:25-36, 1997b.

Gopalakrishna, R. and Jaken, S. Protein kinase C signaling and oxidative stress. *Free Radic Biol Med* 28:1349-1361, 2000.

Gorman, A, McCarthy, et al. Morphological assessment of apoptosis. In: *Techniques in apoptosis. A user's guide.*, edited by Cotter, TG, Martin and SJ. London: Portland Press, 1996, p. 1-20.

Gorman, S.D. and Cristofalo, V.J. Reinitiation of cellular DNA synthesis in BrdU-selected nondividing senescent WI-38 cells by simian virus 40 infection. *J Cell Physiol* 125:122-126, 1985.

Gostissa, M., Hengstermann, A., Fogal, V., et al. Activation of p53 by conjugation to the ubiquitin-like protein SUMO-1. *EMBO J* 18:6462-6471, 1999.

Griffith, O.W. Biologic and pharmacologic regulation of mammalian glutathione synthesis. *Free Radic Biol Med* 27:922-935, 1999.

Griffith, O.W. and Meister, A. Potent and specific inhibition of glutathione synthesis by buthionine sulfoximine (S-n-butyl homocysteine sulfoximine). *J Biol Chem* 254:7558-7560, 1979.

Griffith, O.W. and Mulcahy, R.T. The enzymes of glutathione synthesis: gamma-glutamylcysteine synthetase. *Adv Enzymol Relat Areas Mol Biol* 73:209-209, 1999.

Gu, W. and Roeder, R.G. Activation of p53 sequence-specific DNA binding by acetylation of the p53 C-terminal domain. *Cell* 90:595-606, 1997.

Guillouf, C., Rosselli, F., Krishnaraju, K., Moustacchi, E., Hoffman, B. and Liebermann, D.A. p53 involvement in control of G2 exit of the cell cycle: role in DNA damage-induced apoptosis. *Oncogene* 10:2263-2270, 1995.

Guyton, K.Z., Liu, Y.S., Gorospe, M., Xu, Q.B. and Holbrook, N.J. Activation of mitogen-activated protein kinase by H2O2 - Role in cell survival following oxidant injury. *Journal Of Biological Chemistry* 271:4138-4142, 1996.

Hainaut, P., Hall, A. and Milner, J. Analysis of p53 quaternary structure in relation to sequence-specific DNA binding. *Oncogene* 9:299-303, 1994.

Hainaut, P. and Milner, J. A structural role for metal ions in the \"wild-type conformation of the tumor suppressor protein p53. *Cancer Res* 53:1739-1742, 1993a.

Hainaut, P. and Milner, J. Redox modulation of p53 conformation and sequence-specific DNA binding in vitro. *Cancer Res* 53:4469-4473, 1993b.

Hall, A.G. Review: The role of glutathione in the regulation of apoptosis. *Eur J Clin Invest* 29:238-245, 1999.

Hall, E.J., Astor, M., Bedford, J., et al. Basic radiobiology. *Am J Clin Oncol* 11:220-252, 1988.

Hall, P.A. and Lane, D.P. Tumor suppressors: a developing role for p53? *Curr Biol* 7:R144-R1471997.

Halliwell, B. Antioxidants in human health and disease. *Annual Review Of Nutrition* 16:33-50, 1996.

Halliwell, B., Gutteridge, J.M. and Cross, C.E. Free radicals, antioxidants, and human disease: where are we now? *J Lab Clin Med* 119:598-620, 1992.

Hansen, M.B., Nielsen, S.E. and Berg, K. Re-examination and further development of a precise and rapid dye method for measuring cell growth/cell kill. *J Immunol Methods* 119:203-210, 1989.

Hara, E., Tsurui, H., Shinozaki, A., Nakada, S. and Oda, K. Cooperative effect of antisense-Rb and antisense-p53 oligomers on the extension of life span in human diploid fibroblasts, TIG-1. *Biochem Biophys Res Commun* 179:528-534, 1991.

Harper, J.W., Adami, G.R., Wei, N., Keyomarsi, K. and Elledge, S.J. The p21 Cdk-interacting protein Cip1 is a potent inhibitor of G1 cyclin-dependent kinases. *Cell* 75:805-816, 1993.

Harrod, K.S., Hermiston, T.W., Trapnell, B.C., Wold, W.S. and Whitsett, J.A. Lung-specific expression of adenovirus E3-14.7K in transgenic mice attenuates adenoviral vector-mediated lung inflammation and enhances transgene expression. *Hum Gene Ther* 9:1885-1898, 1998.

Harvey, M., Sands, A.T., Weiss, R.S., et al. In vitro growth characteristics of embryo fibroblasts isolated from p53-deficient mice. *Oncogene* 8:2457-2467, 1993.

Hasty, P., Rivera-Perez, J. and Bradley, A. The length of homology required for gene targeting in embryonic stem cells. *Mol Cell Biol* 11:5586-5591, 1991a.

Hasty, P., Rivera-Perez, J., Chang, C. and Bradley, A. Target frequency and integration pattern for insertion and replacement vectors in embryonic stem cells. *Mol Cell Biol* 11:4509-4517, 1991b.

Haupt, Y., Barak, Y. and Oren, M. Cell type-specific inhibition of p53-mediated apoptosis by mdm2. *EMBO J* 15:1596-1606, 1996.

Haupt, Y., Maya, R., Kazaz, A. and Oren, M. Mdm2 promotes the rapid degradation of p53. *Nature* 387:296-299, 1997.

Haupt, Y., Rowan, S., Shaulian, E., Vousden, K.H. and Oren, M. Induction of apoptosis in HeLa cells by trans-activation-deficient p53. *Genes Dev* 9:2170-2183, 1995.

Hayashi, T., Ueno, Y. and Okamoto, T. Oxidoreductive regulation of nuclear factor kappa B. Involvement of a cellular reducing catalyst thioredoxin. *J Biol Chem* 268:11380-11388, 1993.

Hayes, J.D. and McLellan, L.I. Glutathione and glutathione-dependent enzymes represent a co-ordinately regulated defence against oxidative stress. *Free Radic Res* 31:273-300, 1999.

Hayflick, L. and Moorhead, P. The serial cultivation of human diploid cell strains. *Exp.Cell Res.* 25:6211961.

Hayflick, L. Aging under glass. *Mutat Res* 256:69-80, 1991.

He, Z., Brinton, B.T., Greenblatt, J., Hassell, J.A. and Ingles, C.J. The transactivator proteins VP16 and GAL4 bind replication factor A. *Cell* 73:1223-1232, 1993.

Heffetz, D., Bushkin, I., Dror, R. and Zick, Y. The insulinomimetic agents H2O2 and vanadate stimulate protein tyrosine phosphorylation in intact cells. *J Biol Chem* 265:2896-2902, 1990.

Henderson, C.J., Smith, A.G., Ure, J., Brown, K., Bacon, E.J. and Wolf, C.R. Increased skin tumorigenesis in mice lacking pi class glutathione S-transferases. *Proc Natl Acad Sci U S A* 95:5275-5280, 1998.

Henle, E.S. and Linn, S. Formation, prevention, and repair of DNA damage by iron/hydrogen peroxide. *J Biol Chem* 272:19095-19098, 1997.

Hermeking, H., Lengauer, C., Polyak, K., et al. 14-3-3 sigma is a p53-regulated inhibitor of G2/M progression. *Mol Cell* 1:3-11, 1997.

Herrlich, P. and Bohmer, F.D. Redox regulation of signal transduction in mammalian cells. *Biochem Pharmacol* 59:35-41, 2000.

Ho, Y.S., Magnenat, J.L., Bronson, R.T., et al. Mice deficient in cellular glutathione peroxidase develop normally and show no increased sensitivity to hyperoxia. *J Biol Chem* 272:16644-16651, 1997.

Hockenbery, D.M., Oltvai, Z.N., Yin, X.M., Milliman, C.L. and Korsmeyer, S.J. Bcl-2 functions in an antioxidant pathway to prevent apoptosis. *Cell* 75:241-251, 1993.

Hofmann, K., Bucher, P. and Tschopp, J. The CARD domain: a new apoptotic signalling motif. *Trends Biochem Sci* 22:155-156, 1997.

Hogan BR, Beddington F, Costantini and Lacy E. *Manipulating the Mouse Embryo*, Cold Spring Harbour, NY:Cold Spring Harbour Laboratory Press, 1994.

Hollstein, M., Rice, K., Greenblatt, M.S., et al. Database of p53 gene somatic mutations in human tumors and cell lines. *Nucleic Acids Res* 22:3551-3555, 1994.

Hollstein, M., Shomer, B., Greenblatt, M., et al. Somatic point mutations in the p53 gene of human tumors and cell lines: updated compilation. *Nucleic Acids Res* 24:141-146, 1996.

Honda, R. and Yasuda, H. Association of p19(ARF) with Mdm2 inhibits ubiquitin ligase activity of Mdm2 for tumor suppressor p53. *EMBO J* 18:22-27, 1999.

Hooper, M., Hardy, K., Handyside, A., Hunter, S. and Monk, M. HPRT-deficient (Lesch-Nyhan) mouse embryos derived from germline colonization by cultured cells. *Nature* 326:292-295, 1987a.

Hooper, M., Hardy, K., Handyside, A., Hunter, S. and Monk, M. HPRT-deficient (Lesch-Nyhan) mouse embryos derived from germline colonization by cultured cells. *Nature* 326:292-295, 1987b.

Hopwood, D. and Levison, D.A. Atrophy and apoptosis in the cyclical human endometrium. *J Pathol* 119:159-166, 1976.

Horikoshi, N., Usheva, A., Chen, J., Levine, A.J., Weinmann, R. and Shenk, T. Two domains of p53 interact with the TATA-binding protein, and the adenovirus 13S E1A protein disrupts the association, relieving p53-mediated transcriptional repression. *Mol Cell Biol* 15:227-234, 1995.

Hoyle, G.W., Li, J., Finkelstein, J.B., et al. Emphysematous lesions, inflammation, and fibrosis in the lungs of transgenic mice overexpressing platelet-derived growth factor. *Am J Pathol* 154:1763-1775, 1999.

Huang, C.S., Anderson, M.E. and Meister, A. Amino-acid-sequence and function of the light subunit of rat-kidney gamma-glutamylcysteine synthetase. *J Biol Chem* 268:20578-20583, 1993a.

Huang, C.S., Chang, L.S., Anderson, M.E. and Meister, A. Catalytic and regulatory properties of the heavy subunit of rat- kidney gamma-glutamylcysteine synthetase. *J Biol Chem* 268:19675-19680, 1993b.

Hubbard, R.C., Ogushi, F., Fells, G.A., et al. Oxidants spontaneously released by alveolar macrophages of cigarette smokers can inactivate the active site of alpha 1-antitrypsin, rendering it ineffective as an inhibitor of neutrophil elastase. *J Clin Invest* 80:1289-1295, 1987.

Hupp, T.R. and Lane, D.P. Two distinct signaling pathways activate the latent DNA binding function of p53 in a casein kinase II-independent manner. *J Biol Chem* 270:18165-18174, 1995.

Hupp, T. and Lane, D. Allosteric activation of latent p53 tetramers. *Current Biology* 4:865-875, 1994.

Ide, T., Tsuji, Y., Ishibashi, S. and Mitsui, Y. Reinitiation of host DNA synthesis in senescent human diploid cells by infection with Simian virus 40. *Exp Cell Res* 143:343-349, 1983.

Imagawa, M., Osada, S., Okuda, A. and Muramatsu, M. Silencer binding proteins function on multiple cis-elements in the glutathione transferase P gene. *Nucleic Acids Res* 19:5-10, 1991.

Inbar, O. and Kupiec, M. Homology search and choice of homologous partner during mitotic recombination. *Mol Cell Biol* 19:4134-4142, 1999.

Ishibashi, M., Akazawa, S., Sakamaki, H., et al. Oxygen-induced embryopathy and the significance of glutathione- dependent antioxidant system in the rat embryo during early organogenesis. *Free Radic Biol Med* 22:447-454, 1996.

Ishikawa, T., Bao, J.J., Yamane, Y., et al. Coordinated induction of mrp/gs-x pump and gamma-glutamylcysteine synthetase by heavy-metals in human leukemia-cells. *J Biol Chem* 271:14981-14988, 1996.

Ishizaki, K., Ejima, Y., Matsunaga, T., et al. Increased UV-induced SCEs but normal repair of DNA damage in p53-deficient mouse cells. *Int J Cancer* 58:254-257, 1994.

Israeli, D., Tessler, E., Haupt, Y., et al. A novel p53-inducible gene, PAG608, encodes a nuclear zinc finger protein whose overexpression promotes apoptosis. *EMBO J* 16:4384-4392, 1997.

Itoh, G., Tamura, J., Suzuki, M., et al. DNA fragmentation of human infarcted myocardial cells demonstrated by the nick end labeling method and DNA agarose gel electrophoresis. *Am J Pathol* 146:1325-1331, 1995.

Iwanaga, M., Mori, K., Iida, T., et al. Nuclear factor kappa B dependent induction of gamma glutamylcysteine synthetase by ionizing radiation in T98G human glioblastoma cells. *Free Radic Biol Med* 24:1256-1268, 1998.

Iwata-Ichikawa, E., Kondo, Y., Miyazaki, I., Asanuma, M. and Ogawa, N. Glial cells protect neurons against oxidative stress via transcriptional up-regulation of the glutathione synthesis. *J Neurochem* 72:2334-2344, 1999.

Jackson, M.W. and Berberich, S.J. MdmX protects p53 from Mdm2-mediated degradation. *Mol Cell Biol* 20:1001-1007, 2000.

Jaenisch, R. Transgenic animals. *Science* 240:1468-1474, 1988.

Jamal, S. and Ziff, E.B. Raf phosphorylates p53 in vitro and potentiates p53-dependent transcriptional transactivation in vivo. *Oncogene* 10:2095-2101, 1995.

Janus, F., Albrechtsen, N., Dornreiter, I., Wiesmnller, L., Grosse, F. and Deppert, W. The dual role model for p53 in maintaining genomic integrity. *Cell Mol Life Sci* 12-27, 1999.

Jayaraman, L., Murthy, K.G., Zhu, C., Curran, T., Xanthoudakis, S. and Prives, C. Identification of redox/repair protein Ref-1 as a potent activator of p53. *Genes Dev* 11:558-570, 1997.

Jenkins, J.R., Chumakov, P., Addison, C., Sturzbecher, H.W. and Wade-Evans, A. Two distinct regions of the murine p53 primary amino acid sequence are implicated in stable complex formation with simian virus 40 T antigen. *J Virol* 62:3903-3906, 1988.

Jeyapaul, J. and Jaiswal, A.K. Nrf2 and c-Jun regulation of antioxidant response element (ARE)-mediated expression and induction of gamma-glutamylcysteine synthetase heavy subunit gene. *Biochem Pharmacol* 59:1433-1439, 2000.

Jiang, S., Wu, M.W., Sternberg, P. and Jones, D.P. Fas mediates apoptosis and oxidant-induced cell death in cultured hRPE cells. *Invest Ophthalmol Vis Sci* 41:645-655, 2000.

Johnson, T.M., Yu, Z.X., Ferrans, V.J., Lowenstein, R.A. and Finkel, T. Reactive oxygen species are downstream mediators of p53-dependent apoptosis. *Proc Natl Acad Sci U S A* 93:11848-11852, 1996.

Jones, S.N., Roe, A.E., Donehower, L.A. and Bradley, A. Rescue of embryonic lethality in Mdm2-deficient mice by absence of p53. *Nature* 378:206-208, 1995.

Jordan, A. and Reichard, P. Ribonucleotide reductases. *Annu Rev Biochem* 67:71-98, 1998.

Jost, C.A., Marin, M.C. and Kaelin, W.G.J. p73 is a simian [correction of human] p53-related protein that can induce apoptosis. *Nature* 389:191-194, 1997.

Jurisicova, A., Latham, K.E., Casper, R.F. and Varmuza, S.L. Expression and regulation of genes associated with cell death during murine preimplantation embryo development. *Mol Reprod Dev* 51:243-253, 1998a.

Jurisicova, A., Rogers, I., Fasciani, A., Casper, R.F. and Varmuza, S. Effect of maternal age and conditions of fertilization on programmed cell death during murine preimplantation embryo development. *Mol Hum Reprod* 4:139-145, 1998b.

Jurisicova, A., Varmuza, S. and Casper, R.F. Programmed cell death and human embryo fragmentation. *Mol Hum Reprod* 2:93-98, 1996.

Jurkiewicz, B.A. and Buettner, G.R. Ultraviolet light-induced free radical formation in skin: an electron paramagnetic resonance study. *Photochem Photobiol* 59:1-4, 1994.

Juven, T., Barak, Y., Zauberman, A., George, D.L. and Oren, M. Wild type p53 can mediate sequence-specific transactivation of an internal promoter within the mdm2 gene. *Oncogene* 8:3411-3416, 1993.

Kaelin, W.G.J. The emerging p53 gene family. *J Natl Cancer Inst* 91:594-598, 1999.

Kaghad, M., Bonnet, H., Yang, A., et al. Monoallelically expressed gene related to p53 at 1p36, a region frequently deleted in neuroblastoma and other human cancers. *Cell* 90:809-819, 1997.

Kane, D.J., Sarafian, T.A., Anton, R., et al. Bcl-2 inhibition of neural death: decreased generation of reactive oxygen species. *Science* 262:1274-1277, 1993.

Kastan, M.B., Zhan, Q., el-Deiry, W.S., et al. A mammalian cell cycle checkpoint pathway utilizing p53 and GADD45 is defective in ataxia-telangiectasia. *Cell* 71:587-597, 1992.

Kernohan, N.M., Hupp, T.R. and Lane, D.P. Modification of an N-terminal regulatory domain of T antigen restores p53-T antigen complex formation in the absence of an essential metal ion cofactor. *J Biol Chem* 271:4954-4960, 1996.

Kerr, J.F. Shrinkage necrosis: a distinct mode of cellular death. *J Pathol* 105:13-20, 1971.

Kerr, J.F., Wyllie, A.H. and Currie, A.R. Apoptosis: a basic biological phenomenon with wide-ranging implications in tissue kinetics. *Br J Cancer* 26:239-257, 1972.

Khalak, R., Huyck, H.L. and Pryhuber, G.S. Antagonistic effects of pyrrolidine dithiocarbamate and N-acetyl-L-cysteine on surfactant protein A and B mRNAs. *Exp Lung Res* 25:479-493, 1999.

Kimball, R.E. Oxygen toxicity: augmentation of antioxiant defense mechanisms in the lung. *American Journal Of Physiology* 230 (5):1425-1431, 1976.

Kitteringham, N.R., Powell, H., Clement, Y.N., et al. Hepatocellular response to chemical stress in CD-1 mice: induction of early genes and gamma-glutamylcysteine synthetase. *Hepatology* 32:321-333, 2000.

Klassen, C.D. *Casarett and Doull's Toxicology: the basic Science of poisons*, 5th edition, McGraw-Hill, 1996.

Kluck, R.M., Bossy-Wetzel, E., Green, D.R. and Newmeyer, D.D. The release of cytochrome c from mitochondria: a primary site for Bcl-2 regulation of apoptosis. *Science* 275:1132-1136, 1997.

Knebel, A., Rahmsdorf, H.J., Ullrich, A. and Herrlich, P. Dephosphorylation of receptor tyrosine kinases as target of regulation by radiation, oxidants or alkylating agents. *EMBO J* 15:5314-5325, 1996.

Ko, L.J. and Prives, C. p53: puzzle and paradigm. *Genes Dev* 10:1054-1072, 1996.

Kojima, S., Matsuki, O., Nomura, T., et al. Induction of mRNAs for glutathione synthesis-related proteins in mouse liver by low doses of gamma-rays. *Biochim Biophys Acta* 1381:312-318, 1998a.

Kojima, S., Matsuki, O., Nomura, T., Kubodera, A. and Yamaoka, K. Elevation of mouse liver glutathione level by low-dose gamma-ray irradiation and its effect on CCl4-induced liver damage. *Anticancer Research* 18:2471-2476, 1998b.

Konishi, T., Kagan, V., Matsugo, S. and Packer, L. UV induces oxy- and chromanoxyl free radicals in microsomes by a new photosensitive organic hydroperoxide, N,N'-bis(2-hydroperoxy-2-methoxyethyl)- 1,4,5,8-naphtalene-tetra-carboxylic-diimide. *Biochem Biophys Res Commun* 175:129-133, 1991.

Kotoh, S., Naito, S., Yokomizo, T., Kohno, K., Kuwano, M. and Kumazawa, J. Enhanced expression of gamma-glutamylcysteine synthetase and glutathione S-transferase genes in cisplatin-resistant bladder cancer cells with multidrug resistance phenotype. *Journal Of Urology* 157:1054-1058, 1997.

Kroemer, G. The proto-oncogene Bcl-2 and its role in regulating apoptosis [published erratum appears in Nat Med 1997 Aug;3(8):934]. *Nat Med* 3:614-620, 1997.

Kroemer, G., Petit, P., Zamzami, N., Vayssiere, J.L. and Mignotte, B. The biochemistry of programmed cell death. *FASEB J* 9:1277-1287, 1995.

Kroemer, G., Zamzami, N. and Susin, S.A. Mitochondrial control of apoptosis. *Immunol Today* 18:44-51, 1997.

Kubbutat, M.H., Jones, S.N. and Vousden, K.H. Regulation of p53 stability by Mdm2. *Nature* 387:299-303, 1997.

Kucherlapati, R.S., Eves, E.M., Song, K.Y., Morse, B.S. and Smithies, O. Homologous recombination between plasmids in mammalian cells can be enhanced by treatment of input DNA. *Proc Natl Acad Sci U S A* 81:3153-3157, 1984.

Kumar, T.R., Wiseman, A.L., Kala, G., Kala, S.V., Matzuk, M.M. and Lieberman, M.W. Reproductive defects in gamma-glutamyl transpeptidase-deficient mice. *Endocrinology* 141:4270-4277, 2000.

Kuo, M.T., Bao, J.J., Curley, S.A., Ikeguchi, M., Johnston, D.A. and Ishikawa, T. Frequent coordinated overexpression of the mrp/gs-x pump and gamma-glutamylcysteine synthetase genes in human colorectal cancers. *Cancer Research* 56:3642-3644, 1996a.

Kuo, M.T., Bao, J.J., Curley, S.A., Ikeguchi, M., Johnston, D.A. and Ishikawa, T. Frequent coordinated overexpression of the MRP/GS-X pump and gamma-glutamylcysteine synthetase genes in human colorectal cancers. *Cancer Res* 56:3642-3644, 1996b.

Kuo, M.T., Bao, J.J., Furuichi, M., et al. Frequent coexpression of MRP/GS-X pump and gamma-glutamylcysteine synthetase mRNA in drug-resistant cells, untreated tumor cells, and normal mouse tissues. *Biochemical Pharmacology* 55:605-615, 1998.

Kurata, S. Selective activation of p38 MAPK cascade and mitotic arrest caused by low level oxidative stress. *J Biol Chem* 275:23413-23416, 2000.

Kyle, M.E., Nakae, D., Sakaida, S., Serroni, A. and Farber, J.L. Protein thiol depletion and the killing of cultured hepatocytes by hydrogen peroxide. *Biochem Pharmacol* 38:3797-3805, 1989.

Laird, P.W., Zijderveld, A., Linders, K., Rudnicki, M.A., Jaenisch, R. and Berns, A. Simplified mammalian DNA isolation procedure. *Nucleic Acids Res* 19:4293-4293, 1991.

Lane, D.P. Cancer. p53, guardian of the genome. *Nature* 358:15-16, 1992.

Lanni, J.S. and Jacks, T. Characterization of the p53-dependent postmitotic checkpoint following spindle disruption. *Mol Cell Biol* 18:1055-1064, 1998.

Laster, S.M., Wood, J.G. and Gooding, L.R. Tumor necrosis factor can induce both apoptic and necrotic forms of cell lysis. *J Immunol* 141:2629-2634, 1988.

Lazebnik, Y.A., Cole, S., Cooke, C.A., Nelson, W.G. and Earnshaw, W.C. Nuclear events of apoptosis in vitro in cell-free mitotic extracts: a model system for analysis of the active phase of apoptosis. *J Cell Biol* 123:7-22, 1993.

Lee, F.Y., Vessey, A., Rofstad, E., Siemann, D.W. and Sutherland, R.M. Heterogeneity of glutathione content in human ovarian cancer. *Cancer Res* 49:5244-5248, 1989.

Lee, J.M. Inhibition of p53-dependent apoptosis by the KIT tyrosine kinase: regulation of mitochondrial permeability transition and reactive oxygen species generation. *Oncogene* 17:1653-1662, 1998.

Lee, S., Elenbaas, B., Levine, A. and Griffith, J. p53 and its 14kDa domain recognise primary DNA damage in the form of insertion/deletion mismatches. *Cell* 81:1013-1020, 1995.

Lemaire, C., Andreau, K., Souvannavong, V. and Adam, A. Inhibition of caspase activity induces a switch from apoptosis to necrosis. *FEBS Lett* 425:266-270, 1998.

Lennon, S.V., Martin, S.J. and Cotter, T.G. Dose-dependent induction of apoptosis in human tumour cell lines by widely diverging stimuli. *Cell Prolif* 24:203-214, 1991.

Leveillard, T., Andera, L., Bissonnette, N., et al. Functional interactions between p53 and the TFIIH complex are affected by tumour-associated mutations. *EMBO J* 15:1615-1624, 1996.

Levine, A.J. p53, the cellular gatekeeper for growth and division. *Cell* 88:323-331, 1997.

Levine, R.L., Oliver, C.N., Fulks, R.M. and Stadtman, E.R. Turnover of bacterial glutamine synthetase: oxidative inactivation precedes proteolysis. *Proc Natl Acad Sci U S A* 78:2120-2124, 1981.

Levonen, A.L., Lapatto, R., Saksela, M. and Raivio, K.O. Expression of gamma-glutamylcysteine synthetase during development. *Pediatr Res* 47:266-270, 2000.

Li, R. and Botchan, M.R. The acidic transcriptional activation domains of VP16 and p53 bind the cellular replication protein A and stimulate in vitro BPV-1 DNA replication. *Cell* 73:1207-1221, 1993.

Li, T., Shi, M.M. and Forman, H.J. Correlated transcriptional induction of the regulatory and catalytic subunits of gamma-glutamylcysteine synthetase (gamma-GCS) In rat lung epithelial l2 cells exposed to 2,3-dimethoxy-1,4-naphthoquinone (DMNQ). *FASEB J* 10:2047-2047, 1996.

Li, Y., Huang, T.T., Carlson, E.J., et al. Dilated cardiomyopathy and neonatal lethality in mutant mice lacking manganese superoxide dismutase. *Nat Genet* 11:376-381, 1995.

Li, Y. and Jaiswal, A.K. Human antioxidant-response-element-mediated regulation of type-1 NAD(P)H-quinone oxidoreductase gene-expression - effect of sulfhydryl modifying agents. *Eur J Biochem* 226:31-39, 1994.

Li, Z.Y., Suzuki, Y., Kurozumi, M., Shen, H.Q. and Duan, C.X. Removal of a dimeric form of surfactant protein C from mouse lungs: its acceleration by reduction. *J Appl Physiol* 84:471-478, 1998.

Lieberman, M.W., Wiseman, A.L., Shi, Z.Z., et al. Growth retardation and cysteine deficiency in gamma-glutamyl transpeptidase-deficient mice. *Proc Natl Acad Sci U S A* 93:7923-7926, 1996.

Liu, L. and Wells, P.G. DNA oxidation as a potential molecular mechanism mediating drug-induced birth defects: phenytoin and structurally related teratogens initiate the formation of 8-hydroxy-2'-deoxyguanosine in vitro and in vivo in murine maternal hepatic and embryonic tissues. *Free Radic Biol Med* 19:639-648, 1995.

Liu, R.M., Gao, L., Choi, J. and Forman, H.J. gamma-glutamylcysteine synthetase: mRNA stabilization and independent subunit transcription by 4-hydroxy-2-nonenal. *Am J Physiol* 275:L861-L8691998.

Liu, R.M., Hu, H.P., Robison, T.W. and Forman, H.J. Increased gamma-glutamylcysteine synthetase and gamma-glutamyl- transpeptidase activities enhance resistance of rat lung epithelial l2 cells to quinone toxicity. *American Journal Of Respiratory Cell And Molecular Biology* 14:192-197, 1996.

Liu, Y.S., Guyton, K.Z., Gorospe, M., Xu, Q.B., Lee, J.C. and Holbrook, N.J. Differential activation of ERK, JNK/SAPK and p38/CSBP/RK map kinase family members during the cellular response to arsenite. *Free Radical Biology And Medicine* 21:771-781, 1996.

Livy, D.J. and Wahlsten, D. Tests of genetic allelism between four inbred mouse strains with absent corpus callosum. *J Hered* 82:459-464, 1991.

Lobe, C.G. and Nagy, A. Conditional genome alteration in mice. *Bioessays* 20:200-208, 1998.

Lohrum, M.A. and Vousden, K.H. Regulation and activation of p53 and its family members. *Cell Death Differ* 6:1162-1168, 1999.

Lopes, S., Jurisicova, A., Sun, J.G. and Casper, R.F. Reactive oxygen species: potential cause for DNA fragmentation in human spermatozoa. *Hum Reprod* 13:896-900, 1998.

Lotem, J., Peled-Kamar, M., Groner, Y. and Sachs, L. Cellular oxidative stress and the control of apoptosis by wild-type p53, cytotoxic compounds, and cytokines. *Proc Natl Acad Sci U S A* 93:9166-9171, 1996.

Louis, J.M., McFarland, V.W., May, P. and Mora, P.T. The phosphoprotein p53 is down-regulated post-transcriptionally during embryogenesis in vertebrates. *Biochim Biophys Acta* 950:395-402, 1988.

Loven, D.P. A role for reduced oxygen species in heat induced cell killing and the induction of thermotolerance. *Med Hypotheses* 26:39-50, 1988.

Lowe, S.W., Bodis, S., McClatchey, A., et al. p53 status and the efficacy of cancer therapy in vivo. *Science* 266:807-810, 1994.

Lowe, S.W., Schmitt, E.M., Smith, S.W., Osborne, B.A. and Jacks, T. p53 is required for radiation-induced apoptosis in mouse thymocytes. *Nature* 362:847-849, 1993.

Lu, H. and Levine, A.J. Human TAFII31 protein is a transcriptional coactivator of the p53 protein. *Proc Natl Acad Sci U S A* 92:5154-5158, 1995.

Lu, S.C., Bao, Y., Huang, Z.Z., Sarthy, V.P. and Kannan, R. Regulation of gamma-glutamylcysteine synthetase subunit gene expression in retinal Muller cells by oxidative stress. *Invest Ophthalmol Vis Sci* 40:1776-1782, 1999.

Ludwig, R.L., Bates, S. and Vousden, K.H. Differential activation of target cellular promoters by p53 mutants with impaired apoptotic function. *Mol Cell Biol* 16:4952-4960, 1996.

Luna, L. *Manual of histologic staining methods of the Armed Forces*, New York:McGraw-Hill, 1968. pp. 111-111.

Lutz, R.J. Role of the BH3 (Bcl-2 homology 3) domain in the regulation of apoptosis and Bcl-2-related proteins. *Biochem Soc Trans* 28:51-56, 2000.

MacNee, W. and Rahman, I. Oxidants antioxidants in idiopathic pulmonary fibrosis. *Thorax* 50:S-S1995.

Manna, S.K., Kuo, M.T. and Aggarwal, B.B. Overexpression of gamma-glutamylcysteine synthetase suppresses tumor necrosis factor-induced apoptosis and activation of nuclear transcription factor-kappa B and activator protein-1. *Oncogene* 18:4371-4382, 1999.

Marnett, L.J. Oxyradicals and DNA damage. *Carcinogenesis* 21:361-370, 2000.

Martensson, J., Jain, A., Stole, E., Frayer, W., Auld, P.A. and Meister, A. Inhibition of glutathione synthesis in the newborn rat: a model for endogenously produced oxidative stress. *Proc Natl Acad Sci U S A* 88:9360-9364, 1991.

Matsui, Y., Zsebo, K. and Hogan, B.L. Derivation of pluripotential embryonic stem cells from murine primordial germ cells in culture. *Cell* 70:841-847, 1992.

Matsuzawa, S., Takayama, S., Froesch, B.A., Zapata, J.M. and Reed, J.C. p53-inducible human homologue of Drosophila seven in absentia (Siah) inhibits cell growth: suppression by BAG-1. *EMBO J* 17:2736-2747, 1998.

Matzuk, M.M., Dionne, L., Guo, Q., Kumar, T.R. and Lebovitz, R.M. Ovarian function in superoxide dismutase 1 and 2 knockout mice. *Endocrinology* 139:4008-4011, 1998.

May, P. and May, E. Twenty years of p53 research: structural and functional aspects of the p53 protein. *Oncogene* 18:7621-7636, 1999.

Mayo, L.D., Turchi, J.J. and Berberich, S.J. Mdm-2 phosphorylation by DNA-dependent protein kinase prevents interaction with p53. *Cancer Res* 57:5013-5016, 1997.

McCarthy, S.A., Symonds, H.S. and Van Dyke, T. Regulation of apoptosis in transgenic mice by simian virus 40 T antigen-mediated inactivation of p53. *Proc Natl Acad Sci U S A* 91:3979-3983, 1994.

McConkey, D.J., Hartzell, P., Nicotera, P., Wyllie, A.H. and Orrenius, S. Stimulation of endogenous endonuclease activity in hepatocytes exposed to oxidative stress. *Toxicol Lett* 42:123-130, 1988.

Mehlen, P., Kretz-Remy, C., Preville, X. and Arrigo, A.P. Human hsp27, Drosophila hsp27 and human alphaB-crystallin expression-mediated increase in glutathione is essential for the protective activity of these proteins against TNFalpha-induced cell death. *EMBO J* 15:2695-2706, 1996.

Meira, L.B., Cheo, D.L., Hammer, R.E., Burns, D.K., Reis, A. and Friedberg, E.C. Genetic interaction between HAP1/REF-1 and p53 [letter]. *Nat Genet* 17:145-145, 1997.

Meplan, C., Richard, M.J. and Hainaut, P. Redox signalling and transition metals in the control of the p53 pathway. *Biochem Pharmacol* 59:25-33, 2000.

Merritt, A.J., Allen, T.D., Potten, C.S. and Hickman, J.A. Apoptosis in small intestinal epithelial from p53-null mice: evidence for a delayed, p53-independent G2/M-associated cell death after gamma-irradiation. *Oncogene* 14:2759-2766, 1997.

Messmer, U.K., Ankarcrona, M., Nicotera, P. and Brune, B. p53 expression in nitric oxide-induced apoptosis. *FEBS Lett* 355:23-26, 1994.

Michiels, C. and Remacle, J. Use of the inhibition of enzymatic antioxidant systems in order to evaluate their physiological importance. *Eur J Biochem* 177:435-441, 1988.

Miller, J. and Heath, W. Self-ignorance in the peripheral T-cell pool. *Immun.Rev.* 133:1501993.

Miller, S.D., Moses, K., Jayaraman, L. and Prives, C. Complex formation between p53 and replication protein A inhibits the sequence-specific DNA binding of p53 and is regulated by single-stranded DNA. *Mol Cell Biol* 17:2194-2201, 1997.

Mills, A.A., Zheng, B., Wang, X.J., Vogel, H., Roop, D.R. and Bradley, A. p63 is a p53 homologue required for limb and epidermal morphogenesis. *Nature* 398:708-713, 1999.

Milner, J., Medcalf, E.A. and Cook, A.C. Tumor suppressor p53: analysis of wild-type and mutant p53 complexes. *Mol Cell Biol* 11:12-19, 1991.

Minetti, M., Mallozzi, C., Distasi, A.M. and Pietraforte, D. Bilirubin is an effective antioxidant of peroxynitrite-medicated protein oxidation in human blood plasma. *Arch Biochem Biophys* 352:165-174, 1998.

Ming, X.F., Kaiser, M. and Moroni, C. c-jun N-terminal kinase is involved in AUUUA-mediated interleukin-3 mRNA turnover in mast cells. *EMBO J* 17:6039-6048, 1998.

Miyashita, T. and Reed, J.C. Tumor suppressor p53 is a direct transcriptional activator of the human bax gene. *Cell* 80:293-299, 1995.

Mo Bi Tec. Lambda-PS eukaryotic genomic libraries. (LPS0496). 1996. Wagenstein 5, Gottingen, Germany. (GENERIC)
Ref Type: Catalog

Moellering, D., McAndrew, J., Patel, R.P., et al. Nitric oxide-dependent induction of glutathione synthesis through increased expression of gamma-glutamylcysteine synthetase. *Arch Biochem Biophys* 358:74-82, 1998.

Mohr, L.R. and Trounson, A.O. Comparative ultrastructure of hatched human, mouse and bovine blastocysts. *J Reprod Fertil* 66:499-504, 1982.

Moinova, H.R. and Mulcahy, R.T. An electrophile responsive element (EpRE) regulates p-naphthoflavone induction of the human gamma-glutamylcysteine synthetase regulatory subunit gene - Constitutive expression is mediated by an adjacent AP- 1 site. *J Biol Chem* 273:14683-14689, 1998.

Moinova, H.R. and Mulcahy, R.T. Up-regulation of the human gamma-glutamylcysteine synthetase regulatory subunit gene involves binding of Nrf-2 to an electrophile responsive element. *Biochem Biophys Res Comm* 261:661-668, 1999.

Momand, J., Zambetti, G.P., Olson, D.C., George, D. and Levine, A.J. The mdm-2 oncogene product forms a complex with the p53 protein and inhibits p53-mediated transactivation. *Cell* 69:1237-1245, 1992.

Morales, A., GarciaRuiz, C., Miranda, M., et al. Tumor necrosis factor increases hepatocellular glutathione by transcriptional regulation of the heavy subunit chain of gamma- glutamylcysteine synthetase. *J Biol Chem* 272:30371-30379, 1997a.

Morales, A., Miranda, M. and Fernandezcheca, J.C. Transcriptional regulation of gamma-glutamylcysteine synthetase (gamma-GCS) by TNF: Molecular functional role of NF-kappa B. *Hepatology* 26:249-249, 1997b.

Morales, A., Miranda, M., Sanchezreyes, A., Colell, A., Biete, A. and Fernandezcheca, J.C. Transcriptional regulation of the heavy subunit chain of gamma- glutamylcysteine synthetase by ionizing radiation. *FEBS Lett* 427:15-20, 1998.

Moreau, J.F., Donaldson, D.D., Bennett, F., Witek-Giannotti, J., Clark, S.C. and Wong, G.G. Leukaemia inhibitory factor is identical to the myeloid growth factor human interleukin for DA cells. *Nature* 336:690-692, 1988.

Mori, C., Nakamura, N., Okamoto, Y., Osawa, M. and Shiota, K. Cytochemical identification of programmed cell death in the fusing fetal mouse palate by specific labelling of DNA fragmentation. *Anat Embryol (Berl)* 190:21-28, 1994.

Morita, Y. and Tilly, J.L. Oocyte apoptosis: like sand through an hourglass. *Dev Biol* 213:1-17, 1999.

Morris, G.F., Hoyle, G.W., Athas, G.B., et al. Lung-specific expression in mice of a dominant negative mutant form of the p53 tumor suppressor protein. *J La State Med Soc* 150:179-185, 1998.

Morris, G., Bischoff, J. and Mathews, M. Transcriptional activation of the human proliferating cell nuclear antigen promoter by p53. *Proc Natl Acad Sci U S A* 93:895-899, 1996.

Morris, P.E. and Bernard, G.R. Significance of glutathione in lung-disease and implications for therapy. *Am J Med Sci* 307:119-127, 1994.

Morrison, D., Rahman, I., Lannan, S. and MacNee, W. Epithelial permeability, inflammation, and oxidant stress in the air spaces of smokers. *Am J Respir Crit Care Med* 159:473-479, 1999.

Mortensen, R.M., Conner, D.A., Chao, S., Geisterfer-Lowrance, A.A. and Seidman, J.G. Production of homozygous mutant ES cells with a single targeting construct. *Mol Cell Biol* 12:2391-2395, 1992.

Mulcahy, R.T. and Gipp, J.J. Identification of a putative antioxidant response element in the 5'- flanking region of the human gamma-glutamylcysteine synthetase heavy subunit gene. *Biochem Biophys Res Comm* 209:227-233, 1995.

Mulcahy, R.T., Wartman, M.A., Bailey, H.H. and Gipp, J.J. Constitutive and beta-naphthoflavone-induced expression of the human gamma-glutamylcysteine synthetase heavy subunit gene is regulated by a distal antioxidant response element/TRE sequence. *J Biol Chem* 272:7445-7454, 1997.

Mulier, B., Rahman, I., Watchorn, T., Donaldson, K., MacNee, W. and Jeffery, P.K. Hydrogen peroxide-induced epithelial injury: the protective role of intracellular nonprotein thiols (NPSH). *Eur Respir J* 11:384-391, 1998.

Muller, S., Berger, M., Lehembre, F., Seeler, J.S., Haupt, Y. and Dejean, A. c-Jun and p53 activity is modulated by SUMO-1 modification. *J Biol Chem* 275:13321-13329, 2000.

Muller, T. Expression of c-fos in quiescent swiss 3t3 cells exposed to aqueous cigarette-smoke fractions. *Cancer Research* 55:1927-1932, 1995.

Mummenbrauer, T., Janus, F., Muller, B., Wiesmuller, L., Deppert, W. and Grosse, F. p53 Protein exhibits 3'-to-5' exonuclease activity. *Cell* 85:1089-1099, 1996.

Munoz, E., Zubiaga, A.M. and Huber, B.T. Interleukin-1 induces c-fos and c-jun gene expression in T helper type II cells through different signal transmission pathways. *Eur J Immunol* 22:2101-2106, 1992.

Murphy, K.C., Campellone, K.G. and Poteete, A.R. PCR-mediated gene replacement in Escherichia coli. *Gene* 246:321-330, 2000.

Mustacich, D. and Powis, G. Thioredoxin reductase. *Biochem J* 346 Pt 1:1-8, 2000.

Muyrers, J.P., Zhang, Y., Testa, G. and Stewart, A.F. Rapid modification of bacterial artificial chromosomes by ET-recombination. *Nucleic Acids Res* 27:1555-1557, 1999.

Nakamura, T., Pichel, J.G., Williams-Simons, L. and Westphal, H. An apoptotic defect in lens differentiation caused by human p53 is rescued by a mutant allele. *Proc Natl Acad Sci U S A* 92:6142-6146, 1995.

Nakano, K., Balint, E., Ashcroft, M. and Vousden, K.H. A ribonucleotide reductase gene is a transcriptional target of p53 and p73. *Oncogene* 19:4283-4289, 2000.

Nasr-Esfahani, M.H. and Johnson, M.H. Quantitative analysis of cellular glutathione in early preimplantation mouse embryos developing in vivo and in vitro. *Hum Reprod* 7:1281-1290, 1992.

Nehls, M., Messerle, M., Sirulnik, A., Smith, A.J. and Boehm, T. Two large insert vectors, lambda PS and lambda KO, facilitate rapid mapping and targeted disruption of mammalian genes. *Biotechniques* 17:770-775, 1994.

Nelson, W.G. and Kastan, M.B. DNA strand breaks: the DNA template alterations that trigger p53-dependent DNA damage response pathways. *Mol Cell Biol* 14:1815-1823, 1994.

Neuzil, J., Gebicki, J.M. and Stocker, R. Radical-induced chain oxidation of proteins and its inhibition by chain-breaking antioxidants. *Biochem J* 293 (Pt 3):601-606, 1993.

New, D.A., Coppola, P.T. and Cockroft, D.L. Comparison of growth in vitro and in vivo of post-implantation rat embryos. *J Embryol Exp Morphol* 36:133-144, 1976.

Ngo, E.O., Nutter, L.M., Sura, T. and Gutierrez, P.L. Induction of p53 by the concerted actions of aziridine and quinone moieties of diaziquone. *Chem Res Toxicol* 11:360-368, 1998.

Nicol, C.J., Harrison, M.L., Laposa, R.R., Gimelshtein, I.L. and Wells, P.G. A teratologic suppressor role for p53 in benzo[a]pyrene-treated transgenic p53-deficient mice. *Nat Genet* 10:181-187, 1995.

Nicotera, P., Hinds, T.R., Nelson, S.D. and Vincenzi, F.F. Differential effects of arylating and oxidizing analogs of N-acetyl-p-benzoquinoneimine on red blood cell membrane proteins. *Arch Biochem Biophys* 283:200-205, 1990a.

Nicotera, P., Hinds, T.R., Nelson, S.D. and Vincenzi, F.F. Differential effects of arylating and oxidizing analogs of N-acetyl-p-benzoquinoneimine on red blood cell membrane proteins. *Arch Biochem Biophys* 283:200-205, 1990b.

Nishikawa, Y., Carr, B.I., Wang, M., et al. Growth inhibition of hepatoma cells induced by vitamin K and its analogs. *J Biol Chem* 270:28304-28310, 1995.

Nishimori, H., Shiratsuchi, T., Urano, T., et al. A novel brain-specific p53-target gene, BAI1, containing thrombospondin type 1 repeats inhibits experimental angiogenesis. *Oncogene* 15:2145-2150, 1997.

Nobel, C.S., Burgess, D.H., Zhivotovsky, B., Burkitt, M.J., Orrenius, S. and Slater, A.F. Mechanism of dithiocarbamate inhibition of apoptosis: thiol oxidation by

dithiocarbamate disulfides directly inhibits processing of the caspase-3 proenzyme. *Chem Res Toxicol* 10:636-643, 1997.

Norimura, T., Nomoto, S., Katsuki, M., Gondo, Y. and Kondo, S. p53-dependent apoptosis suppresses radiation-induced teratogenesis. *Nat Med* 2:577-580, 1996.

Novak, A., Goyal, N. and Gronostajski, R.M. Four conserved cysteine residues are required for the DNA binding activity of nuclear factor I. *J Biol Chem* 267:12986-12990, 1992.

O'Connor, PM., Wassermann, K., Sarang, K., Magrath, I., Bohr, VA. and Kohn, KW. Relationship between DNA crosslinks, cell cycle, and apoptosis in Burkitt's lymphoma cell lines differing in sensitivity to nitrogen mustard. *Cancer Res* 51:6550-6557, 1990.

O'Reilly, O. DNA damage and cell cycle checkpoints in hyperoxic lung injury: braking to facilitate repair. *Am J Physiol* 281:L291-L3052001.

Oberosler, P., Hloch, P., Ramsperger, U. and Stahl, H. p53-catalyzed annealing of complementary single-stranded nucleic acids. *EMBO J* 12:2389-2396, 1993.

Ochi, T. Hydrogen-peroxide increases the activity of gamma-glutamylcysteine synthetase in cultured chinese-hamster v79 cells. *Archives Of Toxicology* 70:96-103, 1995.

Offer, H., Wolkowicz, R., Matas, D., Blumenstein, S., Livneh, Z. and Rotter, V. Direct involvement of p53 in the base excision repair pathway of the DNA repair machinery. *FEBS Lett* 450:197-204, 1999.

Ohyama, K., Chung, C.H., Chen, E., et al. p53 influences mice skeletal development. *J Craniofac Genet Dev Biol* 17:161-171, 1997.

Okamoto, K. and Beach, D. Cyclin G is a transcriptional target of the p53 tumor suppressor protein. *EMBO J* 13:4816-4822, 1994.

Okazawa, H., Shimizu, J., Kamei, M., Imafuku, I., Hamada, H. and Kanazawa, I. Bcl-2 Inhibits Retinoic Acid-induced Apoptosis during the Neural Differentiation of Embryonal Stem Cells. *J Cell Biol* 132:955-968, 1996.

Okorokov, A.L., Ponchel, F. and Milner, J. Induced N- and C-terminal cleavage of p53: a core fragment of p53, generated by interaction with damaged DNA, promotes cleavage of the N-terminus of full-length p53, whereas ssDNA induces C-terminal cleavage of p53. *EMBO J* 16:6008-6017, 1997.

Oliner, J.D., Kinzler, K.W., Meltzer, P.S., George, D.L. and Vogelstein, B. Amplification of a gene encoding a p53-associated protein in human sarcomas. *Nature* 358:80-83, 1992.

Oliner, J.D., Pietenpol, J.A., Thiagalingam, S., Gyuris, J., Kinzler, K.W. and Vogelstein, B. Oncoprotein MDM2 conceals the activation domain of tumour suppressor p53. *Nature* 362:857-860, 1993.

Oltvai, Z.N., Milliman, C.L. and Korsmeyer, S.J. Bcl-2 heterodimerizes in vivo with a conserved homolog, Bax, that accelerates programmed cell death. *Cell* 74:609-619, 1993.

Orlowski, M. and Meister, A. Isolation of highly purified gamma-glutamylcysteine synthetase from rat kidney. *Biochemistry* 10:372-380, 1971.

Orr-Weaver, T.L., Szostak, J.W. and Rothstein, R.J. Yeast transformation: a model system for the study of recombination. *Proc Natl Acad Sci U S A* 78:6354-6358, 1981.

Osada, S., Ikeda, T., Xu, M., Nishihara, T. and Imagawa, M. Identification of the transcriptional repression domain of nuclear factor 1-A. *Biochem Biophys Res Comm* 238:744-747, 1997.

Osifchin, N.E., Jiang, D., Ohtani-Fujita, N., et al. Identification of a p53 binding site in the human retinoblastoma susceptibility gene promoter. *J Biol Chem* 269:6383-6389, 1994.

Owen-Schaub, L.B., Zhang, W., Cusack, J.C., et al. Wild-type human p53 and a temperature-sensitive mutant induce Fas/APO-1 expression. *Mol Cell Biol* 15:3032-3040, 1995.

Pani, G., Bedogni, B., Anzevino, R., et al. Deregulated manganese superoxide dismutase expression and resistance to oxidative injury in p53-deficient cells. *Cancer Res* 60:4654-4660, 2000.

Park, E.M., Park, Y.M. and Gwak, Y.S. Oxidative damage in tissues of rats exposed to cigarette smoke. *Free Radic Biol Med* 25:79-86, 1998.

Parks, D., Bolinger, R. and Mann, K. Redox state regulates binding of p53 to sequence-specific DNA, but not to non-specific or mismatched DNA. *Nucleic Acids Res* 25:1289-1295, 1997.

Pavletich, N.P., Chambers, K.A. and Pabo, C.O. The DNA-binding domain of p53 contains the four conserved regions and the major mutation hot spots. *Genes Dev* 7:2556-2564, 1993.

Pesch, J., Brehm, U., Staib, C. and Grummt, F. Repression of interleukin-2 and interleukin-4 promoters by tumor suppressor protein p53. *J Interferon Cytokine Res* 16:595-600, 1996.

Petronilli, V., Costantini, P., Scorrano, L., Colonna, R., Passamonti, S. and Bernardi, P. The voltage sensor of the mitochondrial permeability transition pore is tuned by the oxidation-reduction state of vicinal thiols. Increase of the gating potential by oxidants and its reversal by reducing agents. *J Biol Chem* 269:16638-16642, 1994.

Piacentini, M., Annicchiarico-Petruzzelli, M., Oliverio, S., Piredda, L., Biedler, J.L. and Melino, E. Phenotype-specific \"tissue transglutaminase regulation in human neuroblastoma cells in response to retinoic acid: correlation with cell death by apoptosis. *Int J Cancer* 52:271-278, 1992.

Pierce, R.H., Campbell, J.S., Stephenson, A.B., et al. Disruption of redox homeostasis in tumor necrosis factor-induced apoptosis in a murine hepatocyte cell line. *Am J Pathol* 157:221-236, 2000.

Podda, M., Traber, M.G., Weber, C., Yan, L.J. and Packer, L. UV-radiation depletes antioxidants and causes oxidative damage in a model of human skin. *Free Radic Biol Med* 24:55-65, 1998.

Poelmann, R.E., Mikawa, T. and Gittenberger, d. Neural crest cells in outflow tract septation of the embryonic chicken heart: differentiation and apoptosis. *Dev Dyn* 212:373-384, 1998.

Polyak, K., Xia, Y., Zweier, J.L., Kinzler, K.W. and Vogelstein, B. A model for p53-induced apoptosis. *Nature* 389:300-305, 1997.

Porter, N. Mechanisms for the autoxidation of polyunsaturated lipids. *Acc.Chem.Res.* 262-268, 1986.

Powis, G., Briehl, M. and Oblong, J. Redox signalling and the control of cell growth and death. *Pharmacol Ther* 68:149-173, 1995.

Powis, G., Svingen, B.A. and Appel, P. Quinone-stimulated superoxide formation by subcellular fractions, isolated hepatocytes, and other cells. *Mol Pharmacol* 20:387-394, 1981.

Pratt, R.M. and Greene, R.M. Inhibition of palatal epithelial cell death by altered protein synthesis. *Dev Biol* 54:135-145, 1976.

Prochaska, H.J. and Talalay, P. Regulatory mechanisms of monofunctional and bifunctional anticarcinogenic enzyme inducers in murine liver. *Cancer Res* 48:4776-4782, 1988.

Prost, S., Bellamy, C.O., Clarke, A.R., Wyllie, A.H. and Harrison, D.J. p53-independent DNA repair and cell cycle arrest in embryonic stem cells. *FEBS Lett* 425:499-504, 1998.

Pryor, W.A. Oxy-radicals and related species: their formation, lifetimes, and reactions. *Annu Rev Physiol* 48:657-667, 1986.

Pryor, W. and Davies, K. The radical view: Are you getting dotty? or Do you Know where your dots are? *Free Radic Biol Med* 14:1993.

Qiu, X.B., Schonthal, A.H. and Cadenas, E. Anticancer quinones induce pRb-preventable G2/M cell cycle arrest and apoptosis. *Free Radic Biol Med* 24:848-854, 1998.

Qiu, Y., Benet, L.Z. and Burlingame, A.L. Identification of the hepatic protein targets of reactive metabolites of acetaminophen in vivo in mice using two-dimensional gel electrophoresis and mass spectrometry. *J Biol Chem* 273:17940-17953, 1998.

Radjendirane, V., Joseph, P., Lee, Y.H., et al. Disruption of the DT diaphorase (NQO1) gene in mice leads to increased menadione toxicity. *J Biol Chem* 273:7382-7389, 1998.

Rahman, A., Mulier, B., Gilmour, P., et al. Oxidant-mediated lung epithelial cell tolerance: the role of intracellular glutathione and nuclear factor-kappaB. *Biochemical Pharmacology* 62:787-794, 2001.

Rahman, I., Antonicelli, F. and MacNee, W. Molecular mechanism of the regulation of glutathione synthesis by tumor necrosis factor-alpha and dexamethasone in human alveolar epithelial cells. *J Biol Chem* 274:5088-5096, 1999.

Rahman, I., Bel, A., Mulier, B., Donaldson, K. and MacNee, W. Differential regulation of glutathione by oxidants and dexamethasone in alveolar epithelial cells. *Am J Physiol* 19:L80-L861998.

Rahman, I., Bel, A., Mulier, B., et al. Transcriptional regulation of gamma-glutamylcysteine synthetase-heavy subunit by oxidants in human alveolar epithelial cells. *Biochem Biophys Res Commun* 229:832-837, 1996a.

Rahman, I., Bel, A., Mulier, B., et al. Transcriptional regulation of gamma-glutamylcysteine synthetase-heavy subunit by oxidants in human alveolar epithelial cells. *Biochem Biophys Res Comm* 229:832-837, 1996b.

Rahman, I., Li, X.Y., Donaldson, K., Harrison, D.J. and MacNee, W. Glutathione homeostasis in alveolar epithelial-cells in-vitro and lung in-vivo under oxidative stress. *Am J Physiol* 13:L-L1995.

Rahman, I. and MacNee, W. Oxidative stress and regulation of glutathione in lung inflammation. *Eur Respir J* 16:534-554, 2000.

Rahman, I., Skwarska, E., Henry, M., et al. Systemic and pulmonary oxidative stress in idiopathic pulmonary fibrosis. *Free Radic Biol Med* 27:60-68, 1999.

Rahman, I., Smith, C.D., Antonicelli, F. and MacNee, W. Characterisation of gamma-glutamylcysteine synthetase-heavy subunit promoter: a critical role for AP-1. *FEBS Lett* 427:129-133, 1998.

Rahman, I., Smith, C.D., Lawson, M.F., Harrison, D.J. and MacNee, W. Induction of gamma-glutamylcysteine synthetase by cigarette-smoke is associated with ap-1 in human alveolar epithelial-cells. *Febs Letters* 396:21-25, 1996.

Rainwater, R., Parks, D., Anderson, M., Tegtmeyer, P. and Mann, K. Role of cysteine residues in regulation of p53 function. *Mol Cell Biol* 15:3892-3903, 1995.

Rancourt, R.C., Keng, P.C., Helt, C.E. and Reilly, M.A. The role of p21(CIP1/WAF1) in growth of epithelial cells exposed to hyperoxia. *Am J Physiol Lung Cell Mol Physiol* 280:L617-L6262001.

Ratan, R.R., Murphy, T.H. and Baraban, J.M. Oxidative stress induces apoptosis in embryonic cortical neurons. *J Neurochem* 62:376-379, 1994.

Reaume, A.G., Elliott, J.L., Hoffman, E.K., et al. Motor neurons in Cu/Zn superoxide dismutase-deficient mice develop normally but exhibit enhanced cell death after axonal injury. *Nat Genet* 13:43-47, 1996.

Reid, L.L., Botta, D., Shao, J., Hudson, F.N. and Kavanagh, T.J. Molecular cloning and sequencing of the cDNA encoding mouse glutamate cysteine ligase regulatory subunit. *Biochem Biophys Acta* 1353:107-110, 1997.

Reiners, J.J.J., Mathieu, P., Okafor, C., Putt, D.A. and Lash, L.H. Depletion of cellular glutathione by conditions used for the passaging of adherent cultured cells. *Toxicol Lett* 115:153-163, 2000.

Reinke, V. and Lozano, G. The p53 targets mdm2 and Fas are not required as mediators of apoptosis in vivo. *Oncogene* 15:1527-1534, 1997.

Renzing, J., Hansen, S. and Lane, D.P. Oxidative stress is involved in the UV activation of p53. *J Cell Sci* 109 (Pt 5):1105-1112, 1996.

Rice, G.C., Bump, E.A., Shrieve, D.C., Lee, W. and Kovacs, M. Quantitative analysis of cellular glutathione by flow cytometry utilizing monochlorobimane: some applications to radiation and drug resistance in vitro and in vivo. *Cancer Res* 46:6105-6110, 1986.

Richman, P, and G. PhD Thesis. 81-81. 1975. Cornell University Medical College. (GENERIC)
Ref Type: Thesis/Dissertation

Rodriguez, M.S., Desterro, J.M., Lain, S., Midgley, C.A., Lane, D.P. and Hay, R.T. SUMO-1 modification activates the transcriptional response of p53. *EMBO J* 18:6455-6461, 1999.

Romerdahl, C.A., Stephens, L.C., Bucana, C. and Kripke, M.L. The role of ultraviolet radiation in the induction of melanocytic skin tumors in inbred mice. *Cancer Commun* 1:209-216, 1989.

Rooney, S.A., Young, S.L. and Mendelson, C.R. Molecular and cellular processing of lung surfactant. *FASEB J* 8:957-967, 1994.

Ross, D., Norbeck, K. and Moldeus, P. The generation and subsequent fate of glutathionyl radicals in biological systems. *J Biol Chem* 260:15028-15032, 1985.

Rossi, L., Moore, G.A., Orrenius, S. and O'Brien, P.J. Quinone toxicity in hepatocytes without oxidative stress. *Arch Biochem Biophys* 251:25-35, 1986.

Rotter, V., Schwartz, D., Almon, E., et al. Mice with reduced levels of p53 protein exhibit the testicular giant-cell degenerative syndrome. *Proc Natl Acad Sci U S A* 90:9075-9079, 1993.

Rouvier, E., Luciani, M.F. and Golstein, P. Fas involvement in Ca(2+)-independent T cell-mediated cytotoxicity. *J Exp Med* 177:195-200, 1993.

Royce, F.H., Van, W., Yin, J. and Plopper, C.G. Comparison of regional variability in lung-specific gene expression using a novel method for RNA isolation from lung subcompartments of rats and mice. *Am J Pathol* 148:1779-1786, 1996.

Ruaro, E.M., Collavin, L., Del Sal, G., et al. A proline-rich motif in p53 is required for transactivation-independent growth arrest as induced by Gas1. *Proc Natl Acad Sci U S A* 94:4675-4680, 1997.

Rubin, E.M. and Smith, D.J. Optimizing the mouse to sift sequence for function. *Trends Genet* 13:423-426, 1997.

Rushmore, T.H., Morton, M.R. and Pickett, C.B. The antioxidant responsive element. Activation by oxidative stress and identification of the DNA consensus sequence required for functional activity. *J Biol Chem* 266:11632-11639, 1991.

Russell, J., Wheldon, T.E. and Stanton, P. A radioresistant variant derived from a human neuroblastoma cell line is less prone to radiation-induced apoptosis. *Cancer Res* 55:4915-4921, 1995.

Russo, T., Zambrano, N., Esposito, F., et al. A p53-independent pathway for activation of WAF1/CIP1 expression following oxidative stress. *J Biol Chem* 270:29386-29391, 1995.

Sabapathy, K., Klemm, M., Jaenisch, R. and Wagner, E.F. Regulation of ES cell differentiation by functional and conformational modulation of p53. *EMBO J* 16:6217-6229, 1997.

Sabbatini, P., Lin, J., Levine, A.J. and White, E. Essential role for p53-mediated transcription in E1A-induced apoptosis. *Genes Dev* 9:2184-2192, 1995.

Sachs, L. and Lotem, J. Control of programmed cell death in normal and leukemic cells: new implications for therapy. *Blood* 82:15-21, 1993.

Sagara, Y., Dargusch, R., Chambers, D., Davis, J., Schubert, D. and Maher, P. Cellular mechanisms of resistance to chronic oxidative stress. *Free Radic Biol Med* 24:1375-1389, 1998.

Sah, V.P., Attardi, L.D., Mulligan, G.J., Williams, B.O., Bronson, R.T. and Jacks, T. A subset of p53-deficient embryos exhibit exencephaly. *Nat Genet* 10:175-180, 1995.

Sakaguchi, K., Herrera, J.E., Saito, S., et al. DNA damage activates p53 through a phosphorylation-acetylation cascade. *Genes Dev* 12:2831-2841, 1998.

Sakamaki, H., Akazawa, S., Ishibashi, M., et al. Significance of glutathione-dependent antioxidant system in diabetes-induced embryonic malformations. *Diabetes* 48:1138-1144, 1999.

Sakamuro, D., Sabbatini, P., White, E. and Prendergast, G.C. The polyproline region of p53 is required to activate apoptosis but not growth arrest. *Oncogene* 15:887-898, 1997.

Samali, A., Nordgren, H., Zhivotovsky, B., Peterson, E. and Orrenius, S. A comparative study of apoptosis and necrosis in HepG2 cells: oxidant-induced

caspase inactivation leads to necrosis. *Biochem Biophys Res Commun* 255:6-11, 1999.

Sands, A.T., Suraokar, M.B., Sanchez, A., Marth, J.E., Donehower, L.A. and Bradley, A. p53 deficiency does not affect the accumulation of point mutations in a transgene target. *Proc Natl Acad Sci U S A* 92:8517-8521, 1995.

Santhanam, U., Ray, A. and Sehgal, P.B. Repression of the interleukin 6 gene promoter by p53 and the retinoblastoma susceptibility gene product. *Proc Natl Acad Sci U S A* 88:7605-7609, 1991.

Saraste, A. Morphologic criteria and detection of apoptosis. *Herz* 24:189-195, 1999.

Saraste, A. and Pulkki, K. Morphologic and biochemical hallmarks of apoptosis. *Cardiovasc Res* 45:528-537, 2000.

Sata, N., Klonowski-Stumpe, H., Han, B., Haussinger, D. and Niederau, C. Menadione induces both necrosis and apoptosis in rat pancreatic acinar AR4-2J cells. *Free Radic Biol Med* 23:844-850, 1997.

Sattler, M., Liang, H., Nettesheim, D., et al. Structure of Bcl-xL-Bak peptide complex: recognition between regulators of apoptosis. *Science* 275:983-986, 1997.

Schauenstein, E. and Esterbauer, H. Formation and properties of reactive aldehydes. *Ciba Found Symp* 225-244, 1978.

Schmale, H. and Bamberger, C. A novel protein with strong homology to the tumor suppressor p53. *Oncogene* 15:1363-1367, 1997.

Schneider, E., Montenarh, M. and Wagner, P. Regulation of CAK kinase activity by p53. *Oncogene* 17:2733-2741, 1998.

Schnellmann, R.G., Monks, T.J., Mandel, L.J. and Lau, S.S. 2-Bromohydroquinone-induced toxicity to rabbit renal proximal tubules: the role of biotransformation, glutathione, and covalent binding. *Toxicol Appl Pharmacol* 99:19-27, 1989.

Schreck, R., Albermann, K. and Baeuerle, P.A. Nuclear factor kappa-b - an oxidative stress-responsive transcription factor of eukaryotic cells (A review). *Free Rad Res Comm* 17:221-237, 1992.

Schreck, R., Rieber, P. and Baeuerle, P.A. Reactive oxygen intermediates as apparently widely used messengers in the activation of the NF-kappa-b transcription factor and HIV-1. *EMBO J* 10:2247-2258, 1991.

Schroder, M. and Thorpe S. *Current Protocols in Molecular Biology*, 1987. pp. 6.0.3-6.2.3

Schultz, R. Regulation of zygotic gene activation in the mouse. *Bioessays* 15:5381993.

Schulze-Osthoff, K., Walczak, H., Droge, W. and Krammer, P.H. Cell nucleus and DNA fragmentation are not required for apoptosis. *J Cell Biol* 127:15-20, 1994.

Schwall, R.H., Robbins, K., Jardieu, P., Chang, L., Lai, C. and Terrell, T.G. Activin induces cell death in hepatocytes in vivo and in vitro. *Hepatology* 18:347-356, 1993.

Schwenk, F., Kuhn, R., Angrand, P.O., Rajewsky, K. and Stewart, A.F. Temporally and spatially regulated somatic mutagenesis in mice. *Nucleic Acids Res* 26:1427-1432, 1998.

Sekhar, K.R. and Freeman, M.L. Autophosphorylation inhibits the activity of gamma-glutamylcysteine synthetase. *J Enzyme Inhib* 14:323-330, 1999.

Sekhar, K.R., Long, M., Long, J., Xu, Z.Q., Summar, M.L. and Freeman, M.L. Alteration of transcriptional and post-transcriptional expression of gamma-

glutamylcysteine synthetase by diethyl maleate. *Radiation Research* 147:592-597, 1997a.

Sekhar, K.R., Meredith, M.J., Kerr, L.D., et al. Expression of glutathione and gamma-glutamylcysteine synthetase mRNA is jun dependent. *Biochem Biophys Res Comm* 234:588-593, 1997b.

Selivanova, G., Ryabchenko, L., Jansson, E., Iotsova, V. and Wiman, K.G. Reactivation of mutant p53 through interaction of a C-terminal peptide with the core domain. *Mol Cell Biol* 19:3395-3402, 1999.

Sethi, J.M. and Rochester, C.L. Smoking and chronic obstructive pulmonary disease. *Clin Chest Med* 21:67-86, viii, 2000.

Sharma, M. and Slocum, H.K. Prevention of quinone-mediated DNA arylation by antioxidants. *Biochem Biophys Res Commun* 262:769-774, 1999.

Shatrov, V.A., Ameyar, M., Bouquet, C., et al. Adenovirus-mediated wild-type-p53-gene expression sensitizes TNF-resistant tumor cells to TNF-induced cytotoxicity by altering the cellular redox state. *Int J Cancer* 85:93-97, 2000.

Shaulsky, G., Goldfinger, N., Ben-Ze'ev, A. and Rotter, V. Nuclear accumulation of p53 protein is mediated by several nuclear localization signals and plays a role in tumorigenesis. *Mol Cell Biol* 10:6565-6577, 1990.

Shaw, P., Bovey, R., Tardy, S., Sahli, R., Sordat, B. and Costa, J. Induction of apoptosis by wild-type p53 in a human colon tumor-derived cell line. *Proc Natl Acad Sci U S A* 89:4495-4499, 1992.

Shaw, P., Freeman, J., Bovey, R. and Iggo, R. Regulation of specific DNA binding by p53: evidence for a role for O-glycosylation and charged residues at the carboxy-terminus. *Oncogene* 12:921-930, 1996.

Shay, J.W., Pereira-Smith, O.M. and Wright, W.E. A role for both RB and p53 in the regulation of human cellular senescence. *Exp Cell Res* 196:33-39, 1991.

Shcherbakova, O.G., Lanzov, V.A., Ogawa, H. and Filatov, M.V. Overexpression of bacterial RecA protein stimulates homologous recombination in somatic mammalian cells. *Mutat Res* 459:65-71, 2000.

Shen, Y. and Shenk, T. Relief of p53-mediated transcriptional repression by the adenovirus E1B 19-kDa protein or the cellular Bcl-2 protein. *Proc Natl Acad Sci U S A* 91:8940-8944, 1994.

Shi, M., Iwamoto, T. and Forman, H.J. Quinone-induction of gamma-glutamylcysteine synthetase-activity and messenger-RNA in rat lung epithelial L2 cells. *FASEB J* 8:A-A1994.

Shi, M.M., Iwamoto, T. and Forman, H.J. gamma-Glutamylcysteine synthetase and GSH increase in quinone-induced oxidative stress in BPAEC. *Am J Physiol* 267:L414-L4211994a.

Shi, M.M., Kugelman, A., Iwamoto, T., Tian, L. and Forman, H.J. Quinone-induced oxidative stress elevates glutathione and induces gamma-glutamylcysteine synthetase-activity in rat lung epithelial L2 cells. *J Biol Chem* 269:26512-26517, 1994b.

Shi, Z.Z., Osei-Frimpong, J., Kala, G., et al. Glutathione synthesis is essential for mouse development but not for cell growth in culture. *Proc Natl Acad Sci U S A* 97:5101-5106, 2000.

Shieh, S.Y., Ikeda, M., Taya, Y. and Prives, C. DNA damage-induced phosphorylation of p53 alleviates inhibition by MDM2. *Cell* 91:325-334, 1997.

Shimizu, S., Eguchi, Y., Kosaka, H., Kamiike, W., Matsuda, H. and Tsujimoto, Y. Prevention of hypoxia-induced cell death by Bcl-2 and Bcl-xL. *Nature* 374:811-813, 1995.

Shimizu, T., Iwanaga, M., Yasunaga, A., et al. Protective role of glutathione synthesis on radiation-induced DNA damage in rabbit brain. *Cell Mol Neurobiol* 18:299-310, 1998.

Shrieve, D.C. and Bump, E.A. Heterogeneity of cellular glutathione among cells derived from a murine fibrosarcoma or a human renal cell carcinoma detected by flow cytometric analysis. *Unknown!* 2001.

Shvarts, A., Steegenga, W.T., Riteco, N., et al. MDMX: a novel p53-binding protein with some functional properties of MDM2. *EMBO J* 15:5349-5357, 1996.

Sian, J., Dexter, D.T., Cohen, G., Jenner, P.G. and Marsden, C.D. Comparison of HPLC and enzymatic recycling assays for the measurement of oxidized glutathione in rat brain. *J Pharm Pharmacol* 49:332-335, 1997.

Sierra-Rivera, E., Meredith, M.J., Summar, M.L., et al. Genes regulating glutathione concentrations in X-ray-transformed rat embryo fibroblasts: changes in gamma-glutamylcysteine synthetase and gamma-glutamyltranspeptidase expression. *Carcinogenesis* 15:1301-1307, 1994.

Simondsen, R.P. and Meister, A. Interaction of the d-isomer of gamma-methylene glutamate with an active-site thiol of gamma-glutamylcysteine synthetase. *J Biol Chem* 261:7134-7137, 1986.

Simpson EM, Linder CC, Sargent EE, Davisson MT, Mobraaten LE and Sharp JJ. Genetic variation among 129 substrains and its importance for targeted mutagenesis in mice. *Nature* 16:19-27, 1997.

Slebos, R.J., Lee, M.H., Plunkett, B.S., et al. p53-dependent G1 arrest involves pRB-related proteins and is disrupted by the human papillomavirus 16 E7 oncoprotein. *Proc Natl Acad Sci U S A* 91:5320-5324, 1994.

Slott, V.L. and Hales, B.F. Protection of rat embryos in culture against the embryotoxicity of acrolein using exogenous glutathione. *Biochem Pharmacol* 36:2187-2194, 1987.

Smith, A.G., Heath, J.K., Donaldson, D.D., et al. Inhibition of pluripotential embryonic stem cell differentiation by purified polypeptides. *Nature* 336:688-690, 1988.

Smith, J.R. and Lincoln, D.W. Aging of cells in culture. *Int Rev Cytol* 89:151-177, 1984.

Smith, J.R. and Pereira-Smith, O.M. Replicative senescence: implications for in vivo aging and tumor suppression. *Science* 273:63-67, 1996.

Smith, M.L., Chen, I.T., Zhan, Q., O'Connor, P.M. and Fornace, A.J.J. Involvement of the p53 tumor suppressor in repair of u.v.-type DNA damage. *Oncogene* 10:1053-1059, 1995.

Soltaninassab, S.R., Sekhar, K.R., Meredith, M.J. and Freeman, M.L. Multi-faceted regulation of gamma-glutamylcysteine synthetase. *J Cell Physiol* 182:163-170, 2000.

Soussi, T., Caron, d.F. and May, P. Structural aspects of the p53 protein in relation to gene evolution. *Oncogene* 5:945-952, 1990.

Stacey, A., Schnieke, A., McWhir, J., Cooper, J., Colman, A. and Melton, D.W. Use of double-replacement gene targeting to replace the murine alpha-lactalbumin gene

with its human counterpart in embryonic stem cells and mice. *Mol Cell Biol* 14:1009-1016, 1994.

Stadtman, E.R. Metal ion-catalyzed oxidation of proteins: biochemical mechanism and biological consequences. *Free Radic Biol Med* 9:315-325, 1990.

Stadtman, E.R. and Levine, R.L. Protein oxidation. *Ann N Y Acad Sci* 899:191-208, 2000.

Stahl, F. Meiotic recombination in yeast: coronation of the double-strand-break repair model. *Cell* 87:965-968, 1996.

Stenger, J.E., Mayr, G.A., Mann, K. and Tegtmeyer, P. Formation of stable p53 homotetramers and multiples of tetramers. *Mol Carcinog* 5:102-106, 1992.

Stewart, C.L., Gadi, I. and Bhatt, H. Stem cells from primordial germ cells can reenter the germ line. *Dev Biol* 161:626-628, 1994.

Stewart, N., Hicks, G.G., Paraskevas, F. and Mowat, M. Evidence for a second cell cycle block at G2/M by p53. *Oncogene* 10:109-115, 1995.

Stocker, R. and Peterhans, E. Antioxidant properties of conjugated bilirubin and biliverdin - biologically relevant scavenging of hypochlorous acid. *Free Rad Res Comm* 6:57-66, 1989.

Stone, V., Coleman, R. and Chipman, J.K. Comparison of the effects of redox cycling and arylating quinones on hepatobiliary function and glutathione homeostasis in rat hepatocyte couplets. *Toxicol Appl Pharmacol* 138:195-200, 1996.

Storz, G., Tartaglia, L.A., Farr, S.B. and Ames, B.N. Bacterial defenses against oxidative stress. *Trends Genet* 6:363-368, 1990.

Strange, R., Li, F., Saurer, S., Burkhardt, A. and Friis, R.R. Apoptotic cell death and tissue remodelling during mouse mammary gland involution. *Development* 115:49-58, 1992.

Strasser, A., Harris, A.W., Corcoran, L.M. and Cory, S. Bcl-2 expression promotes B- but not T-lymphoid development in SCID mice. *Nature* 368:457-460, 1994.

Su, B. and Karin, M. Mitogen-activated protein kinase cascades and regulation of gene expression. *Curr Opin Immunol* 8:402-411, 1996.

Subbaramaiah, K., Altorki, N., Chung, W.J., Mestre, J.R., Sampat, A. and Dannenberg, A.J. Inhibition of cyclooxygenase-2 gene expression by p53. *J Biol Chem* 274:10911-10915, 1999.

Sugrue, M.M., Shin, D.Y., Lee, S.W. and Aaronson, S.A. Wild-type p53 triggers a rapid senescence program in human tumor cells lacking functional p53. *Proc Natl Acad Sci U S A* 94:9648-9653, 1997.

Sun, W.M., Huang, Z.Z. and Lu, S.C. Regulation of gamma-glutamylcysteine synthetase by protein- phosphorylation. *Biochem J* 320:321-328, 1996.

Sun, Y., Bian, J., Wang, Y. and Jacobs, C. Activation of p53 transcriptional activity by 1,10-phenanthroline, a metal chelator and redox sensitive compound. *Oncogene* 14:385-393, 1997.

Susin, S.A., Lorenzo, H.K., Zamzami, N., et al. Molecular characterization of mitochondrial apoptosis-inducing factor. *Nature* 397:441-446, 1999.

Symonds, H., Krall, L., Remington, L., et al. p53-dependent apoptosis suppresses tumor growth and progression in vivo. *Cell* 78:703-711, 1994.

Szostak, J.W., Orr-Weaver, T.L., Rothstein, R.J. and Stahl, F.W. The double-strand-break repair model for recombination. *Cell* 33:25-35, 1983.

Takenaka, I., Morin, F., Seizinger, B.R. and Kley, N. Regulation of the sequence-specific DNA binding function of p53 by protein kinase C and protein phosphatases. *J Biol Chem* 270:5405-5411, 1995.

Tamura, T., Ishihara, M., Lamphier, M., et al. An IRF-1-dependent pathway of DNA damage-induced apoptosis in mitogen-activated T lymphocytes. *Nature* 376:596-599, 1995.

Tan, M., Li, S., Swaroop, M., Guan, K., Oberley, L.W. and Sun, Y. Transcriptional activation of the human glutathione peroxidase promoter by p53. *J Biol Chem* 274:12061-12066, 1999.

Tanaka, H., Arakawa, H., Yamaguchi, T., et al. A ribonucleotide reductase gene involved in a p53-dependent cell-cycle checkpoint for DNA damage. *Nature* 404:42-49, 2000.

Tanaka, S., Saito, K. and Reed, J.C. Structure-function analysis of the Bcl-2 oncoprotein. Addition of a heterologous transmembrane domain to portions of the Bcl-2 beta protein restores function as a regulator of cell survival. *J Biol Chem* 268:10920-10926, 1993.

Tanaka, T., Uchiumi, T., Kohno, K., et al. Glutathione homeostasis in human hepatic cells: overexpression of gamma-glutamylcysteine synthetase gene in cell lines resistant to buthionine sulfoximine, an inhibitor of glutathione synthesis. *Biochem Biophys Res Commun* 246:398-403, 1998.

Taper, H.S., Keyeux, A. and Roberfroid, M. Potentiation of radiotherapy by nontoxic pretreatment with combined vitamins C and K3 in mice bearing solid transplantable tumor. *Anticancer Res* 16:499-503, 1996.

Tapper, M.A., Sheedy, B.R., Hammermeister, D.E. and Schmieder, P.K. Depletion of cellular protein thiols as an indicator of arylation in isolated trout hepatocytes exposed to 1,4-benzoquinone. *Toxicol Sci* 55:327-334, 2000.

te Riele, H., Maandag, E.R., Clarke, A., Hooper, M. and Berns, A. Consecutive inactivation of both alleles of the pim-1 proto-oncogene by homologous recombination in embryonic stem cells. *Nature* 348:649-651, 1990.

te Riele, H., Maandag, E. and Berns, A. Highly efficient gene targeting in embryonic stem cells through homologous recombination with isogenic DNA constructs. *Proc Natl Acad Sci U S A* 89:5128-5132, 2000.

Thanislass, J., Raveendran, M. and Devaraj, H. Buthionine sulfoximine-induced glutathione depletion - its effect on antioxidants, lipid-peroxidation and calcium homeostasis in the lung. *Biochem Pharmacol* 50:229-234, 1995.

Thomas, J. and Sies, H. Protein S-thiolation and dethiolation. In: *The post-translational modification of proteins*, edited by Tuboi, S., Taniguchi, N. and Katunuma, N. Boca Raton: CRC press, 1991, p. 35-51.

Thomas, K.R. and Capecchi, M.R. Site-directed mutagenesis by gene targeting in mouse embryo-derived stem cells. *Cell* 51:503-512, 1987.

Thomas, K.R., Deng, C. and Capecchi, M.R. High-fidelity gene targeting in embryonic stem cells by using sequence replacement vectors. *Mol Cell Biol* 12:2919-2923, 1992.

Thomas, K.R., Folger, K.R. and Capecchi, M.R. High frequency targeting of genes to specific sites in the mammalian genome. *Cell* 44:419-428, 1986.

Thomas, M., Jain, S., Kumar, G.P. and Laloraya, M. A programmed oxyradical burst causes hatching of mouse blastocysts. *J Cell Sci* 110 (Pt 14):1597-1602, 1997.

Thomas, M., Massimi, P., Jenkins, J. and Banks, L. HPV-18 E6 mediated inhibition of p53 DNA binding activity is independent of E6 induced degradation. *Oncogene* 10:261-268, 1995.

Thompson, C.B. Apoptosis in the pathogenesis and treatment of disease. *Science* 267:1456-1462, 1995.

Thor, H., Smith, M.T., Hartzell, P., Bellomo, G., Jewell, S.A. and Orrenius, S. The metabolism of menadione (2-methyl-1,4-naphthoquinone) by isolated hepatocytes. A study of the implications of oxidative stress in intact cells. *J Biol Chem* 257:12419-12425, 1982.

Thut, C.J., Chen, J.L., Klemm, R. and Tjian, R. p53 transcriptional activation mediated by coactivators TAFII40 and TAFII60. *Science* 267:100-104, 1995.

Tien, M., Bucher, J.R. and Aust, S.D. Thiol-dependent lipid peroxidation. *Biochem Biophys Res Commun* 107:279-285, 1982.

Tietze, F. Enzymic method for quantitative determination of nanogram amounts of total and oxidized glutathione: applications to mammalian blood and other tissues. *Anal Biochem* 27:502-522, 1969.

Tomonari, A., Nishio, K., Kurokawa, H., et al. Identification of cis-acting DNA elements of the human gamma- glutamylcysteine synthetase heavy subunit gene. *Biochem Biophys Res Comm* 232:522-527, 1997a.

Tomonari, A., Nishio, K., Kurokawa, H., et al. Proximal 5'-flanking sequence of the human gamma-glutamylcysteine synthetase heavy subunit gene is involved in cisplatin-induced transcriptional up-regulation in a lung cancer cell line SBC-3. *Biochem Biophys Res Comm* 236:616-621, 1997b.

Torres, R.M. and Kuhn, R. *The Cologne Guide to Gene Targeting*, 1995. (UnPub)

Toussaint, O., Dumont, P., Dierick, J.F., et al. Stress-induced premature senescence. Essence of life, evolution, stress, and aging. *Ann N Y Acad Sci* 908:85-98, 2000.

Trocino, R.A., Akazawa, S., Ishibashi, M., et al. Significance of glutathione depletion and oxidative stress in early embryogenesis in glucose-induced rat embryo culture. *Diabetes* 44:992-998, 1995.

Tsuboi, S. Elevation of glutathione level in rat hepatocytes by hepatocyte growth factor via induction of gamma-glutamylcysteine synthetase. *J Biochem (Tokyo)* 126:815-820, 1999.

Tsuchiya, K., Mulcahy, R.T., Reid, L.L., Disteche, C.M. and Kavanagh, T.J. Mapping of the glutamate-cysteine ligase catalytic subunit gene (GLCLC) To human-chromosome 6p12 and mouse chromosome 9d-e and of the regulatory subunit gene (GLCLR) To human-chromosome 1p21-p22 and mouse chromosome 3h1-3. *Genomics* 30:630-632, 1995.

Tu, Z. and Anders, M.W. Expression and characterization of human glutamate-cysteine ligase. *Arch Biochem Biophys* 354:247-254, 1998a.

Tu, Z. and Anders, M.W. Identification of an important cysteine residue in human glutamate-cysteine ligase catalytic subunit by site-directed mutagenesis. *Biochem J* 336 (Pt 3):675-680, 1998b.

Tu, Z. and Anders, M.W. Up-regulation of glutamate-cysteine ligase gene expression by butylated hydroxytoluene is mediated by transcription factor AP-1. *Biochem Biophys Res Commun* 244:801-805, 1998c.

Uberti, D., Yavin, E., Gil, S., Ayasola, K.R., Goldfinger, N. and Rotter, V. Hydrogen peroxide induces nuclear translocation of p53 and apoptosis in cells of oligodendroglia origin. *Brain Res Mol Brain Res* 65:167-175, 1999.

Ublacker, G.A., Johnson, J.A., Siegel, F.L. and Mulcahy, R.T. Influence of glutathione S-transferases on cellular glutathione determination by flow cytometry using monochlorobimane. *Cancer Res* 51:1783-1788, 1991.

Ueno, M., Masutani, H., Arai, R.J., et al. Thioredoxin-dependent redox regulation of p53-mediated p21 activation. *J Biol Chem* 274:35809-35815, 1999.

Unger, T., Nau, M.M., Segal, S. and Minna, J.D. p53: a transdominant regulator of transcription whose function is ablated by mutations occurring in human cancer. *EMBO J* 11:1383-1390, 1992.

Upadhyay, S., Li, G., Liu, H., Chen, Y.Q., Sarkar, F.H. and Kim, H.R. bcl-2 suppresses expression of p21WAF1/CIP1 in breast epithelial cells. *Cancer Res* 55:4520-4524, 1995.

Urata, Y., Honma, S., Goto, S., et al. Melatonin induces gamma-glutamylcysteine synthetase mediated by activator protein-1 in human vascular endothelial cells. *Free Radic Biol Med* 27:838-847, 1999.

Urata, Y., Yamamoto, H., Goto, S., et al. Long exposure to high glucose-concentration impairs the responsive expression of gamma-glutamylcysteine synthetase by interleukin-1-beta and tumor-necrosis-factor-alpha in mouse endothelial-cells. *J Biol Chem* 271:15146-15152, 1996.

Van den Eijinde, SM, Boshart, et al. Phosphatidylserine plasma membrane asymmetry in vivo: a pancellular phenomenon which alters during apoptosis. *Cell Death Differ* 4:311-316, 1997.

van Ommen, B., Voncken, J.W., Muller, F. and van Bladeren, P.J. The oxidation of tetrachloro-1,4-hydroquinone by microsomes and purified cytochrome P-450b. Implications for covalent binding to protein and involvement of reactive oxygen species. *Chem Biol Interact* 65:247-259, 1988.

van, H., Robert, O., Dumont, E., et al. Markers of apoptosis in cardiovascular tissues: focus on Annexin V. *Cardiovasc Res* 45:549-559, 2000.

Vayssier, M., Banzet, N., Francois, D., Bellmann, K. and Polla, B.S. Tobacco smoke induces both apoptosis and necrosis in mammalian cells: differential effects of HSP70. *American Journal Of Physiology-Lung Cellular And Molecular Physiology* 19:L771-L7791998.

Venot, C., Maratrat, M., Dureuil, C., Conseiller, E., Bracco, L. and Debussche, L. The requirement for the p53 proline-rich functional domain for mediation of apoptosis is correlated with specific PIG3 gene transactivation and with transcriptional repression. *EMBO J* 17:4668-4679, 1998.

Verhaegh, G.W., Parat, M.O., Richard, M.J. and Hainaut, P. Modulation of p53 protein conformation and DNA-binding activity by intracellular chelation of zinc. *Mol Carcinog* 21:205-214, 1998.

Virchow, R. and Chandler, A. *Cellular pathology as based upon physiological and pathological histology*, New York:Dover Publications, 1859.

Voehringer, D.W., McConkey, D.J., McDonnell, T.J., Brisbay, S. and Meyn, R.E. Bcl-2 expression causes redistribution of glutathione to the nucleus. *Proc Natl Acad Sci U S A* 95:2956-2960, 1998.

Voehringer, D., Hirshberg, D., Xiao, J., et al. Gene microarray identification of redox and mitochondrial elements that control resistance or sensitivity to apoptosis. *Proc Natl Acad Sci U S A* 97:2680-2685, 2000.

Wagner, A.J., Kokontis, J.M. and Hay, N. Myc-mediated apoptosis requires wild-type p53 in a manner independent of cell cycle arrest and the ability of p53 to induce p21waf1/cip1. *Genes Dev* 8:2817-2830, 1994.

Walker, N.I., Bennett, R.E. and Kerr, J.F. Cell death by apoptosis during involution of the lactating breast in mice and rats. *Am J Anat* 185:19-32, 1989.

Walsh, A.C., Li, W., Rosen, D.R. and Lawrence, D.A. Genetic mapping of GLCLC, the human gene encoding the catalytic subunit of gamma-glutamylcysteine synthetase, to chromosome band 6p12 and characterization of a polymorphic trinucleotide repeat within its 5' untranslated region. *Cytogenet Cell Genet* 75:14-16, 1996.

Walsh, G.M., Dewson, G., Wardlaw, A.J., Levi, S. and Moqbel, R. A comparative study of different methods for the assessment of apoptosis and necrosis in human eosinophils. *J Immunol Methods* 217:153-163, 1998.

Wang, D., Kreutzer, D.A. and Essigmann, J.M. Mutagenicity and repair of oxidative DNA damage: insights from studies using defined lesions. *Mutat Res* 400:99-115, 1998a.

Wang, D., Yu, X. and Brecher, P. Nitric oxide and N-acetylcysteine inhibit the activation of mitogen-activated protein kinases by angiotensin II in rat cardiac fibroblasts. *J Biol Chem* 273:33027-33034, 1998b.

Wang, K., Yin, X.M., Chao, D.T., Milliman, C.L. and Korsmeyer, S.J. BID: a novel BH3 domain-only death agonist. *Genes Dev* 10:2859-2869, 1996.

Wang, X., Campos, B., Kaetzel, M.A. and Dedman, J.R. Annexin V is critical in the maintenance of murine placental integrity. *Am J Obstet Gynecol* 180:1008-1016, 1999.

Wang, X.W., Yeh, H., Schaeffer, L., et al. p53 modulation of TFIIH-associated nucleotide excision repair activity. *Nat Genet* 10:188-195, 1995.

Wang, Y., Reed, M., Wang, P., et al. p53 domains: identification and characterization of two autonomous DNA-binding regions. *Genes Dev* 7:2575-2586, 1993.

Warner, H.R. Superoxie dismutase, aging and degenerative disease. *Free Radical Biology And Medicine* 17:249-258, 1994.

Wasserman, W. and Fahl, W. Functional antioxidant responsive elements. *Proc Natl Acad Sci USA* 94:5361-5366, 1997.

Waterman, M.J., Stavridi, E.S., Waterman, J.L. and Halazonetis, T.D. ATM-dependent activation of p53 involves dephosphorylation and association with 14-3-3 proteins. *Nat Genet* 19:175-178, 1998.

Watson, R.W., Rotstein, O.D., Nathens, A.B., Dackiw, A.P. and Marshall, J.C. Thiol-mediated redox regulation of neutrophil apoptosis. *SURGERY* 120:150-158, 1996.

Weber, J.D., Taylor, L.J., Roussel, M.F., Sherr, C.J. and Bar-Sagi, D. Nucleolar Arf sequesters Mdm2 and activates p53. *Nat Cell Biol* 1:20-26, 1999.

Wendland, J., Ayad-Durieux, Y., Knechtle, P., Rebischung, C. and Philippsen, P. PCR-based gene targeting in the filamentous fungus Ashbya gossypii. *Gene* 242:381-391, 2000.

White, E. Life, death and the pursuit of apoptosis. *Genes Dev* 10:1-15, 1996.

Wild, A.C., Gipp, J.J. and Mulcahy, R.T. Overlapping antioxidant response element and PMA response element sequences mediate basal and beta-naphthoflavone-induced expression of the human gamma-glutamylcysteine synthetase catalytic subunit gene. *Biochem J* 332:373-381, 1998.

Wild, A.C., Moinova, H.R. and Mulcahy, R.T. Regulation of gamma-glutamylcysteine synthetase subunit gene expression by the transcription factor Nrf2. *J Biol Chem* 274:33627-33636, 1999.

Wilhelm, D., Bender, K., Knebel, A. and Angel, P. The level of intracellular glutathione is a key regulator for the induction of stress-activated signal transduction pathways including Jun N-terminal protein kinases and p38 kinase by alkylating agents. *Mol Cell Biol* 17:4792-4800, 1997.

Will, Y., Fischer, K.A., Horton, R.A., et al. gamma-glutamyltranspeptidase-deficient knockout mice as a model to study the relationship between glutathione status, mitochondrial function, and cellular function. *Hepatology* 32:740-749, 2000.

Williams, R.L., Hilton, D.J., Pease, S., et al. Myeloid leukaemia inhibitory factor maintains the developmental potential of embryonic stem cells. *Nature* 336:684-687, 1988.

Winn, L.M. and Wells, P.G. Phenytoin-initiated DNA oxidation in murine embryo culture, and embryo protection by the antioxidative enzymes superoxide dismutase and catalase: evidence for reactive oxygen species-mediated DNA oxidation in the molecular mechanism of phenytoin teratogenicity. *Mol Pharmacol* 48:112-120, 1995.

Winn, L.M. and Wells, P.G. Evidence for embryonic prostaglandin H synthase-catalyzed bioactivation and reactive oxygen species-mediated oxidation of cellular macromolecules in phenytoin and benzo[a]pyrene teratogenesis. *Free Radic Biol Med* 22:607-621, 1997.

Wong, E.A. and Capecchi, M.R. Homologous recombination between coinjected DNA sequences peaks in early to mid-S phase. *Mol Cell Biol* 7:2294-2295, 1987.

Woods, J.R., Plessinger, M.A. and Fantel, A. An introduction to reactive oxygen species and their possible roles in substance abuse. *Obstetrics And Gynecology Clinics Of North America* 25:219-230, 1998.

Wu, A.L. and Moye-Rowley, W.S. GSH1, which encodes gamma-glutamylcysteine synthetase, is a target gene for yAP-1 transcriptional regulation. *Mol Cell Biol* 14:5832-5839, 1994.

Wu, F.Y., Chang, N.T., Chen, W.J. and Juan, C.C. Vitamin K3-induced cell cycle arrest and apoptotic cell death are accompanied by altered expression of c-fos and c-myc in nasopharyngeal carcinoma cells. *Oncogene* 8:2237-2244, 1993.

Wu, H., Liu, X. and Jaenisch, R. Double replacement: strategy for efficient introduction of subtle mutations into the murine Col1a-1 gene by homologous recombination in embryonic stem cells. *Proc Natl Acad Sci U S A* 91:2819-2823, 1994.

Wu, H.H. and Momand, J. Pyrrolidine dithiocarbamate prevents p53 activation and promotes p53 cysteine residue oxidation. *J Biol Chem* 273:18898-18905, 1998.

Wu, K.I., Pollack, N., Panos, R.J., Sporn, P.S. and Kamp, D.W. Keratinocyte growth factor promotes alveolar epithelial cell DNA repair after H2O2 exposure. *American Journal Of Physiology-Lung Cellular And Molecular Physiology* 19:L780-L7871998.

Wubah, J.A., Ibrahim, M.M., Gao, X., Nguyen, D., Pisano, M.M. and Knudsen, T.B. Teratogen-induced eye defects mediated by p53-dependent apoptosis. *Curr Biol* 6:60-69, 1996.

Wyllie, A.H., Kerr, J.F. and Currie, A.R. Cell death in the normal neonatal rat adrenal cortex. *J Pathol* 111:255-261, 1973.

Wyllie, A.H., Kerr, J.F. and Currie, A.R. Cell death: the significance of apoptosis. *Int Rev Cytol* 68:251-306, 1980.

Xia, F., Wang, X., Wang, Y.H., et al. Altered p53 status correlates with differences in sensitivity to radiation-induced mutation and apoptosis in two closely related human lymphoblast lines. *Cancer Res* 55:12-15, 1995.

Xiao, H., Pearson, A., Coulombe, B., et al. Binding of basal transcription factor TFIIH to the acidic activation domains of VP16 and p53. *Mol Cell Biol* 14:7013-7024, 1994.

Xie, T., Belinsky, M., Xu, Y. and Jaiswal, A.K. ARE- and TRE-mediated regulation of gene expression. Response to xenobiotics and antioxidants. *J Biol Chem* 270:6894-6900, 1995.

Xiong, Y., Hannon, G.J., Zhang, H., Casso, D., Kobayashi, R. and Beach, D. p21 is a universal inhibitor of cyclin kinases. *Nature* 366:701-704, 1993.

Yaguchi, M., Miyazawa, K., Katagiri, T., et al. Vitamin K2 and its derivatives induce apoptosis in leukemia cells and enhance the effect of all-trans retinoic acid. *Leukemia* 11:779-787, 1997.

Yamamoto, M., Yoshida, M., Ono, K., et al. Effect of tumor suppressors on cell cycle-regulatory genes: RB suppresses p34cdc2 expression and normal p53 suppresses cyclin A expression. *Exp Cell Res* 210:94-101, 1994.

Yanez, R.J. and Porter, A.C. Gene targeting is enhanced in human cells overexpressing hRAD51. *Gene Ther* 6:1282-1290, 1999.

Yang, A., Schweitzer, R., Sun, D., et al. p63 is essential for regenerative proliferation in limb, craniofacial and epithelial development. *Nature* 398:714-718, 1999.

Yang, A., Walker, N., Bronson, R., et al. p73-deficient mice have neurological, pheromonal and inflammatory defects but lack spontaneous tumours. *Nature* 404:99-103, 2000.

Yang, E., Zha, J., Jockel, J., Boise, L.H., Thompson, C.B. and Korsmeyer, S.J. Bad, a heterodimeric partner for Bcl-XL and Bcl-2, displaces Bax and promotes cell death. *Cell* 80:285-291, 1995.

Yang, J., Liu, X., Bhalla, K., et al. Prevention of apoptosis by Bcl-2: release of cytochrome c from mitochondria blocked. *Science* 275:1129-1132, 1997.

Yao, K.S., Godwin, A.K., Johnson, S.W., Ozols, R.F., Odwyer, P.J. and Hamilton, T.C. Evidence for altered regulation of gamma-glutamylcysteine synthetase gene-expression among cisplatin-sensitive and cisplatin-resistant human ovarian-cancer cell-lines. *Cancer Research* 55:4367-4374, 1995.

Yao, K.S., Xanthoudakis, S., Curran, T. and O'Dwyer, P.J. Activation of AP-1 and of a nuclear redox factor, Ref-1, in the response of HT29 colon cancer cells to hypoxia. *Mol Cell Biol* 14:5997-6003, 1994.

Yew, P.R., Liu, X. and Berk, A.J. Adenovirus E1B oncoprotein tethers a transcriptional repression domain to p53. *Genes Dev* 8:190-202, 1994.

Yin, Y., Solomon, G., Deng, C. and Barrett, J.C. Differential regulation of p21 by p53 and Rb in cellular response to oxidative stress. *Mol Carcinog* 24:15-24, 1999.

Yin, Y., Terauchi, Y., Solomon, G.G., et al. Involvement of p85 in p53-dependent apoptotic response to oxidative stress. *Nature* 391:707-710, 1998.

Yokote, H., Nishio, K., Arioka, H., et al. The C-terminal domain of p53 catalyzes DNA-renaturation and strand exchange toward annealing between intact ssDNAs and

toward eliminating damaged ssDNA from duplex formation through preferential recognition of damaged DNA by a duocarmycin. *Mutat Res* 409:147-162, 1998.

Yonish-Rouach, E., Borde, J., Gotteland, M., Mishal, Z., Viron, A. and May, E. Induction of apoptosis by transiently transfected metabolically stable wt p53 in transformed cell lines. *Cell Growth Differ* 1:39-47, 1994.

Yoshida, T., Maulik, N., Ho, Y.S., Alam, J. and Das, D.K. H(mox-1) constitutes an adaptive response to effect antioxidant cardioprotection: A study with transgenic mice heterozygous for targeted disruption of the Heme oxygenase-1 gene. *Circulation* 103:1695-1701, 2001.

Zamzami, N., Marchetti, P., Castedo, M., et al. Sequential reduction of mitochondrial transmembrane potential and generation of reactive oxygen species in early programmed cell death. *J Exp Med* 182:367-377, 1995.

Zamzami, N., Marzo, I., Susin, S.A., et al. The thiol crosslinking agent diamide overcomes the apoptosis-inhibitory effect of Bcl-2 by enforcing mitochondrial permeability transition. *Oncogene* 16:1055-1063, 1998.

Zamzami, N., Susin, S.A., Marchetti, P., et al. Mitochondrial control of nuclear apoptosis. *J Exp Med* 183:1533-1544, 1996.

Zastawny, T.H., Dabrowska, M., Jaskolski, T., et al. Comparison of oxidative base damage in mitochondrial and nuclear DNA. *Free Radic Biol Med* 24:722-725, 1998.

Zhang, Y., Buchholz, F., Muyrers, J.P. and Stewart, A.F. A new logic for DNA engineering using recombination in Escherichia coli. *Nat Genet* 20:123-128, 1998.

Zhang, Y., Riesterer, C., Ayrall, A.M., Sablitzky, F., Littlewood, T.D. and Reth, M. Inducible site-directed recombination in mouse embryonic stem cells. *Nucleic Acids Res* 24:543-548, 1996.

Zheng, M. and Storz, G. Redox sensing by prokaryotic transcription factors. *Biochem Pharmacol* 59:1-6, 2000.

Zhou, J.A.J.W.S.H.a.P.C. A role for p53 in base excision repair. *EMBO J* 20:914-923, 2001.

Ziegler, A., Jonason, A.S., Leffell, D.J., et al. Sunburn and p53 in the onset of skin cancer. *Nature* 372:773-776, 1994.

Zoratti, M. and Szabo, I. The mitochondrial permeability transition. *Biochim Biophys Acta* 1241:139-176, 1995.

Zou, H., Henzel, W.J., Liu, X., Lutschg, A. and Wang, X. Apaf-1, a human protein homologous to C. elegans CED-4, participates in cytochrome c-dependent activation of caspase-3. *Cell* 90:405-413, 1997.

Appendix II: Solutions

RNA Solutions

DEPC treated water

diethylpyrocarbonate (DEPC) in double distilled water	0.01% (w/v)

Stand overnight at room temperature

Autoclave solution prior to use

5X First strand buffer

Tris-HCl, pH8.3	250mM
KCl	375mM
M_gCl_2	15mM

DNA solutions

PCR buffers

Standard PCR 10X buffer

Tris-HCl pH8.0	20mM
KCl	50mM
$MgCl_2$	15mM

Hi-Fidelity 50X polymerase buffer

Glycerol	50%
Tris HCl pH 7.5	0.8mM
KCl	1.0mM
$(NH_4)_2SO_4$	0.5mM
EDTA	2.0mM
β-mercaptoethanol	0.1Mm

Hi-Fidelity 10X reaction buffer

Tricine-KOH (pH9.2)	40mM
KOAc	15mM
$Mg(OAc)_2$	3.5mM
BSA	75μg/ml

Agarose gel electrophoresis reagents

Agarose gels

For DNA fragments >500bp	0.8% w/v agarose in TBE buffer
For DNA fragments <500bp	3% w/v agarose and 1% Nu Sieve (Flowgen) in TBE buffer

Tracking dye

Bromophenol blue	0.1%
EDTA	0.1M
Glycerol	50% v/v

TBE buffer

Tris	0.89M
Boric acid	0.89M
EDTA	0.002M

Plasmid isolation

Antibiotic Luria Broth

NaCl	1% (w/v)
Bactotryptone	1% (w/v)
Yeast extract	5% (w/v)
Agar	2% (w/v)

Make up in dH2O, adjust to pH 7.0 with 5N NaOH.

Autoclave, cool to 55^0C and add 50mg/ml of filter-sterilised ampicillin.

Resuspension Solution

Tris.HCl (pH=8.0)	50mM
EDTA (pH=8.0)	10mM

Autoclave and store at 4°C

Add 100µg/ml RNase A

Lysis Solution

NaOH	200mM
SDS	1%

Neutralisation Solution

Potassium Acetate (pH 5.5)	3M

Equilibration buffer

NaCl	750mM
MOPS pH 7.0	50mM
Isopropanol	15%
Triton X-100	0.15%

Wash buffer

NaCl	1.0M
MOPS pH 7.0	50mM
Isopropanol	15%

Elution buffer

NaCl	1.25M
MOPS pH 8.5	50mM
Isopropanol	15%

TE Buffer

Tris.Cl (pH=7.5)	10mM
EDTA (pH=8.0)	1mM

Sequencing

5X Sequenase Reaction buffer

Tris-HCl, pH 7.5	200mM
$MgCl_2$	100mM
NaCl	250mM

Enzyme dilution buffer

Tris-HCl, pH 7.5	10mM
DTT	5mM
EDTA	0.1mM
Acetylated BSA	0.5mg/ml

Termination mixes

All four mixes contain,

dATP	80μM
dCTP	80μM
dGTP	80μM
dTTP	80μM
NaCl	50mM

In addition the 'A' mix contains 8μM ddATP, the 'C' mix 8μM ddCTP etc.

Stop solution

Formamide	95% v/v
EDTA	20mM
Bromophenol Blue	0.5g/l
Xylene cyanol FF	0.5g/l

Gel solution

Urea	250g
19:1, 40% acrylamide stock	75mls
10X TBE	50mls
dH_2O	175mls

Gel fix solution

Methanol	10%
Acetic Acid	10%

in dH_2O.

Southern analysis

Depurination Solution

HCl	0.2M

Denaturation Solution

NaCl	1.5M
NaOH	0.5M

Neutralisation Solution

NaCl	1.5M
Tris-HCl, pH 7.2	1M

20 X SSC

NaCl	3M
Trisodium citrate	0.3M

pH to 7.0 with 1M HCl

High Prime

Klenow polymerase	1U/µl
dATP	0.125mM
dCTP	0.125mM
dGTP	0.125mM
dTTP	0.125mM
5X reaction buffer in glycerol	50% (v/v)

Dextran sulphate solution

Dissolve 50g dextran sulphate in 300mls of dH_2O

Pre-Hybridisation Solution

SSC	15mls 20x
SDS	5mls 10%
Dextran sulphate solution	30mls

Wash solutions, in order of ascending stringency

I	2x SSC + 1% SDS in dH2O
II	1x SSC + 1% SDS in dH2O
III	0.5x SSC + 1% SDS in dH2O
IV	0.25x SSC + 0.1% SDS in dH2O
V	0.1x SSC + 0.1% SDS in dH2O

Library plating

LB++ broth:

Prepare LB broth as described in section "Plasmid isolation" and add to final concentration:

$MgSO_4$	10mM
Maltose	0.2%

Store at room temperature.

1M $MgSO_4$:

Filter sterilize, store at room temperature.

SM (per litre)

NaCl	5.8g
$MgSO_4.7H_2O$	2.0g
Tris.Cl, pH7.5	1M50ml

Autoclave, add 5ml 2% gelatin solution (autoclaved separately).

Store at room temperature.

LB/MgSO4 plates:

Prepare LB broth as described in section "Plasmid isolation" and add to a final concentration

$MgSO_4$	10mM

Pour plates and store at 4°C.

LB/top agarose:

Prepare LB as described above and add to a final concentration:

$MgSO_4$	10mM

Agarose (7.2g/l), autoclave.

Store at room temperature.

Maltose, 20% in H_2O

Filter sterilize, store at room temperature

ES cell culture solutions

Medium for ES cell culture

BHK-21 G-MEM (Life Technologies)	500ml
100x Non-Essential Amino Acids (Life Technologies)	5ml
100x Sodium Pyruvate (100mM, Life Technologies)	5m
100X L-Glutamine (200mM, Life Technologies)	5ml
LIF (use at 1:500)	500µl
100mM β mercaptoethanol solution	500µl
FBS/FCS serum for ES cells	50ml

(25mls Fetal Calf Serum (Sigma): 25mls Newborn Calf Serum (Life Technologies))

100mM β-mercaptoethanol solution

1000x β-mercaptoethanol (Sigma)	100µl
dH_2O	14.1mls

Filter sterilise solution through 0.2µm filter.

Store at 4°C.

LIF was prepared by the transfection of Cos-7 cells and subsequent harvesting of the conditioned medium (Smith et al., 1988)

10X PBS

KCl	2.0g/l
KH_2PO_4	2.0g/l
NaCl	80.0g/l
$Na_2HPO_4.7H_2O$	21.60g/l

1X Trypsin-EDTA

Trypsin	0.5g
EDTA	2.0g

(Made up to 1l with modified Puck's Saline A)

Freeze Media (FM)

Culture media	40% v/v
Serum	50% v/v
Dimethyl Sulphoxide	10% v/v

ES Cell Lysis Buffer

Tris-HCl, pH 8.5	100mM
EDTA	5mM
SDS	0.2%
NaCl	200mM
Proteinase K	100µg per ml

Antibiotic supplements for selection

For 500mls media

5X Gancyclovir: 50µl 10,000X

200µg/ml G418: 500µl of stock G418: Disslove 4.0g G418 in 20mls PBS, aliquot and store at –20°C.

Free Radical Biology & Medicine, Vol. 32, No. 2, pp. 187–196, 2002

0891-5849/02/$–see front matter

ELSEVIER

PII S0891-5849(01)00792-4

Original Contribution

GLUTATHIONE AND P53 INDEPENDENTLY MEDIATE RESPONSES AGAINST OXIDATIVE STRESS IN ES CELLS

JONATHAN P. COE,* IRFAN RAHMAN†, NATHALIE SPHYRIS,* ALAN R. CLARKE,‡ and DAVID J. HARRISON*

*CRC Laboratories, Department of Pathology and †ELEGI Respiratory Medicine Unit, University of Edinburgh, Edinburgh, UK; and ‡School of Biosciences, Cardiff University, Cardiff, UK

(*Received* 16 *March* 2001; *Accepted* 8 *November* 2001)

Abstract—We have investigated the roles of the antioxidant glutathione and p53 in the response of embryonic stem (ES) cells to oxidative stress. ES cells express γGCS, a critical enzyme in glutathione (GSH) biosynthesis. Treatment with the pro-oxidant menadione led to elevation of GSH, a strong apoptotic response and reduced clonogenic survival. Addition of BSO, a specific γGCS inhibitor depleted GSH pools and prevented the menadione-induced increase in GSH, sensitizing cells to oxidative insult. Although p53 status had no bearing on either the basal levels of GSH or the menadione-induced GSH response, the levels of menadione-induced apoptosis were reduced in the absence of p53. We conclude that the pathways involving p53 and GSH act independently to protect against the deleterious effects of oxidative damage. Furthermore, the presence of an intact p53 pathway confers a long-term growth advantage post oxidative stress. Thus, in the absence of p53 ES cells bearing genotoxic damage are less likely to be propagated, suggesting that p53-dependent apoptosis acts to limit the deleterious effects of oxidative stress during early development.

Keywords—GSH, p53, Apoptosis, ROS, ES cells, Free radicals

INTRODUCTION

Oxidants produced during normal metabolism or following exposure to xenobiotics may adversely affect embryogenesis by causing DNA strand breaks, lipid peroxidation, and protein degradation. Disruption of the intracellular redox equilibrium also affects the balance between cell death, proliferation, and senescence [1,2]. Cellular mechanisms to maintain redox homeostasis and curb injury inflicted by reactive oxygen species (ROS), the main source of oxidative stress, include a complex array of chemical and enzymatic ROS-scavengers, damage sensors, and response effectors.

A key determinant in the maintenance of the redox equilibrium is the tripeptide glutathione (GSH). GSH is produced via a two-step pathway, the first of which is rate-limiting and catalyzed by gamma glutamylcysteine synthetase (γGCS). This enzyme is composed of two subunits, a heavy subunit containing the active site (γGCS*h*) and a regulatory light subunit (γGCS*l*). GSH is the most abundant intracellular nonprotein thiol which affords protection against oxidative stress directly, via conjugation, or indirectly as a co-factor in repair reactions catalyzed by glutathione *S*-transferases (GST) and glutathione peroxidases (GPx) [3].

Several lines of evidence also point to a role for the stress-surveillance transcription factor, p53, in the response to oxidative stress [4,5]. In response to a variety of stress signals, p53 co-ordinates the cellular processes of cell cycle arrest, senescence, apoptosis [6–8], and directly participates in DNA repair via the base excision repair (BER) pathway [9]. Considerable attention has also been focused on the contribution of p53 in embryonic development. p53 is expressed at high levels in embryos up to day 11 post fertilization, and then levels rapidly decline, as reviewed [10]. As such, undifferentiated ES cells express high levels of p53 and respond to UV-induced damage by undergoing apoptosis, whereas differentiated cells have lower levels of p53 and are relatively UV resistant [11]. Furthermore, p53 levels and activity are modulated with the degree of differentiation

Address correspondence to: Dr. I. Rahman, ELEGI Laboratory, Respiratory Medicine Unit, University of Edinburgh, Medical School, Teviot Place, Wilkie Building, Edinburgh EH8 9AG, UK; Tel: +44 (0131) 651-1523; Fax: +44 (0131) 651-1558; E-Mail: ir@srv1.med.ed.ac.uk.

[11–13], with expression throughout later gestation becoming isolated to developing nervous tissue [13].

Although p53 null mice were found to be viable, an increased incidence of exencephaly and associated defects in neural tube development suggests a role for p53 in neural tube closure [14,15]. Embryos deficient for a negative regulator of p53, mdm2, are non-viable at an early stage. However, viability of mdm2 null mice is fully restored in the absence of p53, suggesting that regulation of p53 activity is critical for embryogenesis and its overexpression is detrimental to development [16].

Several studies have attributed the cause of drug-induced birth defects to oxidative DNA damage [17,18]. A role for p53 as a teratological suppressor was suggested on the basis of the ability of p53 to inhibit the effects of the pro-oxidant and teratogen benzo[a]pyrene on mouse embryonic development, possibly by protection against ROS-induced DNA damage [17–19].

A large body of evidence also implicates ROS in the induction of apoptosis [20–22], and p53 activation [5,23]. Intriguingly, many of the early transcripts induced by p53 prior to the onset of apoptosis are involved in the regulation of ROS and are thought to increase ROS formation [24]. Since antioxidants, including GSH, can rescue cells from apoptosis, ROS have been implicated as downstream effectors in the execution phase of cell death [25–27]. Furthermore, the gene encoding GPx was found to be transactivated by p53 [28], linking the p53-signaling pathway with the regulation of antioxidants.

The majority of studies investigating the toxicity of oxidative stress have utilized the culture of primary or transformed cell lines for limited periods of time. ES cells, the pluripotent progenitors of all subsequent development, proliferate continuously in culture. However, ES cells are nontransformed and exhibit normal growth and responses to damage characteristic of that in vivo. These traits permit analysis of the immediate and long-term effects of oxidative stress on healthy mammalian cells. Such experiments have not, to the author's knowledge, been used before with ES or other cell types.

We used ES cells to investigate the role of GSH and p53 in the response to oxidative stress induced by the pro-oxidant and chemotherapy quinone, menadione (MQ) [29,30]. MQ can diffuse across the plasma membrane and initiate a toxic "redox cycle" with molecular oxygen, a reaction that can generate ROS including H_2O_2, $^1O_2$, $O_2^{\bullet -}$, and, in the presence of metal ions, the highly unstable and deleterious hydroxyl radical, $OH^{\bullet}$. MQ can also react directly with protein sulfhydryl (SH) groups. This ability of MQ to arylate protein SH-groups to form MQ-protein conjugates, an event not dependent upon the presence of iron, is well documented [31]. Thus, metabolism of MQ can exert oxidative stress by two routes: arylation or oxidation.

MQ can introduce single strand breaks in DNA, though this damage has been dissociated from immediate cell death in hepatocytes [32] and fibroblasts [5]. In embryonic development, however, such damage to DNA propagated through successive rounds of replication may accumulate to the detriment of the organism.

We present evidence that suggests p53 and GSH, through discrete mechanisms, modulate the immediate and long-term viability of ES cells under oxidative stress. This alteration in viability is mediated, at least in part, by p53-dependent and -independent signaling pathways that delete damaged embryonic cells.

MATERIALS AND METHODS

ES cell culture and experimental treatments

ES cells were maintained in GMEM BHK-21 supplemented with nonessential amino acids, sodium pyruvate, L-glutamine, 10% fetal calf serum (Life Technologies, Paisley, UK), β-mercaptoethanol (Sigma Chemical Co., St. Louis, MO, USA), and leukemia inhibitory factor. 0.3×10^6 cells/well were seeded in gelatinized 6 well plates (Greiner Laboratories, Solingen, Germany) and propagated at 37°C in 5% CO_2.

Three hours after seeding the medium was replaced with normal medium, or media containing 100 μM BSO (Sigma) and incubated for 16 h. At the end of the 16 h pretreatment the medium was discarded and the cells rinsed once with warm PBS. Subsequently, cells were incubated with serum-free media with or without 35 μM MQ (Sigma) for 90 min. 35 μM MQ was selected on the basis of baseline kill experiments indicating that, at this dose, BSO optimally reduced ES cell viability (data not shown). Following MQ exposure, cells were rinsed twice with warm PBS and incubated with complete media until analysis.

Derivation of p53-null embryonic stem cells by high G418 selection

The p53−/− ES cell line HG287 was derived from the hemizygous line R72 by high G418 selection [33]. R72 cells were previously derived from E14 [34] by targeting the p53 locus with a neomycin resistance cassette [7].

γGCS RT-PCR

RNA was isolated from subconfluent ES cells with TRIzol Reagent (Life Technologies) and total RNA reverse transcribed using Superscript II (Life Technolo-

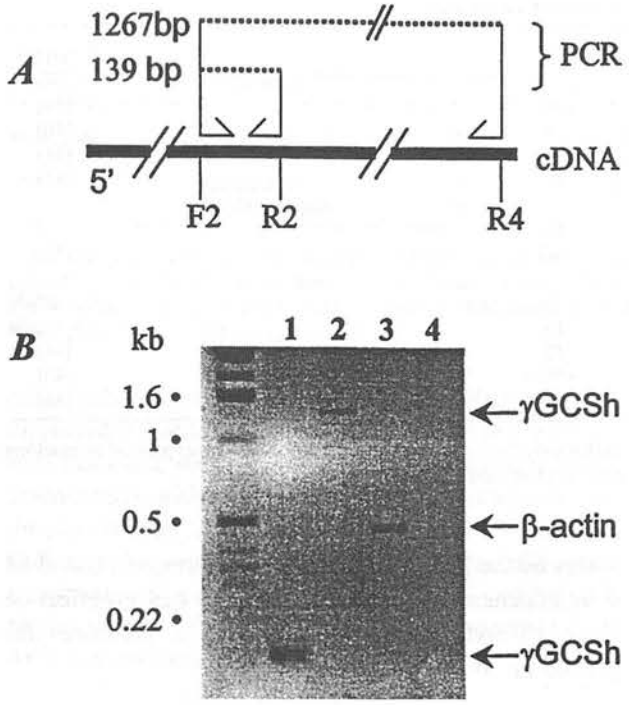

Fig. 1. ES cells express *γGCSh* transcripts. RT-PCR strategy to detect the presence of *γGCS* mRNA in ES cells. (A) Dashed lines represent PCR products, solid line cDNA. *γGCSh* exonic primers F2 + R2 generate a 139bp product, F2+ R4 a 1267bp product. (B) Agarose gel electrophoresis of RT-PCR performed on total RNA isolated from subconfluent ES cells. Lane 1: PCR with F2 + R2, lane 2: F2 + R4, lane 3: positive control amplifying the housekeeping gene encoding β-actin (450 bp product), lane 4: negative control.

gies) according to the manufacturer's instructions. To detect γGCS mRNA, PCR was performed on ES cell cDNA. Oligonucleotide primers were designed on the basis of the published sequence of γGCS*h* cDNA [35], and the housekeeping gene, β-actin (Stratagene, La Jolla, CA, USA). γGCS*h* primer sequences (5′-3′);

F2: AGGAGAAAAGGTTGTCATCAATG,

R2: CAAATCCCATGGCATCCATGTA

R4: CAAGTAACTCTGGGCATTCACA (Fig. 1A).

PCR was run in a Hybaid Omnigene cycler as follows: 94°C, 45 s: 56°C, 30 s: 72°C, 60 s, for 30 cycles. PCR products were analyzed on a 4% agarose gel.

MTT assay

ES cell viability was determined by the modified tetrazolium salt 3-(4-5-dimethylthiazoyl-2-yl) 2-5-diphenyl-tetrazolium bromide (MTT) assay as described [36]. Briefly, 600 μl of MTT (5 mg/ml in PBS) was added to each well after treatment. Samples were incubated for 3 h at 37°C, washed once with PBS and left to dry, prior to the addition of 1.5 ml dimethyl formamide (DMSO). The optical densities at 590 nm were measured using a 96 well multiscanner autoreader (Dynatech MR 5000), with DMSO as a blank.

Clonogenic survival assay

Cells were plated in triplicate at a range of cell densities and treated with MQ and BSO as described above. Plates were maintained for 10 days, then fixed in 70% ethanol for 10 min and stained with 10% Giemsa prior to counting clones.

Quantification of apoptosis by direct counts of acridine orange stained cells

Cells were trypsinized, washed in PBS and fixed in 90% ethanol: 10% formalin. Fixed single cell suspensions were stained with acridine orange solution (10 μg/ml) and observed under fluorescence microscopy. Apoptotic ES cells were identified by their condensed chromatin, fragmented nuclei and smaller size [37]. The number of apoptotic cells in relation to total cell number was scored in triplicate. In total, 600 cells were counted for each sample.

Intracellular GSH levels

GSH levels were measured according to the method of Tietze et al. [38]. Briefly, cells were trypsinized, washed in PBS and stored at −70°C. Pellets were thawed slowly on ice before addition of 0.5 ml ice-cold 0.6% sulfosalicyclic acid/0.01% Triton X-100. The cells were lysed by freeze-thawing and repeated vortexing. Samples were pelleted at 4°C and the supernatant stored at −70°C.

Assays were performed in triplicate. Samples (10 μl) were incubated at room temperature with 8 units/ml glutathione reductase in the presence of 0.4 mg/ml DTNB (5, 5′ dithiobis-2-nitrobenzoic acid). Following addition of 0.4 mg/ml NADPH (β-nicotinamide adenine dinucleotide phosphate) the change in absorbance at 412 nm was recorded using a Dynex-TC Multiplate reader. A standard curve was established for each plate using GSH in the range of 0.167–2.5 nmoles. Results were expressed per mg of total protein. Sample protein concentration was determined by the Bio-Rad assay, using BSA as a standard.

Statistical analysis

All data sets were analyzed using the software package SigmaStat version 2.03 (SPSS, Chicago, IL, USA). When comparing two groups Normality and Equal Variance are automatically tested. Where these criteria are

Table 1. Levels of GSH in Different Cell Types

Cell type	Basal [GSH]	Reference
Human alveolar carcinoma, A549	150	[39]
Human hepatocarcinoma, HepG2	71	[40]
Bovine arterial endothelium	20	[41]
Rat lung epithelial, L2	18	[42]
Mouse embryonic epithelial:		
BDC-1 (wild type)	18	[43]
GCS-1 (*γGCSh−/−*)	ND	[43]
Mouse embryonic stem, ES:		
HM-1 (wild-type)	16	this article
HG287 (p53−/−)	16	this article
Rat embryo	12	[44]
Mouse 2 cell embryo	*0.4	[45]
Mouse blastocyst	*0.2	[45]

Illustrates the GSH level of ES cells in comparison to levels of intracellular GSH detected in other tissues. All GSH values are expressed as nmol/mg protein except values marked *, expressed as pmol/embryo. ND = no detectable level of GSH.

met parametric (unpaired *t*) tests were applied, where these criteria were not met nonparametric (Mann-Whitney rank sum) tests were applied.

RESULTS

ES cells synthesize γGCS transcipts

We wished to characterize the response of ES cells to oxidative stress. To detect the presence of a GSH-dependent antioxidant system in ES cells, we tested for the expression of γGCS, which catalyses the rate-limiting step in *de novo* glutathione biosynthesis. *γGCSh* transcripts were detected by RT-PCR performed on ES cell lysates (Fig. 1).

Partial GSH depletion does not affect ES cell viability

Having established the presence of *γGCS* transcripts in ES cells, the intracellular levels of free GSH in wild-type (HM-1) and p53−/− (HG287) ES cells were measured as described. GSH levels in ES cells are comparable with levels found in the early embryo (Table 1).

We measured ES cell GSH levels following treatment with the GSH-modulating agent BSO (DL-buthionine-(S,*R*)-sulfoximine). BSO, a specific and irreversible inhibitor of γGCS [46], has been shown to reduce the levels of GSH in many cell types. ES cells GSH levels were measured after incubation with a range of BSO concentrations. BSO lowered GSH levels, although the reduction was similar for all BSO concentrations within the 25–250 μM range employed (Fig. 2). For subsequent experiments concentrations of 100 μM BSO were used, which gave approximately 70% GSH depletion.

In order to estimate the tolerance of wild-type and p53−/− ES cells to low GSH, we analyzed the consequences of BSO on cellular viability. We estimated viability by the MTT assay, which measures mitochondrial dehydrogenase activity. 100 μM BSO had no effect on the MTT index (Table 2), even when incubated for periods up to 48 h (data not shown).

MQ reduces viability in a GSH- and p53-dependent manner

Next, we analyzed the immediate response of ES cells to MQ-induced oxidative stress, with viability scored through the MTT assay. Figure 3 shows that the viability of both wild-type and p53−/− ES cells was compro-

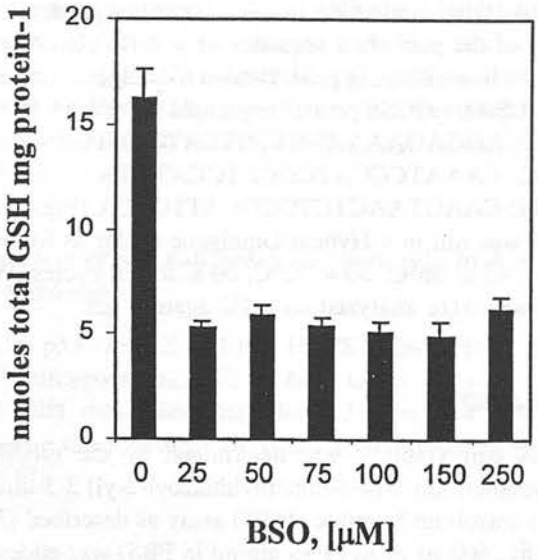

Fig. 2. Effect of BSO on ES cell GSH levels. GSH content of wild-type ES cells after incubation for 16 h with a gradient of BSO concentrations or without BSO. Results are mean SEM values from three independent experiments. The corresponding values for p53−/− cells were indistinguishable (data not shown).

Table 2. Toxicity of BSO Towards Wild-type and p53−/− ES Cells

Genotype	Treatment	n	GSH (nmoles/mg protein)	GSH reduction (%)	Cell viability (%)
Wild-type	Untreated	18	16.1 ± 1.5	0	100
	BSO 100 μM	9	4.93 ± 0.45	69.82 ± 2.10*	102.5 ± 1.26
p53−/−	Untreated	9	16.01 ± 1.9	0	100
	BSO 100 μM	9	4.54 ± 0.7	70.4 ± 2.81‡	98.8 ± 2.35

ES cells were treated for 16 h with 100 μM BSO in full media. Immediately after treatment, cytosolic extracts were prepared by freeze-thawing and ultrasound. Samples were stored at −20°C until analysis of GSH levels via the Tietze method. Cell viability 24 h post BSO exposure was evaluated using the MTT assay. Data are mean ± SEM values from at least nine independent experiments performed in triplicate. GSH reduction: * and ‡, t-test p = .001 vs. untreated value.

mised following exposure to 35 μM MQ. Wild-type cells displayed a sustained decrease in viability in the period post treatment, dropping to 34% of control values at 7 h. Pretreatment with BSO augmented MQ cytotoxicity, reducing viability to less than 5% of control levels at 7 h. Following exposure to MQ with or without BSO pretreatment, p53−/− ES cells displayed a considerably higher viability than their wild-type counterparts up to 48 h post exposure to MQ.

MQ induces p53-independent modulation of free GSH levels

In order to assess any alteration in the level of GSH subsequent to oxidative stress, GSH levels were monitored in ES cells at different time points post exposure to MQ. Following a 90 min incubation with 35 μM MQ, wild-type ES cells showed a rapid elevation of free GSH levels, peaking at 24 h post exposure before subsiding to basal levels 48 h post exposure (Fig. 4). The fluctuation of GSH levels seen in untreated controls is consistent with the degree of confluency, as reported for culture for other cell types.

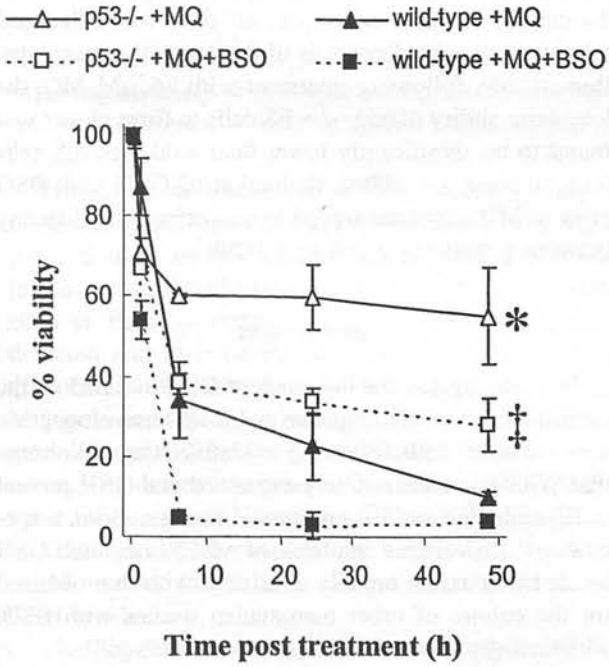

Fig. 3. Effect of BSO on MQ-induced cytotoxicity in wild-type and p53−/− ES cells. Cell viability at various time points immediately post 35 μM MQ exposure was evaluated by the MTT assay. Error bars represent SEM of three independent experiments. * and ‡ indicate the difference in comparison to wild-type ES cells treated with MQ only (p = < .001 t-test) and with MQ + BSO (p = < .001 t-test), respectively.

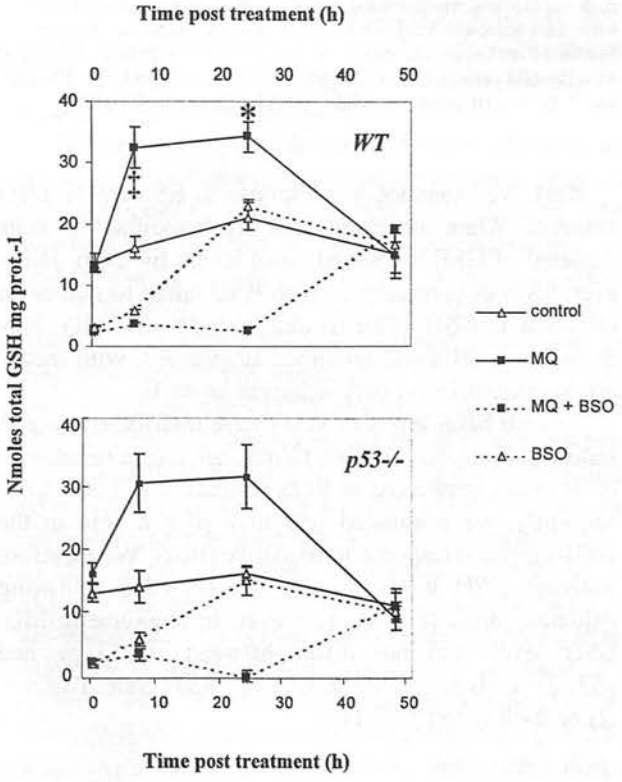

Fig. 4. GSH response of ES cells to oxidative stress. Total free GSH levels in wild-type (top panel) and p53−/− ES cells (lower panel) post 35 μM MQ and BSO treatment. Cells received either no pretreatment (solid lines), or BSO pretreatment (dashed lines). Subsequently, cells were transiently incubated in serum free media with 35 μM MQ (solid boxes) or without MQ (open triangles). Time at 0 h = end of the MQ treatment. Error bars represent SEM values of three independent experiments. *Indicates the difference in comparison to MQ-treated p53−/− ES cells (p = 1.0 t-test), and ‡ signifies the difference compared to untreated wild-type cells (p = .005 t-test).

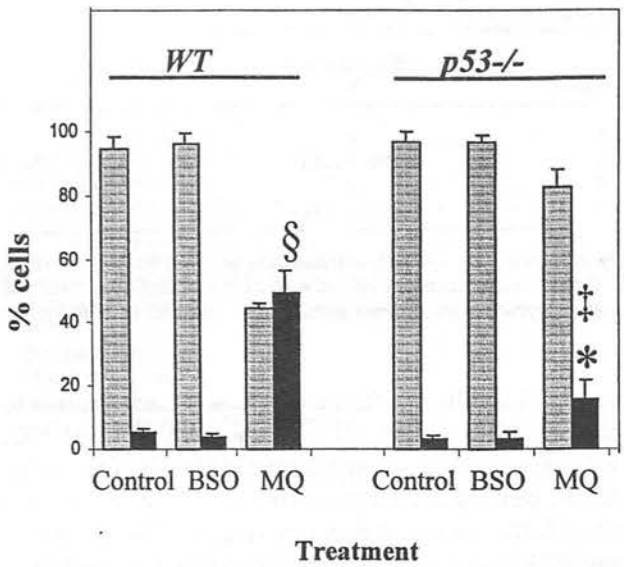

Fig. 5. Effect of BSO or MQ on the induction of apoptosis. ES cells were treated with 100 μM BSO or 35 μM MQ treatment and the rate of apoptosis examined. Shaded bars represent percentage of intact cells, solid bars percentage of apoptotic cells. Cell death was examined 7 h post removal of 35 μM MQ and the percentage apoptosis occurring in each experiment was assessed directly, using morphological criteria. Error bars represent SEM values from three independent experiments. Statistical indicators are shown as: §, (p = .001 t-test) vs. untreated wild-type ES cells; ‡, (p = 0.026 t-test) vs. untreated p53−/− ES cells, and *, (p = .001 t-test) vs. wild-type ES cells exposed to MQ.

Next, we examined the response of ES cells to BSO removal. When incubated with fresh media, ES cells depleted of GSH recovered basal levels by 24 h. However, ES cells preincubated with BSO failed to induce an elevation in GSH when treated with 35 μM MQ. Furthermore, GSH levels remained suppressed, with recovery to control levels only achieved at 48 h.

Though basal levels of GSH were unaffected by p53 status, p53 has been shown to transactivate a number of other genes implicated in ROS regulation [23,26]. Consequently, we postulated p53 may play a role in the GSH-mediated response to oxidative stress. We therefore analyzed GSH levels in p53−/− ES cells following oxidative stress (Fig. 4). However, in response to MQ, GSH levels did not differ between wild-type and p53−/− cells at 6 h (Mann Whitney Rank Sum Test p = .2) or 24 h (t-test p = 1).

MQ induces apoptosis in wild-type and p53−/− ES cells

As MTT does not distinguish between growth arrest and cell death, we investigated the mechanism underlying the reduction in cellular viability associated with exposure to MQ. The mode of cell death was determined directly using morphological criteria after staining with acridine orange (Fig. 5) [35]. No difference in the rate of apoptosis was detected between untreated and BSO-treated cell cultures, consistent with analogous MTT indices. A considerable proportion (52.47% ± 3.73) of wild-type ES cells exposed to MQ had entered apoptosis 6 h following MQ removal (t-test p = .001), concordant with the observed reduction in the MTT index at this time. p53−/− ES cells also exhibited an apoptotic response (15.88% ± 3.57, t-test p = .026). However, the incidence was considerably reduced in comparison to wild-type cells (t-test p = .001), consistent with a large population of p53−/− cells remaining viable at 48 h post MQ exposure.

MQ treatment reduces clonogenic survival, a phenomenon accentuated by p53 deficiency

In comparison to wild-type ES cells, p53−/− ES cells are refractory to apoptosis at 6 h after exposure to MQ and display an immediate survival advantage over wild-type cells, manifested up to 48 h post exposure. To ascertain whether loss of p53 conferred a continued growth advantage over an extended period, we compared the clonogenic survival of wild-type and p53−/− ES cells after exposure to MQ. A difference in plating efficiency was observed, with wild-type cells showing a plating efficiency of 85.4% compared to p53−/− cells. To control for this difference, all data was calculated relative to untreated controls of the respective genotype. Remarkably, following treatment with 35 μM MQ, the long-term ability of p53−/− ES cells to form clones was found to be significantly lower than wild-type ES cells (Fig. 6, t-test $p < .006$). Reduction of GSH with BSO prior to MQ exposure served to exacerbate the disparity between genotypes (t-test p = .029).

DISCUSSION

We investigated the influence of GSH and p53 on the immediate apoptotic response and long-term clonogenic survival of ES cells following oxidative stress. We show that *γGCSh* is constitutively expressed and GSH present in ES cells, the earliest embryonic lineage. BSO, a specific and irreversible inhibitor of γGCS, depleted GSH levels by an extent broadly consistent with that obtained for the culture of other mammalian tissues with BSO, which ranges from < 75% [47] to > 90% [48].

ROS can cause single strand breaks in DNA, initiate nuclear translocation and activation of wild-type p53 [23,49]. We show that ES cells are sensitive to oxidative challenge and respond by initiating apoptosis, a process widely regarded as important in normal development. The ES cell response also entails a rapid and transient

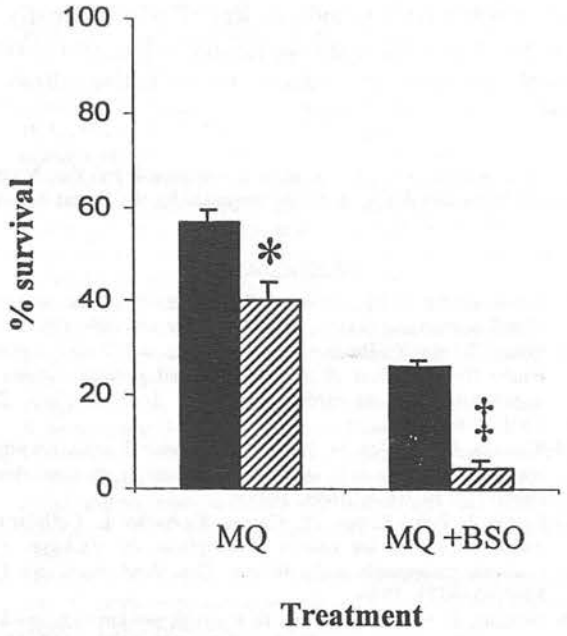

Fig. 6. Clonogenic survival of ES cells following exposure to oxidative stress. The long-term viability of ES cells after exposure to 35 μM MQ with or without prior 100 μM BSO treatment was determined. Wild-type ES cells are represented as solid bars and p53−/− cells as striped bars. Error bars represent SEM values of three independent experiments. *Indicates the statistical significance in comparison to wild-type ES cells treated with MQ only ($p = < .006$ t-test), and ‡ represents the significance in comparison to wild-type ES cells treated with MQ + BSO ($p = .029$ t-test).

elevation of GSH. This phenomenon parallels studies exposing a variety of cell types to MQ, and is thought to perform a protective function against oxidative damage [44,50].

However, an initial fall in GSH levels, evident in other cell types, was not observed in ES cells. The Tietze method used in this study measures total glutathione levels, reduced and oxidized. However GSH-conjugates such as PrSSG, formed by arylation reactions, are not detected and their formation would register as a loss of glutathione. It is therefore probable that GSH scavenges MQ-generated ROS, and that arylation reactions are not predominant in ES cells. Indeed, raised GSSG levels are commonly detected in other cell lines treated with MQ or other modes of oxidative stress [39,51]. Thus oxidation of GSH to GSSG, coupled with rapid GSH synthesis, could account for the lack of a preliminary fall in total GSH levels.

The generation of a *γGCSh*−/− embryonic cell line has revealed GSH is not required for normal growth in culture [43]. In this study, we show GSH deficiency augmented MQ cytotoxicity in both wild-type and p53−/− ES cells, reflecting a protective role of GSH. That BSO prevented the elevation in GSH indicates this response is normally mediated by an amplified rate of GSH synthesis. Together, this data indicates ES cells have a functional GSH-dependent detoxification system, which although dispensable for growth under normal conditions becomes necessary in the response against oxidative stress.

Conversely, p53−/− ES cells display an immediate survival advantage compared to wild-type cells. A battery of redox-regulation genes, including GPx, GST, and oxidoreductases have been identified as downstream effectors of p53 signaling [24,28]. We therefore reasoned that p53 may have a role in the GSH response to oxidative stress, possibly through modulation of γGCS expression. We found that the steady state levels of GSH in wild-type and p53−/− ES cells were identical. This makes a role for p53 in basal transcription of *γGCSh* or related enzymes unlikely, and is consistent with the notion that p53 transcribes target genes only when activated by cellular injury. However, the GSH response profiles of wild-type and p53−/− ES cells under oxidative stress were statistically indistinguishable. This is strong evidence that oxidative stress induces GSH via a mechanism independent of p53. Candidate mechanisms include other redox-sensitive transcription factors, such as NF-κB and AP-1. These have been shown to elevate GSH in a variety of cell types, coincident with an up-regulation of *γGCSh* [51–54].

Whilst MQ initiates apoptosis in both p53−/− and wild-type ES cell lines, the immediate apoptotic response was significantly reduced in p53−/− ES cells. This indicates the presence of distinct p53-dependent and -independent apoptotic pathways. Others have shown p53 is necessary for inducing apoptosis in response to oxidative stress [55]. However, Aladjem et al. observed only p53-independent apoptosis in response to ribonucleotide depletion and DNA damage, whilst Corbet et al. showed both p53-dependent and delayed p53-independent apoptosis in response to UV [37,56]. These findings serve to underline the complex role played by p53 in the apoptotic response of embryonic cells to damage.

The lower incidence of apoptosis observed in p53−/− ES cells at 6 h does not necessarily imply an attenuated p53−/− apoptotic response. Others have revealed, with extended time courses, the presence of a delayed wave of p53-independent apoptosis [57–59]. Thus the lower apoptotic index observed at 6 h post MQ treatment is interpreted as a kinetic shift, rather than a reduced response *per se*. This is also in agreement with the "primed to die" function where, even in the absence of p53, ES cells recognize injury and activate a death pathway. Because ROS act as downstream mediators in some apoptotic pathways it is possible that MQ, via ROS generation, may directly activate apoptotic factors in the absence of the p53 protein [60].

It should be noted that, as well as DNA damage

inflicted by MQ and the subsequent induction of apoptosis, the embryonic toxicity of MQ may manifest via a subtle reprogramming of gene expression. Such alterations are difficult to monitor in vitro and could effect cellular changes not detected within this study.

We observed the immediate growth advantage and reduced apoptotic response of p53−/− ES cells exposed to MQ translated into a lower clonogenic survival than wild-type cells in the long-term. This is consistent with a role for p53 as teratological suppressor, originally proposed due to the ability of p53 to limit the teratogolic effects of benzo[a]pyrene [19], and later cyclophosphamide, on mouse embryonic development [61]. However, there are exceptions. While fetal lethality in wild-type mice embryos exposed to irradiation was greater than in p53−/− mice, p53−/− mice showed more lesions [62]. Moreover, Wubah and colleagues demonstrated the genotoxic agent 2-chloro-2-deoxyadenosine caused a 73% incidence of eye abnormalities in wild-type embryos, compared with 52% and 2% in p53+/− and p53−/− embryos, respectively [63]. Clearly further work is required to resolve these apparent differences in p53 functionality.

In the absence of p53 (although immediate survival is higher) surviving ES cells are very likely to carry a high level of cellular damage. Normally this injury would be repaired through p53-dependent DNA mechanisms, such as BER, and failure to repair would trigger p53-dependent cell death. In the absence of p53, we hypothesize this level of damage is sufficient to initiate delayed p53-independent mechanisms that prevent propagation, leading to reduced long term survival. These mechanisms may include p53-independent apoptosis and permanent withdrawal from the cell cycle. This is in agreement with the conclusions reached by Frenkel et al., who showed p53−/− embryos, upon irradiation, display not only altered patterns of apoptosis but accentuated levels of delayed death compared to their wild-type counterparts [59]. This is also consistent with the view that in development loss of cells is less detrimental to the organism than retention of damaged cells. It should be remembered that these results reflect early organogenesis (< 10 d post fertilization) and may not be the case for later development, where p53 levels decrease with differentiation.

In conclusion, we propose that in the absence of functional p53, MQ-induced DNA breaks accrue and activate alternative embryonic death pathways that prevent the persistence of genetic lesions in differentiated cells. These mechanisms are perhaps reliant upon other p53 family members, such as the homologues p63 and p73. GSH may serve to limit MQ-induced DNA damage and therefore indirectly prevent induction of both p53-dependent and -independent death pathways. Investigation of pathways and independent of p53 is clearly an area that may yield a greater understanding of developmental abnormalities induced by oxidative stress *in utero*.

Acknowledgements — This work was supported by the Norman Salvesen Trust and AICR. A.R.C is supported by the Royal Society.

REFERENCES

[1] Powis, G.; Briehl, M.; Oblong, J. Redox signalling and the control of cell growth and death. *Pharmacol. Ther.* **68:**149–173; 1995.
[2] Wang, D.; Yu, X.; Brecher, P. Nitric oxide and N-acetylcysteine inhibit the activation of mitogen-activated protein kinases by angiotensin II in rat cardiac fibroblasts. *J. Biol. Chem.* **273:** 33027–33034; 1998.
[3] Rahman, I.; MacNee, W. Lung glutathione and oxidative stress: implications in cigarette smoke-induced airway disease. *Am. J. Physiol.* **277:**L1067–L1088; 1999.
[4] Lotem, J.; Peled-Kamar, M.; Groner, Y.; Sachs, L. Cellular oxidative stress and the control of apoptosis by wild-type p53, cytotoxic compounds, and cytokines. *Proc. Natl. Acad. Sci. USA* **93:**9166–9171; 1996.
[5] Renzing, J.; Hansen, S.; Lane, D. P. Oxidative stress is involved in the UV activation of p53. *J. Cell Sci.* **109:**1105–1112; 1996.
[6] Lane, D. P. Cancer. p53, guardian of the genome. *Nature* **358:** 15–16; 1992.
[7] Clarke, A. R.; Purdie, C. A.; Harrison, D. J.; Morris, R. G.; Purdie, C. C.; Hooper, M. L.; Wyllie, A. H. Thymocyte apoptosis induced by p53-dependent and independent pathways. *Nature* **362:**849–852; 1993.
[8] Levine, A. J. p53, the cellular gatekeeper for growth and division. *Cell* **88:**323–331; 1997.
[9] Zhou, J.; Ahn, J.; Wilson, S. H.; Prives, C. A role for p53 in base excision repair. *EMBO J.* **20:**914–923; 2001.
[10] Choi, J.; Donehower, L. A. p53 in embryonic development: maintaining a fine balance. *Cell. Mol. Life Sci.* **55:**38–47; 1999.
[11] Sabapathy, K.; Klemm, M.; Jaenisch, R.; Wagner, E. F. Regulation of ES cell differentiation by functional and conformational modulation of p53. *EMBO J.* **16:**6217–6229; 1997.
[12] Louis, J. M.; McFarland, V. W.; May, P.; Mora, P. T. The phosphoprotein p53 is down-regulated post-transcriptionally during embryogenesis in vertebrates. *Biochim. Biophys. Acta* **950:** 395–402; 1988.
[13] Komarova, E. A.; Chernov, M. V.; Franks, R.; Wang, K.; Armin, G.; Zelnik, C. R.; Chin, D. M.; Bacus, S. S.; Stark, G. R.; Gudkov, A. V. Transgenic mice with p53-responsive lacZ: p53 activity varies dramatically during normal development and determines radiation and drug sensitivity in vivo. *EMBO J.* **16:**1391–1400; 1997.
[14] Armstrong, J. F.; Kaufman, M. H.; Harrison, D. J.; Clarke, A. R. High-frequency developmental abnormalities in p53-deficient mice. *Curr. Biol.* **5:**931–936; 1995.
[15] Sah, V. P.; Attardi, L. D.; Mulligan, G. J.; Williams, B. O.; Bronson, R. T.; Jacks, T. A subset of p53-deficient embryos exhibit exencephaly. *Nat. Genet.* **10:**175–180; 1995.
[16] Jones, S. N.; Roe, A. E.; Donehower, L. A.; Bradley, A. Rescue of embryonic lethality in Mdm2-deficient mice by absence of p53. *Nature* **378:**206–208; 1995.
[17] Winn, L. M.; Wells, P. G. Evidence for embryonic prostaglandin H synthase-catalyzed bioactivation and reactive oxygen species-mediated oxidation of cellular macromolecules in phenytoin and benzo[a]pyrene teratogenesis. *Free Radic. Biol. Med.* **22:**607–621; 1997.
[18] Liu, L.; Wells, P. G. DNA oxidation as a potential molecular mechanism mediating drug-induced birth defects: phenytoin and structurally related teratogens initiate the formation of 8-hydroxy-2′-deoxyguanosine in vitro and in vivo in murine maternal hepatic and embryonic tissues. *Free Radic. Biol. Med.* **19:**639–648; 1995.

[19] Nicol, C. J.; Harrison, M. L.; Laposa, R. R.; Gimelshtein, I. L.; Wells, P. G. A teratologic suppressor role for p53 in benzo-[a]pyrene-treated transgenic p53-deficient mice. *Nat. Genet.* **10:** 181–187; 1995.

[20] Lowe, S. W.; Bodis, S.; McClatchey, A.; Remington, L.; Ruley, H. E.; Fisher, D. E.; Housman, D. E.; Jacks, T. p53 status and the efficacy of cancer therapy in vivo. *Science* **266:**807–810; 1994.

[21] Symonds, H.; Krall, L.; Remington, L.; Saenz-Robles, M.; Lowe, S.; Jacks, T.; Van Dyke, T. p53-dependent apoptosis suppresses tumor growth and progression in vivo. *Cell* **78:**703–711; 1994.

[22] Kroemer, G.; Zamzami, N.; Susin, S. A. Mitochondrial control of apoptosis. *Immunol. Today* **18:**44–51; 1997.

[23] Uberti, D.; Yavin, E.; Gil, S.; Ayasola, K. R.; Goldfinger, N.; Rotter, V. Hydrogen peroxide induces nuclear translocation of p53 and apoptosis in cells of oligodendroglia origin. *Brain Res. Mol. Brain Res.* **65:**167–175; 1999.

[24] Polyak, K.; Xia, Y.; Zweier, J. L.; Kinzler, K. W.; Vogelstein, B. A model for p53-induced apoptosis. *Nature* **389:**300–305; 1997.

[25] O'Connor, P. M.; Wassermann, K.; Sarang, K.; Magrath, I.; Bohr, V. A.; Kohn, K. W. Relationship between DNA crosslinks, cell cycle, and apoptosis in Burkitt's lymphoma cell lines differing in sensitivity to nitrogen mustard. *Cancer Res.* **51:**6550–6557; 1990.

[26] Lennon, S. V.; Martin, S. J.; Cotter, T. G. Dose-dependent induction of apoptosis in human tumour cell lines by widely diverging stimuli. *Cell Prolif.* **24:**203–214; 1991.

[27] Johnson, T. M.; Yu, Z. X.; Ferrans, V. J.; Lowenstein, R. A.; Finkel, T. Reactive oxygen species are downstream mediators of p53-dependent apoptosis. *Proc. Natl. Acad. Sci. USA* **93:**11848–11852; 1996.

[28] Tan, M.; Li, S.; Swaroop, M.; Guan, K.; Oberley, L. W.; Sun, Y. Transcriptional activation of the human glutathione peroxidase promoter by p53. *J. Biol. Chem.* **274:**12061–12066; 1999.

[29] Taper, H. S.; Keyeux, A.; Roberfroid, M. Potentiation of radiotherapy by nontoxic pretreatment with combined vitamins C and K3 in mice bearing solid transplantable tumor. *Anticancer Res.* **16:**499–503; 1996.

[30] Yaguchi, M.; Miyazawa, K.; Katagiri, T.; Nishimaki, J.; Kizaki, M.; Tohyama, K.; Toyama, K. Vitamin K2 and its derivatives induce apoptosis in leukemia cells and enhance the effect of all-trans retinoic acid. *Leukemia* **11:**779–787; 1997.

[31] Di Monte, D.; Ross, D.; Bellomo, G.; Eklow, L.; Orrenius, S. Alterations in intracellular thiol homeostasis during the metabolism of menadione by isolated rat hepatocytes. *Arch. Biochem. Biophys.* **235:**334–342; 1984.

[32] Coleman, J. B.; Gilfor, D.; Farber, J. L. Dissociation of the accumulation of single-strand breaks in DNA from the killing of cultured hepatocytes by an oxidative stress. *Mol. Pharmacol.* **36:**193–200; 1989.

[33] Mortensen, R. M.; Conner, D. A.; Chao, S.; Geisterfer-Lowrance, A. A.; Seidman, J. G. Production of homozygous mutant ES cells with a single targeting construct. *Mol. Cell. Biol.* **12:**2391–2395; 1992.

[34] Hooper, M.; Hardy, K.; Handyside, A.; Hunter, S.; Monk, M. HPRT-deficient (Lesch-Nyhan) mouse embryos derived from germline colonization by cultured cells. *Nature* **326:**292–295; 1987.

[35] Reid, L. L.; Botta, D.; Shao, J.; Hudson, F. N.; Kavanagh, T. J. Molecular cloning and sequencing of the cDNA encoding mouse glutamate cysteine ligase regulatory subunit. *Biochim. Biophys. Acta* **1353:**107–110; 1997.

[36] Hansen, M. B.; Nielsen, S. E.; Berg, K. Re-examination and further development of a precise and rapid dye method for measuring cell growth/cell kill. *J. Immunol. Methods* **119:**203–210; 1989.

[37] Corbet, S. W.; Clarke, A. R.; Gledhill, S.; Wyllie, A. H. P53-dependent and -independent links between DNA-damage, apoptosis and mutation frequency in ES cells. *Oncogene* **18:**1537–1544; 1999.

[38] Tietze, F. Enzymic method for quantitative determination of nanogram amounts of total and oxidized glutathione: applications to mammalian blood and other tissues. *Anal. Biochem.* **27:**502–522; 1969.

[39] Rahman, I.; Bel, A.; Mulier, B.; Lawson, M. F.; Harrison, D. J.; MacNee, W.; Smith, C. A. Transcriptional regulation of gamma-glutamylcysteine synthetase-heavy subunit by oxidants in human alveolar epithelial cells. *Biochem. Biophys. Res. Commun.* **229:** 832–837; 1996.

[40] Galloway, D. C.; Blake, D. G.; Shepherd, A. G.; McLellan, L. I. Regulation of human gamma-glutamylcysteine synthetase: coordinate induction of the catalytic and regulatory subunits in HepG2 cells. *Biochem. J.* **328:**99–104; 1997.

[41] Shi, M. M.; Iwamoto, T.; Forman, H. J. gamma-Glutamylcysteine synthetase and GSH increase in quinone-induced oxidative stress in BPAEC. *Am. J. Physiol.* **267:**L414–L421; 1994.

[42] Shi, M. M.; Kugelman, A.; Iwamoto, T.; Tian, L.; Forman, H. J. Quinone-induced oxidative stress elevates glutathione and induces gamma-glutamylcysteine synthetase-activity in rat lung epithelial L2 cells. *J. Biol. Chem.* **269:**26512–26517; 1994.

[43] Shi, Z. Z.; Osei-Frimpong, J.; Kala, G.; Kala, S. V.; Barrios, R. J.; Habib, G. M.; Lukin, D. J.; Danney, C. M.; Matzuk, M. M.; Lieberman, M. W. Glutathione synthesis is essential for mouse development but not for cell growth in culture. *Proc. Natl. Acad. Sci. USA* **97:**5101–5106; 2000.

[44] Ishibashi, M.; Akazawa, S.; Sakamaki, H.; Matsumoto, K.; Yamasaki, H.; Yamaguchi, Y.; Goto, S.; Urata, Y.; Kondo, T.; Nagataki, S. Oxygen-induced embryopathy and the significance of glutathione-dependent antioxidant system in the rat embryo during early organogenesis. *Free Radic. Biol. Med.* **22:**447–454; 1996.

[45] Gardiner, C. S.; Reed, D. J. Synthesis of glutathione in the preimplantation mouse embryo. *Arch Biochem. Biophys.* **318:**30–36; 1995.

[46] Griffith, O. W.; Mulcahy, R. T. The enzymes of glutathione synthesis: gamma glutamylcysteine synthetase. *Adv. Enzymol. Relat. Areas Mol. Biol.* **73:**209–259; 1999.

[47] Lu, S. C.; Bao, Y.; Huang, Z. Z.; Sarthy, V. P.; Kannan, R. Regulation of gamma-glutamylcysteine synthetase subunit gene expression in retinal Muller cells by oxidative stress. *Invest. Ophthalmol. Vis. Sci.* **40:**1776–1782; 1999.

[48] Aliosman, F.; Antoun, G.; Wang, H.; Ranjagopal, S.; Gagucas, E. Buthionine sulphoximine induction of gamma-glutamyl-L-cysteine synthetase gene-expression, kinetics of glutathione depletion and resynthesis, and modulation of carmustine-induced DNA-DNA cross-linking and cytotoxicity in human glioma-cells. *Mol. Pharmacol.* **49:**1012–1020; 1996.

[49] Messmer, U. K.; Ankarcrona, M.; Nicotera, P.; Brune, B. p53 expression in nitric oxide-induced apoptosis. *FEBS Lett.* **355:**23–26; 1994.

[50] Trocino, R. A.; Akazawa, S.; Ishibashi, M.; Matsumoto, K.; Matsuo, H.; Yamamoto, H.; Goto, S.; Urata, Y.; Kondo, T.; Nagataki, S. Significance of glutathione depletion and oxidative stress in early embryogenesis in glucose-induced rat embryo culture. *Diabetes* **44:**992–998; 1995.

[51] Rahman, I.; Antonicelli, F.; MacNee, W. Molecular mechanism of the regulation of glutathione synthesis by tumor necrosis factor-alpha and dexamethasone in human alveolar epithelial cells. *J. Biol. Chem.* **274:**5088–5096; 1999.

[52] Mulcahy, R. T.; Wartman, M. A.; Bailey, H. H.; Gipp, J. J. Constitutive and beta-naphthoflavone-induced expression of the human gamma-glutamylcysteine synthetase heavy subunit gene is regulated by a distal antioxidant response element/TRE sequence. *J. Biol. Chem.* **272:**7445–7454; 1997.

[53] Sekhar, K. R.; Meredith, M. J.; Kerr, L. D.; Soltaninassab, S. R.; Spitz, D. R.; Xu, Z. Q.; Freeman, M. L. Expression of glutathione and gamma-glutamylcysteine synthetase mRNA is *jun* dependent. *Biochem. Biophys. Res. Commun.* **234:**588–593; 1997.

[54] Morales, A.; Miranda, M.; Sanchezreyes, A.; Colell, A.; Biete, A.; Fernandezcheca, J. C. Transcriptional regulation of the heavy subunit chain of gamma- glutamylcysteine synthetase by ionizing radiation. *FEBS Lett.* **427:**15–20; 1998.

[55] Yin, Y.; Terauchi, Y.; Solomon, G. G.; Aizawa, S.; Rangarajan,

P. N.; Yazaki, Y.; Kadowaki, T.; Barrett, J. C. Involvement of p85 in p53-dependent apoptotic response to oxidative stress. *Nature* **391**:707–710; 1998.

[56] Aladjem, M. I.; Spike, B. T.; Rodewald, L. W.; Hope, T. J.; Klemm, M.; Jaenisch, R.; Wahl, G. M. ES cells do not activate p53-dependent stress responses and undergo p53-independent apoptosis in response to DNA damage. *Curr. Biol.* **8**:145–155; 1998.

[57] Clarke, A. R.; Gledhill, S.; Hooper, M. L.; Bird, C. C.; Wyllie, A. H. p53 dependence of early apoptotic and proliferative responses within the mouse intestinal epithelium following gamma-irradiation. *Oncogene* **9**:1767–1773; 1994.

[58] Merritt, A. J.; Allen, T. D.; Potten, C. S.; Hickman, J. A. Apoptosis in small intestinal epithelial from p53-null mice: evidence for a delayed, p53-independent G2/M-associated cell death after gamma-irradiation. *Oncogene* **14**:2759–2766; 1997.

[59] Frenkel, J.; Sherman, D.; Fein, A.; Schwartz, D.; Almog, N.; Kapon, A.; Goldfinger, N.; Rotter, V. Accentuated apoptosis in normally developing p53 knockout mouse embryos following genotoxic stress. *Oncogene* **18**:2901–2907; 1999.

[60] Qiu, X. B.; Schonthal, A. H.; Cadenas, E. Anticancer quinones induce pRb-preventable G2/M cell cycle arrest and apoptosis. *Free Radic. Biol. Med.* **24**:848–854; 1998.

[61] Moallem, S. A.; Hales, B. F. The role of p53 and cell death by apoptosis and necrosis in 4-hydroperoxycyclophosphamide-induced limb malformations. *Development* **125**:3225–3234; 1998.

[62] Norimura, T.; Nomoto, S.; Katsuki, M.; Gondo, Y.; Kondo, S. p53-dependent apoptosis suppresses radiation-induced teratogenesis. *Nat. Med.* **2**:577–580; 1996.

[63] Wubah, J. A.; Ibrahim, M. M.; Gao, X.; Nguyen, D.; Pisano, M. M.; Knudsen, T. B. Teratogen-induced eye defects mediated by p53-dependent apoptosis. *Curr. Biol.* **6**:60–69; 1996.

ABBREVIATIONS

BSO—DL-buthionine-[S,R]-sulphoximine
ES—embryonic stem
γGCS—gamma glutamylcysteine synthetase
γGCS*h*—γGCS heavy subunit
γGCS*l*—γGCS light subunit
GPx—glutathione peroxidase
GSH—reduced glutathione
GSSG—oxidized glutathione
GST—glutathione transferases
MQ—menadione
ROS—reactive oxygen species